

## University of Southampton Research Repository

Copyright © and Moral Rights for this thesis and, where applicable, any accompanying data are retained by the author and/or other copyright owners. A copy can be downloaded for personal non-commercial research or study, without prior permission or charge. This thesis and the accompanying data cannot be reproduced or quoted extensively from without first obtaining permission in writing from the copyright holder/s. The content of the thesis and accompanying research data (where applicable) must not be changed in any way or sold commercially in any format or medium without the formal permission of the copyright holder/s.

When referring to this thesis and any accompanying data, full bibliographic details must be given, e.g.

Thesis: Author (Year of Submission) "Full thesis title", University of Southampton, name of the University Faculty or School or Department, PhD Thesis, pagination.

Data: Author (Year) Title. URI [dataset]



**University of Southampton**

Faculty of Environmental and Life Science

School of Ocean and Earth Science

**Stress in paradise: Reconstructing Late Holocene hydroclimate to investigate the  
role of drought in the timing of human migration and colonisation in the tropical  
South Pacific**

by

**Charlotte Victoria Hipkiss**

ORCID ID: 0000-0001-6379-079X

Thesis for the degree of Doctor of Philosophy

November 2023



# University of Southampton

## Abstract

Faculty of Environmental and Life Science

School of Ocean and Earth Science

Doctor of Philosophy

Stress in paradise: Reconstructing Late Holocene hydroclimate to investigate the role of drought in the timing of human migration and colonisation in the tropical South Pacific

by

Charlotte Victoria Hipkiss

The South Pacific was the final frontier of human colonisation on Earth. Human migration across the Pacific occurred in two waves, the first started 3000 yr BP and saw the Lapita civilisation colonise remote Oceania eastward to Samoa. After a long pause of 2000 years, the second occurred at approximately 1000 yr BP and saw the colonisation of eastern Polynesia out to the three corners of the Polynesian Triangle. Reasons for these migrations are contested, but climate is increasingly thought to have been a factor. Despite high levels of precipitation in this region, drought is prevalent and palaeoclimate evidence suggests the South Pacific has experienced shifts between dry and wet periods throughout the past three thousand years. Drought has significant repercussions for small Pacific islands, affecting both water and food resources.

The aim of this thesis is to identify how the climate has changed over the Holocene in this region and to assess whether changing climate was a pivotal driver in the timing of human migration and colonisation. Using a sequence of cores from Emaotfer Swamp located on the island of Efate in Vanuatu and Lake Tiriara, located on the island of Mangaia in the Southern Cook Islands, this study utilises a multi-proxy approach, which includes stable isotopes ( $\delta^{13}\text{C}$  and  $\delta^{15}\text{N}$  from organic matter as well as  $\delta^{18}\text{O}$  and  $\delta^{13}\text{C}$  from carbonate) as well as Itrax  $\mu\text{XRF}$  profiles and diatoms to create new palaeo records. This thesis presents new 9,200 and 2,500-year environmental and climatic record from Emaotfer Swamp and Lake Tiriara respectively. The key findings from the palaeoenvironmental records show evidence for a shift towards dry conditions around  $500\text{-}2300 \pm 160$  yr BP in the Emaotfer record and  $1590\text{-}860 \pm 126$  cal yr BP and  $650\text{-}470 \pm 102$  yr BP in the Tiriara record. This indicates that there was a notable change in hydroclimate conditions around the second wave of human migration into Eastern Polynesia and in the relatively early stages of colonisation. To unravel the connection between climate and impacts on island life, this thesis also presents a new socio-ecological model of prehistoric Pacific island life. The model identifies the impact of changing hydroclimate on agricultural carrying capacity and population dynamics to reinforce the evidence for a potential connection between the changing climate identified by palaeoenvironmental records and the dynamics of early Pacific island societies. The model outputs suggest that drought has a greater impact on population dynamics the closer to the absolute carrying capacity the population gets and that severity of the drought rather than the frequency is the key factor determining the impact of a drought on agricultural outputs and population dynamics. This thesis offers firstly, new insights into climatic and hydrological change during the Holocene, across the two waves of human migration in the tropical South Pacific - a region that is relatively under-represented in terms of palaeo-environmental research. Secondly, this thesis presents a new socio-ecological model of Pacific island life that provides insights into the pressure of environmental change on these early Polynesian societies following colonisation.



# Table of Contents

<b>Table of Contents</b> .....	<b>i</b>
<b>Table of Tables</b> .....	<b>ix</b>
<b>Table of Figures</b> .....	<b>xi</b>
<b>Research Thesis: Declaration of Authorship</b> .....	<b>xix</b>
<b>COVID-19 Impact Statement</b> .....	<b>xxi</b>
<b>Acknowledgements</b> .....	<b>xxii</b>
<b>Definitions and Abbreviations</b> .....	<b>xxiii</b>
<b>Chapter 1 Introduction</b> .....	<b>1</b>
1.1 Pacific Climate .....	1
1.2 Pacific Palaeoclimate.....	2
1.3 Human Migration and Colonisation of the Pacific .....	4
1.4 The focus of this study .....	5
1.5 Thesis Structure.....	5
<b>Chapter 2 Literature Review</b> .....	<b>7</b>
2.1 Introduction.....	7
2.2 Human Colonisation of the Pacific .....	7
2.3 Environment/Climate-human interactions .....	12
2.3.1 Diet of the Pacific islanders .....	15
2.3.2 Voyaging & Migration .....	17
2.3.3 Conflict .....	19
2.3.4 Environment/Climate-human interactions summary .....	20
2.4 South Pacific Climate and Precipitation .....	21
2.5 Pacific palaeo-precipitation records .....	25
2.5.1 Climate and the first wave of migration and initial colonisation period .....	27
2.5.2 Climate and the second wave of migration and colonisation of Polynesia .....	33
2.5.2.1 Mediaeval Climate Anomaly .....	35
2.5.2.2 Little Ice age to present.....	38
2.6 Modelling prehistoric societies .....	43

## Table of Contents

2.6.1	Approaches for modelling of socio-ecological systems.....	47
2.6.1.1	Agent-based .....	47
2.6.1.2	Systems dynamics .....	48
2.6.1.3	Other modelling approaches .....	50
2.7	Summary .....	53
<b>Chapter 3</b>	<b>Aims and Objectives.....</b>	<b>55</b>
3.1	Introduction .....	55
3.2	Changes in hydroclimate in the tropical South Pacific during the Late Holocene ..	56
3.3	Modelling island life.....	57
3.4	Palaeoclimate and Archaeological records of the tropical South Pacific .....	58
<b>Chapter 4</b>	<b>Regional Setting and Site Description .....</b>	<b>59</b>
4.1	Introduction .....	59
4.2	Emaotfer Swamp – Efate, Vanuatu.....	62
4.2.1	Geography of Vanuatu and Efate .....	62
4.2.2	Climate of Efate.....	62
4.2.3	Geological setting of Efate .....	63
4.2.4	Vegetation of Efate .....	64
4.2.5	Colonisation of Vanuatu .....	64
4.2.6	Emaotfer Swamp.....	65
4.3	Lake Tiriara – Mangaia, Cook Islands.....	67
4.3.1	Geography of the Cook Islands and Mangaia .....	67
4.3.2	Climate of Mangaia .....	67
4.3.3	Geological setting of Mangaia .....	68
4.3.4	Vegetation of Mangaia .....	71
4.3.5	Colonisation of the Southern Cook Islands.....	71
4.3.6	Lake Tiriara.....	72
<b>Chapter 5</b>	<b>Palaeoenvironmental Methods .....</b>	<b>75</b>
5.1	Sediment Coring and site stratigraphy .....	75
5.2	Magnetic Susceptibility.....	75
5.3	Geochemistry - Itrax $\mu$ XRF .....	76

5.4	Sedimentology.....	80
5.5	Inorganic isotopes .....	81
5.5.1	$\delta^2\text{H}$ and $\delta^{18}\text{O}$ in Modern lake water.....	81
5.5.2	Carbonate $\delta^{18}\text{O}$ record in Lake Sediments.....	81
5.5.3	Conceptual Model for $\delta^{18}\text{O}$ in Tropical Lakes .....	87
5.5.4	Carbonate $\delta^{13}\text{C}$ record in Lake Sediments .....	89
5.6	Organic Proxies.....	90
5.6.1	Total Organic Carbon, Total Nitrogen and C/N ratio .....	90
5.6.2	Carbon and Nitrogen Isotopes .....	91
5.6.2.1	$\delta^{13}\text{C}_{\text{Organic}}$ .....	91
5.6.2.2	$\delta^{15}\text{N}$ .....	93
5.7	Diatom analysis .....	94
5.8	Chronology .....	95
5.8.1	$^{210}\text{Pb}$ & $^{137}\text{Cs}$ .....	95
5.8.2	Radiocarbon/ $^{14}\text{C}$ .....	98
5.8.3	Tephrochronology .....	99
<b>Chapter 6</b>	<b>Environmental Change in Vanuatu .....</b>	<b>101</b>
6.1	Introduction.....	101
6.2	Chronology .....	101
6.2.1	Radiocarbon/ $^{14}\text{C}$ .....	101
6.2.2	Tephrochronology .....	102
6.2.3	Rbacon Age Model .....	103
6.3	Magnetic Susceptibility .....	106
6.4	Loss-On-Ignition .....	107
6.5	$\mu\text{XRF}$ Geochemistry .....	107
6.5.1	Principal Component Analysis.....	110
6.6	Organic Proxies.....	113
6.6.1	Total Organic Carbon.....	113
6.6.1.1	TOC vs $\text{LOI}_{550}$ .....	113

## Table of Contents

6.6.2	Total Nitrogen .....	114
6.6.3	C/N ratio.....	115
6.6.4	Organic $\delta^{13}\text{C}$ and $\delta^{15}\text{N}$ .....	116
6.7	Inorganic Proxies.....	117
6.7.1	$\delta^{18}\text{O}$ and $\delta^{13}\text{C}$ .....	117
6.8	Palaeoenvironmental change in Vanuatu during the Holocene.....	120
6.8.1	Interpretation of the Emaotfer Swamp sequence.....	120
6.8.2	Evidence for a Wet event in zone E-3 – 8031-7926 cal yr BP $\pm$ 809 .....	126
6.8.3	Evidence for drought event in zone E-5 - 6644-7424 $\pm$ 623 cal yr BP .....	127
6.8.4	Evidence for drought event at the transition between zone E-7 and E-8.....	128
6.9	Summary .....	130
<b>Chapter 7 Environmental Change in the Southern Cook Islands .....</b>		<b>133</b>
7.1	Introduction .....	133
7.2	Chronology.....	133
7.2.1	$^{14}\text{C}$ .....	133
7.2.2	$^{210}\text{Po}/^{210}\text{Pb}$ and $^{137}\text{Cs}$ .....	134
7.2.3	Rbacon Age Model.....	137
7.3	Magnetic Susceptibility.....	138
7.4	Loss-On-Ignition .....	139
7.5	$\mu\text{XRF}$ Geochemistry.....	140
7.5.1	Principal Component Analysis .....	143
7.6	Organic Proxies .....	146
7.6.1	Total Organic Carbon and Nitrogen .....	146
7.6.2	C/N ratio.....	147
7.6.3	Organic $\delta^{13}\text{C}$ and $\delta^{15}\text{N}$ .....	148
7.7	Inorganic Proxies.....	149
7.7.1	$\delta^2\text{H}$ and $\delta^{18}\text{O}$ in modern water .....	149
7.7.2	Inorganic $\delta^{18}\text{O}$ and $\delta^{13}\text{C}$ record.....	151
7.8	Diatoms.....	154

7.9	Palaeoenvironmental change in the Cook Islands during the Late Holocene .....	157
7.9.1	Interpretation of the Lake Tiriara Sequence .....	157
7.9.1.1	Pre-human arrival – 2500 – 950 yr BP .....	157
7.9.1.2	Post-human arrival – 950 yr BP to present .....	159
7.9.2	Evidence for drought events within the Tiriara sequence .....	164
7.9.2.1	Zone M-2 - 1678-1594 ± 126 cal yr BP .....	164
7.9.2.2	End of Zone M-3 - 1594-859 ± 126 cal yr BP .....	166
7.9.2.3	Zone M-5 - 647-470 ± 102 cal yr BP .....	167
7.9.3	Evidence for a palaeotsunami within the Tiriara sequence.....	169
7.9.4	Use of Ti/inc as a precipitation proxy.....	173
7.10	Summary .....	177
<b>Chapter 8</b>	<b>Modelling Prehistoric Polynesian Island Life .....</b>	<b>179</b>
8.1	Introduction.....	179
8.2	Socio-ecological system of the Prehistoric Polynesians.....	180
8.2.1	Hydrology .....	181
8.2.2	Demography .....	182
8.2.3	Land and water management .....	183
8.3	Conceptual Model .....	186
8.4	Model Development .....	190
8.4.1	Vensim.....	190
8.4.2	Creating the Model .....	190
8.5	Model parameterisation .....	193
8.5.1	Population .....	196
8.5.2	Carrying Capacity.....	197
8.5.3	Food Availability .....	197
8.5.4	Precipitation .....	199
8.5.4.1	Palaeo Reconstruction Rainfall Data Set .....	201
8.6	Sensitivity Analysis and Model Validation .....	204
8.6.1	Sensitivity Testing.....	205

## Table of Contents

8.7	Results.....	207
8.7.1	Scenario model outputs.....	207
8.7.2	Scenario drought and population metrics.....	210
8.7.3	Palaeo Scenario.....	212
8.7.3.1	1000-year palaeo sequence.....	212
8.7.3.2	2000-year palaeo sequence.....	215
8.7.4	Palaeo drought and population metrics.....	217
8.7.5	Model Evaluation and Interpretation.....	219
8.7.6	Limitations/Further development.....	225
8.8	Summary.....	227
<b>Chapter 9</b>	<b>Discussion.....</b>	<b>229</b>
9.1	Introduction.....	229
9.2	Palaeoenvironmental change surrounding periods of human migration and colonisation in the tropical South Pacific.....	229
9.2.1	Palaeoenvironmental change in Early to Mid-Holocene and surrounding first wave of migration c. 3000 yr BP.....	229
9.2.2	Palaeoenvironmental change surrounding second wave of migration c. 1000 yr BP/MCA.....	233
9.2.3	Palaeoenvironmental change in the MCA-LIA transition c. 1300 AD.....	237
9.2.4	Palaeoenvironmental change surrounding the LIA c.650-100 yr BP through to present.....	237
9.3	Was drought/changing hydroclimate a driver of human migration in the tropical South Pacific during the late Holocene?.....	238
9.3.1	Drought and the first wave of migration into Remote Oceania c. 3000 yr BP.....	239
9.3.2	Drought and the “Long Pause”.....	240
9.3.3	Drought and the second wave of migration into Eastern Polynesia c. 1000 yr BP.....	246
9.3.4	Drought and subsequent colonisation of Eastern Polynesia - 1300 AD event.....	250

9.4 Summary .....	252
<b>Chapter 10 Conclusions.....</b>	<b>253</b>
10.1 Overview.....	253
10.2 Main Findings .....	254
10.2.1 Environmental/Climatic change in Vanuatu over the Holocene .....	254
10.2.2 Environmental/climatic change in the Southern Cook Islands over the Late Holocene .....	255
10.2.3 Modelling Prehistoric Polynesian Island Life .....	256
10.2.4 Hydroclimate change over key periods of human migration and colonisation 256	
10.2.5 Drought as a driver of migration.....	257
10.3 Recommendations for future research.....	258
10.4 Final Thoughts .....	260
<b>Appendix A Palaeo-precipitation records .....</b>	<b>263</b>
<b>Appendix B Archaeology data sources .....</b>	<b>265</b>
<b>Appendix C Calibration values for the isotope measurements.....</b>	<b>267</b>
<b>Appendix D Diatom pictures .....</b>	<b>269</b>
<b>Appendix E R code for model metrics .....</b>	<b>271</b>
<b>List of References .....</b>	<b>273</b>



## Table of Tables

Table 2.1: Different types of ENSO events, the region they affect and the associated impacts - taken from (Murphy et al, 2014). .....	23
Table 5.1: Overview of the XRF elements or ratios utilised within this thesis along with example references from tropical and sub-tropical lakes. Adapted from Davies et al, 2015. ....	78
Table 5.2: Summary of parameters used in tephra glass shard analysis .....	100
Table 6.1: <sup>14</sup> C dates from Emaotfer Swamp, Vanuatu. ....	102
Table 6.2: Breakdown of XRF zones for Emaotfer Swamp sequence and a description of major changes in elemental profiles. ....	108
Table 7.1: <sup>14</sup> C dates from Lake Tiriara, Mangaia. ....	134
Table 7.2: Breakdown of XRF zones for Lake Tiriara sequence and a description of major changes in elemental profiles. ....	142
Table 8.1: List of parameters, stocks and outputs used within the Mangaia socio-ecological model. ....	193
Table 8.2: The statistical and drought characteristics of the different rainfall scenarios .....	200
Table 8.3: Palaeo rainfall scenarios, the associated dinosterol iteration values .....	204
Table 8.4: Drought characteristics of the model scenarios .....	207
Table 10.1: Table of studies included in the map in the literature review that focus on hydroclimate in tropical South Pacific used in <b>Error! Reference source not found.</b> ....	263
Table 10.2: Archaeology figure sources used in Figure 9.4 – adapted and updated from Field and Lape (2010) .....	265
Table 10.3: MCS and CCS calibration standards for inorganic isotopes $\delta^{18}\text{O}$ and $\delta^{13}\text{C}$ .....	267
Table 10.4: BROCC3 calibration standards for organic isotopes $\delta^{13}\text{C}$ and $\delta^{15}\text{N}$ . ....	268
Table 10.5: Spirulina calibration standards for organic isotopes $\delta^{13}\text{C}$ and $\delta^{15}\text{N}$ . ....	268



## Table of Figures

Figure 2.1: Map identifying the timing of colonisation of different regions of the Pacific. Dotted black lines denote migration pauses. (Redrawn and adapted from map presented by Matisoo-Smith (2015). .....	9
Figure 2.2: Cycle of island life following migration into a new archipelago. ....	13
Figure 2.3: Map of average annual precipitation with the location of the ITCZ and SPCZ in relation to Vanuatu (yellow box) and the Southern Cook Islands (red box).....	22
Figure 2.4: Nov-April total rainfall (mm) for the South Pacific region. The lines represent SPCZ locations during different phases of IPO and SOI. Solid white line: -SOI/+IPO; dashed white line: -SOI/-IPO; solid black line: +SOI/-IPO; dashed black line: +SOI/+IPO. (Figure from Lorrey et al, 2012) .....	24
Figure 2.5: Map identifying the location of palaeo-records relating to precipitation. Colour denotes the type of record; Pink – Coral, Dark Blue - Marine, Purple – Saline Lakes, Light blue – Freshwater Lake, Orange- Stalagmite, Brown- Swamp. ....	26
Figure 2.6: Overview diagram of key palaeo records of hydroclimate change in the tropical pacific from 3400 yr BP to present. Yellow lines mark the start of the two waves of human migration. ....	28
Figure 2.7: Overview diagram of key palaeo records of hydroclimate change in the tropical pacific from 1200 yr BP to present. Orange box marks the duration of the MCA and the purple box marks the duration of the LIA. ....	34
Figure 2.8: Flow chart for developing a system dynamics model - taken from Ding et al (2018)	49
Figure 4.1 Images displaying the average rainfall/location of the SPCZ during A – the period 1971-2000, B – over El Niño years and C – over La Niña years. The yellow box denotes the location of Vanuatu, the white box denotes the location of the Southern Cook Islands .....	60
Figure 4.2: Map highlighting the location of: A - Vanuatu and the Cook Islands within the tropical South Pacific with the areas denoting the extent of Micronesia (purple), Melanesia (blue) and Polynesia (green) indicated. B –the island of Efate within Vanuatu. C –Mangaia within the Southern Cook Islands. ....	61

## Table of Figures

Figure 4.3: Average monthly precipitation and temperature for Vanuatu (BOM, 2020; WMO, 2020).....	62
Figure 4.4: Geological map of Efate (left) redrawn and simplified from Dickinson et al (2013) and Kinston et al (2014) and an elevation profile (right) produced from SRTM data available from USGS Earth Explorer. Yellow dot denotes location of Emaotfer Swamp.....	63
Figure 4.5: Inset map identifies the location of Emaotfer Swamp within Efate. Main figure shows Emaotfer Swamp site map identifying the Teouma River, ocean, housing and the Teouma archaeological site (yellow dot). ....	66
Figure 4.6: Annual precipitation (blue bars) and temperature (black line) in the Cook Islands (BOM, 2020).....	68
Figure 4.7: Geology (top) and elevation profile (bottom) for the island of Mangaia. Yellow dot denotes the location of Lake Tiriara.....	69
Figure 4.8: Simplified cross-section of Mangaia where the volcanic core is surrounded by upraised makatea escarpment. Top row is the Mangaian name for each land section and below the common name for each land section. Redrawn and adapted from Allen (1969) and Kirch (2017).....	70
Figure 4.9: Lake Tiriara site map identifying the Makatea plateau, swamp lowlands, pondfields and the 2016 coring location (red dot) for the sediments used in this report and the approximate location of the Chague-Goff et al (2016) core (yellow dot).....	73
Figure 5.1: Image showing different components of Itrax core scanner from Croudace et al (2006) .....	77
Figure 5.2: Diagram illustrating the connections between the different constraints of $\delta^{18}\text{O}_{\text{carb}}$ in lake sediments (from Leng and Marshall, 2004).....	83
Figure 5.3: Process to extract carbon dioxide from carbonate ready for analysis on a mass spectrometer.....	86
Figure 5.4: Diagram illustrating conceptual model for shifts in environmental proxies during wet (A) and dry (B) conditions in tropical lake systems. Adapted from Hassall (2017). ....	88

Figure 5.5: Fractionation pathways for $\delta^{13}\text{C}$ in and around the lake environment - from Cohen (2003).....	90
Figure 5.6: Plot of C/N ratio against $^{13}\text{C}$ and the relative position of different types of plant organic matter (adapted from Meyer, 2003). .....	92
Figure 5.7: Graph denoting the different processes affecting $^{15}\text{N}$ and $^{13}\text{C}$ and how they impact on the isotopic values (Finlay and Kendall, 2007). .....	93
Figure 5.8: Diagram showing the different pathways of $^{210}\text{Pb}$ into a depositional environment such as a lake (Taken from Dinsley, Gowing and Marriott (2019), original source Oldfield and Appleyby (1984). .....	96
Figure 6.1: Panels show different elements of the chemical fingerprint of tephra shards for the identified tephra layer at Emaotfer compared to known Kuwae deposits. ...	103
Figure 6.2: Age model generated by the Rbacon package for Emaotfer Swamp. This is the unweighted age model and colours denote the material used for each date. Green = Plant macrofossil, Blue = Bulk sediment and Brown = Peat. ....	104
Figure 6.3: Age model generated by the Rbacon package for Emaotfer Swamp. This is the weighted age model and colours denote the material used for each date. Green = Plant macrofossil, Blue = Bulk sediment and Brown = Peat. ....	105
Figure 6.4: Plots of the loss-on-ignition at 550 and 950 °C along with the magnetic susceptibility data for the Emaotfer core sequence. Red line denotes the start of the first wave of human migration into Remote Oceania. Blue line is loess smoothed. ....	106
Figure 6.5: Plots of XRF geochemistry data for the Emaotfer core sequence. Grey zones relate to the XRF zones described in Table 6.2. Red line denotes the start of the first wave of human migration into Remote Oceania. Blue line is loess smoothed. ....	109
Figure 6.6: Plots showing the relationship between Sr, Ti and Ca in the Emaotfer core sequence. ....	110
Figure 6.7: Principal component analysis for the Emaotfer Swamp sequence with data point colour denoting the zones laid out in the XRF section. ....	111
Figure 6.8: Pearson correlation values between each XRF element for the Emaotfer Swamp sediments. Where boxes are crossed out it denotes that the p-value for that correlation was higher than 0.05.....	112

## Table of Figures

Figure 6.9: Scatterplot showing the relationship between TOC and LOI <sub>550</sub> for Emaotfer Swamp. .....	114
Figure 6.10: TOC, TN, $\delta^{13}\text{C}$ (‰ VPDB), $\delta^{15}\text{N}$ (‰ Air) and C/N for Emaotfer Swamp. Red line denotes the start of the first wave of human migration into Remote Oceania. Blue line is loess smoothed. ....	115
Figure 6.11: Plot showing the C/N and $\delta^{13}\text{C}$ (‰ VPDB) data for Emaotfer Swamp and how it relates to typical algae, C <sub>3</sub> and C <sub>4</sub> plant values. Colours denote the zone.....	117
Figure 6.12: Plot showing the Ca/inc, CO <sub>2</sub> yield data, $\delta^{13}\text{C}_{\text{inorganic}}$ (‰ VPDB) and $\delta^{18}\text{O}$ (‰ VPDB) for the Emaotfer Swamp core sequence. Red line denotes the start of the first wave of human migration into Remote Oceania. Blue line is loess smoothed. ....	119
Figure 6.13: Plot showing the relationship between inorganic $\delta^{13}\text{C}$ (‰ VPDB) and $\delta^{18}\text{O}$ (‰ VPDB) from Emaotfer Swamp with a line of best fit and displaying the r-squared value. .....	120
Figure 7.1: Plot of Po-210 activity going down through the Lake Tiriara core top sequence. ...	135
Figure 7.2: Plot of the linear regression of the natural logarithm of the Po-210 data from 66-100 cm down through Lake Tiriara core sequence with the linear regression equation and r-squared value reported. ....	136
Figure 7.3: Age model generated by the Rbacon package for Lake Tiriara. This is an unweighted age model and colours denote the material used for each date. Green = Plant macrofossil and Blue = Bulk sediment. ....	137
Figure 7.4: Plots showing the LOI <sub>550</sub> , LOI <sub>950</sub> and magnetic susceptibility data for the Mangaia sequence. ....	139
Figure 7.5: Plots showing the XRF geochemistry data for the Mangaia sequence. Red line denotes the start of the second wave of human migration into eastern Polynesia...	141
Figure 7.6: Plots showing the relationship between Sr, and Ti against Ca in the Tiriara core sequence. ....	143
Figure 7.7: Principal component analysis plot for PCA 1 and PCA2 of the Mangaian sediments.	144
Figure 7.8: Correlation matrix for the selected $\mu\text{XRF}$ elements for Lake Tiriara. Crosses denote correlations that are not statistically significant. The coloured boxes are visually	

illustrating the strength of the correlation using the scale to the right of the plot. .....	145
Figure 7.9: Plots showing the C/N, $\delta^{13}\text{C}_{\text{org}}$ (‰ VPDB), $\delta^{15}\text{N}$ (‰ Air), TN and TOC data from the Mangaia sequence.....	147
Figure 7.10: Plot showing the C/N against the $\delta^{13}\text{C}$ (‰ VPDB) values for each zone of the Mangaia sequence. Boxes denote typical values for lacustrine algae (purple box), $\text{C}_3$ (green box) and $\text{C}_4$ plants (yellow box).....	149
Figure 7.11: Plot showing the $^2\text{H}$ and $^{18}\text{O}$ for rain events in the tropical Pacific, freshwater lakes taken from Maloney <i>et al</i> (2019) and Lake Tiriara. ....	150
Figure 7.12: Plots showing the inorganic $\delta^{13}\text{C}$ (‰ VPBD), $\delta^{18}\text{O}$ (‰ VPBD), Ca/inc XRF and $\text{CO}_2$ yield data from the Mangaia sequence. Blue line is loess smoothed. ....	153
Figure 7.13: Plot showing the relationship between inorganic $\delta^{13}\text{C}$ (‰ VPBD) and $\delta^{18}\text{O}$ (‰ VPBD) from Lake Tiriara, Mangaia with a line of best fit and displaying the r-squared value. ....	154
Figure 7.14: Stratigraphic plot for the relative abundance of diatom types from Lake Tiriara.	156
Figure 7.15: Charcoal count data from the Lake Tiriara sequence plotted against the age model presented in section 7.2.3. - data from Temple-Brown (2018). ....	162
Figure 7.16: Plot showing the Ti/inc XRF data from Lake Teroto (Sear et al, 2020) (top) and Lake Tiriara (this thesis) over the past 2,500 years. Blue line is loess smoothed..	174
Figure 7.17: Plot of wet season (Nov-Apr) rainfall data from Rarotonga and Mangaia with linear regression value – data from KNMI climate explorer (2023). ....	175
Figure 7.18: Changes in the lake area between 2005 and 2019 for both Lake Tiriara and Lake Teroto calculated using satellite images in google earth. ....	176
Figure 8.1: Conceptual model of the Mangaia socio-ecological system split into external environmental, internal social and the socio-environmental interface. ....	189
Figure 8.2: “Tradeoffs in model building between generality, precision and realism.” Taken from Troy et al 2015 .....	191
Figure 8.3: Conceptual model of the Mangaia socio-ecological system split into external environmental, internal social and the socio-environmental interface. This	

## Table of Figures

version denotes the components that were selected as part of the final socio-ecological model.....	192
Figure 8.4: Visualisation of the Vensim model structure .....	195
Figure 8.5: Graph identifying how the metrics of impact and recovery are measured. Red lines denote drought events. Taken from Kuil et al 2019. ....	201
Figure 8.6: The quantitative precipitation reconstruction covering the past 2,000 years from Lake Lanoto'o in Samoa - taken from Sear et al (2020) with a loess smoother running through the points giving the running mean precipitation value. The red area denotes the minimum and maximum error associated with the dinosterol reconstruction. ....	203
Figure 8.7: Sensitivity test outputs for A - crop calorie availability, B - maximum population growth and C - Labour required plotted against the baseline of food availability output from Scenario 6.1. ....	206
Figure 8.8: Outputs from the system dynamics Vensim model for Mangaia. The outputs are broken down into the four scenarios run as per Table 8.2. Within each panel the colours represent the 10 iterations of each scenario. ....	209
Figure 8.9: Graph showing the outputs from the drought and population metrics produced for the rainfall data for scenarios 3 and 4.....	211
Figure 8.10: Model outputs for the 1000-year palaeo scenario showing the agricultural carrying capacity, population and rainfall outputs .....	214
Figure 8.11: Model outputs for the 2000-year palaeo scenario showing the agricultural carrying capacity, population and rainfall outputs. ....	216
Figure 8.12: Graph showing the outputs from the drought and population metrics produced for the 2000-year palaeo scenario.....	218
Figure 8.13: Graph showing the outputs from the drought and population metrics produced for the 1000-year palaeo scenario.....	218
Figure 8.14: Model output from Kohala model showing population change over time taken from Kirch et al (2012). ....	221
Figure 8.15: Total food availability model output from the model scenario 4. ....	222

- Figure 8.16: Total food availability model output from the palaeo scenarios. Red box highlights a period of conflict in Mangaian history and the green box highlights a period where food production improved as per Kirch (2017). Grey lines denote the breaks between different periods of Mangaian history with the name of each period labelled as per Kirch (2017).....222
- Figure 9.1: Comparison between palaeo records from Australia, Melanesia and Polynesia. A – Emaotfer Swamp  $\delta^{18}\text{O}$  (‰ VPBD) record from Efate, Vanuatu (this thesis), B –  $\delta^2\text{H-C}_{26}$  (‰ VSMOW) biomarker record from Lake Lanoto’o, Samoa (Hassall, 2017), C – Ti/inc record from Lake Lanoto’o, Samoa (Hassall, 2017), D –  $\delta^2\text{H-C}_{26}$  (‰ VSMOW) biomarker record from Lake Teroto, Atiu, Cook Islands (Hassall, 2017), E – Annual Mean Precipitation (mm/year) derived from carbon isotope ratios from Eastern Australia (Barr et al, 2019) and F - Botryococcene (‰) from Lake Junco – Galapagos (Zhang et al, 2014). Blue box denotes the wet event identified in the Emaotfer Swamp record, red box denotes dry period identified in Emaotfer Swamp record and purple boxes denote the start of the two periods of human migration in the tropical Pacific. ....232
- Figure 9.2: Comparison between palaeo records from Melanesia and Western Polynesia over the past 3,000 years. A –Emaotfer Swamp  $\delta^{18}\text{O}$  record from Efate, Vanuatu (this thesis), B – Diatom record from Emaotfer Swamp, Vanuatu (Wirrmann et al, 2011), C - Ostracod record from Emaotfer Swamp, Vanuatu (Wirrmann et al, 2011), D -  $\delta^2\text{H-dinosterol}$  (‰ VSMOW) biomarker record from Lake Emaotul, Vanuatu (Maloney et al, 2022). E -  $\delta^2\text{H-dinosterol}$  (‰ VSMOW) biomarker record from Lake Lanoto’o, Samoa (Maloney et al, 2022), F –  $\delta^2\text{H-dinosterol}$  (‰ VSMOW) biomarker record from Lac Lanutavake, Wallis (Maloney et al, 2022). Purple boxes denote the start of two waves of human migration, the red box denotes start of dry period, the blue box denotes start of wetter condition.235
- Figure 9.3: Comparison between palaeo records from Polynesia. A - Lake Tiriara  $\delta^{18}\text{O}$  record from Mangaia, Southern Cook Islands (this thesis), B –  $\delta^2\text{H}$  Dinosterol (‰ VSMOW) record from Lake Teroto - Atiu, Southern Cook Islands (Sear et al, 2020), C – Ti/Ca record from Apu Bay, Society Islands (Toomey et al, 2016), D –  $\delta^2\text{H}$  Dinosterol (‰ VSMOW) record from Lake Lanoto’o – Upolu, Samoa (Sear et al, 2020) and E – Botryococcene (‰) from Lake Junco – Galapagos Zhang et al, 2014) .The red and blue rectangles denote the MCA and LIA periods respectively. The purple lines represent the timing of the two waves of human

Table of Figures

migration in the tropical South Pacific. Yellow denotes the tsunami layer event timing from the Mangaia sequence. .... 236

Figure 9.4: Main features of the archaeological records of major archipelagos of the tropical South Pacific. Information taken from sources listed in appendix B – redrawn and adapted from Goff and Nunn (2016). Red boxes denote drier hydroclimate conditions as suggested by the Emaotfer and Mangaia sediment sequences. 249

## Research Thesis: Declaration of Authorship

Print name: CHARLOTTE VICTORIA HIPKISS

Title of thesis: Stress in paradise: Reconstructing Late Holocene hydroclimate to investigate the role of drought in the timing of human migration and colonisation in the tropical South Pacific

I declare that this thesis and the work presented in it are my own and has been generated by me as the result of my own original research.

I confirm that:

1. This work was done wholly or mainly while in candidature for a research degree at this University;
2. Where any part of this thesis has previously been submitted for a degree or any other qualification at this University or any other institution, this has been clearly stated;
3. Where I have consulted the published work of others, this is always clearly attributed;
4. Where I have quoted from the work of others, the source is always given. With the exception of such quotations, this thesis is entirely my own work;
5. I have acknowledged all main sources of help;
6. Where the thesis is based on work done by myself jointly with others, I have made clear exactly what was done by others and what I have contributed myself;
7. None of this work has been published before submission

Signature: ..... Date: .....



## COVID-19 Impact Statement

A vast majority of the research presented in this thesis was conducted during the COVID-19 pandemic and the subsequent year(s) when a new way of working was unfolding. The pandemic began early in the second year of my PhD studies and has had an effect on most aspects of the work presented in this thesis. Due to the impact of the pandemic, a number of significant changes were made to the focus and course of the thesis to ensure successful completion. The work presented in this thesis is therefore the product of modified scheme of research and the use of already available core material. Originally, the main analytical chapters would have required field work in the Pacific region in the summer of 2020, which due to the pandemic, became impossible to execute. Instead, I made use of core material that had been collected by my supervisors on past visits to the Pacific, which limited the scope of my thesis to what was already available. Also, this thesis depended on access to a number of laboratory facilities for sediment analysis that due to the pandemic were closed for a number of months delaying the onset of main data collection due to delay in pilot study results and compressing the timeline for the completion of subsequent analysis and interpretation. The final analytical chapter that presents the socio-ecological model was originally supposed to be a third palaeo chapter providing a cross-section of change across the South Pacific region. Every effort was made to reduce the impact of the pandemic on this thesis. However, the COVID-19 pandemic was an unprecedented event and it was not possible to mitigate all of the impacts that effected this thesis.

## Acknowledgements

Firstly, I would like to thank my supervisors David Sear, Pete Langdon and Justin Sheffield for their guidance and advice throughout my PhD. Particularly David as my lead supervisor who kept us all going through the covid-19 pandemic by chatting about gardening, baking and a bit of work.

I'd like to thank my friend and PhD companion, Nichola Strandberg who has been with me through this PhD journey since day one and has been supportive, always offered help, posted samples to me on multiple occasions and was willing to look at my data whenever I asked.

Thank you to my friends from the PhD hub, Nathaniel, Becca, Sofia, Marjorie, Georgina, Luke, Martin, Rebecca, Winfred and everyone else. Thanks also to my officemates, Molly, Beth, Chloe and Gustavo who put up with me and listened to me rant and rave about things that just weren't quite working.

I'd like to thank Dr Ben Pears, Dr Ali Monteath and Dr Thierry Fonville for their advice and guidance on palaeo methods over the years. I would also like to thank the lab manager Peter Morgan and lab technicians James Fielding, Kamil Zahorski, Luke Everett for their assistance through my time at Southampton. Thanks to Professor Mel Leng & Dr Jack Lacey for hosting me at BGS to complete vital lab work and assistance with/feedback on the data. Thanks to Dr Tom Bishop of the University of Manchester for his advice around ITRAX data and data analysis. Thanks to Dr Shane Cronin for running the tephra sample for the EMB sequence. Thanks also to Dr Philippa Ascough of SUERC for her feedback on NEIF grant proposal and further assistance with dating strategy for the palaeo sequences. Also, the radiocarbon small samples required the expertise of Dr Xiaomei Xu at the Keck Carbon Cycle AMS Facility, University of California, Irvine, USA. Thanks to Dr Pawel Gaca of GAU-Radioanalytical at NOCS for hosting me to prepare Po-210 samples at NOCs and running the samples for us when our chemistry lab was down.

This work was supported by the Natural Environment Research Council [grant number NE/L002531/1]. Support for isotope and radiocarbon data collection was provided by NEIF under grant NE/S011587/1 (allocation number 2356.0321).

Finally, I'd like to thank my family – Jack, Ellie, Ron, Gary, Emily and my grandparents but particularly my Mum, who was always there to pick me up when I was down and never doubted that I could do this.

## Definitions and Abbreviations

<sup>137</sup> Cs	Caesium-137 (radioisotope)
<sup>13</sup> C	Carbon-13 (stable isotope)
<sup>13</sup> C <sub>inorg</sub>	Inorganic Carbon-13 (stable isotope)
<sup>13</sup> C <sub>org</sub>	Organic Carbon-13 (stable isotope)
<sup>15</sup> N	Nitrogen-15 (stable isotope)
<sup>18</sup> O	Oxygen-18 (stable isotope)
<sup>210</sup> Pb	Hydrogen-2/Deuterium (stable isotope)
<sup>210</sup> Pb	Lead-210 (radioisotope)
<sup>210</sup> Po	Polonium-210 (radioisotope)
ABM	Agent-based model
AD	Anno Domini
AMS	Accelerated Mass Spectrometry
BN	Bayesian network
C/N	Carbon-nitrogen ratio
Ca.	Circa
Cal yr BP	Calibrated radiocarbon years before present (1950 AD)
CCM	Coupled-component model
ENSO	El Niño Southern Oscillation
ITCZ	Intertropical Convergence Zone
KBM	Knowledge-based model
LIA	Little Ice Age
LOI	Loss-on-ignition
LOI <sub>550</sub>	Loss-on-ignition at 550 °C
LOI <sub>950</sub>	Loss-on-ignition at 950 °C
masl	Metres above sea level
Mag sus	Magnetic susceptibility

## Definitions and Abbreviations

MCA .....	Mediaeval Climate Anomaly – synonymous with MWP
MWP .....	Mediaeval Warm Period – synonymous with MCA
PCA.....	Principal component analysis
$r^2$ .....	Linear regression
SD.....	System dynamics
SOI.....	Southern Oscillation Index
SPCZ .....	South Pacific Convergence Zone
SSS.....	Sea Surface Salinity
SST .....	Sea Surface Temperature
TDIC.....	Total dissolved inorganic carbon
TN.....	Total Nitrogen
TOC .....	Total organic carbon
VPDB .....	Vienna Pee Dee Belemnite
VSMOW2 .....	Vienna Standard Mean Ocean Water 2
XRF .....	X-Ray Fluorescence
yr BP.....	Radiocarbon years before present (1950 AD)
$\delta$ .....	Delta
$\mu$ XRF .....	Micro X-Ray Fluorescence

## Chapter 1 Introduction

The Pacific Ocean is a vast region that covers a surface area that is greater in size than the total land surface area of the planet (NOAA, 2022). It is home to over 30,000 islands and nearly all of them are in the South Pacific Ocean (United Nations, 1983; Burns, 2001). There are 15 island nations in the Pacific Ocean including New Zealand, 1 US state and 32 non-sovereign territories that include islands such as American Samoa, Easter Island, French Polynesia and New Caledonia (United Nations, 2022). These islands represent the last region on earth to be colonised by humans and today they are home to approximately 12.3 million people (Kirch, 1997; Secretariat of the Pacific Community, 2020). The Pacific islands are split into three geographical and cultural groups called Melanesia, Micronesia and Polynesia (Secretariat of the Pacific Community, 2011) – illustrated in figure 2.1. in chapter 2. The culture of Pacific islanders is intrinsically tied to the natural environment (Duncan, 2011), which stems from traditional practices that have been present on the islands for thousands of years that have allowed these island communities to survive as conditions changed through time both climatically and environmentally (United Nations, 2012). Pacific islanders are economically and culturally heavily reliant upon the natural resources of the islands they live on (Duncan, 2011), but are both space and resource limited, dependent upon rainfall for their food and water security (Secretariat of the Pacific Community, 2011; Dixon-Jain *et al.*, 2014).

### 1.1 Pacific Climate

Whilst Pacific climate is characterised by high levels of rainfall that in some parts can exceed five metres annually, South Pacific islands are also the location of some of the most severe water shortage problems on the globe (White *et al.*, 2007). The seasons in the tropical Pacific are characterised by rainfall – with wet and dry seasons - rather than temperature, which remains relatively constant year-round. Rainfall in the tropical South Pacific is primarily controlled by the South Pacific convergence zone (SPCZ), an offshoot of the Intertropical Convergence Zone (ITCZ). The SPCZ is a convective band of rain clouds that stretches from Papua New Guinea, thousands of kilometres southeast to French Polynesia (Brown *et al.*, 2020). Climate in the Pacific is also regulated by a number of modes of climate variability such as El Niño Southern Oscillation (ENSO) and the inter-decadal Pacific

oscillation (IPO) that affect sea surface temperature and atmospheric pressure which in turn impacts upon wind and air temperatures (McGree et al, 2016). These climatic oscillations also influence the location, extent and intensity of the SPCZ (Lorrey *et al.*, 2012; Haffke and Magnúsdóttir, 2013; Brown *et al.*, 2020). Thus, drought is a prominent feature in Pacific climate, particularly during ENSO events, which are strongly related to precipitation anomalies (McGree et al, 2016). Due to climate change, annual rainfall is projected to rise in the equatorial Pacific but drop in the region to the east of French Polynesia (Dixon-Jain *et al.*, 2014). However, models produce a large range of projected change in precipitation so there is considerable uncertainty as to the magnitude and extent of projected change (IPCC, 2022).

In the tropical South Pacific, precipitation is vitally important for the food and water security of the 12.3 million Pacific islanders who depend on reliable precipitation for survival (Dixon-Jain *et al.*, 2014; Secretariat of the Pacific Community, 2020). This will have been the case historically, with growing evidence that climate - specifically drought, may have influenced the decisions of early humans to migrate east across the Pacific (Anderson, 2002; Goodwin, Browning and Anderson, 2014; Nunn and Kumar, 2018; Sear *et al.*, 2020). Palaeo records also suggest that shifts in precipitation were larger and longer than observed in the instrumental record (McGree et al, 2016). Thus, it is important to utilise palaeoclimatic records so that we are able to place modern day changes and future scenarios within a longer-term context and understand the full range of climatic variability exhibited in that region and to understand the climatic context of Pacific human history.

## 1.2 Pacific Palaeoclimate

The Pacific covers almost a third of the planet (NOAA, 2022) and yet it is a region we know relatively little about in terms of climate variability on sub-decadal to millennial timescales despite the region's importance in influencing global climate (Brown *et al.*, 2020). At the sub-decadal level we still struggle with resolving El Niño events and at the millennial scale level, we know even less, given most palaeo records in this region come from either corals – that are high resolution but cover very short timescales - or marine sediments which focus only on the million year plus scale due to relatively low sedimentation rates (e.g. Gorman *et al.*, 2012; Mamo et al, 2013). Hence, there is a major gap in our understanding of Holocene climate change in this region. Promising archives of longer-term palaeoclimate

can be found in sedimentary archives that have accumulated at relatively high rates throughout the Holocene. These archives include lakes and swamps. Lake sediments potentially offer continuous long-term records going back millennia. Recent evidence from lake sediment archives in the Pacific has demonstrated the potential to provide long (c.7000+ yr records Sear et al., 2020; Gosling *et al.*, 2020) and higher resolution (50-150 yr resolution, Sear et al., 2020; Atwood et al., 2014) hydroclimate records from the Pacific islands. However, in the South Pacific islands, lake sediment archives are relatively scarce, becoming less abundant moving eastward across the Pacific. For example, in the Southern Cook Islands, lakes are only present due to tectonic uplift that created their biogenic limestone known locally as makatea. These escarpments made of ancient coral that surrounds the island and traps runoff from the volcanic core to form swamps and lakes at the interior side of the makatea (Wood, 1978; Stoddart, Woodroffe and Spencer, 1990; Ellison, 1994; Parkes, 1994).

As well as obstacles with resolution and availability of records, there is also the challenge of irregular temporal coverage in the palaeo record from the Pacific. The palaeoenvironmental records from this region are typically biased towards the past 1-2,000 years, which includes the so-called 'Common Era'. This temporal bias is likely due to a combination of a relative paucity of suitable palaeoenvironmental archives and research interests surrounding the two climatic shifts called the Medieval Climate Anomaly and the Little Ice Age along with the second wave of migration into eastern Polynesia, all of which fall within the past 2,000 years. However, human history in this region dates back beyond 2000 yr BP. Further palaeoenvironmental work needs to be conducted within the tropical Pacific to refine our understanding of climatic change in this region during the Holocene but particularly over the past 3,000 years which also covers the period when humans started to colonise the western Pacific islands but also beyond.

The impact of climate on ancient civilisations has been widely studied in other regions and examples extend across the globe. For example, it has been suggested that drought played a role in the fall of the Maya civilisation in Central America (Kuil *et al.*, 2016), collapse of Mediterranean societies during the Bronze Age (Kaniewski et al, 2015) and impacted Native American cultures between 11th and 13th centuries (Benson *et al.*, 2007). However, climate-human interactions have yet to be properly resolved in the Pacific region. Current climate models (e.g. CMIP5/6 GCM's) do not represent SPCZ dynamics accurately and its

behaviour over longer timescales is uncertain (IPCC, 2022). Hence, new records are required to address the lack of understanding of long-term hydroclimate variability, which has hampered efforts to test the climate hypothesis as a driver of migration and settlement in the South Pacific.

### **1.3 Human Migration and Colonisation of the Pacific**

The Pacific region represents the final frontier of human colonisation of the planet. People started to move into remote Oceania approximately 3000 yr BP, moving through the Solomon Islands, Vanuatu, New Caledonia, Fiji and Tonga before finally stopping once reaching Samoa. Following a long pause of around 2000 years (Sear *et al.*, 2020; Ioannidis *et al.*, 2021), humans started a second wave of migration that started in the Cook Islands and reached out to the three corners of the Polynesian triangle of Hawaii, Easter Island and New Zealand (Ioannidis *et al.*, 2021). The two sites in Vanuatu and the Southern Cook Islands are located in pivotal archaeological locations as they both represent some of the first islands colonised by humans in the first and second waves of migration respectively (Bedford *et al.*, 2006; Kirch, 2017b). The southern Cook Islands in particular are recognised as gateway islands for migration into Eastern Polynesia (Allen and Wallace, 2007) granting the opportunity to study the connections between hydroclimate change and human dispersal and activity in the Pacific during both major migration phases.

Different ideas have been put forward as potential drivers of human colonisation of the Pacific such as development of navigational skills and canoe technology, culture and changing climate (Cochrane, 2018; Irwin *et al.*, 2022). It has been suggested that the climate – specifically drought - may have put pressure on the resources of certain islands, particularly as populations grew, and that this may have forced the Polynesians to migrate eastwards (Anderson, 2002; Goodwin, Browning and Anderson, 2014; Nunn and Kumar, 2018; Sear *et al.*, 2020). This drought hypothesis draws on evidence from palaeoenvironmental and archaeological studies from across the Pacific and seeks to understand whether drought played a role in the timing of migration and subsequent colonisation. Research conducted in the tropical South Pacific has alluded to drought being a potential driver in migration and social change (Nunn, 2000a; Nunn and Britton, 2001; Allen, 2006; Anderson, Chappell, *et al.*, 2006; Field and Lape, 2010; Goodwin, Browning and Anderson, 2014; Goff and Nunn, 2016; Sear *et al.*, 2020). The Pacific region is a relatively

under-studied region in terms of environmental change so the development of new palaeoenvironmental records is important to be able to place the corpus of archaeological knowledge of the Pacific into an environmental and climatic context.

#### **1.4 The focus of this study**

The purpose of this study is to reconstruct climate over the past 3,000 years with the aim to tie together climate and archaeological records to understand whether climate, but specifically drought, played a role in the timing of human migration and subsequent colonisation of islands in the tropical South Pacific. To do this, this study will present two new palaeoenvironmental records from Emaotfer Swamp in Vanuatu and Lake Tiriara in the Cook Islands, which represent key archaeological locations in relation to the two waves of human migration into the Pacific. These records will utilise a multi-proxy approach that includes  $\mu$ XRF, sedimentology, organic and inorganic stable isotopes ( $\delta^{13}\text{C}$  and  $\delta^{15}\text{N}$  from organic matter as well as  $\delta^{18}\text{O}$  and  $\delta^{13}\text{C}$  from carbonate) and diatoms to build new hydroclimate records in the tropical South Pacific over key periods in Pacific human history. To follow on from the palaeo work, to tangibly connect together climatic change and its impact on island life, this study will also develop and utilise a system dynamics model to examine the connection between changing precipitation, agriculture and population dynamics in a prehistoric Polynesian socio-ecological system. The model will use a combination of experimental and reconstructed palaeo-rainfall datasets to assess how climate change over the late Holocene affected the case study island of Mangaia located within the Cook Islands.

#### **1.5 Thesis Structure**

In chapter 2, the existing literature surrounding this thesis is reviewed and knowledge gaps are identified. Following on from this, chapter 3 lays out the aims and objectives of this thesis. Chapter 4 covers the regional setting and site descriptions for Emaotfer Swamp in Vanuatu and Lake Tiriara in the Cook Islands. Chapter 5 presents and describes the methods utilised to generate a chronology and palaeoenvironmental records for the core sequences from both sites. In chapters 6 and 7 the results for the core sequence from Emaotfer Swamp and Lake Tiriara respectively, are discussed and an interpretation of the records from both sites is offered. Following this, in chapter 8, the model building and the results from

## Chapter 1

modelling experiments are presented and discussed, exploring the potential impact of climate on prehistoric Polynesian island life during the late Holocene. Chapter 9 offers a discussion of the main themes of the thesis including palaeoenvironmental change in the tropical South Pacific during the late Holocene and the reconstruction of hydroclimate around the time of the two waves of human migration amongst the Pacific Islands. The chapter considers a range of evidence to evaluate whether drought in particular may have acted as a driver in those waves of human migration and societal change in prehistoric Polynesian island life. Finally, chapter 10 presents the overall conclusions and main findings of this thesis along with recommendations for future research.

## Chapter 2 Literature Review

### 2.1 Introduction

To address the aims of the thesis, a review of the key literature is needed to present our current understanding of key topics and highlight any gaps in our current knowledge. This chapter begins by introducing the timeline of human colonisation of the Pacific providing a chronological timeline that has structured different aspects of this thesis. The next section of this review covers environment/climate-human interactions including a range of aspects of island life including diet, voyaging and conflict to demonstrate the evident connections between island life and Pacific climate. The second half of this chapter moves onto our understanding of South Pacific climate and precipitation both today through instrumental and satellite data and in the past through palaeoenvironmental records. The palaeoenvironmental records are framed around the chronology of the two waves of human migration. The review then moves onto looking at modelling of prehistoric societies and the range of approaches available. This chapter concludes with a brief summary of the key messages from all the different aspects of the literature covered.

### 2.2 Human Colonisation of the Pacific

There has been debate throughout the years about the origin of Pacific Islanders and the timing of their arrival into remote Oceania and Eastern Polynesia. Famously, in 1947, the Norwegian Thor Heyerdahl sailed a replica Polynesian raft from South America to French Polynesia in an attempt to prove that Polynesians could have been descended from South American rather than Asian origins (Heyerdahl, 1950). This theory was subsequently disproven with evidence from linguistics (Pawley, 2007), archaeology (Kirch, 2017a) and later genetics (Ioannidis *et al.*, 2021). It is now widely accepted that humans migrated down through South East Asia approximately 45,000 yr BP and moved through Papua New Guinea and into the Solomon Islands (O'Connor and Hiscock, 2014; Kirch, 2017a). This was possibly facilitated by lower sea levels and the existence of land bridges allowing humans to travel across this landscape (Irwin, 1992; O'Connor and Hiscock, 2014; Kirch, 2017a). The history of human colonisation of the Pacific is a story of three parts; the first

## Chapter 2

Lapita migration into remote Oceania, the c.2000 year “long pause” and the second wave of migration into Eastern Polynesia (adapted from Goff et al., 2012).

The first wave of migration into remote Oceania occurred c.3000 yr BP by the Lapita civilisation – see Figure 2.1. During this phase, humans sailed eastward across Melanesia moving through the Solomon Islands, down the Santa Cruz islands and onto the Vanuatu archipelago. It has been suggested that the initial move into remote Oceania and the revelation of new unclaimed resources and land may have provided the motivation for rapid human expansion across Melanesia (Bedford and Spriggs, 2014). The first arrival of humans into Vanuatu is dated to 3100-2900 BP on Aore Island with other islands in the archipelago following soon after at around 3000 yr BP for Malakula, Efate and Erromango (Bedford and Spriggs, 2014). Dates from New Caledonia match closely to those from Vanuatu with Lapita colonisation of these islands also being dated to around 3000 cal yr BP (Cochrane, 2018). From New Caledonia, moving eastward, human arrival in Fiji required a significant ocean voyage, navigating a jump of 850 km whilst fighting against the currents and westward blowing winds (Irwin, 1992; Kirch, 2017a). Based on a review of radiocarbon dates from across multiple islands, people first arrived into Viti Levu approximately 3050-2950 cal BP and this is currently the earliest known evidence for Lapita colonisation in Fiji (Clark and Anderson, 2009a). Human arrival in Tonga is dated to  $2838 \pm 8$  cal BP using U/Th dating on artefacts from the earliest known settlement located on the island of Tongatapu and this also represents human arrival into Polynesia (Burley *et al.*, 2015). For Samoa, the earliest dates for human arrival are around 2900 to 2700 cal BP which come from archaeological findings at Ferry Berth on the island of Upolu (Gosling *et al.*, 2020). This first wave of migration into remote Oceania is considered a rapid phase of movement across Melanesia that is described as a “radiocarbon instant” (Bedford and Spriggs, 2014; Kirch, 2017a) where it is typically not possible to differentiate which sites came first within standard error between any of the islands colonised in this first wave.

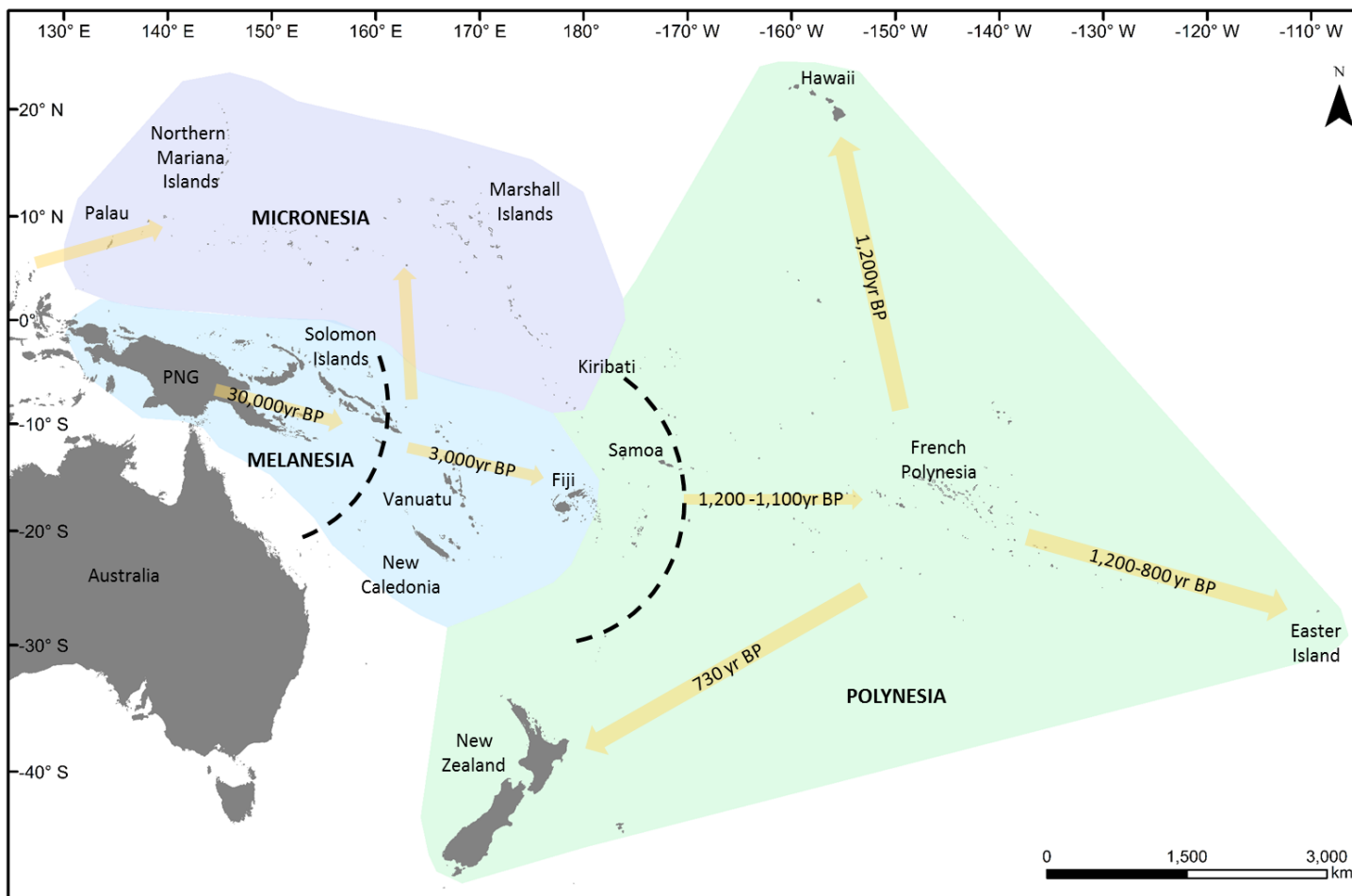


Figure 2.1: Map identifying the timing of colonisation of different regions of the Pacific. Dotted black lines denote migration pauses. (Redrawn and adapted from map presented by Matisoo-Smith (2015).

Following this first wave, there was a break in eastward migration and humans did not voyage any further into Polynesia for approximately 2000 years; this gap in migration was dubbed the “long pause” (Kirch, 2017a). There has been debate on the cause of this long pause, with some citing climate (Dickinson, 2003) or a delay in development of navigation and maritime technology (Anderson, Chappell, *et al.*, 2006). Some have suggested that the long pause is just indicative of how difficult it was to traverse the vast gap between west and east Polynesia (Anderson, Chappell, *et al.*, 2006; Hunt and Lipo, 2017). Others have suggested that palaeotsunamis could have been the cause of this long pause due to the impact tsunamis would have had on the primarily coastal-based populations through loss of knowledge (due to casualties) and resources that enable long-distance voyaging (Goff, McFadgen, *et al.*, 2012). Another explanation that is proffered is the duration of the hydro-isostatic mid-Holocene high stand that left sites that would typically be targeted for colonisation, uninhabitable as they were submerged by the ocean at this time (Dickinson, 2003). Further to this, there is also debate surrounding the length of the long pause which primarily revolved around the earliest dates for settlement in the Cook Islands, which are considered the “gateway islands” into Eastern Polynesia during the 2<sup>nd</sup> wave of human colonisation (Allen and Wallace, 2007). According to a review of radiocarbon dates from across eastern Polynesia by Wilmshurst (Wilmshurst *et al.*, 2011) and archaeological studies from the oldest sites in the Southern Cook Islands (Allen and Wallace, 2007), human arrival could have occurred as late as 700 yr BP or 1250 AD. Yet, palaeoenvironmental studies from the Southern Cook Islands contradict this timeline and dated human arrival to as far back as 2500 yr BP (Ellison, 1994; Chagué-Goff *et al.*, 2016) suggesting a gap of around 500 years between migration waves. However, Anderson (1995) drew these dates of colonisation into question and his scepticism proved to be justified as more recent archaeological and palaeoenvironmental work has refined these chronologies. It is now widely agreed that the break between migration waves was somewhere between these two timeframes. An early date for colonisation of the Cook Islands - and thus the timing of the 2<sup>nd</sup> migration wave into eastern Polynesia - set at 900-1100 AD or 1050 – 850 yr BP (Kirch, 2017b; Sear *et al.*, 2020; Ioannidis *et al.*, 2021) setting the gap between the 1<sup>st</sup> and 2<sup>nd</sup> wave of migration at around 2000 years.

The earliest evidence for Humans arrival in French Polynesia is derived from a coastal settlement on Mo’orea dated at 950-550 yr BP (Kahn and Sinoto, 2017). Whilst a new

chronology for Vaito'otia-Fa'ahia has provided a date of human colonisation for Huahine at around 900-790 yr BP (Anderson *et al.*, 2019). Genetic evidence put arrival at around 900 yr BP (Ioannidis *et al.*, 2021). Evidence from a number of sites across French Polynesia, including the Marquesas and Gambier Archipelagos suggest that humans had discovered these islands as early as 1100-1000 yr BP (Kirch *et al.*, 2010; Allen, 2014; Conte and Molle, 2014). However, actual colonisation of the more eastward and southern archipelagos such as the Marquesas, Bass and Gambier Islands occurred later around 750 yr BP (Kennett *et al.*, 2006; Kirch *et al.*, 2010; Allen, 2014; Ioannidis *et al.*, 2021). The remainder of the Polynesian triangle was colonised within a few hundred years and concluded with human arrival in Easter Island by around 750 yr BP (Hunt and Lipo, 2006, 2008), Hawaii by 730-689 yr BP (Rieth *et al.*, 2011) and New Zealand by 670 yr BP (Wilmshurst *et al.*, 2008; Ioannidis *et al.*, 2021). It is estimated that by 650 yr BP (1300 AD) humans had essentially colonised all the islands in the tropical South Pacific region (Wilmshurst *et al.*, 2011; Ioannidis *et al.*, 2021). This was undoubtedly an impressive feat in global human history as it involved early Pacific peoples navigating thousands of kilometres of open ocean in an outrigger style canoe. Travelling against prevailing winds and currents to find small pockets of viable land within hundreds of thousands of square kilometres of ocean, successfully colonise these, and survive for generations, adapting to whatever landscape and climate they encounter. Though there is now evidence of shifting climate providing "voyaging windows" and advances in voyaging technology that may have assisted with long distance sea voyaging in this region (Anderson, Chappell, *et al.*, 2006; Irwin *et al.*, 2022) which will be discussed later in this chapter.

There is still uncertainty in terms of the timing, rate and extent of migration across the tropical Pacific as well as issues around our understanding of how the colonisation worked – whether it was a simple two wave migration or made up of more complex stages (as per Sear *et al.* (2020)). The key gap is our understanding of the role of the environment in all this, and why so little local environmental and climatic data is available. The next section will delve into environment/climate-human relations in more detail.

### 2.3 Environment/Climate-human interactions

The impact of climate on ancient civilisations has been widely studied and examples extend across the globe. For example, it has been suggested that drought played a role in the fall of the Maya civilisation in Central America (Kuil *et al.*, 2016), the collapse of Mediterranean societies during the Bronze Age (Kaniewski, Guiot and Van Campo, 2015) and impacted Native American cultures between 11th and 13th centuries (Benson *et al.*, 2007). However, climate-human interactions have yet to be properly resolved in the Pacific region.

For the tropical South Pacific, there is existing research on climate-human interactions though it is focused on the so-called “1300 AD event” that led to significant changes in Pacific Society (Nunn, 2003; Goff and Nunn, 2016). This time period is significant in terms of climate as it sits within the transition between the Little Ice Age and the Medieval Climate Anomaly. Research carried out by Nunn and colleagues found that during this period of climate variability there were significant cultural changes and the outbreak of warfare on islands all across the tropical South Pacific. Nunn (2000) suggests that this period saw a significant drop in both sea level (approximately 1.15 m between 1270-1475 AD) and temperature (approximately 1.5 °C) across the Pacific basin along with a rise in ENSO frequency and precipitation. The potential impacts of these changes included a drop in productivity from coral reefs which were a key food supply for Pacific Islanders, erosion of island interiors and subsequent sedimentation downstream in low-lying land and stress on ecosystems (Nunn, 2000a). Research surrounding climate-human interactions prior to 1300 AD is limited. Many studies have mentioned the role of climate as a potential driver of migration or its impact on human populations (Nunn, 2000a; Nunn and Britton, 2001; Allen, 2006; Anderson, Chappell, *et al.*, 2006; Field and Lape, 2010; Goodwin, Browning and Anderson, 2014; Goff and Nunn, 2016; Sear *et al.*, 2020) but more in the capacity of an incidental remark rather than critically analysing climate as a potential factor in human migration in the Pacific. It is conceivable that climate did have a role to play in island life during this time and still does to this day.

New evidence from the Cook Islands suggest this dry period started 200-300 years before the 1300 AD event (Sear *et al.*, 2020) and actually coincided with the 2<sup>nd</sup> wave of migration into eastern Polynesia. Other work has also suggested that climate played a

role in the timing of voyaging in the tropical South Pacific (Anderson, Chappell, *et al.*, 2006; Goodwin, Browning and Anderson, 2014). Furthermore, it is thought that the climatic oscillations active in the Pacific region cause shifts in the SPCZ and the associated droughts could have affected the food and water resources of prehistoric Pacific island communities (Anderson, 2001; Kirch, 2017a).

Figure 2.2 illustrates the cycle of island life in the tropical South Pacific over the past 3,000 years. It's broken down into four stages; arrival/discovery, colonisation, establishment and development adapted from the settlement phases used in Sear *et al* (2020). The evidence for this model of island life comes from a range of studies across archaeology (Kirch, 1994, 2017a, 2017b; Anderson, 2001, 2002, 2014; Field, 2004; Bedford and Spriggs, 2008; Valentin *et al.*, 2010; Field and Lape, 2010; Burley, Sheppard and Simonin, 2011; Kinaston, Bedford, *et al.*, 2014; Goodwin, Browning and Anderson, 2014; Allen, 2015; Irwin *et al.*, 2022), palaeoenvironmental studies (Allen, 2006; Kennett *et al.*, 2006; Allen and Craig, 2009; Allen *et al.*, 2011; Allen and Mcalister, 2013; Sear *et al.*, 2020; Strandberg *et al.*, 2023) and ethnohistoric accounts (Williams, 1837; Gill, 1894; Hiroa, 1934; Reilly, 2009). Each will be discussed in turn with the aim of laying out the typical history of colonisation following migration and the interactions between the prehistoric Pacific community and the environment through time.

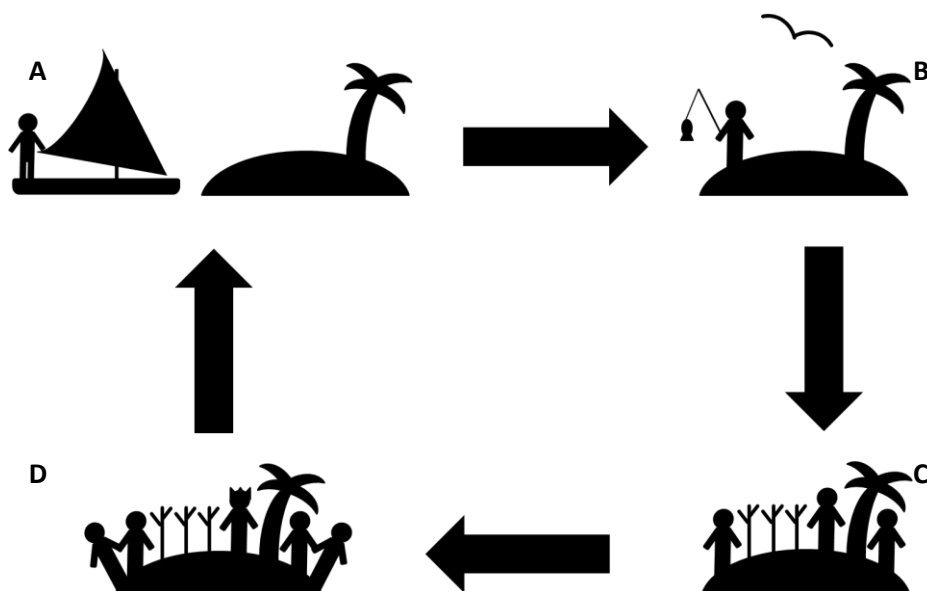


Figure 2.2: Cycle of island life following migration into a new archipelago.

**Stage 1: Arrival/Discovery** – This is not necessarily a period of permanent occupation, could be occasional visits or temporary occupation when particular resources are bountiful. The population would be dependent on wild natural resources that are found in abundance on that particular island e.g., fish, wild birds, wild fruit/vegetation. There would not be any significant environmental impact from a small and/or temporary population so it is unlikely that there would be a signal in sedimentary records indicating human presence at this stage. Figure 2.2-A

**Stage 2: Colonisation** – Humans now permanently occupy the island, predominantly in coastal regions. The food resources they depend upon are primarily wild resources. However, the founding population would have brought cultigens with them e.g. Colocasia Taro species (Valentin *et al.*, 2010) but these are not yet extensively cultivated. The colonisers released domesticates such as pigs onto the island as well as some unintended stowaways like the Pacific rat. There is likely to still be a strong connection with other islands through trade. There will be at least a small impact on the environment that with certain proxies could be picked up in the sedimentary record. Figure 2.2-B

**Stage 3: Establishment** – The population has been steadily growing over generations. Wild resources have become relatively depleted under increased population pressure and people have now moved inland to start cultivating the land more widely to increase food production. Inland settlements are now more dominant. There is likely still some contact with other islands. The vulnerability of the population is relatively low in comparison to other stages in the cycle as the population is at a sustainable level with a mix of food resources available and contact/trade with other populations is still open. There is a significant impact on the environment that can be picked up in sedimentary records. Figure 2.2-C

**Stage 4: Development** – The population has grown exponentially since arrival and now likely is reaching the upper limits of the carrying capacity of the island. All available and suitable land is cultivated to provide for a larger population. The connections between islands have broken down over time. There will have been some significant developments in terms of social structure such as the development of chiefdoms or a generally more complex social hierarchy. Due to the population pressure on the land, there are outbreaks of warfare between social groups. The vulnerability of the population is high due to overpopulation, availability of resources per person and environmental degradation.

There is development of new advances in technology such as canoes, fishhooks, irrigation systems etc. The population has a very significant impact on the environment that can be picked up in the sedimentary record. Figure 2.2-D

The cycle of human-environment interactions in the tropical South Pacific presented has clear parallels with the stages of growth suggested in resilience theory literature; consolidation, transformation and release, reorganisation and innovation (Anderies and Hegmon, 2011). In subsequent sections different aspects of Pacific island life will be presented and the connection between that aspect and the environment examined.

### 2.3.1 Diet of the Pacific islanders

As laid out in the section above, the types of resources that islanders depended upon for sustenance changed through time depending on the stage of settlement and the associated population and environmental pressures. In the past two decades, stable isotope data including  $\delta^{13}\text{C}$ ,  $\delta^{15}\text{N}$  and  $\delta^{34}\text{S}$  has allowed researchers to discern the diets of early Pacific islanders using bone collagen from cemetery sites (Valentin *et al.*, 2006; Commendador *et al.*, 2013; Kinaston, Bedford, *et al.*, 2014; Herrscher *et al.*, 2018). One example of this is from Teouma, one of the earliest Lapita sites uncovered in remote Oceania and dated to ca.3000-2900 yr BP and located on the island of Efate in Vanuatu (Petchey *et al.*, 2014). It is the location of a number of burial sites that have been attributed to some of the first humans to arrive into remote Oceania. Isotopic data from this site shows that early Pacific islanders initially utilised wild marine and terrestrial resources to feed their fledgling communities (Kinaston *et al.*, 2014). However, over time, diets changed as populations grew, wild marine and terrestrial resources depleted and horticulture emerged. Research by Valentin *et al.* (2006) looking at changing diets in Cikobia, Fiji found that during the late prehistoric/historic period on this island, vegetables made up a significant portion of the islanders diet during this time and the intake of marine resources dropped in comparison to the Lapita diet observed in Teouma for example. These findings were also reflected in data from Rapa Nui (also known as Easter Island) where a comparison between isotopic data from different islands indicated that those living on Easter Island were more heavily dependent on terrestrial resources for their food (Commendador *et al.*, 2013). This all coincides with the concept of “transported landscapes” where both the Lapita and later the Polynesians took both

cultigens and animals with them when they travelled in search of new land and introduced them to the landscapes they discovered (Valentin *et al.*, 2010). There were exceptions to this pattern possibly because the physical limitations of an island or a small population size do not enable or require the development of horticulture respectively (Herrscher *et al.*, 2018). Nevertheless, horticulture became important in island life as island communities grew and developed and often settlements focused around good agricultural land (Kirch, 1994, 2017a). On Atiutaki in the Cook Islands, data from human, pig and dog samples provided insights and connections between the diet of people and animals on this island. Both marine and agricultural food sources were an important part of the diet of the islanders. It is also noted that cyclones in the 14<sup>th</sup> century had severe impacts on reefs that potentially took centuries to recover, causing depressions in certain fish stocks (Allen and Craig, 2009). Cyclones occur more frequently under El Niño conditions in the Cook Islands as the position of the SPCZ dictates the cyclone generation zone due to characteristic cyclonic wind shear (de Scally, 2008). Some researchers have also attributed the poisoning of reef fish by ciguatera algae as a driver of migration. One study linked climatic changes, specifically positive PDO phases, with increased incidence of ciguatera fish poisoning (Rongo *et al.*, 2009). The consumption of poisoned fish causes illness so it has been suggested that during periods of high incidence of ciguatera fish poisoning, populations typically dependent on reef fish for a food source would have to look for alternative food sources, potentially driving migration to new lands (Rongo *et al.*, 2009). The poisoning of reef fish by ciguatera is possibly just one symptom of changing climatic conditions that put pressure on a range of island ecosystems including the reef fish and populations dependent upon them.

In Polynesia, agriculture was primarily rain-fed (Quintus and Cochrane, 2018a) so changes in the climate would have significant impact upon food security for Pacific islanders who over time become more and more reliant on agricultural resources to support their growing populations. Rainfall gradients even across individual islands would influence the types of cultigens introduced in certain areas (Kirch, 1994). On islands where irrigation systems were developed, populations were possibly slightly less vulnerable to climatic change due to the storage of water in these systems, e.g. Taro pondfields (Allen, 1969) but this would only be a temporary stopgap that could not withstand prolonged shifts to drier conditions. Furthermore, wild resources are also impacted by changes in

environmental conditions. The example from Atiutaki with the depletion of reef fish stocks following cyclones provides evidence of this. It is clear that climate plays an important role in both agricultural and wild resource availability.

When conditions are difficult and communities are running close to the maximum carrying capacity of the island, pressure on resources increases (Brandt and Merico, 2015). To relieve this pressure two mechanisms that are primarily used in Pacific history are migration and warfare. This became palpable later in Pacific history when war and conflict broke out and was often focused around areas of fertile land or involved the losing side having to forfeit their productive lands to the victor. Evidence for this comes from both archaeological (Field, 2003; Field and Lape, 2010; Kirch, 2017b) and ethnohistoric evidence passed down through oral histories (Gill, 1894; Hiroa, 1934; Reilly, 2009) and examples come from many islands including Tikiopia, Mangaia and Hawai'i (Kirch, 1984).

### 2.3.2 Voyaging & Migration

There has been a debate in the literature on exactly how Pacific islanders managed to migrate across thousands of kilometres of open ocean. As discussed, there were two waves of migration into the Pacific. The first approx. 3,000 years ago, when the Lapita civilisation migrated from near Oceania into remote Oceania (i.e., W to E) through to Samoa and the second was approx. 1,000 years ago when eastern Polynesia was colonised.

Early traditionalist ideas on migration and long-distance seafaring said that the development of new maritime technologies such as the outrigger canoe, enabled humans to cross the Pacific Ocean. Early migrations into the Pacific to Vanuatu and New Caledonia could have been accomplished on sailing rafts and traditionalists also assumed the existence of double canoes that could sail windward (Anderson, 2014). However, in recent times the timing of technological advances - specifically sails – and the existence of double canoes during the Polynesian migration has been drawn into question and instead suggestions that advantageous sailing conditions would also have been required (Anderson, 2014). Within the literature, climate has been brought up as a potential driver in both the Lapita migration into remote Oceania (Duprey *et al.*, 2014; Cochrane, 2018) and the Polynesian migration into eastern Polynesia (Sear *et al.*, 2020). Some suggest that

Pacific Islanders did not have the maritime technology required to sail against the prevailing winds and instead migration across the South Pacific islands required shifts in climatic conditions that were brought about by ENSO (Anderson, Chappell, *et al.*, 2006). Typically, the prevailing winds and currents in the tropical South Pacific do not favour eastward migration as they respectively blow and flow from east to west against the direction of travel. However, during El Niño years the currents and winds become reversed (Murphy, Power and Mcgree, 2014) offering opportunities for voyaging eastward. Goodwin *et al.* (2014) found that Polynesian migration was facilitated by shifting wind conditions brought about by climatic change in the Late Holocene and also likely offered the motivation too as climatic change impacted on island life, particularly in the central eastern Pacific.

After initial colonisation, long-distance seafaring and movement between populations eventually stopped. Following the Lapita colonisation of remote Oceania, there was still contact with near Oceania populations until 2700 cal yr BP after which evidence for contact between populations stopped (Cochrane, 2018). Similarly, following the migration into eastern Polynesia and colonisation of the Polynesian triangle, long-distance voyaging between different island groups had stopped by 550-450 cal yr BP (Goodwin, Browning and Anderson, 2014; Goff and Nunn, 2016). Following colonisation, an island's individual cultural identity would diverge and evolve leading to a breakdown in social connections over generations and eventually resulting in voyaging between islands coming to an end (Reepmeyer, 2021). Another explanation could be that increasing populations across the region and strain on resources reduced trade between islands or perhaps a drop in favourable climatic conditions required to make the journey during this period.

Voyaging/migration can act as a potential mechanism for managing overpopulation or to seek out new resources during times of stress *i.e.*, drought. However, the literature suggests that not only could climate be a push factor for migration but long-distance voyaging also required certain climatic conditions in order to be successful (Anderson, Chappell, *et al.*, 2006; Goodwin, Browning and Anderson, 2014).

### 2.3.3 Conflict

Conflict and warfare are prominent aspects of Polynesian history (Dinapoli and Morrison, 2017) especially during the mid-second millennium. The rise of conflict during this period is likely because previous mechanisms of relieving pressure on resources due to overpopulation were no longer viable. During the Lapita period and the initial colonisation of remote Oceania, the societal response to resource pressure - due to the impact of climatic change but specifically drought - was to migrate to vacant archipelagos as conflict over land and food increased (Goodwin, Browning and Anderson, 2014). However, by 1300 AD every island in the South Pacific had been colonised (Wilmshurst *et al.*, 2011; Ioannidis *et al.*, 2021) so migrating to new islands was no longer possible. Pressure then continued to increase until conflict breaks out. Work conducted by Field and Lape (2010) also noted this connection between climate and conflict as they found that anomalous dry periods where levels of rainfall were below average were linked with the building of 99% of fortifications on the islands of the tropical Pacific during the Little Ice Age. They found that the link between drought and conflict was possibly stronger from 1100 to 1900 AD following the start of the second wave of human migration in this region. Other work on this front found that in Fiji, population responses to reaching island carrying capacity led them to build fortifications to protect resources but variable climatic conditions during the LCO/LIA transition actually led to increased cooperation between populations and the development of social hierarchies (Field, 2004). This was definitely not a Pacific wide phenomenon however, as Kirch states, “war is the ultimate cultural control on overpopulation” (Kirch, 1984, p. 201) and it was also a way to appropriate more agricultural land from weaker groups (Kirch, 1984, p. 206). Evidence for warfare comes from a number of islands including Tikopia, Futuna and Mangaia, driven primarily by overpopulation, food shortages and limited agricultural resources (Kirch, 1984, 2017b). These pressures would have been exacerbated by a variable climate, as drought would severely affect water security, which in turn would bring about greater food shortages and reduce yields to agricultural resources. In fact, some of the “most politically powerful and highly competitive chieftainships developed” not in the wetter windward parts of the island but in drier leeward landscapes in Hawai’i and the Society Islands (Kirch, 1984). It is clear that overpopulation during this development stage of settlement with evolution of social complexity was primarily a social process but it is worth considering whether

variable climate played a role in speeding up some of these processes by reducing the carrying capacity of Pacific islands.

#### **2.3.4 Environment/Climate-human interactions summary**

In summary, climate has been cited as a potential driver of migration (Duprey *et al.*, 2014; Cochrane, 2018; Sear *et al.*, 2020) as well as other aspects of prehistoric Pacific island life including, voyaging (Anderson, Chappell, *et al.*, 2006; Goodwin, Browning and Anderson, 2014), diet (Kirch, 1994), conflict (Kirch, 1984, 2017b; Nunn, 2000a; Field and Lape, 2010) and adaptation of agricultural technology (Kirch, 1994; Quintus and Cochrane, 2018a, 2018b). Considering the different aspects of Pacific island life and the history of the tropical South Pacific there are a number of hypotheses surrounding climate and prehistoric island life that have developed through this discussion and they are:

- Climate, specifically rainfall amount and variability, played an important part in prehistoric island life.
- Early Pacific islanders were vulnerable to variations in climate due to the impact on often limited food and water resources
- Drought played a role in the timing of the waves of human migration into the tropical South Pacific during the Late Holocene.
- Drought periods occurred at around 900 AD and 1300 AD

In order to test these hypotheses, we need to be able to understand how past climatic changes have influenced Pacific societies, and we need to ensure we have accurate and robust data on the climate from across the Pacific and precise age models. Conditions in the Pacific basin vary across different north-south and east-west gradients and so it is important not to assume that the responses will be the same island group to island group or even that the defined MCA and LIA periods in European climate will translate directly into the same kind of changes in the Pacific (Allen, 2006). This suggested link between societal and environmental changes still needs testing with long-term high resolution continuous and relevant palaeo-records that go back beyond the start of colonisation. This could provide a window into how environmental changes translated into specific drivers of colonisation in the Pacific.

The next sections of this literature review will examine our current understanding of the characteristics of South Pacific climate and controls specifically on rainfall variability.

Following this, our current understanding of past climate over key periods in Pacific human history will be explored and finally a summary of existing studies that look to combine our knowledge of climatic and social change in models of prehistoric Pacific island life.

## **2.4 South Pacific Climate and Precipitation**

In the first instance, our understanding of the climate of the tropical South Pacific comes from modern observations and data. We know that the South Pacific is a region characterised by high levels of rainfall that in some parts can exceed 5 metres annually (see Figure 2.3) but it is also the location of some of the most severe water shortage problems on the globe (White et al., 2007). Rainfall in the tropical South Pacific is primarily produced by convective climatic features such as the Intertropical Convergence Zone (ITCZ), West Pacific monsoon and the South Pacific Convergence Zone (SPCZ) (Kuleshov et al., 2014). An off-shoot of the Intertropical Convergence Zone, the SPCZ is a band of convective rain clouds that stretches from the West Pacific Warm Pool south-east across to French Polynesia (Figure 2.3) and acts as a major source of freshwater to the South Pacific islands via precipitation (van der Wiel et al., 2015). The SPCZ is strongest in austral summer, which results in well-defined dry winter and wet summer seasons (Australian Bureau of Meteorology and CSIRO, 2011).

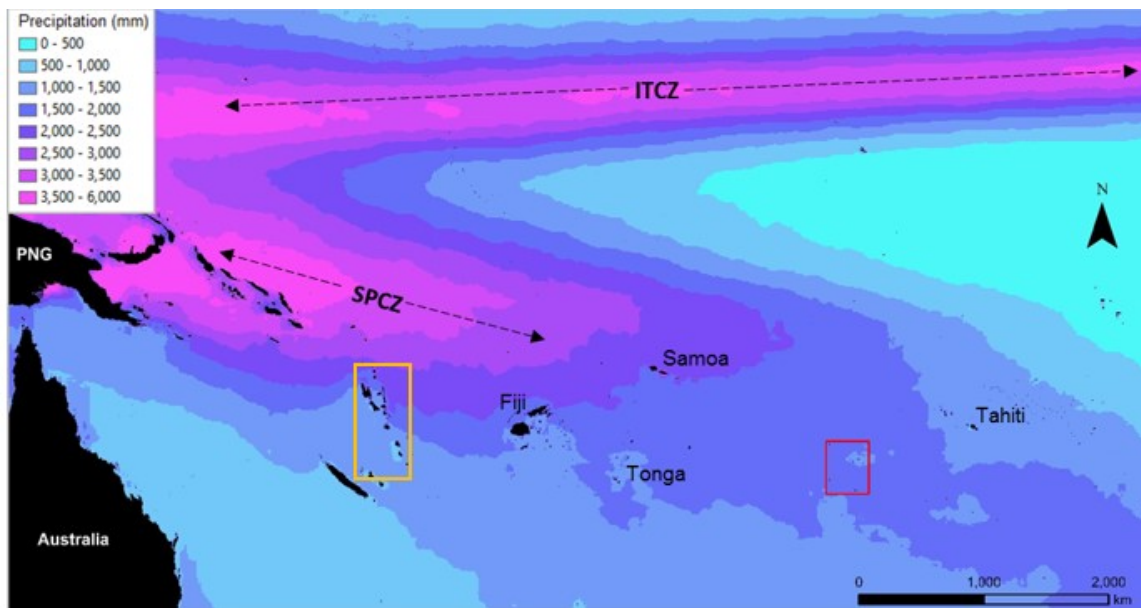
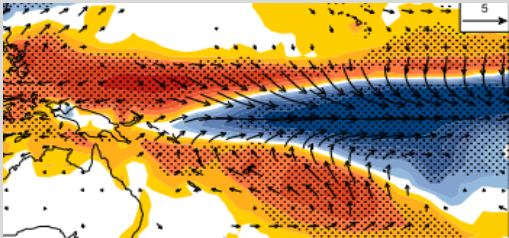
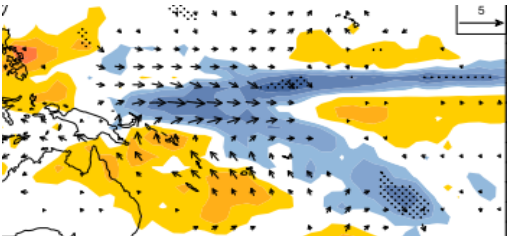
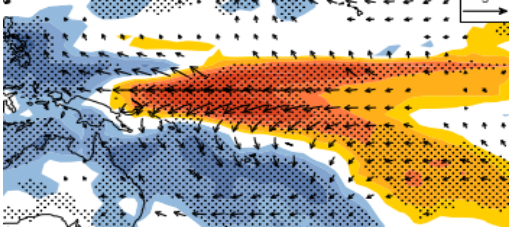


Figure 2.3: Map of average annual precipitation with the location of the ITCZ and SPCZ in relation to Vanuatu (yellow box) and the Southern Cook Islands (red box).

There are a number of climatic oscillations at work in the Pacific region - such as the Inter-decadal Pacific Oscillation (IPO), the Pacific Decadal Oscillation (PDO) and El Niño Southern Oscillation (ENSO) (McGree, Schreider and Kuleshov, 2016; Newman *et al.*, 2016) - that influence the strength, extent and position of the SPCZ and operate over a range of time scales (Folland *et al.*, 2002; Brown *et al.*, 2020). The different phases of these climatic oscillations cause the contraction or expansion and shift in the location of the SPCZ, which significantly alters the amount of rainfall that falls on the Pacific islands – particularly those north and south of the SPCZ - providing increased rainfall in some and drought in others depending on the direction of movement (Cai *et al.*, 2014, 2015; van der Wiel *et al.*, 2015; Higgins *et al.*, 2020). This rainfall variability affects the availability of water resources on Pacific islands where surface and ground-water can be limited and are dependent on precipitation for recharge (Duncan, 2011). Whilst El Niño is generally referred to as a single entity, there are three different classifications of El Niño events known as the Central Pacific El Niño (CPE) and the Eastern Pacific El Niño (EPE) and the third type is known as a mixed El Niño (ME) (Table 2.1). El Niño events are separated into different types as they have different characteristics in terms of sea surface temperature patterns and wind strength and direction as well as varying impact on rainfall responses. Whilst CPE can have significant impacts on the climate system in the Pacific, the extreme zonal El Niño episodes occur during EPEs and this kind of El Niño is where we see the greatest SST anomalies and the

most significant changes in rainfall (Murphy, Power and Mcgree, 2014). ENSO events also bring about significant changes in the prevailing wind direction on an inter-annual basis (Duprey *et al.*, 2014).

Table 2.1: Different types of ENSO events, the region they affect and the associated impacts - taken from (Murphy *et al.*, 2014).

Type of ENSO event	Mean wet season rainfall anomalies (mm/day-1) and surface winds	Niño Region & Impacts
<b>Cold Tongue El Niño (CTE) / East Pacific El Niño (EPE)</b>		Niño 3 – The most significant changes in SST gradients and reversal of surface winds leading to notable changes in rainfall with extreme wet and dry anomalies.
<b>Warm Pool El Niño (WPE) / Central Pacific El Niño (CPE)</b>		Niño 4 - Differences in rainfall anomalies are low and changes are inconsistent.
<b>Mixed El Niño (ME)</b>		Niño 3-4 - Similar to the CTE in terms of impact but on a lower scale in terms of SST and rainfall changes.
<b>La Niña</b>		Niño 3-4 - Opposite pattern from El Niño events. Enhancement of typical climatic conditions.

The PDO and IPO are oscillations that occur over longer time periods than ENSO, with phases lasting around 20 to 30 years and affecting the entire Pacific basin (NIWA, 2023). Both PDO and IPO represent low frequency variability in the Pacific Ocean and are defined by changes in SST (Hernández *et al.*, 2020). The IPO for example, sees below average SSTs in tropical Pacific during negative phases (Peng *et al.*, 2015; Hernández *et al.*, 2020) and opposite conditions during positive phases (Peng *et al.*, 2015).

Furthermore, the operation of different timescales of oscillations can result in compound events whereby IPO and ENSO interact to produce distinct precipitation variability by shifting the location of the SPCZ (Power *et al.*, 1999; Lorrey *et al.*, 2012) as shown in Figure 2.4. Variability in the position of the SPCZ during ENSO and IPO has been shown to influence the duration, magnitude and intensity of drought in the Pacific over inter-annual to inter-decadal timescales respectively (McGree, Schreider and Kuleshov, 2016).

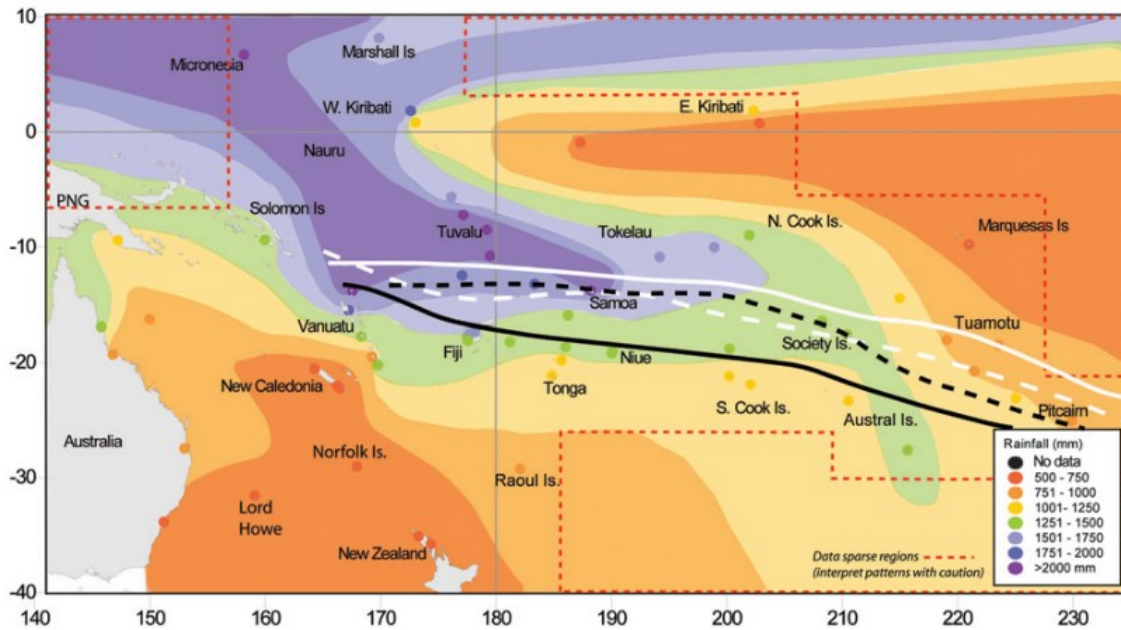


Figure 2.4: Nov-April total rainfall (mm) for the South Pacific region. The lines represent SPCZ locations during different phases of IPO and SOI. Solid white line: -SOI/+IPO; dashed white line: -SOI/-IPO; solid black line: +SOI/-IPO; dashed black line: +SOI/+IPO. (Figure from Lorrey *et al.*, 2012)

Drought is caused and defined by a severe shortage of precipitation and it is a natural hazard that affects agriculture and water resources (Mishra and Singh, 2010). It is different from other types of natural hazards as it does not occur instantaneously but builds up over time and can last for years whilst affecting large areas (Below *et al.*, 2007). The number of Pacific-based studies focusing on drought in the modern age where we have instrumental and satellite data is growing (e.g. Dixon-Jain *et al.*, 2014; McGree, Schreider and Kuleshov, 2016) and are helping to develop our wider understanding. However, longer term records going back 400+ years, show that climatic oscillation patterns in the past 30 years - such as ENSO which influence drought events - are unusual in comparison to the record over the

past four centuries (Freund *et al.*, 2019). If only instrumental records are used to express the range of precipitation variability and resulting droughts, then the natural variability in these climatic events may not be fully represented. Palaeoenvironmental records can expand our understanding of the true natural variability of Pacific hydroclimate – which represents the connection between climate and the hydrological cycle (NWS, 2023) - and these types of archives can also help position current and future scenarios of drought within a longer-term context.

## 2.5 Pacific palaeo-precipitation records

In the past, most terrestrial palaeo-records from the Pacific region focus on proxies relating to vegetation changes, fires and indicators of human arrival (e.g., Burney *et al.*, 1995; Allen *et al.*, 2011; Gosling *et al.*, 2020) rather than palaeoclimatological change in the Pacific. However, the number of palaeoclimatic studies in this region is growing and each one helps build our understanding of how climate has changed in this region during the Holocene. **Error! Reference source not found.** shows the type of archive and location of the palaeoenvironmental studies that have been conducted within the South Pacific islands that specifically relate to hydroclimate. The Pacific region is a region that proves more difficult to study compared to other parts of the world due to the relative isolation of its islands and the technical requirements that need to be overcome to collect records from potential archives. There is a paucity of precipitation records that are continuous, high resolution with a long temporal range, particularly from the central Pacific, which inhibits our understanding of climatic change across the South Pacific basin in the geological past (Toomey *et al.*, 2016). Palaeoenvironmental records come from a range of environmental archives and in the Pacific a majority are either marine sediments, coral, stalagmites or terrestrial, which includes swamp/peatlands and lake sediments. Each type of archive has its own advantages and disadvantages when studying climatic change. Marine sediments often cover very long time periods, but sediment accumulation is slow so temporal resolution is low. Corals have good temporal resolution but often only capture short snapshots in time that can be sporadic. Stalagmites similar to coral also have good temporal resolution but often do not cover long time periods and typically only have records spanning hundreds instead of thousands of years. Terrestrial records can have good

temporal resolution and can cover long time periods (i.e., thousands of years) though typically not as far back as marine sediments.

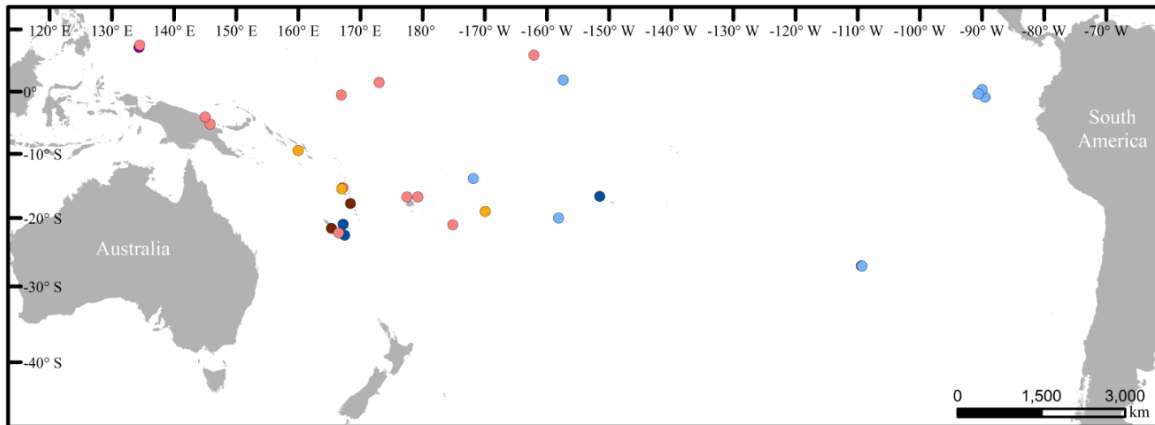


Figure 2.5: Map identifying the location of palaeo-records relating to precipitation. Colour denotes the type of record; Pink – Coral, Dark Blue - Marine, Purple – Saline Lakes, Light blue – Freshwater Lake, Orange- Stalagmite, Brown- Swamp.

Many studies compare the records they are presenting with other records from the region but often these records will be from sites on the fringes of the Pacific basin or beyond and often from continental areas (e.g. Smittenberg *et al.*, 2011; Atwood *et al.*, 2021). Comparison between these types of records should be done with care as sites that are either on or near continents will have different types of processes influencing their archives. Continental climate is primarily controlled by the large seasonal changes of heating and cooling of the land, which is more pronounced than that of the ocean (Ramage, 1995; Holden, 2017) whereas the ocean and atmosphere act as the main controls on maritime climate and rainfall is generally convective (Neale and Slingo, 2003; Schroeder, 2009). Here we will focus on palaeo records that come from within the Pacific basin rather than peripheral or continental sites to avoid continental effects within the climate record. In this section, in line with the focus of this thesis, the existing work on the Pacific climate record has been divided into two time periods surrounding the two waves of human migration into the Pacific.

For discussion purposes, the records are also going to be split geographically within the time periods. For clarity, the South Pacific will be broken down into northern (Kiribati, Outlying Pacific Atolls), western (Vanuatu, Fiji, Samoa, New Caledonia), central (Cook Islands, French Polynesia) and eastern (Easter Island, Galapagos) South Pacific regions.

### **2.5.1 Climate and the first wave of migration and initial colonisation period**

The palaeoclimate surrounding the first wave of migration into eastern Polynesia has been more relatively understudied than the second has. Figure 2.6 shows an overview of the key climate commentaries from a range of studies taken from across the Pacific region leading up to and following the first and second wave of migration into remote Oceania. It is clear from Figure 2.6 that a vast number of these records do not extend back to the first wave of human migration into the Pacific.

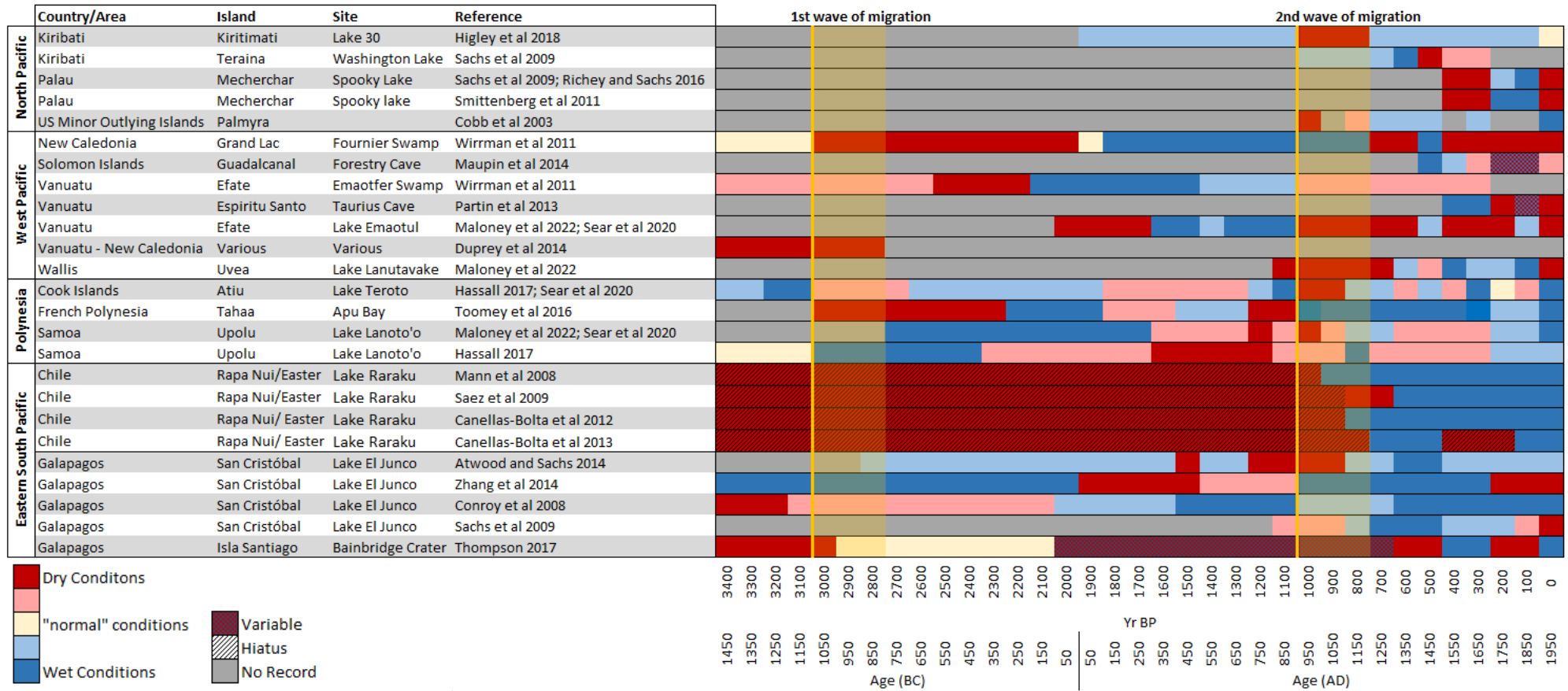


Figure 2.6: Overview diagram of key palaeo records of hydroclimate change in the tropical Pacific from 3400 yr BP to present. Yellow lines mark the start of the two waves of human migration.

From the western South Pacific, one record that has presented an insight into the climate during this time is a study conducted by Duprey *et al.* (2014) who produced an isotopic record from giant clams found at archaeological sites in New Caledonia and Vanuatu. Using the shells, they attempted to identify the differences between the modern climate state and the climate state around the time of the Lapita migration, which occurred approximately 3000 yr BP. The data suggested that the mean state was drier between 3600 and 2800 yr BP in Vanuatu and New Caledonia based on carbon isotopes. However, there were mixed results based on oxygen isotopes which signify whether conditions were cooler or warmer (Duprey *et al.*, 2014). Whilst this record has limited sample number and covers only relatively short snapshots in time it also is one of the few studies that attempts to identify whether climate was a factor in the first wave of migration into remote Oceania by the Lapita from the Solomon Islands. Another study also located in Vanuatu - but this time utilising a terrestrial archive - used sediments taken from the Emaotfer Swamp to reconstruct past environmental change. Wirmann *et al.* (2011) showed that between 3100 to 2500 yr BP there was a drop in water levels at Emaotfer Swamp and a change in the vegetation in the landscape from rainforest to open forest which they interpret as a potential dry period. However, they do note this vegetation change could be due to human activity in the area as the Vanuatu archipelago were some of the first islands to be colonised by Pacific islanders. Furthermore, the sequence from Emaotfer is carbonate rich making dating difficult and adding uncertainty to the age model. Similarly, a record from the Fournier Swamp in New Caledonia, which lies around 400 km south of Vanuatu, found that between 2750-2000 yr BP a cool and dry climate prevailed (Wirmann *et al.*, 2011). From 2600-2000 yr BP they suggest that the increase of andesine in the sediment is evidence of a rise in erosion, which would be caused by a decrease in vegetation due to the drier conditions. However, in other studies, an increase in erosion can also be attributed to human activity in the area (Sear *et al.*, 2020) and this period does follow the colonisation of New Caledonia by humans (Cochrane, 2018). Nevertheless, a study identifying the dynamics of the SPCZ over the Holocene using sites from Samoa and the Cook Islands found that from 4,000 to 2,700 cal yr BP the SPCZ was moving to a more northwest position but it's position was highly variable during this time (Hassall, 2017). During 2800-1500 yr BP the SPCZ appears to have contracted bringing lower levels of rainfall to the region southwest of the SPCZ which is reflected in the

terrestrial records from Vanuatu and New Caledonia (Wirrmann, Eagar, *et al.*, 2011; Wirrmann, Sémah, *et al.*, 2011).

From the central South Pacific, due to the paucity of “conventional palaeoclimate archives” (Toomey *et al.*, 2016, p.491), a study from French Polynesia instead opted to investigate an off-shore sediment record from Apu Bay in Tahaa. This record is one of the few oceanic records that goes beyond the Common Era. The sediment profile goes back 3000 yr BP and uses the XRF ratio Ti/Ca as an indicator of terrestrial in-wash into the bay which is caused by higher levels of rainfall (Toomey, Donnelly and Tierney, 2016). The record shows that there is a gradual increase in mean precipitation through the late Holocene but around 3000 yr BP conditions were notably drier than any time in the last 2000-3000 years. The interpretation of this record has to be done with care however as the choice of proxy would likely have been influenced by human activity from 1000 yr BP altering the natural pattern of Ti/Ca in the latter part of the record as it is understood that increasing rates of Ti can be linked to the arrival of humans and clearance of the land (Sear *et al.*, 2020) and indeed, from 1000 yr BP there is an upward shift in the average Ti/Ca values at the approximate time of human arrival in the Society Islands around 1050 yr BP (Ioannidis *et al.*, 2021).

In the eastern South Pacific, some of the oldest and longest records available in the South Pacific come from Easter Island on the south-eastern edge of the Polynesian triangle. Easter Island sits in relative isolation being 2,000 km from the next nearest island and 3,500 km from the nearest continental land. It has a subtropical climate prone to drought, no reef and with a small surface area of 164km<sup>2</sup> and relatively little in terms of natural resources (Hixon *et al.*, 2019). It was one of the last places in the Polynesian triangle to be colonised (approximately 750 yr BP or 1200 AD (Hunt and Lipo, 2008; Mulrooney, 2013; Ioannidis *et al.*, 2021)) and has captured the imagination of the scientific community as well as the general public for its story of ecological collapse and the Moai statues that sit in testament to the civilisation that first lived on the island.

There are three studies by Mann *et al.* (2008), Sáez *et al.* (2009) and Cañellas-Boltà *et al.* (2012) from Lake Raraku that reconstruct the hydroclimate during the Holocene for Easter Island. Earlier work conducted by Mann *et al.* (2008) struggled with dating the sediments from Rano Raraku because of floating reed mats, reed roots and potential in-wash of old carbon from the watershed. Later works by Sáez *et al.* (2009) and Cañellas-

Boltà *et al.* (2012) improved on the work done by Mann *et al.* (2008) and both presented a 34,000 year record. However, both similarly had chronology issues due to in-wash of older material and contamination due to modern roots growing into the sediments, which introduces uncertainty in the timing of changes in these records. During the mid-Holocene (8700-4500 yr BP) the site was a swamp before it dried up and sedimentation stopped (Cañellas-Boltà *et al.*, 2012). Each of the three records from this site has the hiatus present, all of which are dated to within 4500 yr BP to 800 yr BP (Mann *et al.*, 2008; Sáez *et al.*, 2009; Cañellas-Boltà *et al.*, 2012). Another record from the Rano Aroi mire provides an alternative 70,000 year record from Easter Island however this record does not cover the Late Holocene due to remobilisation of the sediment sequence caused by human activity in the area (Margalef *et al.*, 2014). All the records developed from Easter Island sediments have a hiatus in the record which sits approximately at 4410-770 yr BP (Mann *et al.*, 2008; Sáez *et al.*, 2009; Cañellas-Boltà *et al.*, 2012; Margalef *et al.*, 2014) which is interpreted as a drought as the lake dried up. The sedimentary hiatus in the Easter Island records does mean there is a significant gap in the hydroclimate record for this island but nonetheless does provide evidence of a significant dry period after 4410 yr BP but prior to 770 yr BP.

Another example from the eastern South Pacific comes from the Galapagos Islands, an archipelago that sits approximately 1000 km off the west coast of Ecuador. Despite sitting at the peripheral edge of the South Pacific basin, a number of palaeo records from the Galapagos hold important information about ENSO variability and changes in hydroclimate in the eastern South Pacific over the Holocene. Multiple studies have been conducted on Lake El Junco, likely due to it being the only permanent freshwater lake in the Galapagos. It is located on the island of San Cristobal and is also a highland site sitting 675 m above sea level. A study conducted at this site by Conroy *et al.* (2008) utilised grain size data along with C/N ratios to reconstruct hydroclimate and ENSO variability across the Holocene. The record indicated that the wettest period during the Holocene was between 2000 and 1500 yr BP indicated by increase in the silt percentage in the grain size record. This period also saw the greatest rate of ENSO variability. Notable increases in the precipitation record occur at 3200 and 2000 yr BP. The driest periods in this record occurred 3800 – 3200 yr BP which is evidenced by an increase in the amount of clay in the sediment that Conroy *et al.* (2008) interpret as a drying out of the lake bed.

Two further studies were conducted on El Junco by Zhang et al. (2014) and Atwood and Sachs (2014) that focused on the lipid biomarker record and algal blooms to reconstruct climate. Overall, Zhang et al (2014) found that the Late Holocene was a period with frequent and strong ENSO activity. Conditions were wetter in the Galapagos from around 4000 yr BP till 2000 yr BP, after which conditions became much drier for at least 500 years and was characterised by weaker El Niños. Atwood and Sachs (2014) also use lipid biomarkers for their record but utilise the D/H ratios to create a 3000 year record of ENSO and hydroclimate change. The oldest part of the record going back to 3000 yr BP seems to indicate hydroclimate was relatively stable and overall wetter conditions based on botryococcene C<sub>34</sub> and dinosterol  $\delta D$ , which are biomarkers associated with algae and plants respectively. Though there are fewer data points in the deeper record for some of the proxies compared to younger sediments. However, all the records from El Junco have well constrained age models that provide some confidence in the timing of changes from these records.

One record comes from the Bainbridge Crater Lake, which sits in contrast to El Junco as it is a low lying hypersaline coastal lake on the island of Isla Santiago. This record offers an independent view on ENSO conditions and hydroclimate in this region with a new archive and alternative proxies that allow for a comparison between records. The chronology for this site is not as well constrained as others in the Galapagos, particularly between 4500-2000 yr BP, where there is a wider spread of <sup>14</sup>C dates. Nevertheless, Thompson *et al.* (2017) suggest that the carbonate laminations that are present in the record between 3500 and 3000 yr BP are indicative of cooler drier conditions that are concentrating the carbonate ions so they precipitate out. They hypothesise that this change in conditions is caused by an increase in the frequency of La Niña conditions.

To summarise, during this first wave of migration into remote Oceania records from the western South Pacific indicate that climatic conditions were dry either during this initial wave of humans into the region or during colonisation in the centuries after. Similarly, the record from Apu Bay also suggests drier conditions around 3000 yr BP in central South Pacific during this initial wave of colonisation. The records from Easter Island also all indicate that conditions were relatively dry from around 4000 yr BP right up until the end of the MCA after which conditions become more humid/wetter. Easter Island does sit on the fringes of the SPCZ zone so has relatively low levels of annual rainfall ranging from

500 to 2000 mm/year (Mann *et al.*, 2008; Sáez *et al.*, 2009; Cañellas-Boltà *et al.*, 2016). Rainfall is highly variable year to year and so Easter Island is susceptible to frequent droughts as a result (Mann *et al.*, 2008; Sáez *et al.*, 2009). Evidence from the Galapagos is slightly conflicting, perhaps due to chronological errors. However, it is clear that there are relatively few records covering this period of migration and a number of the archives are located in the eastern Pacific, thousands of kilometres away from the region being colonised during this time. Furthermore, a number of the records from the western South Pacific struggle with untangling human and climate signals in their sequences. It is vital that more palaeoenvironmental data covering this first phase of colonisation into remote Oceania is produced so that it is possible to place this wave of migration into a fully coherent environmental and climatic context.

### **2.5.2 Climate and the second wave of migration and colonisation of Polynesia**

The palaeoclimate surrounding the second wave of migration into eastern Polynesia has been more extensively studied than the first. A number of studies have focused on Pacific climate within the Common Era which is the period from 1 AD to 2000 AD. Before examining the climate record for this period, it is important to note there are two key periods in terms of global climate during the Common Era that are commonly noted in palaeoclimatic studies and provide a useful frame of reference for considering records from this period. The first is the Mediaeval Climatic Anomaly (MCA) also known as the Mediaeval Warm Period (MWP) that occurred between 950-1250 AD and the second is the Little Ice Age (LIA) which occurred between 1300-1850 AD (Mann *et al.*, 2009). These periods are also important in terms of the Pacific climate and human history during this period. Figure 2.7 shows an overview of the key climate commentaries from a range of studies taken from across the Pacific region leading up to and following the second wave of migration into Eastern Polynesia.



### 2.5.2.1 Mediaeval Climate Anomaly

There are a number of coral records from across the Pacific including Palmyra (Cobb *et al.*, 2003; Nurhati, Cobb and Di Lorenzo, 2011), Fiji (Linsley *et al.*, 2004; Bagnato *et al.*, 2005; Dassie *et al.*, 2014), Palau (Osborne *et al.*, 2014), Vanuatu (Kilbourne *et al.*, 2004), Tonga (Dassie *et al.*, 2018), French Polynesia (Boiseau *et al.*, 1998) and the Cook Islands (Linsley *et al.*, 2004; Dassie *et al.*, 2018) that provide observations on hydroclimate change, though more specifically ENSO. They often provide good temporal resolution – down to sub-annual - but poor time coverage typically only going back to a maximum of 200 yr BP, making corals customarily an impractical palaeoclimate archive for understanding climate during the prehistoric human occupation of the Pacific. Contrary to this trend, one of the longest coral records was presented by Cobb *et al.* (2003) from Palmyra Island, an outlying atoll sitting north of the Northern Line Islands. They present a series of coral records at a monthly resolution, covering five time slices across the last 1,100 years including both the MCA and the LIA. Their key finding in terms of hydroclimate was that the 10<sup>th</sup> century presented the coolest and/or driest conditions of the last 1,100 years. Corals can be difficult to interpret as there are a number of variables that influence coral isotopic values such as SST, SSS and SOI and in addition to this, the interaction between the ocean and atmosphere can introduce additional noise into the record (Cobb *et al.*, 2003; Quinn *et al.*, 2006, 2017). This makes it difficult to discern precipitation proxies from other processes in coral records (Cobb *et al.*, 2003; Maupin *et al.*, 2014). Despite this, Cobb *et al.* (2003) have shown that corals can provide useful insights and they can plug gaps in spatial coverage where terrestrial archives are lacking. This study does however sit in the North Pacific Ocean and whilst it may be influenced by shifts in the ITCZ, it is well beyond the influence of the SPCZ.

In the western South Pacific, a more recent study that looked at the climatic context for the second wave of migration into Polynesia suggested that a prolonged drought in the tropical South Pacific was occurring when humans started moving eastward into Polynesia (Sear *et al.*, 2020). Evidence from three different sites across the South Pacific including Vanuatu, Samoa and the Cook Islands, all indicated that around 900-1000 AD there was a notable shift towards drier conditions at the start of the MCA. These records are also supported by a robust chronology that provides confidence in the timing of these

changes. A record from Samoa and the Cook Islands found that between 1700 -725 yr BP there was a significant northward shift in the ITCZ and SPCZ axis moved southwest. This would have brought about drier conditions in the Cook Islands but wetter conditions for Samoa based on Ca/Ti ratio and total organic carbon data respectively (Hassall, 2017) in contrast to Sear et al (2020). Another study in this region conducted by Maloney et al (2022) has produced records of changing precipitation by using  $\delta D$  in dinosterols primarily in the western South Pacific with sites in Samoa, Vanuatu and Wallis islands. They also found that drier conditions dominated throughout the MCA across their three sites but data from Vanuatu and Samoa showed they experienced a 17-19‰ shift in values towards drier conditions whereas the data from Wallis and Futuna only showed a maximum 8‰ shift. This indicates that whilst dry conditions may have dominated this region during the MCA, not all archipelagos experience the same major changes in precipitation. A number of the records from the Maloney et al (2022) data are produced from the same sequences utilised in Sear et al (2020) so this study benefits from the same robust chronology that provides confidence in the timing of these changes. The study from Fournier Swamp by Wirrmann et al (2011) in New Caledonia sits in contrast to the rest of the west South Pacific by suggesting that wetter conditions predominated the period between 1800-900 cal yr BP which covers the start of this second migration wave into Polynesia. However, they do note a “global phenomenon” at 1080-750 cal yr BP but attribute it to wetter conditions evidenced by the development of mangroves which is then followed swiftly by a change to drier conditions from 750 cal yr BP. This disparity in terms of the timing of wet/dry shifts could be due to age model issues as these changes are noted in a core sequence that had problems with remobilisation.

In the central South Pacific, the Apu Bay record from Tahaa, indicated that French Polynesia experienced a wetter MCA, which sits in stark contrast to other records from the Pacific. This is because Tahaa sits on the NE fringes of the SPCZ, so conditions were wetter in French Polynesia during human migration into eastern Polynesia and this sequence also suggests that there was also a decline in hurricane activity providing a higher chance of voyaging success. A northward shift in the SPCZ axis as suggested by Hassall (2017) could explain the higher rate of rainfall for French Polynesia that usually sits to the northeast of the typical SPCZ axis. Similarly, tree ring records from the fringes of the Pacific basin were found to be strongly connected to SPCZ dynamics and identified

the MCA as dry, El Niño dominated period with extreme multiyear eastward shifts in the SPCZ (Higgins *et al.*, 2020).

In the Northern South Pacific, a study from a lake on Kiritimati Island, Kiribati utilising geochemical and sedimentological data to reconstruct climate over the last 1000 years. This record is congruent with the records from the west South Pacific with dry conditions during MCA from 900 to 1200 AD (Higley, Conroy and Schmitt, 2018). This record corroborates the theory of a more northerly ITCZ during this time though the timing of this change could be disputed as the age model has large errors particularly around the LIA period.

In the eastern South Pacific, on Easter Island all the palaeoenvironmental records have a hiatus from approximately 4410-770 yr BP. Mann *et al.* (2008) suggested that following the end of the hiatus around 770 yr BP, close to the end of the MCA, conditions were likely wetter as the lake levels rose again allowing sedimentation to restart but additional data on the climate signal beyond this is inconclusive due to human activity. Work conducted by Sáez *et al.* (2009) agreed and found that the MCA was a drier period as indicated by the hiatus but the end of the MCA was likely a more humid period as evidenced by vegetation changes in that part of the sequence.

In the Galapagos, multiple studies have been conducted on Lake El Junco located on the island of San Cristobal. The study by Conroy *et al.* (2008) found that overall, there is a pattern of increasingly wetter conditions through the Holocene in the eastern Pacific. Zhang *et al.* (2014) found that there was then a shift to more frequent and intense El Niño events from 1000 yr BP for 400 years. Results from a study by Atwood and Sachs (2014) found that prior to the start of the MCA there was a wetter period from 1450-1250 yr BP which represents the wettest part of the entire record but found similar pattern with drier conditions dominant in the period 1000-800 yr BP likely due to the ITCZ migrating northward during this time. Another record from the Bainbridge Crater, from Isla Santiago within the Galapagos, suggests that there was a notable increase in the frequency of ENSO events from around 2000 – 1750 yr BP for at least 1000 years till 700 yr BP during the MCA (Thompson *et al.*, 2017).

### 2.5.2.2 Little Ice age to present

In the western South Pacific, there are studies that focus particularly on deriving a precipitation record in the South Pacific using speleothems in Niue, Vanuatu and the Solomon Islands (Rasbury and Aharon, 2006; Partin *et al.*, 2013; Maupin *et al.*, 2014). These types of archives are particularly useful as they often provide a high-resolution record of climatic change, but like coral, also only cover a relatively short time period. For example, the record from the Solomon Islands has a sample resolution of four months but going back only 600 years (Maupin *et al.*, 2014). It does however contain the LIA period and shows that conditions during this time were initially drier than present with conditions getting progressively wetter from 1400 AD but difficult to tell as variability across the record makes the shift subtle. Another record from Vanuatu offers a 446 year sequence with a sub-annual resolution and similarly finds that conditions were slightly drier and more variable than average during the LIA due to an equatorward shift in the SPCZ (Partin *et al.*, 2013). The record from Niue has hiatuses where sedimentation stopped. These records have provided useful climatological data over the period following the initial colonisation of Polynesia to provide a full picture of climatic change during this period. However, it is essential to develop long-term precipitation records in the SPCZ region and South of the SPCZ region which are areas most heavily impacted by drought and also place the changes during the LIA into a longer-term climatic context.

The study carried out by Maloney *et al.* (2022) that included records from Samoa, Vanuatu and Wallis and Futuna using dinosterols also included observations on the LIA. Overall though, there is a lack of cohesion between different records in relation to the LIA. The Uvea sequence from Wallis shows a subtle u-shaped pattern of precipitation across the LIA with wetter values as the LIA starts and ends but slightly drier mid-LIA values. Whereas the Samoa and Vanuatu sequences both show a much more substantial shift from wet to dry conditions and back during the middle of the LIA. Though the LIA wet-dry changes are all still wet relative to the conditions at the start of the MCA. The study conducted by Hassall (2017) contrastingly shows that the SPCZ was in a more NW position during the LIA with drier conditions noted in Samoa during this time and wetter in the Cook Islands. Whereas, the record from Emaotfer swamp suggested an increase in El Niño events from 1000 to 300 yr BP across both the MCA and LIA, which typically indicates dry conditions throughout for Vanuatu (Wirmann, Eagar, *et al.*, 2011). The

contrast between these records shows that conditions through the LIA were variable across this region.

In the central South Pacific, the Apu Bay record indicated a drier LIA in contrast to other records, specifically those in the western South Pacific. However, another study from the central South Pacific by Sachs et al (2009) used microbial mats, molecular and isotopic indicators of rainfall from Washington Island to build long-term precipitation records. They found that conditions were dry all the way through from 980 AD possibly to 1640 AD or even late eighteenth century, which covers both the MCA and LIA. Though it is important to note that the LIA shows a major shift toward drier values around 1400 AD compared to those from the MCA, so this represents a shift from dry to drier conditions, which is on trend with the record from Apu Bay. This work was then built upon by Smittenberg et al (2011) who further developed the record from Palau to generate an approximately 10,000 year old record from the marine spooky lake using hydrogen isotopic ratio ( $\delta D$ ) of lipids. They presented only two sections of the sequence covering the early Holocene and the LIA with a substantial gap in the middle. They found that either a more El Niño like mean state dominated during the LIA or there was a more southerly mean latitude of ITCZ which presented with greater SPCZ rainfall and lower ITCZ rainfall perhaps accounting for the differences between Apu Bay and Washington Island. However, since the LIA there has likely been a Northern migration of ITCZ. Another record from the central South Pacific - a lake sediment record from Kiritimati Island - found that during the LIA there was a change towards conditions similar to modern between 1200 to 1400 CE and shift to even drier in Washington Lake at 1420 CE suggesting a southward shift of ITCZ near the beginning of the LIA.

From the eastern South Pacific, the records from Lake Raraku on Easter Island found that following the drier MCA, there was a shift from around 1150 AD to a more humid environment that allowed for peat deposits to start forming again and then wetter conditions with the start of the LIA (Sáez *et al.*, 2009; Cañellas-Boltà *et al.*, 2012). The records from El Junco in the Galapagos by Zhang et al (2014) and Atwood and Sachs (2014) similarly found that the strong and frequent El Niño events persisted through the MCA into the LIA with an even wetter pezriod around 600-650 yr BP just prior to the onset of the LIA after which drier conditions have persisted from 200 yr BP till present. The Bainbridge Crater Lake record shows siliciclastic laminae and an increase in pollen

concentration from 410 to 330 yr BP, which indicates wetter mid-LIA conditions but otherwise conditions from the end of the MCA to present was characterised by low ENSO activity and drier conditions from 300 yr BP until 50 yr BP. This is evidenced by gypsum deposits and the lack of diatoms in the record but in the last 100 years conditions have become wetter and the frequency of El Niño events have increased (Thompson *et al.*, 2017). There is disagreement between the record at Bainbridge Crater and the other records from the Galapagos, primarily over the timing of certain changes which Thompson *et al.* (2017) has put down to a lag in the response of highland sites compared to lowland records such as this one. There is some disagreement between the Atwood and Sachs (2014) record and the one from Conroy et al (2008) from the same El Junco site – Atwood and Sachs (2014) suggest higher El Niño rainfall from 700-100 yr BP (1250-1850 AD) whilst Conroy et al's suggests rainfall intensity similar to or lower than modern conditions. Also Conroy et al has the maximum amount of sand at 2000-1600 yr BP (50 BC to 350 AD) interpreted as high rainfall - but this is not mirrored in El Niño rainfall index from Atwood and Sachs (2014).

A study conducted by Atwood et al (2021) looked to compare palaeo data and model outputs of tropical hydroclimate over the past 2000 years. The study heavily focuses on continental sites where Monsoon systems play a prominent role in the hydroclimate and the number of sites within the tropical South Pacific included in the comparison is low. They remark that the LIA signal is absent in terrestrial records from the maritime continent which is inconsistent with a number of terrestrial studies from across the maritime Pacific (e.g. Sachs *et al.*, 2009; Partin *et al.*, 2013; Maloney *et al.*, 2022). For the MCA, both model and data agree that conditions were dry in the Eastern Pacific and Mesoamerica from 800-1000 AD. When comparing the palaeo data and some CESM models they found that conditions were wetter during the LIA in the maritime continent (western pacific) and dry conditions dominated in the central tropical pacific. However, there is a discrepancy between data and model outputs for the eastern pacific as the Galapagos data indicates wetter conditions with LIA whilst models indicate drying or no change.

Higley et al (2018) also offer a synthesis of hydroclimate Pacific palaeo records that cover the MCA-LIA period and suggest that there is no “consistent spatial or temporal pattern of variability” during this time (Higley *et al.*, 2018, p. 354). However, this study shares a

similar flaw in that there are only four records included in their synthesis within the maritime Pacific and of those only two are in the central Pacific, the rest come from the Galapagos - which sits on the eastern fringes of the basin - and continental records. Records from the Galapagos are useful particularly in relation to the reconstruction of hydroclimate and ENSO but should not be used in place of records from the Pacific islands. The effects of El Niño events are difficult to quantify and these records are providing a more qualitative record of ENSO activity (i.e., stronger vs weaker, increase and decrease). Depending on the type of El Niño event (e.g. cold tongue, warm pool) – see Table 2.1 - each can have a very different effect in terms of short-term changes to climate. Depending on where an island sits upon the SPCZ axis can mean drastically different climate signal. Therefore, it is important to build up local records to quantify the changes across the basin over time.

To summarise, the timing of the second wave of human migration coincides with the start of the MCA, approximately 900-1000 yr BP. During this time the western South Pacific and Easter Island became drier but areas in the central South Pacific and the Galapagos became wetter likely due to a northward expansion of the ITCZ and shift of SPCZ northward also (Sear *et al.*, 2020). Whereas, during the LIA conditions were reversed with generally wetter conditions in the western South Pacific and Easter Island and drier in the central and eastern Pacific. Though it appears that climate during the LIA was variable and different archipelagos experienced a slightly different pattern of change during this time, which was possibly dependent on where they sat in relation to the SPCZ.

Data-model comparisons or data synthesis from the tropical South Pacific can prove inconclusive (e.g. Smittenberg *et al.*, 2011; Atwood *et al.*, 2021) though this is due in part to the inability of models to represent SPCZ dynamics (Brown *et al.*, 2020) but also the lack of palaeo records from island archives utilised as part of the comparison or synthesis and an over-dependence on continental records. For example, for the tropical Pacific region the data-model comparison by Atwood *et al.* (2021) had only two records covering the South Pacific and one for the central Pacific, this would not provide a representative picture of regional climate so their model comparison is dominated by continental records. A comparison between these types of records should be done with care as sites that are either on or near continents will have different types of processes influencing their archives that are controlled by a mix of similar and different processes to those of

Pacific Islands (Ramage, 1995; Neale and Slingo, 2003; T. Schroeder, 2009; Holden, 2017). The South Pacific is a vast space and it would be incorrect to assume that records from the periphery of the basin are representative of the whole region. The SPCZ dominates the climate system in the tropical South Pacific and palaeo records from Pacific Islands are uniquely placed to capture this and how it has changed through time. However, there has been some success using remote records to reconstruct aspects of South Pacific climate. Higgins et al (2020) compared tree-ring records with instrumental SPCZi and model outputs and found that remote tree ring records were able to reconstruct 58% of the variance in the instrumental record and offered insights into changes during the MCA and LIA in the tropical South. However, Higgins et al (2020) admit that movement in the location of the SPCZ over the MCA may not be due to ENSO but instead related to shifts in ocean-atmospheric patterns. This highlights the importance of the development of long-term records from islands within the tropical South Pacific to continue building our knowledge on Pacific hydroclimate in order to continue developing models that can properly represent SPCZ dynamics.

When discussing climatic change over the late Holocene in relation to human activities and societal change it is important to have relevant records in the associated regions but it is also vital to have a robust chronology to be able to tie together climate and archaeological records in the Pacific (Field and Lape, 2010). The example from the Fournier Swamp in New Caledonia (Wirrmann *et al.*, 2011) showed how errors in the chronology can shift our understanding of the timing of change and can make it difficult to draw connections between different types of records such as palaeoenvironmental and archaeological.

It is clear from Figure 2.7 that there is disagreement between different records within the same regions of the Pacific. This can be due to a range of issues such as dating error, local vs regional signals, misinterpretation etc. As discussed, records from the same region or even the same site can provide conflicting data (e.g. Conroy *et al.*, 2008; Atwood and Sachs, 2014; Maloney *et al.*, 2022). Having a good range of palaeoenvironmental records both temporally and spatially allows for inter-comparison between different archives (e.g., Easter Island) and can provide certainty where archives disagree (e.g. Galapagos Islands). The relative scarcity of records that date back beyond the Common Era, i.e., the last 2000 years, makes it difficult to make a full assessment of what the climatic context of the first wave of migration looked like. More work is required to produce records that

extend back further to fill this gap. For the second wave of migration, the complexity lies in understanding where the spatial boundary sits between wet and dry. Even within the western Pacific, records from the same region show different rates of change through the MCA and the LIA (Maloney *et al.*, 2022), which cross over with key archaeological/social changes in the tropical South Pacific. More work is also required to provide clarity in regional changes during this period. To be able to draw conclusions about how climate may have influenced human/society activity, it is vital to have reliable and accurate reconstructions of South Pacific palaeoclimate covering the past 3,000 years (Allen, 2006).

## 2.6 Modelling prehistoric societies

Archaeological studies have provided us with a wealth of information about prehistoric island life, and climatic/environment palaeo-reconstructions, allowing us to test these changes against possible drivers such as climate. The development of digital technologies over the decades has made modelling of systems easier with accessible user-friendly visual interfaces that allow researchers to reconstruct the dynamics of prehistoric societies in a formal and systematic way (Barton *et al.*, 2012; El Sawah *et al.*, 2017).

Computational models can be particularly useful in archaeology where it is not possible to go into the field and make direct observations as the objects of study are buried in time. Narratives of social change can be tested and become the subject of experimentation. Archaeological data can be used to suggest parameters for the models and the outputs truth-tested against empirical data and current working theories of how the socio-ecological system functions (Barton *et al.*, 2012). Models have been developed to investigate prehistoric societies worldwide covering topics such as the collapse of the Kayenta Anasazi in Long House Valley, Arizona (Axtell *et al.*, 2002) and the Maya civilisation from Central America (Heckbert, 2013; Kuil *et al.*, 2016) and in the Pacific region as well. Examples include Erickson and Gowdy's (2000) study identifying how institutional change in Tikopia and Easter Island affect the relationship between natural resources systems and population growth and the connection between human behaviour of the Tsembaga and environmental degradation in New Guinea (Anderies, 1998) as well as many others, some of which will be more closely examined here. It is also worth mentioning those studies that utilise GIS based software to understand societal behaviour

and change as it is still a form of formalising these systems using computational methods. Examples of these studies include the development of social complexity and fortification building in Fiji (Field, 2004), land use and settlement patterns through time and space in Easter Island (Mulrooney, 2013) and reconstructing agricultural strategies in Samoa (Shapiro, 2020). In this section however, we will look at the development of socio-ecological models that focus on prehistoric island life in the tropical South Pacific and how these have developed over time.

As with the palaeoclimatic records, modellers have also been drawn to the mystery of Rapa Nui (Easter Island). A wave of papers modelling Easter Island started with the original Brander and Taylor paper (1998) which proffered an adapted predator-prey model to help understand population dynamics and attempt to uncover the mystery of Rapa Nui. It inspired a host of new studies using their model as a base (e.g. Dalton and Coats, 2000; Erickson and Gowdy, 2000; Reuveny and Decker, 2000; Pezzey and Anderies, 2003; Dalton, Coats and Asrabadi, 2005). However, most of these models were seeking to develop the original model further by including elements of resource management, human behaviour and developing institutions rather than environmental factors. There has been perhaps too much focus put on one island amongst thousands as many researchers have been keen to draw parallels between the socio-ecological disaster of Easter Island and global patterns of human-environment interconnections (Kirch, 1997; Rainbird, 2002; Brandt and Merico, 2015). Island abandonment or what could be considered societal collapse – at least on an island scale – occurred on the islands of Pitcairn and Henderson (Anderson, 2001). Both of these islands sit on the path between western and central Polynesia and Easter Island but have had little attention whereas Easter Island has been continuously occupied by humans since colonisation but has received a great deal of attention likely due to its use as a modern analogue and the alluring and unique Moai statues.

However, despite earlier models focusing on population dynamics and societal behaviour and change, a model developed by Brandt and Merico (2015) that builds on work done by Basener *et al.* (2008) also focuses on Easter Island but builds in an agricultural component as well as the introduction of rats to the island as per the Basener *et al.* (2008) model. They also compare model outputs to radiocarbon datasets, which are used in the study as a proxy of clearance rates. The Brandt and Merico (2015) study considers carrying

capacity as a control on population and their model starts to consider the environmental context more than any of the previous models. Nevertheless, a majority – if not all - of the Easter Island models that look at this island as a socio-ecological system, do not consider climate but instead suggest that human society, their activities and behaviours are the main sources of change on the island (Merico, 2017). There is a research bias amongst archaeologists and anthropologists to overemphasise the influence of human society within a system and provide little or no environmental context as this is not the lens they typically use to view their field of study (Allen, 2006). As discussed in section 2.3.4, climate has played a role in prehistoric Pacific island life, though to what extent is contested. It would be fair to comment that not incorporating climate into a socio-ecological model focused on tropical South Pacific islands would be a serious omission of an important variable in the study of an agriculturally dependent prehistoric society.

An example of a model focusing on socio-ecological island systems in the South Pacific comes from Hamilton and Kahn (2007) who presented a population model based in a space-limited environment e.g. an island. They applied this model to the 'Opunohu Valley on Moorea, French Polynesia. They built in a more complex agricultural aspect compared to those produced for Easter Island, which considers the multi-cropping characteristic of the Polynesian agroecology. Using the model, they calculated the carrying capacity of the 'Opunohu Valley based on the amount of food that can be produced if all cultivable land was utilised. The model was later built upon by Puleston and Tuljapurkar (2008) who included a more complex breakdown of population age classes which overall increases the carrying capacity of the island as children and elderly would require a lower calorie intake compared to adult workers. The work done by Hamilton and Kahn (2007) and Puleston and Tuljapurkar (2008) raises the interesting question of what other factors play into the carrying capacity of a finite space. Both models calculate carrying capacity based on the agricultural production of the area. Agricultural production is dependent upon a range of environmental factors including soil, nutrients and climate, which are not represented in these models.

An example of a model that includes those environmental factors that control agricultural yield is the study from Kirch et al (2012) presenting the Hawai'i biocomplexity project. The multi-disciplinary Hawai'i biocomplexity project looks at modelling the impact of agricultural intensification on population dynamics but concentrates on the leeward

Kohala field system from Hawai'i Island. The model includes an element of climate as part of its productivity calculations, but it is focused on agricultural intensification as the main driver of change in the area. A limitation of the study is its narrow focus in terms of space and the absence of climate as a driver similar to other Pacific socio-ecological models. This study does however consider the wider environmental context as part of the model. In Hawai'i, like other Pacific islands, the rainfall is variable. Even within individual islands, the rainfall is highly variable due to the high elevation of the islands creating large contrasts between the windward and leeward sides of the islands and this is represented in this model to help calculate agricultural yield. However, the rainfall record used as part of this study is a historical one rather than a palaeoclimate reconstruction due to the availability of data. The model provides useful insights into the potential impact of the intensification of agriculture on the Kohala region, but it makes it difficult to draw connections between the archaeological and climatological records over the prehistoric period as it does not include climate data covering that period.

Other models have looked at the impact of climatic change on an agriculturally dependent prehistoric society. Kuil *et al.* (2016) developed a socio-hydrological model to identify the impacts of changing climate - but in particular rainfall - on food availability and the influence this may have had on the collapse of the Maya civilisation. The main aim of the model was to identify the role of reservoirs that the Maya built to handle times of water stress and how the population dealt with drought both with and without reservoirs. The model also utilises palaeoclimatic records to drive their model allowing them to explore their hypothesis around drought and the collapse of the Maya civilisation. Whilst this model assesses just one aspect of socio-hydrological dynamics (the role of reservoirs), it is a good example of how palaeo-climatic archives and modelling can come together to help answer archaeological questions.

To date, a model focusing on the hydrological record and how it might impact on human society has not been produced for the South Pacific region. The studies examined in this section have shown the development of socio-ecological models of the tropical South Pacific region and elsewhere, but each has limitations that are holding back insights into the connection between climate and prehistoric Pacific society. A model similar in format to the Kuil *et al.* (2016) is currently missing from the modelling literature surrounding the tropical South Pacific.

### 2.6.1 Approaches for modelling of socio-ecological systems

There is a substantial amount of literature surrounding the modelling of socio-ecological systems, particularly surrounding regime shifts or as part of an integrated environmental assessment. Primarily these types of study focus on modern day socio-ecological systems that are looking to represent current environments to understand how stakeholder/management decisions or environmental change will impact on these systems however they have also been applied to prehistoric societies (Barton *et al.*, 2012). As discussed in the previous section, modelling can be a useful tool in the field of archaeology to help build our understanding of past societies but also the socio-ecological systems that they were a part of (Barton *et al.*, 2012). There are a number of approaches to model prehistoric societies and socio-ecological systems though here the focus will be on agent-based models and system dynamics models, which are prominent in the literature. Other modelling approaches that can be used to understand socio-ecological systems include statistical, equilibrium, coupled component, knowledge-based models and Bayesian networks which will also be discussed briefly.

#### 2.6.1.1 Agent-based

Agent-based models (ABM) as the name suggests constructs a simulated space in which a number of agents are able to interact amongst one another and their environment. The agents act as autonomous entities that interact or communicate according to a set of predefined rules (Ding *et al.*, 2018). Agents within the model can change their behaviour based on changes to their environment either through action or adaptation. ABMs are particularly useful for systems where multiple stakeholders test the impact of policy decisions and are used to understand the result of interactions between and learning of different model agents (Schulze *et al.*, 2017). There are a range of software available to develop ABMs including Cormas, NetLogo and Repast or alternatively ABM can be developed using programming languages such as C, Java and Python (Kelly *et al.*, 2013; Ding *et al.*, 2018). The difficulty with ABMs is that they require detailed data on the processes in order to parameterise the model as incomplete information can lead to inaccuracies in prediction and forecasting and excluding those processes with limited data can lead to poor outputs and inhibits the social learning aspect of the model (Kelly *et al.*,

2013). The models tend to be highly complex, require high levels of computational resources and generate irreproducible outputs (Kelly *et al.*, 2013; Schulze *et al.*, 2017). However, those irreproducible outputs are also known as emergent behaviour and can prove to be more useful than those models where the behaviour is summarised across significant aspects of the system (Jakeman *et al.*, 2006). ABMs are also not as adept at simulating feedback loops (Kelly *et al.*, 2013) – which are important in socio-ecological systems - as other modelling approaches. There has been a rise in the number of studies utilising bottom-up models such as agent-based modelling to understand prehistoric socio-ecological systems (Perry and O’Sullivan, 2018). The MayaSim model developed by Heckbert (2013) provides one example of an agent-based model used to look at prehistoric socio-ecological system and the collapse of the Maya civilisation.

### 2.6.1.2 Systems dynamics

Systems dynamics (SD) has been around since the late 1950s. It was coined by Jay Forrester during his time at Massachusetts Institute for Technology and was first called “industrial dynamics” (El Sawah *et al.*, 2017). Despite being originally developed to model business growth, SD has acted as one of the primary forbearers of socio-ecological modelling. In 1972, in their book *Limits to growth*, Meadows *et al.* utilised SD to demonstrate how policy impacted on socio-ecological systems. This put SD forward as an effective tool to model socio-ecological systems and develop our understanding of them and to this day, SD is still widely used for this purpose (El Sawah *et al.*, 2017). The concepts of SD are derived from fields such as mathematics, engineering and physics making them interdisciplinary in nature (Sterman, 2002). The modeller can formalise a conceptual model of a system using SD software and appropriate differential equations to create a computational representation of the system they are studying - see Figure 2.8 (Kelly *et al.*, 2013; Filatova, Polhill and van Ewijk, 2016). The different parts of the system are represented using a combination of “stocks” which can also be known as accumulators or levels that essentially represent the different variables and “flows” also known as rates which represent the processes that alter the stock elements of the model (Kelly *et al.*, 2013; Filatova, Polhill and van Ewijk, 2016; El Sawah *et al.*, 2017). SD is also useful for representing feedback loops in systems between variables and often where one

variable feeds back into itself (Filatova et al., 2016). The benefits of using SD is that it provides a tool that allows users to develop a better understanding of the system they are studying and how it works (El Sawah *et al.*, 2017). It enables users to determine system thresholds and shifts in the system state between stable and unstable. A number of SD software are available (e.g., Vensim, Stella, Powersim) that provide a graphical interface that is easily accessible to those without coding skills and they do not require a high level of computational resources to run. However, one of the pitfalls with SD is that the user-friendly interfaces encourages model over-complexity (Kelly *et al.*, 2013). Also, similar to statistical and equilibrium models, SD is not typically able to deal well with spatial scale change. SD are typically fixed in terms of model structure and are not able to develop naturally unless parameters are changed which alter the overall structure of the model (Heckbert (2010) in (Filatova, Polhill and van Ewijk, 2016)). For understanding the interactions between humans and the environment in the past, system dynamics models are ideal as they can fill the gaps where archaeological and palaeo-data are typically either proxy derived or come with a certain level of uncertainty, SD provides the method to test assumptions and theories.

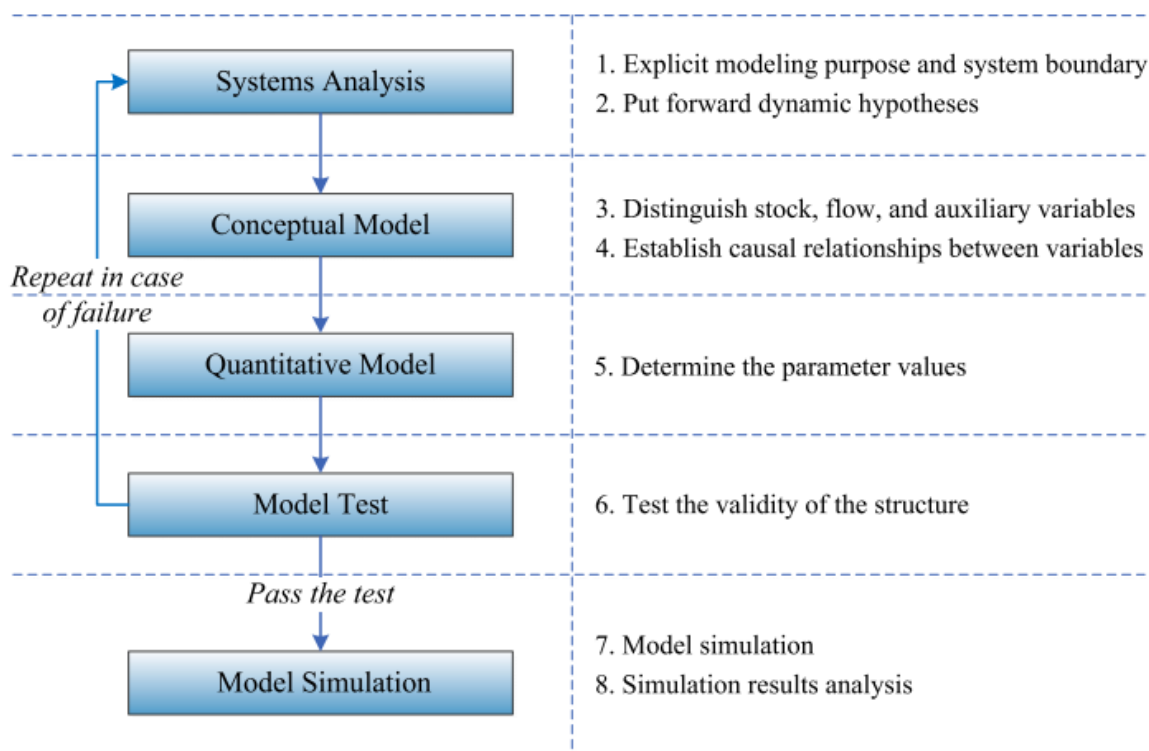


Figure 2.8: Flow chart for developing a system dynamics model - taken from Ding et al (2018)

An example of the use of system dynamics modelling in the prehistoric Pacific comes from the adapted version of the predator-prey model, specifically the Lotka-Volterra model - though often described as a 'dynamic' model - especially for Easter Island with the original Brander and Taylor paper (1998) inspiring a whole host of new studies using their model as a base (e.g. Dalton and Coats, 2000; Erickson and Gowdy, 2000; Reuveny and Decker, 2000; Pezzey and Anderies, 2003; Dalton, Coats and Asrabadi, 2005) and added on aspect that dealt with resource management, changing human behaviour and developing institutions.

### **2.6.1.3 Other modelling approaches**

There are a range of other modelling approaches that are less frequently used that will be introduced and assessed in this section. These include statistical models, knowledge-based models (KBM), Bayesian networks (BN) and coupled component models (CCM).

Statistical models identify socio-ecological change through statistical analysis of time-series data. An advantage of using statistical models is that they can uncover correlations between variables within the model and explain the causal processes (Filatova, Polhill and van Ewijk, 2016). However, the disadvantage of statistical models is that they have the capacity to become overly complex and they require large data sets that provide a time series for both dependent and independent variables (Filatova, Polhill and van Ewijk, 2016). Statistical models are particularly good for studying ecological regime shifts but currently have only been tested on this aspect of socio-ecological modelling so there is uncertainty as to the ability of statistical models to represent other elements of socio-ecological systems (Filatova, Polhill and van Ewijk, 2016). This type of model was used to reconstruct the impact of climate change in Europe from 1500-1800 AD and how it led to socio-ecological catastrophes using a series of long time series historical data (Zhang *et al.*, 2011). A statistical model could be an effective method to reconstruct past socio-ecological systems where excellent long-term data sets are available but particularly where systems are prehistoric, reliable and consistent data is not always available.

Knowledge-based models (KBMs) are a type of model that utilises a series of known facts and rules about how the system works that are then formalised into a logic-based model

(Kelly *et al.*, 2013). The advantage of KBMs is that they learn how the system works directly from the user rather than the data which is then formalised in a series of rules that explain how the system works within the model (Yan *et al.*, 2006; Kelly *et al.*, 2013). The disadvantage of KBMs is that to keep them relevant, the knowledge that informs the model needs to be kept up to date so that it provides a true representation of the system. Also, it is not always possible to formalise complex systems into a knowledge-based model. An example of a KBM that has been used in socio-ecological context comes from Giordano and Liersch (2012), who utilised technical knowledge from the local community in Uzbekistan in conjunction with a GIS-based system to monitor river basin soil salinity. However, KBM are not likely to be suitable for palaeo/archaeological modelling as KBM requires knowledge for all relevant processes and components before they can be constructed as part of the model.

Bayesian networks are a form of statistical multivariate model that produce probabilistic graphical outputs, but unlike SD, is typically unable to model dynamic feedback loops (Aguilera *et al.*, 2011; D. N. Barton *et al.*, 2012). The connection between one variable and another is either where one influences or is influenced by another within a BN model, there is never a two-way relationship between them (Barton *et al.*, 2012). The advantage of using BNs is that they are able to overcome potential gaps in data for variables by bringing together a range of information to determine the likely relationship between variables (Chen and Pollino, 2012). They are also useful for developing a deeper understanding of the individual components of complex causal chains by dealing with them each separately (Kelly *et al.*, 2013). The downfall of BNs is that in order to be used in a practical way, they often need to break down continuous variables into a discrete form which notably decreases the precision of variable relationships built into the model that in turn result in inaccurate model outcomes (Kelly *et al.*, 2013). Bayesian networks would be useful in archaeological-based research - where there is likely to be ambiguity and gaps in the data - as it is able to deal with uncertainty and can assign probability to outputs (Till *et al.*, 2018). However, the inability of Bayesian networks to deal with feedback loops makes it a difficult approach to utilise in the study of socio-ecological systems, which often has to deal with these kinds of processes. Bayesian network models has been used to study prehistoric socio-ecological system from the Iberian Peninsula but specifically the study was interested in the advent of farming in the region and utilises the

Bayesian networks aspect on both independent and dependent variables (Palacios, Barcelo and Delgado, 2022).

As the name suggests, Coupled-component models (CCM) combines different model approaches - such as the ones already described in this section - to create a hybrid model that is able to handle an interdisciplinary system that draws on “social, economic and biophysical components” (Kelly *et al.*, 2013, p. 172). The benefit of using CCM is that it is possible to incorporate dynamic feedbacks as part of CCM and provide detailed portrayals of individual components and how they tie together. Due to this though, a disadvantage of CCM is that the breadth of their scope can be limited if the components are presented with a high level of detail (Kelly *et al.*, 2013). An example of the use of CCM in socio-ecological systems is the project MedLand that utilises components that represent small-holder farming, landscape evolution and vegetation change to study the interaction between social and environmental processes throughout the Anthropocene (Barton *et al.*, 2016). CCM are useful for studying past socio-ecological systems but typically only within a finite scope, such as the Hawai'i biocomplexity project which focuses down on the leeward Kohala field system, one subset of the agricultural system of the island (Kirch *et al.*, 2012). Where a study would benefit from a wider breadth of scope, alternative methodological approaches may be required.

In summary, there are a number of modelling approaches available and each offers its own advantages and disadvantages. In terms of modelling a prehistoric socio-ecological system, Agent-based and statistical models are not suitable as they require detailed data (Kelly *et al.*, 2013; Filatova, Polhill and van Ewijk, 2016) of a quality and length that is not possible when studying pre-contact societies. KBM models similarly require knowledge for all relevant processes and components (Kelly *et al.*, 2013) whereas SD models do not need that same level of detail and can fill the gaps where archaeological and palaeo-data are lacking (El Sawah *et al.*, 2017). SD provides the method to test assumptions and theories on systems we do not fully understand. Bayesian models likely offer the best alternative modelling approach as they can deal with uncertainty and produce probabilistic graphical outputs. However, SD models are able to incorporate feedback loops whereas Bayesian models are not, which are an intrinsic aspect of socio-ecological systems (Aguilera *et al.*, 2011; Barton *et al.*, 2012). This makes SD the ideal approach for developing a socio-ecological model of prehistoric island dynamics.

## 2.7 Summary

Climate has been cited as a potential driver of migration (Duprey *et al.*, 2014; Cochrane, 2018; Sear *et al.*, 2020) as well as other aspects of prehistoric Pacific island life including, voyaging (Anderson, Chappell, *et al.*, 2006; Goodwin, Browning and Anderson, 2014), diet (Kirch, 1994; Allen and Wallace, 2007) and conflict (Kirch, 1984, 2017b; Nunn, 2000a; Field and Lape, 2010).

Pacific precipitation is primarily regulated by the SPCZ, which in turn is controlled by a range of climatic oscillations such as the El Niño Southern Oscillation that cause significant shifts in rainfall patterns on an inter-annual basis. Palaeo-climate records from the region have provided evidence of a highly variable climate through the past 3,000 years with multiple shifts from dry to wet conditions during the Late Holocene. There is clearly some ambiguity surrounding the climate beyond the past 2,000 years, but specifically the first wave of migration into remote Oceania and the rate and extent of change during periods such as the MCA and LIA during the second wave of migration into Polynesia and subsequent settlement in the region.

Archaeological records from this region are growing and the South Pacific was one of the final regions on Earth to be colonised by people (Kirch, 1997) so human history in this region is not as deeply buried in time as other parts of the world. This offers a unique opportunity to study human-environment interactions in this region. From the extensive archaeological records coming from the Pacific the review of different aspects of Pacific island life such as diet, migration, voyaging and conflict all point towards the influence that climate has on each of these elements.

Relatively little work has been done on modelling prehistoric Pacific island life and it is clear that a socio-ecological model that utilises palaeoclimatic data to reconstruct the impact of climatic change on prehistoric Pacific island life, is currently missing from the literature. The palaeoclimate literature from the tropical South Pacific clearly outlines how variable precipitation has been in this region over the past 3,000 years and archaeological literature outlines how climate has played an important role in Pacific island life prior to European contact. New work is required to combine this element into a model to reconstruct the consequences of changing climate on prehistoric Pacific island life.

## Chapter 2

The modelling literature has developed rapidly over the past few decades and now there are easily accessible and powerful tools for reconstructing past socio-ecological environments and developing our understanding of these and how different factors, such as climate, influence such societies. A range of modelling approaches are available for the study of socio-ecological systems, but agent-based and system dynamics modelling are the most regularly used particularly in relation to past systems and also are supported by accessible and user-friendly software and support. Other modelling approaches include statistical, knowledge-based, Bayesian network and coupled-component. Each approach has benefits and trade-offs that need to be considered when designing a modelling approach to tackle a research problem. For the prehistoric tropical Pacific where there is not a good breadth of time series data, gaps in both knowledge and data for all variables and a need for breadth of scope then an approach like System Dynamics is likely to be the best solution.

## Chapter 3 Aims and Objectives

### 3.1 Introduction

The purpose of this study is to reconstruct climate over the past 3,000 years with the aim to tie together climate and archaeological records to understand whether climate, but specifically drought, played a role in the timing of human migration and subsequent colonisation of islands in the tropical South Pacific. This study focuses on the past 3,000 years, which is important, as this encompasses both phases of migration within the Pacific islands (approx. 3000 and 1000 yr BP). The development of 3,000-year palaeo records in key archaeological locations would allow a comparison with archaeological records including the known periods of migration and colonisation to test the specific human–climate interaction in the South Pacific using this site-specific concept (Blockley *et al.*, 2018). As discussed in the literature review, there is a scarcity of palaeoclimatic records from the Pacific region dating back to the first wave of migration into remote Oceania and there is a level of ambiguity surrounding the rate and extent of rainfall changes around the second wave of migration into Polynesia. Whilst there has been an increase in the number of records coming out from the Pacific region in the past few decades (Hassall, 2017) there is still a significant disparity between the Pacific and other more well studied regions such as the North Atlantic basin. Further work is required to build up our understanding of hydroclimate change over the late Holocene in the tropical South Pacific. Furthermore, modelling has proven to be a useful tool in the field of archaeology (Barton *et al.*, 2012), creating an experimental reconstruction of socio-ecological systems that we can use to test theories of social change. There are a number of examples of socio-ecological models that attempt to reconstruct some element of prehistoric Pacific island life (e.g. Brander and Taylor, 1998; Hamilton and Kahn, 2007; Kirch *et al.*, 2012; Brandt and Merico, 2015). However, to date, none have incorporated social, agricultural and climatic elements alongside palaeoclimatic data in an attempt to draw connections between archaeological data and palaeoclimatic archives in the Pacific region. There is currently a gap in the literature on how late Holocene climatic change impacted on prehistoric Pacific island life. To resolve these knowledge gaps, this thesis has the following aims:

- Reconstruct late Holocene hydroclimate over the past 3000 years from lacustrine sediments using a multi-proxy approach.
- Understand how climate likely impacted on food security and population dynamics in prehistoric Polynesia
- Assess the new and existing evidence on whether drought played a role in the prehistoric migrations within the tropical South Pacific.

To achieve the above aims, a series of objectives have been identified for this thesis which are divided into three sections – one section per aim - and are as follows:

### **3.2 Changes in hydroclimate in the tropical South Pacific during the Late Holocene**

There is a relative paucity of palaeoclimate records across the South Pacific region (Toomey et al, 2016) considering it has a larger surface area than Eurasia, the largest continental area on Earth. Many more records need to be developed in this region to help advance our understanding of climatic change through time and at a resolution that allows links to be drawn between them and archaeological records. There is a particular gap in records dating back beyond 2000 yr BP within the central and western Pacific. Furthermore, this thesis also seeks to utilise a mix of proxies including stable isotopes ( $\delta^{13}\text{C}$ ,  $\delta^{15}\text{N}$  and  $\delta^{18}\text{O}$ ), which have been used on Pacific records previously but  $\delta^{18}\text{O}$  from carbonate has not yet been used on lacustrine archives in this region. There has been a shift in recent years toward utilising biomarkers such as dinosterols and other lipids (e.g. Sachs *et al.*, 2009; Atwood and Sachs, 2014; Zhang et al, 2014; Hassall, 2017; Sear *et al.*, 2020; Maloney *et al.*, 2022). Whilst dinosterols, biomarkers and lipids are a useful proxy that have provided new data from challenging archives, they often come with large error bars both on isotopic and age values due to the amount of sediment required. Additionally, relatively little is known about the modern contexts of these proxies so there are a number of unknowns in terms of lake-specific effects, signal pathways and so on that limit the usefulness of dinosterols, biomarkers and lipids at this stage (Leng and Henderson, 2013; Ladd *et al.*, 2021; Maloney *et al.*, 2022). The use of a multi-proxy approach is important as it allows us to develop our understanding of local changes

within the basin and lake itself along with the response of proxies to both internal and external drivers (Birks and Birks, 2006). Therefore, in order to reconstruct late Holocene hydroclimate over the past 3000 years using a multi-proxy approach, this thesis has the following objectives:

1. Determine whether  $\delta^{18}\text{O}$  from carbonate can be used on tropical lake sediments to develop a hydroclimate record for tropical South Pacific.
2. Develop new terrestrial records from lake sediments using a multi-proxy approach including  $\delta^{13}\text{C}$  and  $\delta^{15}\text{N}$  from organic matter and inorganic stable isotopes  $\delta^{13}\text{C}$  and  $\delta^{18}\text{O}$  from carbonate, geochemistry and diatom analysis.

### 3.3 Modelling island life

As discussed in Chapter 2, modelling has been a useful tool for looking at prehistoric population dynamics (Puleston and Tuljapurkar, 2008; Roman, Bullock and Brede, 2017) and socio-ecological change (Anderies, 1998; Kirch *et al.*, 2012; Heckbert, 2013; Brandt and Merico, 2015), both globally and within the Pacific region. It has also been used to understand the role of changing climatic conditions and its impact on other prehistoric civilisations such as the Maya in central America where drought is thought to have played a role in societal collapse (Kuil *et al.*, 2016). The use of models to represent socio-ecological systems can help us to understand the impact that changing precipitation has on prehistoric Polynesian island life and resolutely tie together palaeoclimatological and archaeological data. It provides a tangible connection between palaeoclimate data and the societies that are impacted by these changes rather than qualitative observations of climatic and societal change and how they may be related. Considering this, the objectives of this thesis in relation to modelling prehistoric island life are:

3. Develop a conceptual model to represent the connections between climate, food security and the island population.
4. From 3, develop a socio-ecological system dynamics model – a relatively simplistic model that represents the key parts of the system, to see if changing these has an impact on food availability and population dynamics.

5. Dependent upon 2), use newly acquired or existing hydroclimate data to simulate the potential impacts on food security over the past 2-3,000 years to assess whether drought was a driver of human migration in the prehistoric Pacific.
6. Experiment with the model to calculate the magnitude, duration and frequency of drought required to significantly impact on food availability and population dynamics.

### **3.4 Palaeoclimate and Archaeological records of the tropical South Pacific**

Several studies have suggested that climate has played a role not only in the timing of human migration (Duprey *et al.*, 2014; Cochrane, 2018) but also on societal changes following colonisation (Nunn, 2000a; Field and Lape, 2010; Goff and Nunn, 2016). It would be valuable to provide an updated synthesis of both climate and archaeological records from across the Pacific. A synthesis of some key archaeological moments within the history of the Pacific was provided by Goff and Nunn (2016) in their discussion of using rapid societal change as an indicator for environmental change. The intent of this thesis is to expand on this to provide more examples linked to the oceanic South Pacific and link it more explicitly to climate records from the region. To this end, the objectives concerning palaeoclimate and archaeological records from the tropical South Pacific are:

7. Develop a synthesis of existing palaeoclimate records from within the tropical South Pacific relating to hydroclimate
8. Compare new data to existing records to create a comprehensive overview of changes across the Pacific during the Late Holocene.
9. Develop a synthesis of archaeological data to generate a timeline of key changes within human history of the South Pacific over the past 3,000 years but with particular emphasis on the two sites of the new hydroclimate data – Mangaia, Cook Islands and Efate, Vanuatu.
10. Assess the new and existing evidence on whether drought played a role in the prehistoric colonisation and migrations within the tropical South Pacific.

## Chapter 4 Regional Setting and Site Description

### 4.1 Introduction

The two sites chosen to meet the aims and objectives of this thesis are Emaotfer Swamp in Vanuatu located with Melanesia and Lake Tiriara in the Cook Islands located in Polynesia – see Figure 4.1. These sites were selected for three reasons; firstly, as discussed in section 1.4, rainfall in the South Pacific is primarily controlled by the SPCZ amongst other climatic regimes such as ENSO and IPO (McGree et al., 2016; Brown *et al.*, 2020). Both sites sit in an SPCZ sensitive area whereby changes in its location can cause a shift in the amount of precipitation these islands receive making them vulnerable to changing climate. Figure 4.1 illustrates this and shows the average location of the SPCZ and rainfall across the South Pacific followed by the changes in SPCZ location and rainfall during El Niño and La Niña years. Secondly, Vanuatu and the Southern Cook Islands sit in important locations in terms of the migration history of the Pacific (Sear *et al.*, 2020). Vanuatu was one of the first archipelagos colonised by the Lapita in the first wave of migration into remote Oceania around 3000 yr BP (Bedford and Spriggs, 2014; Cochrane, 2018). The Southern Cook Islands similarly were some of the first islands colonised in the final Polynesian wave of migration and they were considered “gateway islands” for migration into the remotest parts of the Polynesian triangle (Allen and Wallace, 2007). The third reason is that both Emaotfer Swamp and Lake Tiriara are also located locally to key archaeological sites – Teouma burial site (Bedford et al, 2006; Petchey *et al.*, 2014) and the Tangatatau Rockshelter (Kirch, 2017b) respectively - allowing potential connections to be drawn between the palaeo-records developed at Emaotfer swamp and Lake Tiriara to the archaeological record in each region.

This chapter is divided between Emaotfer Swamp in Vanuatu and Lake Tiriara in the Cook Islands. For each site, the key characteristics in terms of climate, geology and vegetation will be identified. This section will also detail the colonisation history of the Pacific in relation to both Vanuatu and the southern Cook Islands and will conclude with a description of each of the sites utilised for this thesis.

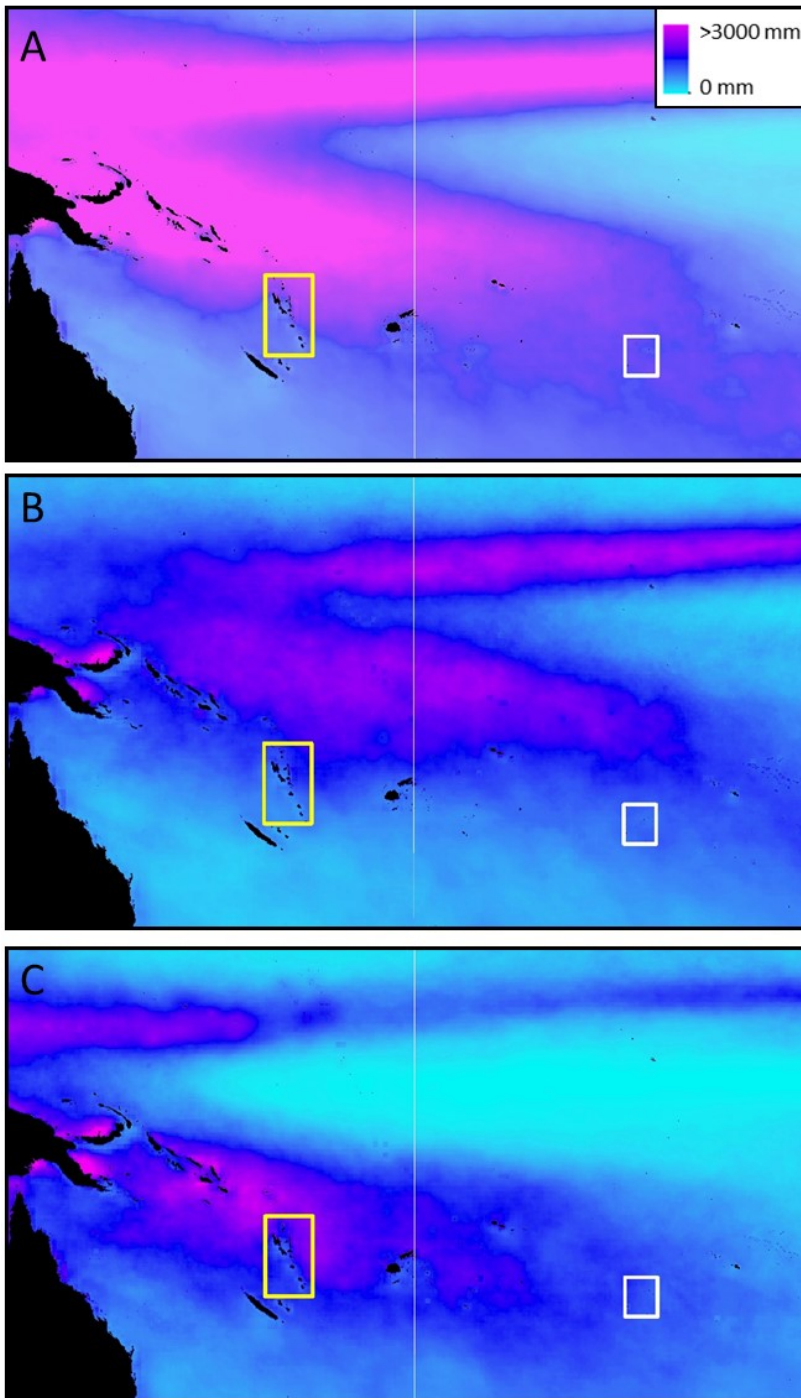


Figure 4.1 Images displaying the average rainfall/location of the SPCZ during A – the period 1971-2000, B – over El Niño years and C – over La Niña years. The yellow box denotes the location of Vanuatu, the white box denotes the location of the Southern Cook Islands

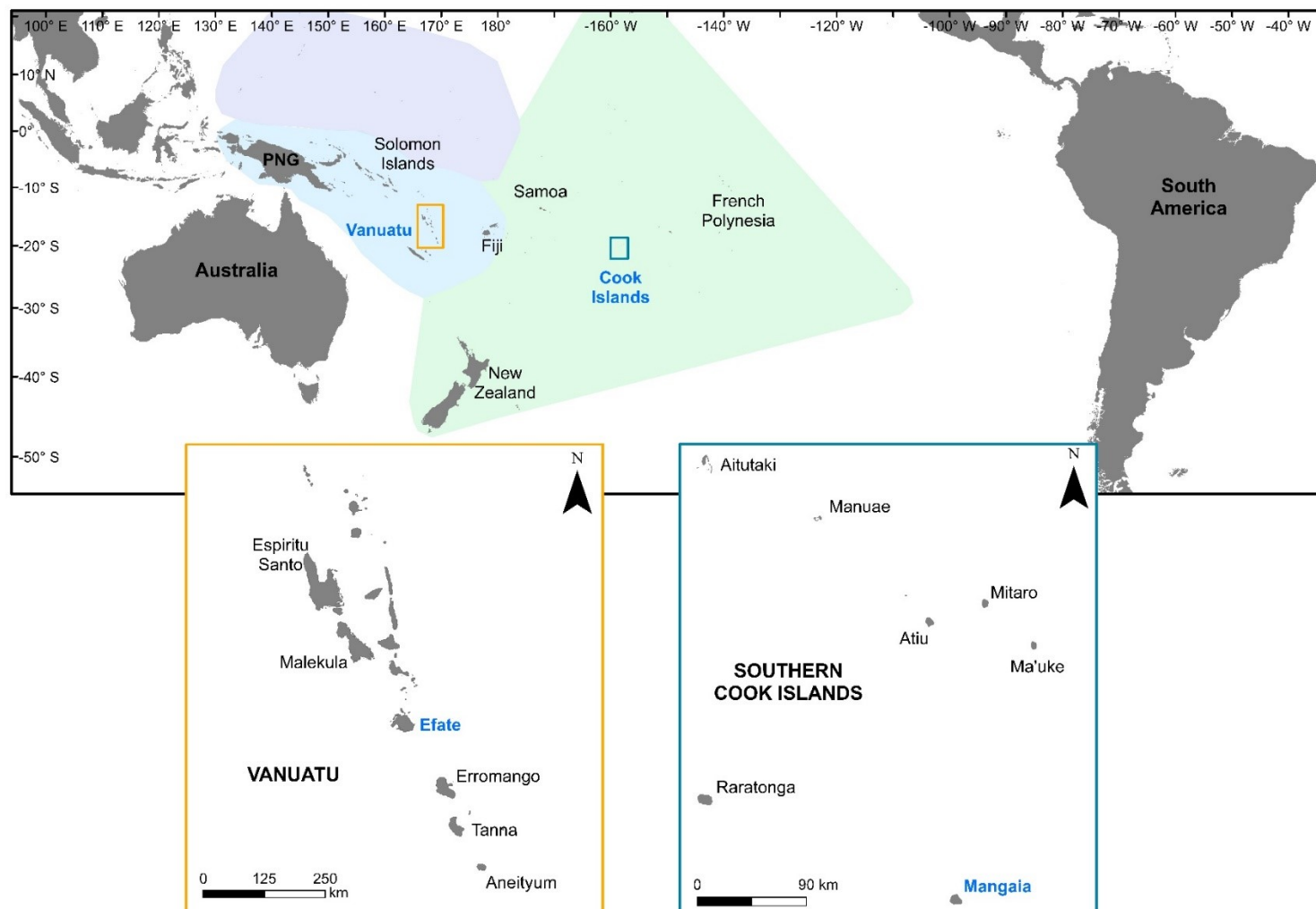


Figure 4.2: Map highlighting the location of: A - Vanuatu and the Cook Islands within the tropical South Pacific with the areas denoting the extent of Micronesia (purple), Melanesia (blue) and Polynesia (green) indicated. B –the island of Efeate within Vanuatu. C –Mangaia within the Southern Cook Islands.

## 4.2 Emaotfer Swamp – Efate, Vanuatu

### 4.2.1 Geography of Vanuatu and Efate

Vanuatu is a South Pacific island nation that is made up of ~83 islands with a recorded population of 272,459 as of 2016 (VNSO, 2009, 2016). Vanuatu covers an area of 612,300 km<sup>2</sup> and is located 2,394 km off the Northeast coast of Australia (VNSO, 2016). Efate (17°39'35.9"S, 168°23'48.0"E) sits within the centre of the Vanuatu archipelago and is the third largest island as well as home to the country’s capital, Port Vila.

### 4.2.2 Climate of Efate

Vanuatu, like most South Pacific island nations, has a well-defined wet and dry season. The wet season typically runs from November to April and the dry season runs from May to October. In Efate, the average annual rainfall is 2862mm and average monthly temperatures remain relatively stable throughout the year ranging between 23 and 27°C (Australian Government Bureau of Meteorology, 2023) – see Figure 4.3. Rainfall is variable as Vanuatu sits on the southern edge of the SPCZ so typically sees less (more) rainfall during El Niño (La Niña) years where the SPCZ contracts (expands) and shifts northeast (southwest) – see Figure 4.1.

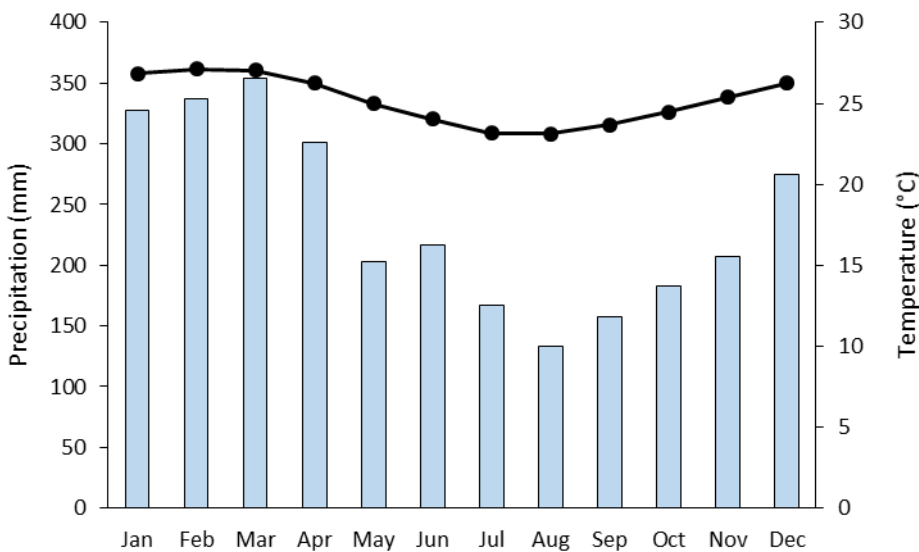


Figure 4.3: Average monthly precipitation and temperature for Vanuatu (BOM, 2020; WMO, 2020).

### 4.2.3 Geological setting of Efate

Efate is a composite high island that is part of the Neogene New Hebrides volcanic arc. It is composed of a volcanic centre of marine pumice breccias that started forming in the Miocene and were uplifted during the early Pleistocene (approx. 1.6 Ma), reaching a maximum elevation of 647 m (Wirrmann, Eagar, *et al.*, 2011; Dickinson *et al.*, 2013). The volcanic central highlands of Efate are encompassed by uplifted limestone - primarily composed of ancient coral - which has formed gently sloping terraces around the steeper inner highlands which are approximately 200 kyr in age (Dickinson *et al.*, 2013) – see Figure 4.4.

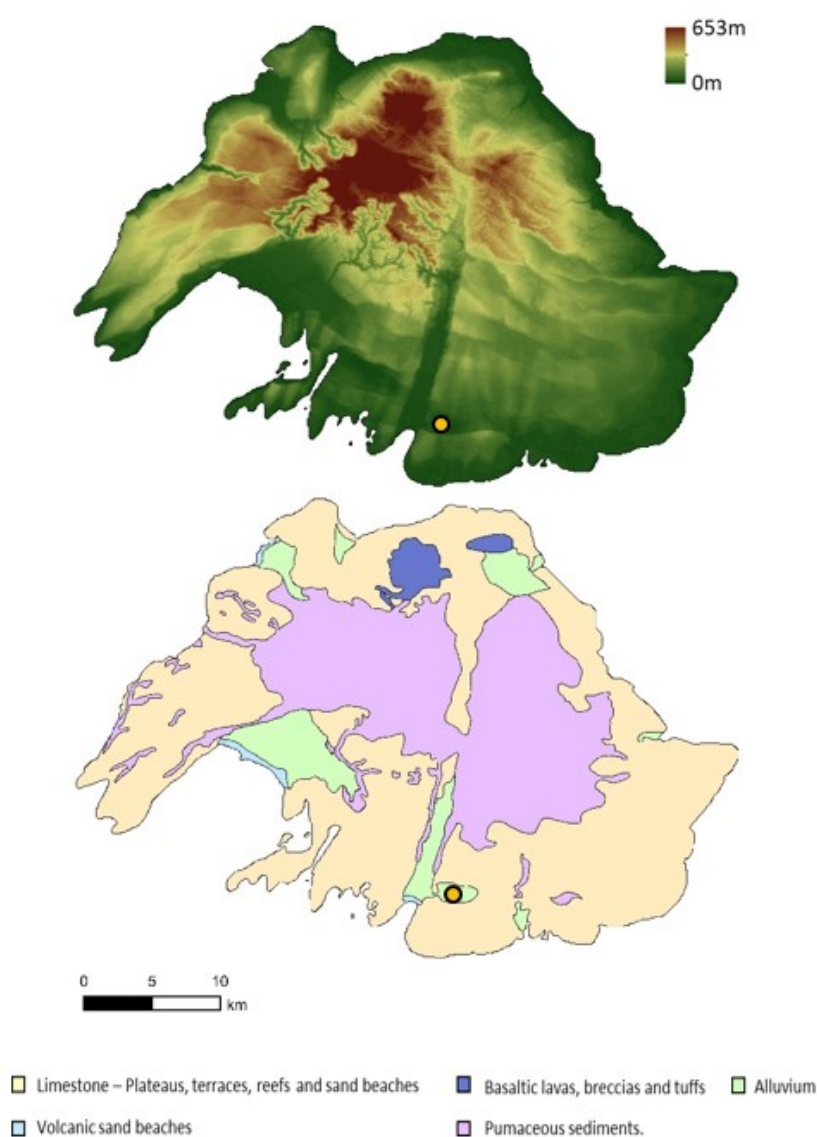


Figure 4.4: Geological map of Efate (left) redrawn and simplified from Dickinson et al (2013) and Kinston et al (2014) and an elevation profile (right) produced from SRTM data available from USGS Earth Explorer. Yellow dot denotes location of Emaotfer Swamp.

#### 4.2.4 Vegetation of Efate

To date, there is no comprehensive study of the vegetation for the island of Efate though the local vegetation around Emaotfer Swamp is discussed later in this chapter (see section 4.2.6.). A recent land cover assessment carried out in 2018 details general vegetation types across the island (Donlan, 2018) and it shows that the highlands of Efate are dominated by forest. As you move out radially towards the limestone plateau the vegetation changes from forest to grassland. Large areas of cultivated land cover part of the southern plateau, though smaller patches of cultivated land appear all along the coast of Efate, usually close to settlements.

#### 4.2.5 Colonisation of Vanuatu

The tropical Pacific Islands were the final frontier of the human colonisation of Earth (Matisoo-Smith, 2015). Over the past three and a half thousand years, there have been phases of colonisation and abandonment of islands across the Pacific (Anderson, 2001)(Irwin, 1992; Nunn, 2000; Anderson, 2001) with Polynesians sailing against dominant prevailing winds, eastwards into remote Oceania (Anderson *et al.*, 2006; Goodwin *et al.*, 2014). Humans arrived into South-East Asia, migrated southwards, and by about 30,000 years ago had reached the Solomon Islands where colonisation paused for over 25,000 years. Approximately 3,000 yr BP, migration resumed with the Lapita society moving eastward into remote Oceania through the island archipelagos of Melanesia (Cochrane, 2018) – see Figure 2.1. Vanuatu was colonised by humans during this first wave of migration and at least 30 Lapita archaeological sites have now been identified across Vanuatu (Bedford and Spriggs, 2014). On the southern coast of Efate, a key archaeological site - the Teouma Lapita cemetery – was discovered in 2004 (Kinaston, Buckley, *et al.*, 2014). Over 100 well-preserved skeletons were discovered along with Lapita pottery at the site which have provided valuable insights into Lapita society – particularly in relation to the diet of these early Lapita settlers (Bedford, Spriggs and Regenvanu, 2006; Valentin *et al.*, 2010; Kinaston, Buckley, *et al.*, 2014). Evidence from Teouma has put human colonisation and settlement within Efate and Vanuatu more generally at around 3200 to 3000 yr BP (Bedford *et al.*, 2006) but this was later revised to an earliest date of 3000 yr BP by Petchey *et al.* (2014).

#### 4.2.6 Emaotfer Swamp

Emaotfer swamp (17°47'08.5"S, 168°24'12.2"E) is a freshwater swamp located in Southern Efate - It is approximately 1.5km long and 0.9km wide, covers a total area of 0.95 km<sup>2</sup> and sits at an elevation of 17 masl (Wirrmann, Eagar, *et al.*, 2011) – see Figure 4.5. The Teouma River sits 2 km west of the site and whilst there is no clear inflow to Emaotfer, a long shallow drainage channel is reported to extend from the south-east arm of the swamp. This may act as an overflow channel during times of high rainfall and there is a small tidal stream that comes within 200-400 m of the site (Kalfatak and Jaensch, 2014). Site visits showed that this stream is well below the level of the swamp, so unlikely to be connected. The vegetation found around the edges and on the swamp itself are primarily grasses (*Poaceae*), sedges (*Cyperaceae*) and ferns as well as water lilies (*Numphaeaceae*) (Combettes et al, 2015). The swamp area is encompassed by a low-level forest (Kalfatak and Jaensch, 2014) which comprises *Barringtonia*, *Pandanus*, *Erythrina* and *Hibiscus* species (Kalfatak and Jaensch, 2014; Combettes et al, 2015). Beyond this, the landscape has been more heavily influenced by humans (Combettes et al, 2015) and primarily consists of cultivated or fallow land, settlements or grassland.

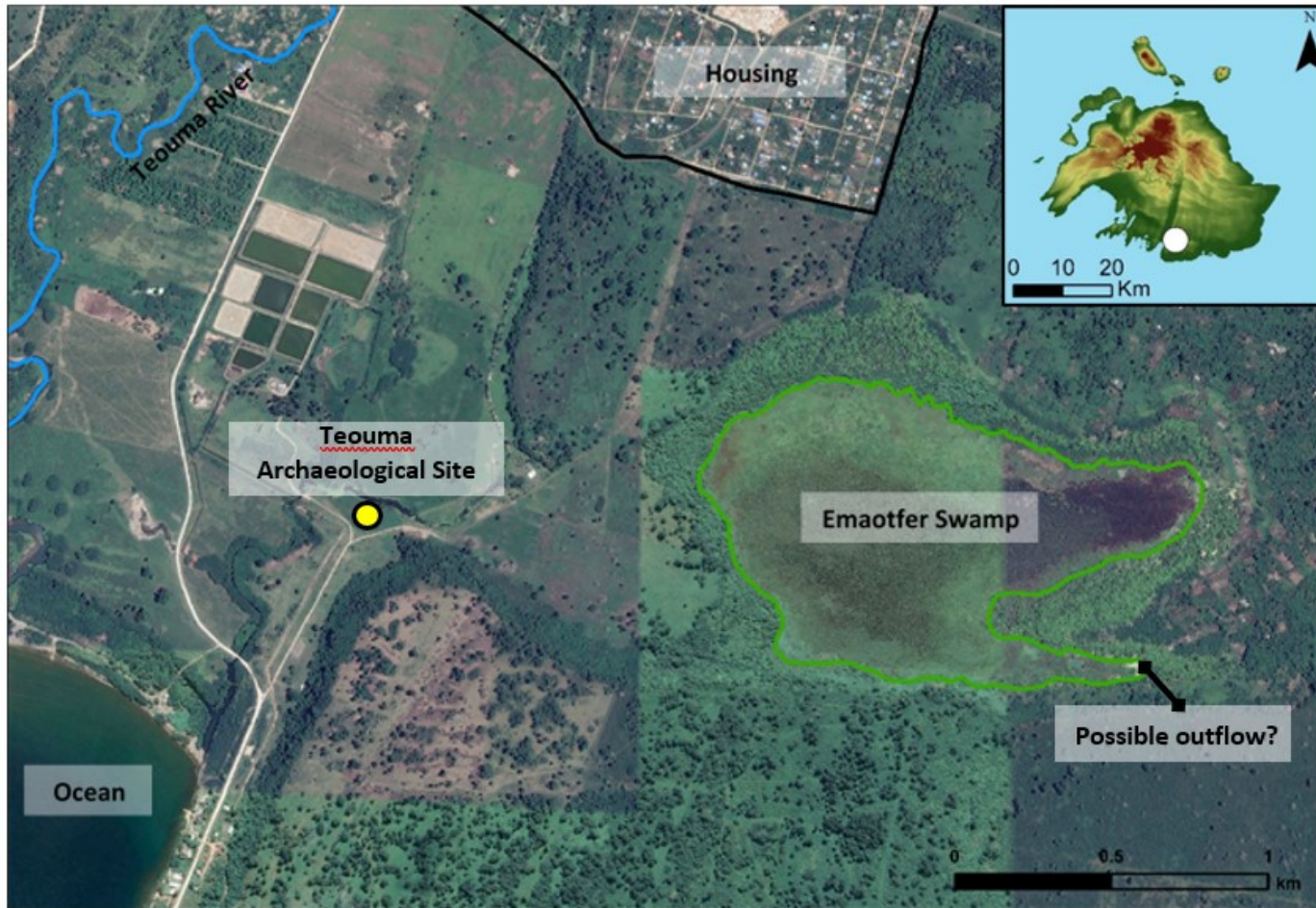


Figure 4.5: Inset map identifies the location of Emaotfer Swamp within Efaté. Main figure shows Emaotfer Swamp site map identifying the Teouma River, ocean, housing and the Teouma archaeological site (yellow dot).

### **4.3 Lake Tiriara – Mangaia, Cook Islands**

#### **4.3.1 Geography of the Cook Islands and Mangaia**

The Cook Islands are a South Pacific island nation made up of 15 islands that are geographically split into a northern and southern group and have a recorded total population of 17,434 in 2016 census (Cook Islands Statistics Office, 2018). The islands are located more than 5,000 km from Australia and stretch across two million square kilometres between American Samoa and French Polynesia (Figure 4.2). Mangaia is the southernmost island of the Cook Islands

#### **4.3.2 Climate of Mangaia**

The Cook Islands are located in a key position in relation to the SPCZ as they sit just beyond the typical average extent of the SPCZ (Figure 4.1). This means that these islands are particularly sensitive to SPCZ movements as it shifts in response to changing climatic oscillations. The Cook Islands have a well-defined wet (December-May) and dry (June-November) season with mean temperatures relatively constant for the year, only ranging between 25 and 28°C (Figure 4.6). Average annual rainfall for Mangaia is between 1900 to 2050 mm/year (Thompson, 1986). Rainfall is variable as the Southern Cook Islands sit on the southeastern edge of the SPCZ so falls within the convective rain band during neutral and La Niña years but see a significant decrease in rainfall during El Niño years when the Southern Cook Islands fall outside the SPCZ rainfall band.

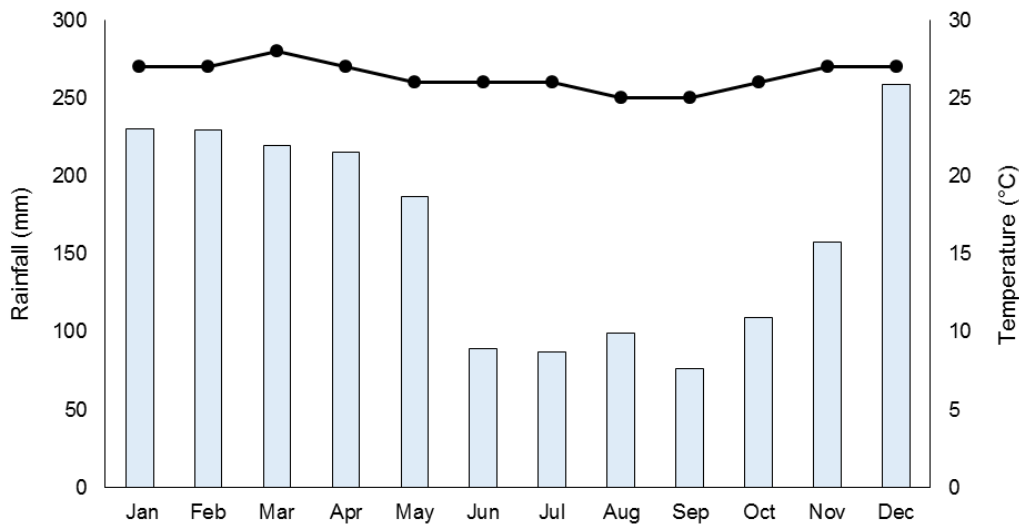


Figure 4.6: Annual precipitation (blue bars) and temperature (black line) in the Cook Islands (BOM, 2020).

### 4.3.3 Geological setting of Mangaia

Mangaia is a composite high island located in the southern Cook Islands group (Nunn *et al.*, 2016). In terms of the morphology, Mangaia has an inner eroded volcanic basaltic cone that rises to a maximum elevation of 168m (Ellison, 1994) and is estimated to be approximately 17-19 million years old (Dalrymple *et al.*, 1975) – see Figure 4.7.

Around the inner volcanic cone is an encircling outer makatea zone, which is composed from an ancient raised limestone reef (Wood, 1978). The makatea rises as a sharp escarpment, which reaches a maximum height of 70 metres and is 700 to 2000 metres wide. The makatea formed during the mid-Tertiary and is approximately 17 Ma old but emerged likely during the late Tertiary to Quaternary (Yonekura *et al.*, 1988). Between these two zones lies lowland swamp that develops at the edge of the radially draining volcanic cone where water becomes trapped when it meets the makatea cliffs forming wetlands and lakes (Ellison, 1994; Parkes, 1994) (Figure 4.8).

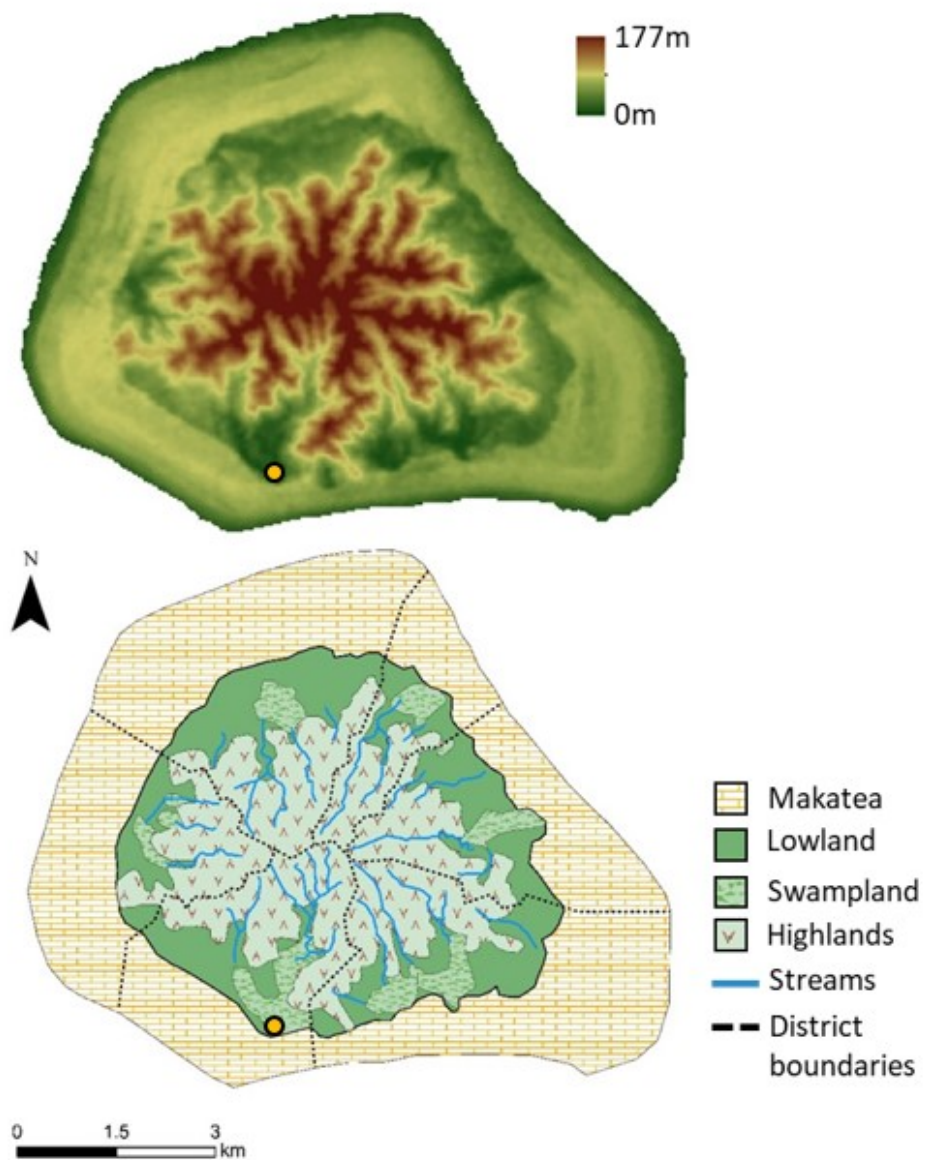


Figure 4.7: Geology (top) and elevation profile (bottom) for the island of Mangaia. Yellow dot denotes the location of Lake Tiriara.

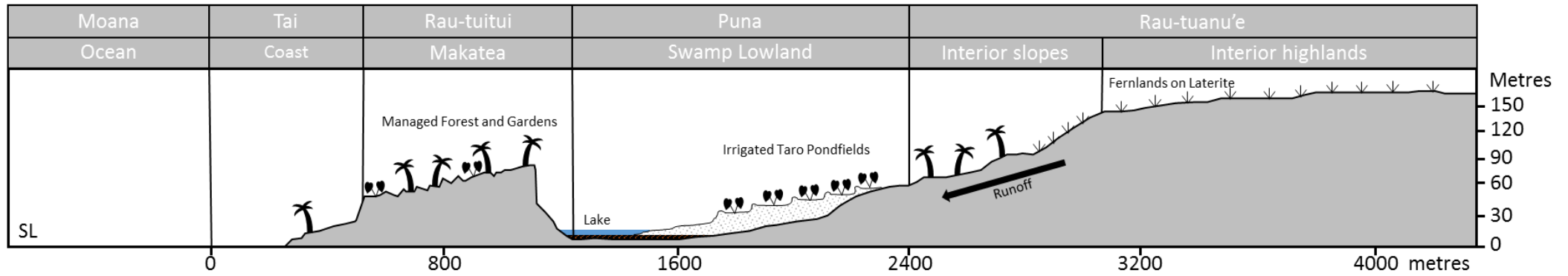


Figure 4.8: Simplified cross-section of Mangaia where the volcanic core is surrounded by upraised makatea escarpment. Top row is the Manganian name for each land section and below the common name for each land section. Redrawn and adapted from Allen (1969) and Kirch (2017).

#### 4.3.4 Vegetation of Mangaia

The volcanic cone is dominated by introduced plant species whilst vegetation on the makatea is dominated by native species (Merlin, 1991). The reason for this discrepancy is that the makatea is not useful as agricultural land whereas the inner volcanic plateau was cultivated for crops (Merlin, 1991; Parkes, 1994). On Mangaia, the central part of the island is dominated by introduced species including pineapple, cassava, and bananas, which are remnants of the transformation of this landscape for agricultural uses. There are also grasses such as maiden silvergrass and woody species like the whistling pine tree, guava, and Noni present (Merlin, 1991). The vegetation on the Makatea are mostly wood and herbaceous plants with species such as Pandan, Zebra wood, Ficus, leafflower trees and white mulberry amongst others (Merlin, 1991).

#### 4.3.5 Colonisation of the Southern Cook Islands

Following the 1,700 year pause after the first Lapita migration that had reached as far as Samoa and Tonga, the colonisation of the rest of the Polynesian triangle commenced c.1100-1200 cal yr BP (Kahn, 2014) – see Figure 2.1. The Southern Cook Islands have been described as “gateways” for this final phase of human migration into Eastern Polynesia (Allen and Wallace, 2007) and so the timing of human arrival on these islands has been widely debated. Wilmshurst et al (2011) suggested that the southern Cook Islands were colonised around 1250 – 1281 AD (ca. 700-670 cal yr BP) based on a meta-analysis of radiocarbon dates from archaeological sites. For Mangaia, work by Ellison (1994) put the arrival of humans on the island at 2500 yr BP where they suggested that a small temporary population may have arrived as evidenced by charcoal and then later indications of environmental disturbance through the presence of clay bands from 1900-1800 yr BP followed by major forest clearance about 1650 yr BP. Work by Chague-Goff et al (2016) narrowed the window of human arrival to 1552–2017 yr BP. These dates however are contentious and a recent analysis of archaeological evidence puts the arrival and initial settlement of Mangaia at c. AD 1000 with permanent habitation established by c. AD 1300 (Kirch, 2017b).

### 4.3.6 Lake Tiriara

Lake Tiriara (21°57'03.9"S 157°55'45.7"W) (Figure 4.9) is located in the Veitatei drainage basin between the volcanic cone and makatea boundary on the south side of Mangaia and is now the only lake on the island likely due to its low elevation and Ellison (1994) reports that it is filling in rapidly. It has an area of approximately 0.2 km<sup>2</sup> and has a maximum depth of 1.2 metres as recorded in 2016 (Sear and Langdon, pers comm, Sept 2018). The limnology of Lake Tiriara is not well understood. Lake temperature was reported to be 27.6 °C with a pH of 7.37 and conductivity of 1,693 µS cm<sup>-1</sup> as stated by Schabetsberger et al (2009). Tiriara is thought to be connected to the ocean via 700 metre long tunnels through the makatea (Ellison, 1993; Chagué-Goff *et al.*, 2016).

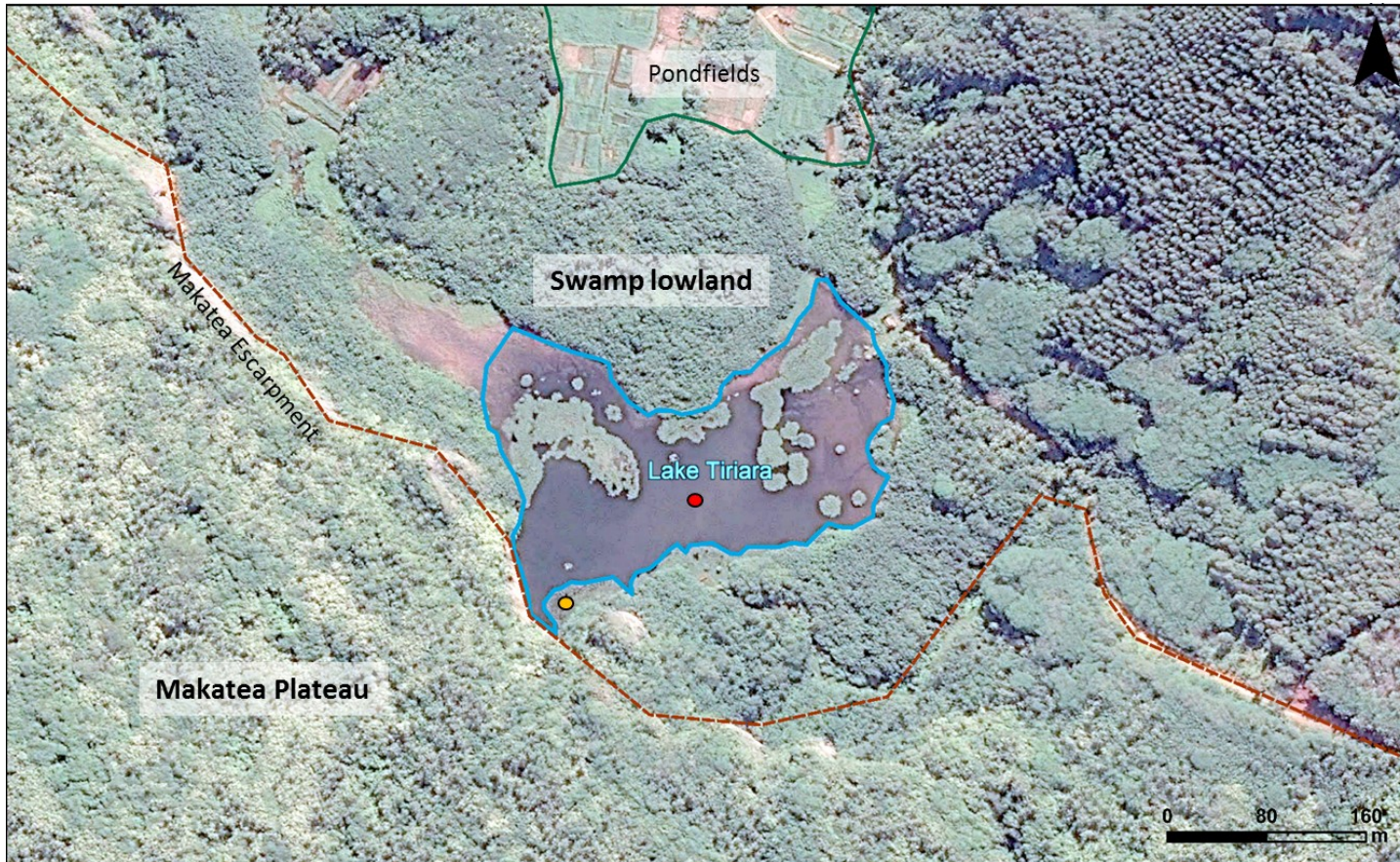


Figure 4.9: Lake Tiriara site map identifying the Makatea plateau, swamp lowlands, pondfields and the 2016 coring location (red dot) for the sediments used in this report and the approximate location of the Chague-Goff et al (2016) core (yellow dot).



## Chapter 5 Palaeoenvironmental Methods

### 5.1 Sediment Coring and site stratigraphy

The Mangaia lake sediments were taken from the deepest parts of the lake during a coring campaign in July 2016 using a GeoCore piston system (GeoCore, 2023), with cores sealed and stored at 4°C in the cold stores at SOGES, University of Southampton. A UWITEC gravity-type corer was used to extract the youngest sediments and maintain the water-sediment interface. The sediments from Lake Tiriara, Mangaia went down to a maximum depth of 840 cm and are mainly composed of gyttja, silty/clay lake sediments. This thesis utilises the top-most 560 cm of sediment to focus analysis on the period just prior to and including human occupation of Mangaia.

The Emaotfer sediments were taken from the swamp during an expedition in August 2019. The sediments of Emaotfer Swamp went down to a maximum depth of 294cm. A gouge corer was used to extract the sediments in continuous 1 metre sections, from these a u-channel section was taken, and these were transported back to the UK to be stored at the University of Southampton's cold stores. Cores were correlated using loss-on-ignition, magnetic, and Itrax geochemistry data to make a master core stratigraphy. Probe data was not collected due to the inaccessibility of the site caused by the presence of standing water.

### 5.2 Magnetic Susceptibility

Magnetic susceptibility is a non-destructive, quick and simple tool that can be used to measure a material's magnetisability (Dearing, 1999a). Sources of magnetic material could come from external sources such as volcanic ash (tephra), aeolian dust and pollution and internal sources and processes such as reductive diagenesis (Dearing, 1999b). This method has been used since the 1970s on a range of materials including lake sediments, offering insights into changes in erosion, hydrology, climate and pollution through time (Dearing, 1999b).

The magnetic susceptibility of the Emaotfer Swamp and Lake Tiriara cores was measured using the Bartington Instruments MS2K at 1cm resolution. To correct and account for the

background level of magnetism, each of the individual measurements of the sediment core were taken between a pair of blank air measurements as per Dearing (1999a).

### 5.3 Geochemistry - Itrax $\mu$ XRF

Developed during the early 1990s,  $\mu$ XRF core scanning has become an important and frequently used tool in a range of environmental study areas including palaeolimnology. One such example of these analytical apparatus is the Itrax  $\mu$ XRF core scanner produced by Cox Analytical Systems. Micro-XRF core scanning has provided a valuable, quick and non-destructive method for analysing the geochemistry of sediments at a high resolution that can offer a wealth of information relating to changes in lacustrine catchments through time. It can offer insights into factors such as in-wash, biological productivity, redox processes and the occurrence of hazardous events (e.g. flooding, volcanic eruption, Tsunami) (Davies et al, 2015). The high-resolution profile produced can also be used to infer sediment mineralogy and depositional environment.

Prior to any sub-sampling, the sediment cores for Emaotfer Swamp and Lake Tiriara were scanned using an Itrax XRF core scanner (Cox Analytical Systems, Gothenburg) located at the British Ocean Sediment Core Research Facility in Southampton. The Itrax core scan data comprises a set of X-Ray Fluorescence ( $\mu$ XRF) spectral data at 200 $\mu$ m resolution as well as high-resolution optical and radiograph images. The Itrax principle involves irradiating a sediment core with an intense X-ray beam that excites atoms of elements in the sediment core producing secondary X-rays that are characteristic of each element. For each sediment increment measured, an X-ray fluorescence spectrum is recorded (Rothwell and Croudace, 2015) which are analysed to generate a continuous element profile (from Al to U) for the core scanned - Figure 5.1.

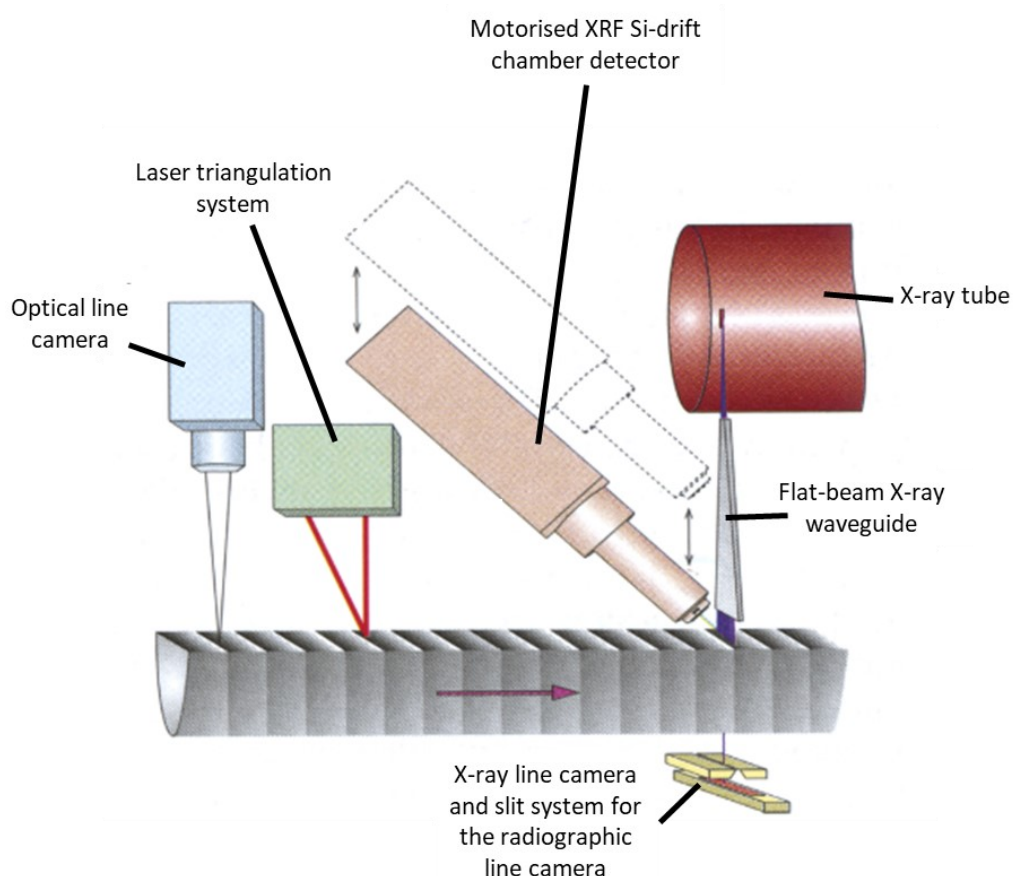


Figure 5.1: Image showing different components of Itrax core scanner from Croudace et al (2006)

The cores were scanned using a molybdenum tube with a voltage of 45kV and the current set at 40mA with an exposure time of 20 seconds. For the purposes of this thesis, the Itrax data was averaged at a 1cm resolution to allow for a comparison to other data sets produced from the core material. Where individual elements are presented individually rather than ratios, the element is normalised against the Compton/incoherent scatter to account for water and organic content as per Sear et al (2020) and Gosling et al (2020). Table 5.1 lists the XRF proxies that were used during this project and the interpretation derived from that proxy. The terrestrial, freshwater biogenic and marine geochemical indicators are based on previous work in Tiriara by Chagué-Goff *et al* (2016a) and the review by Davies, Lamb and Roberts (2015) and examples from the wider literature that are cited within the table.

Table 5.1: Overview of the XRF elements or ratios utilised within this thesis along with example references from tropical and sub-tropical lakes. Adapted from Davies et al, 2015.

	Element or Ratio	Purpose/Interpretation (with increase in element/ratio)	Reference
Terrestrial	Titanium (Ti) & Iron (Fe)	Terrestrial Input – increase in precipitation washes more terrestrial material from the basin into the lake	Chague-Goff et al (2016); Sear et al (2020)
	Manganese/Iron (Mn/Fe)	Redox processes - increase in this ratio indicates oxic bottom water.	Burn and Palmer (2014);
	Bromine (Br)	Marine influence – particularly in near coastal lakes due to ocean spray Organic content – increasing Br is associated with an increase in organic content	Evans et al (2019); Chague-Goff et al (2016)
Marine	Chlorine (Cl)	Marine influence – particularly in near coastal lakes due to ocean spray	Chague-Goff et al (2016)
	Sulphur (S)	Marine influence – higher presence of S and sulphates in ocean water compared to fresh Precipitation of gypsum - when concentrated in water column due to high levels of evaporation	Burnett et al (2011); Burn and Palmer (2014); Chague-Goff et al (2016)
	Calcium (Ca)	Increased in-lake carbonate precipitation - when concentrated in water column due to high levels of evaporation Marine influence – connection to ocean allowing input of ocean water or sediments	Burn and Palmer (2014); Burnett et al (2011); Chague-Goff et al (2016)
Freshwater	Silica (Si)	Increase in productivity – increase biogenic silica from diatoms Increase in terrestrial input - increase in precipitation washes more terrestrial material from the basin into the lake	Chague-Goff et al (2016); Burnett et al (2011)

Both Ti and Fe are indicators of erosion (Cohen, 2003; Davies et al, 2015) and both typically align with the magnetic susceptibility in sediment records (Davies et al, 2015). These elements are often paired as Ti and Fe are found as Ti-Fe rich magnetite or Fe–Ti oxides in silts but Ti is particularly useful as it is not utilised as part of in-lake processes so is a reliable indicator of terrestrial in-wash from the wider catchment into the lake (Davies et al, 2015; Evans *et al.*, 2019). Peaks in Ti can also occur due to human disturbance of the

catchment e.g. advent of agriculture and can also indicate the presence of tephra layers within the sediments (Davies et al, 2015).

Fe, however, is involved in other lake processes and can be used in conjunction with Mn as a redox proxy. Peaks in the Mn/Fe ratio in lake sediments can indicate when there is enhanced mixing within the water column and the bottom water becomes oxic (Cohen, 2003; Davies et al, 2015; Evans *et al.*, 2019). The interpretation is based upon Mn being more soluble compared to Fe in anoxic conditions, leading to a lower level of preservation of Mn relative to Fe. During oxic conditions, Mn is unable to easily dissolve into the water column so becomes preferentially preserved in the lake sediments, compared to periods of anoxia, thus producing a higher Mn/Fe ratio value (Cohen, 2003; Burn and Palmer, 2014; Evans *et al.*, 2019). This ratio has previously been used in tropical and subtropical lakes in New Zealand and Jamaica to identify periods of oxidation at the bottom of the lake (Burn and Palmer, 2014; Evans *et al.*, 2019).

Si can be a proxy for either increase in terrestrial in-wash or an increase in productivity (Cohen, 2003; Chagué-Goff *et al.*, 2016; Evans *et al.*, 2019). An increase in Si is typically due to an increase in biogenic silica, which is largely formed from diatoms and often there is a correlation between the amount of biogenic silica and TOC within lake sediments due to this overall increase in productivity (Cohen, 2003). In other lakes, Si can also be highly correlated with other terrestrial proxies such as Ti and Fe indicating that it is also a signal for terrestrial in-wash and it has also been used as an indicator of tephra presence (Kylander *et al.*, 2011, 2012; Chagué-Goff *et al.*, 2016).

The presence of Br can indicate higher organic content in lake sediments as Br binds with organic material and is preserved in the sediment sequence (Davies et al, 2015; Evans *et al.*, 2019) whilst the presence of Cl can indicate the presence of tephra or organic compounds in lake sediments (Evans *et al.*, 2019). Br along with Cl and also the ratio Br/Cl have also been used as indicators of increasing marine influence (Chagué-Goff *et al.*, 2016). Br is present in the ocean as bromide salts and Cl similarly is present as sea salts and in marine organics that can enter lakes either through sea spray or fluvial or subterranean connections from lakes to the ocean (Evans *et al.*, 2019). A comparison of Br to other marine proxies such as Cl or S alongside organic proxies such as TOC or LOI<sub>550</sub> is required to interpret this XRF profile.

The primary function of the Ca XRF profile for Emaotfer Swamp and Lake Tiriara is the identification of carbonates within the lake sediment sequence. The relationship between Ca and other elemental profiles such as Sr and S can assist in identifying minerals such as calcium carbonate ( $\text{CaCO}_3$ ), aragonite ( $\text{SrCO}_3$ ) and gypsum ( $\text{CaSO}_4$ ) that can precipitate in lakes due to evaporative concentration (Burn and Palmer, 2014; Davies *et al.*, 2015; Evans *et al.*, 2019). A comparison of Ca to terrestrial proxies such as Ti can also identify whether carbonates are allochthonous or autochthonous in nature (Cohen, 2003; Evans *et al.*, 2019).

As discussed, S has been used as a proxy for gypsum ( $\text{CaSO}_4$ ) precipitation when correlated with Ca (Burn and Palmer, 2014; Chagué-Goff *et al.*, 2016). S can also be useful for discerning between freshwater and marine sediments as S and sulphates are much more abundant in ocean water than fresh so significant shift could indicate marine influence on a freshwater system (Cohen, 2003).

The interpretation of XRF data will usually be site specific, as processes may work differently across a range of sites. It is also important to evaluate XRF data in conjunction with other elemental XRF profiles and additional proxy information to develop the palaeoenvironmental interpretation (Davies *et al.*, 2015), as Table 5.1 shows there are a range of interpretations just for XRF data alone.

## 5.4 Sedimentology

Loss-on-ignition (LOI) is an inexpensive and relatively quick method to identify the water, organic and potentially carbonate content of lake sediments (Boyle, 2001). It involves weighing the samples before and after burning off different elements in a muffle furnace – 550°C for organics and 950°C for carbonate - and the resulting weight loss determines the percentage contribution within the sediment. Loss-on-ignition was used to determine organic and carbonate content at 1 cm resolution across both the Lake Tiriara and Emaotfer Swamp sequences. However, due to the amount of material available the Emaotfer Swamp sequence is not continuous and instead 1cm LOI samples were taken where material was left over from isotopic samples. The samples were processed as per method described by Heiri *et al.* (2001) whereby samples were put in the furnace at 550°C

for 4 hours and 950°C for 2 hours. For this study, LOI<sub>950</sub> was of particular interest as it can be used as a proxy for carbonate content because at temperatures over 900 °C carbon dioxide (CO<sub>2</sub>) is evolved from carbonates leaving oxides and the resulting weight loss can indicate at the amount of carbonate present in the sediments (Heiri *et al*, 2001). There is some error associated with LOI, as changes in exposure time and sample size can produce significantly different results (Heiri *et al*, 2001). Due to this, Heiri et al (2001) called for a standard protocol to be applied for LOI across laboratories and the protocol they suggest was implemented here.

## 5.5 Inorganic isotopes

### 5.5.1 $\delta^2\text{H}$ and $\delta^{18}\text{O}$ in Modern lake water

The modern lake characteristics should be studied to help account for any variables that may influence the isotopic values of the lake water (Leng and Marshall, 2004). Providing isotopic values for modern lake water can help provide context for palaeoenvironmental data from the same site. Modern lake water isotope values can also assist in identifying whether the lake is evaporative when it is compared to the values for regional rainfall using the local meteoric water line (LMWL). If a lake plots close to or on the LMWL then its waters are isotopically similar to local rainfall, whereas if it sits off the LMWL then there is likely to be fractionation happening through evaporation and it would sit on a local evaporation line that diverges from the LMWL (Leng and Marshall, 2004). Modern lake water samples were taken from Lake Tiriara during the coring expeditions in 2016. The water was stored in screw-cap bottles and stored in cold storage (~4°C) at the Geography and Environmental Science laboratories at the University of Southampton. Samples were sent to the British Geological Survey for analysis of water <sup>2</sup>H and <sup>18</sup>O using the GV Isoprime and EuroPyrOH with in-house standards. Results are reported as ‰ VSMOW2 (Vienna Standard Mean Ocean Water 2)

### 5.5.2 Carbonate $\delta^{18}\text{O}$ record in Lake Sediments

Oxygen isotopes preserved in lake sediments have been used in palaeoenvironmental research since the 1950s to reconstruct both precipitation and temperature changes (Leng and Henderson, 2013) crucial to which is a full understanding of the stable isotope

system. They can be employed from either biogenic or authigenic sources preserved in lake sediments (Leng and Marshall, 2004; Bradley, 2015) and are thought to reflect changes in temperature or the isotopic composition of the lake water on formation (Leng and Marshall, 2004). Oxygen isotopes have a high potential for reconstructing records of hydroclimate as they require small sample sizes and can be linked to changes in hydroclimate (Leng, 2006; Kurita, 2013). The second challenge is accounting for the main controls and constraints that influence the  $\delta^{18}\text{O}$  (Figure 5.2) – temperature,  $\delta^{18}\text{O}_{\text{water}}$  and disequilibrium effects (Leng and Henderson, 2013). Changes in temperature causes a change in the rate of isotope fractionation between lake water and carbonates by approximately 0.24‰ per 1°C (Leng and Marshall, 2004). However, in tropical regions the temperatures remain relatively constant year round and climate is defined by wet and dry seasons rather than winter and summer (Australian Bureau of Meteorology and CSIRO, 2011) (see Figure 4.6) indicating that the influence of temperature on the rate of fractionation here should be limited (Cohen, 2003; Bird *et al.*, 2020). The isotopic composition of  $\delta^{18}\text{O}_{\text{water}}$  in lacustrine environments is primarily a function of precipitation (Leng and Marshall, 2004). This can vary however for lakes in regions where evaporation heavily influences lake hydrology are subject to kinetic fractionation where the lake water becomes enriched in heavier  $^{18}\text{O}$  as lighter  $^{16}\text{O}$  is preferentially evaporated. In tropical regions, evaporation authigenic and biogenic carbonates are formed within the water column taking up the isotopic signature of the lake, which are then preserved in the lake sediments. Biogenic carbonates are a function of shell formation on lake dwelling organisms such as ostracods whilst authigenic carbonates are precipitated following evaporation and resultant concentration of minerals or as part of the photosynthesis of lake flora. However, any disequilibrium or vital effects need to be accounted for where possible – particularly with biogenic sources of carbonate (Leng and Marshall, 2004). Thus, in these tropical South Pacific lakes, because evaporation is regionally dominant over temperature changes (Cohen, 2003), hydroclimate changes should be the dominant control on carbonate isotopic variation in the absence of other direct controls, for example marine incursions, offering the potential for studying past precipitation patterns (Kurita, 2013).

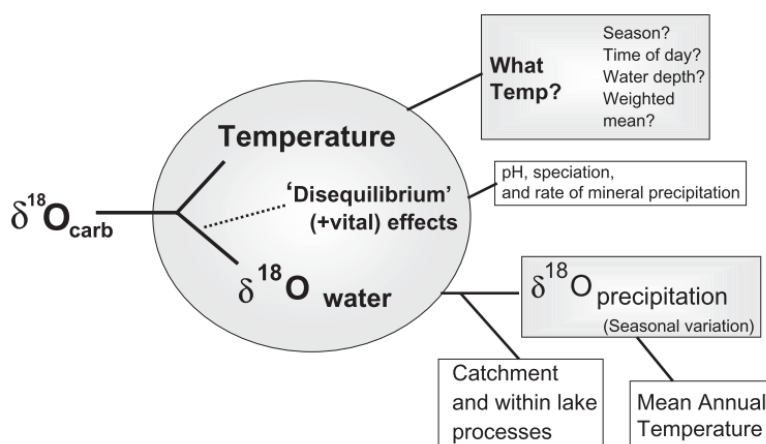


Figure 5.2: Diagram illustrating the connections between the different constraints of  $\delta^{18}\text{O}_{\text{carb}}$  in lake sediments (from Leng and Marshall, 2004).

The  $\delta^{18}\text{O}$  record can also be influenced by the size of the lake in comparison to the catchment, residence time and air mass sources. The modern lake characteristics should be studied to help account for these variables (Leng and Marshall, 2004).  $\delta^{18}\text{O}_{\text{water}}$  is controlled by  $\delta^{18}\text{O}_{\text{precipitation}}$  - the variable in the system we are looking to reconstruct - but also the catchment and processes going on within the lake itself. In lake systems where groundwater input is dominant, the effects of shifting P/E balance can be relatively muted as the groundwater reduces the sensitivity of the system to climatic changes (Lamb *et al.*, 2000). A study looking at a sequence from Lake Tilo in Ethiopia, found that groundwater input into the lake was responsible for a high level of fluctuations of isotopic values for  $\delta^{13}\text{C}$  and  $\delta^{18}\text{O}$  (~15‰) meaning the ratio between  $\delta^{13}\text{C}$  and  $\delta^{18}\text{O}$  had to be used specifically to disentangle different drivers and infer climatic change in the authigenic calcite record (Lamb *et al.*, 2000). Closed lakes will have much larger shifts in  $\delta^{18}\text{O}$  values in the order of 5‰ to greater than 10‰ compared to open lakes where variations in  $\delta^{18}\text{O}$  values are much smaller with only 1 to 2‰ of variation (Leng and Marshall, 2004). Though typically, the groundwater in the region had notably lower  $\delta^{18}\text{O}$  values than the local rainfall, with up to 5‰ difference between rainfall and groundwater sources not associated with hot springs (Lamb *et al.*, 2000), which would therefore alter the lake  $\delta^{18}\text{O}$  towards lower values than if the lake was fed by rainfall alone. In addition to the effects of closed versus open lakes, the size of the lake and its associated residence time also has an important impact on  $\delta^{18}\text{O}$  values (Leng and Marshall, 2004). Smaller lakes with residence times of less than a year generally produce more negative values (Leng and Marshall, 2004). For example, Lake Kail in Guatemala has an area of 0.01km<sup>2</sup> with a max

depth of 3m and had a  $\delta^{18}\text{O}$  range of -9 to -5‰ VPDB through the Holocene (Stansell *et al.*, 2020). Whereas large lakes with residence times approaching hundreds of years typically have positive values (Leng and Marshall, 2004). For example, Lake Awassa in Ethiopia has an area of 92km<sup>2</sup> with a max depth of 23m and had a  $\delta^{18}\text{O}$  range of +0.5 to +7 ‰ VPDB through the Holocene (Lamb *et al.*, 2002). Whilst these two systems may be quite different, this highlights the range of  $\delta^{18}\text{O}$  values that are possible across a range of sites. To be able to interpret  $\delta^{18}\text{O}$  records one needs to be able to account for the different controls at the study site, both in space and time. Further to this, fractionation rates vary between carbonate species (Leng and Marshall, 2004) so it is important to identify whether the carbonate species changes through a core sequence as this could have implications for the interpretation of the  $\delta^{13}\text{C}$  and  $\delta^{18}\text{O}$  records if the carbonate species changes through the sequence (Lamb *et al.*, 2000). For example, a record from Moon Lake in the USA saw a 2‰ difference in  $\delta^{18}\text{O}$  values between aragonite and calcite laminae (Valero-Garcés *et al.*, 1997), which would have had the potential to be misinterpreted as an environmental or climatic change if carbonate mineralogy had not been determined.

$\delta^{18}\text{O}$  is a well utilised proxy in many - primarily temperate - regions of the world (Leng and Marshall, 2004), but has not been routinely used on lacustrine archives in the South Pacific islands. It has been successfully used in tropical regions to reconstruct hydroclimatological and hydrological changes in lakes in South America (Schwalb, Burns and Kelts, 1999; Bird *et al.*, 2011; Blard *et al.*, 2011) and Africa (Gasse and Fontes, 1989; Gasse, 2002; Lamb *et al.*, 2005). Oxygen isotopes have also been used successfully in the Pacific region to reconstruct precipitation using stalagmite records taken from Solomon Islands and Vanuatu (Partin *et al.*, 2013; Maupin *et al.*, 2014). These records provide high temporal resolution (four month resolution in the Solomon Islands), but are relatively short only encompassing the last 400-600 years (Partin *et al.*, 2013; Maupin *et al.*, 2014).

111 bulk samples were prepared for oxygen isotope analysis from the Mangaia sequence and 85 from the Emaotfer sequence. The sampling strategy was based on existing age models for these sites by establishing the approximate accumulation rate for each core. For the Mangaia cores, samples were taken every 10 cm over the top part of the sequence, but this is increased to one sample every 5 cm between 140 and 260 cm. For the Emaotfer core, samples were taken every 5 cm over the top part of the sequence, but

sampling increased to one sample every 2 cm from 195 cm to the bottom of the core. In both sets of cores, the sampling interval was increased within the cores where the approximate location of human arrival sat within the sequence based on existing age models and previous work at these sites.

The samples were taken to the British Geological Survey (BGS) at Keyworth for processing and were prepared using methodology provided by BGS (Leng, 2018). The preparation of  $^{18}\text{O}$  samples involved leaving them in sodium hypochlorite overnight to bleach the sediment, the beakers are then topped up with deionised water, left to settle overnight and then rinsed three more times before being dried. Carbon dioxide ( $\text{CO}_2$ ) is then extracted from the samples using the process described in Figure 5.3. When the  $\text{CO}_2$  is extracted, the amount of gas released is measured in millibars prior to freezing in the collection vessels. This data is not typically utilised, but in this thesis, the amount of  $\text{CO}_2$  being released will be used as an indicator of the presence of carbonate within the sediments where the  $\text{LOI}_{950}$  proves to be lacking. The  $\text{CO}_2$  extracted from the samples were analysed using the VG Optima and Thermo Finnigan MAT 253 at the British Geological Survey. Samples were calibrated using MCS and CCS international standards. Results are reported as per mil, ‰ VPDB (Vienna Pee Dee Belemnite) for  $\delta^{13}\text{C}$  and  $\delta^{18}\text{O}$  from carbonate. A large number of samples from Mangaia did not produce data for  $\delta^{18}\text{O}$  and  $\delta^{13}\text{C}$  as it became apparent during analysis that carbonate was not consistently precipitated throughout the core.



### 5.5.3 Conceptual Model for $\delta^{18}\text{O}$ in Tropical Lakes

Seasons in tropical regions are defined by changes in precipitation rather than changes in temperature, as such, the isotopic composition of lake water at low elevation tropical sites is controlled principally by changes in the hydroclimate. During wetter conditions, precipitation acts as a source of relatively enriched  $^{16}\text{O}$  as it is preferentially evaporated from ocean water, replenishing the lake, leading to an increase in the lake level and causing a relative drop in the  $^{18}\text{O}$  content in the lake water. It is expected that the higher levels of precipitation will lead to an increase in soil in-wash into the lake, evidenced by an increase in terrigenous material within the lake sediments. Conversely, during drier conditions, evaporation increases whilst input into the lake via precipitation decreases,  $^{16}\text{O}$  is preferentially evaporated from the lake water as it is isotopically lighter and the lake level drops causing the residual lake water to become  $^{18}\text{O}$  enriched. During this time, it is also expected that there will be a decrease in soil in-wash and thus a relative drop in terrigenous material in the sediments. Both Conroy et al (2008) and Thompson et al (2017) found that during periods of drier climate there were higher rates of carbonate precipitation at both Genovesa Crater Lake and Bainbridge Crater Lake respectively. Based on this, theoretically, the records should show higher (lower) carbonate precipitation and lower (higher) diatom concentrations during dry (wet) periods. The specific challenge in using oxygen isotopes from makatea lake systems in the Pacific, is that they can be connected periodically to the surrounding ocean via groundwater percolation or cave systems (Ellison, 1994; Chagué-Goff *et al.*, 2016; Hassall, 2017). This results in potential changes in salinity that is a particular source of uncertainty when trying to reconstruct precipitation, as marine incursions would see a shift in the  $\delta^{18}\text{O}$  in the lake water due to higher fractions of  $^{18}\text{O}$  in seawater (approximate  $\delta^{18}\text{O}$  value of 0‰) (Rao *et al.*, 1987; Darling, 2004; Darling *et al.*, 2006). Therefore, it is important to be able to differentiate between periods of drier conditions and of marine incursions since both would register as an increase in the ratio of  $\delta^{18}\text{O}$  in the lake water. Any shifts in the salinity of the lake either through changes in the marine input into the lake or the freshening of the lake through long-term persistent high levels of precipitation will influence the algal community composition and will emerge in either marine or freshwater biogenic mineralogy within the sediments. It has also been suggested

that the brackish natures of these lake systems will lead to the presence of Sr in the sediments due to flocculation of in-washed soils (Hassall, 2017). Significant inputs of marine water into the lake system may also cause an increase in the  $\delta^{18}\text{O}$  signature whereas during fresher periods the  $\delta^{18}\text{O}$  signature should reflect hydroclimate changes. This model is to be tested using data presented in this study and is illustrated in Figure 5.4.

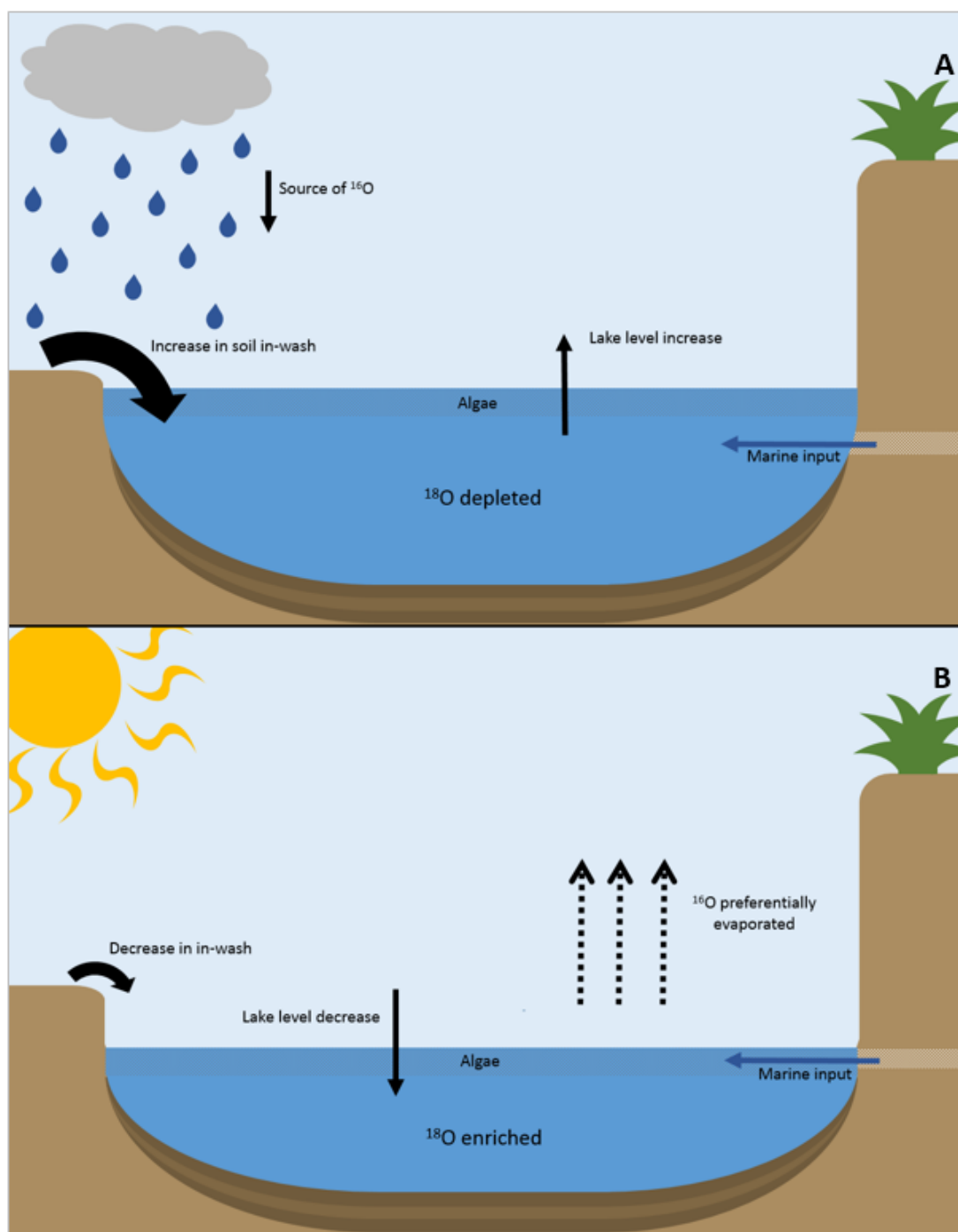


Figure 5.4: Diagram illustrating conceptual model for shifts in environmental proxies during wet (A) and dry (B) conditions in tropical lake systems. Adapted from Hassall (2017).

#### 5.5.4 Carbonate $\delta^{13}\text{C}$ record in Lake Sediments

When analysing the carbon dioxide produced from carbonate sediments, two isotopes are analysed – the first is  $\delta^{18}\text{O}$  discussed above and the second is the inorganic  $\delta^{13}\text{C}$  ( $\delta^{13}\text{C}_{\text{inorganic}}$ ). The  $\delta^{13}\text{C}_{\text{inorganic}}$  is typically a reflection of the total dissolved inorganic carbon (TDIC) present in the water on formation. Changing  $\delta^{13}\text{C}_{\text{inorganic}}$  values can indicate a change in the inflowing waters, higher levels of lake productivity in the form of photosynthesis or a change in the exchange of carbon dioxide between the atmosphere and TDIC (Leng and Marshall, 2004). The  $\delta^{13}\text{C}$  values can assist with differentiating between these processes as generally  $\delta^{13}\text{C}$  TDIC values reflect the allochthonous input of terrestrial carbon from  $\text{C}_3$  (-25‰ to -32‰) and  $\text{C}_4$  (-10‰ to -15‰) plants but also the autochthonous lake sources such as in-lake plants or plankton (-40 and -20‰) which can affect TDIC (Valero-Garcés *et al.*, 1997; Leng and Marshall, 2004). Typically, the inflow of groundwater would decrease  $\delta^{13}\text{C}$  values (Li and Ku, 1997; Leng and Marshall, 2004; Liutkus *et al.*, 2005) with values for groundwater or river waters coming in roughly around -10% to -15% due to plant respiration and  $\text{CO}_2$  generation from soils washed in from the surrounding catchment (Leng and Marshall 2004). However, at both Lake Tiriara and Emaotfer Swamp the surrounding catchment geology in the form of the makatea escarpment and raised coralline limestone terraces respectively offering another possible  $\delta^{13}\text{C}$  source. Marine carbonates typically have a  $\delta^{13}\text{C}$  value of 0‰ VPDB (Valero-Garcés *et al.*, 1997). Where groundwater meets a limestone catchment, the effect can be a much higher  $\delta^{13}\text{C}$  value of -3‰ to +3‰ due to water eroding and dissolving the surrounding geology releasing the carbon from the marine carbonate into the groundwater (Andrews *et al.*, 1997; Leng and Marshall, 2004). Figure 5.5 illustrates some more of the fractionation pathways for  $\delta^{13}\text{C}$  within a lake and the associated values.

There are several examples of the use of  $\delta^{13}\text{C}$  from carbonate in tropical regions as an indicator of environmental and hydrological change. For example, a record from Lake 30 in Kiritimati uses  $\delta^{13}\text{C}$  from carbonate as a proxy for changes in inflow of groundwater and productivity, where lower  $\delta^{13}\text{C}$  would indicate groundwater input and higher  $\delta^{13}\text{C}$  indicates higher levels of photosynthesis (Wyman *et al.*, 2021). Similarly, a record from Lake Kail in Guatemala utilises  $\delta^{13}\text{C}$  from carbonate as part of their hydroclimate reconstruction and found that the covariance between  $\delta^{18}\text{O}$  and  $\delta^{13}\text{C}$  in carbonates

occurred during dry conditions when lake levels were lower, and the lake was disconnected from inflowing waters creating a closed system (Stansell *et al.*, 2020). These examples highlight how  $\delta^{13}\text{C}$  from carbonates can be a useful proxy for hydrological change.

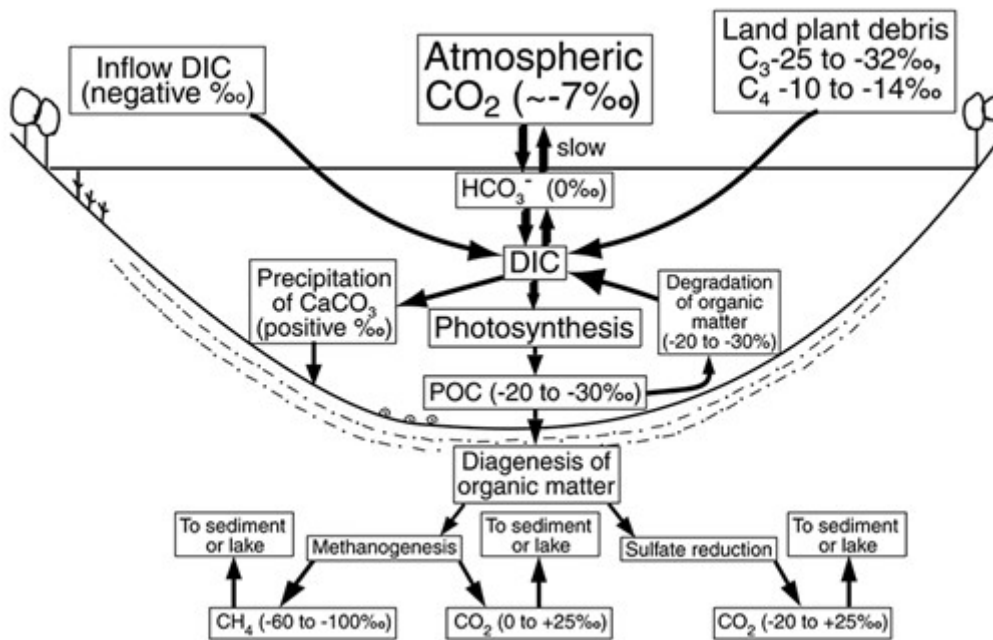


Figure 5.5: Fractionation pathways for  $\delta^{13}\text{C}$  in and around the lake environment - from Cohen (2003).

## 5.6 Organic Proxies

### 5.6.1 Total Organic Carbon, Total Nitrogen and C/N ratio

Organic matter of lake sediments can provide important insights into how lakes, their surrounding catchment and even how climate has changed through time (Meyers and Teranes, 2001). Total organic carbon (TOC) is a useful tool for inferring the organic content of sediment and is the preferred method over LOI due to the associated error attached to the LOI method (Meyers and Teranes, 2001). Typically, organic matter from plants is made up of approximately 50% carbon so if the TOC carbon value is doubled that should provide an estimate of the organic content of the sediment. Considering this, there should be a strong relationship between the TOC and the  $\text{LOI}_{550}$  record as both act as indicators for total organic content (Meyers and Teranes, 2001).

The ratio of total organic carbon and total nitrogen (C/N) is a useful tool in palaeolimnological studies as it is used as an indicator of the proportion of autochthonous and allochthonous produced organic matter that often are connected with changing levels of in lake productivity or in-wash respectively (Cohen, 2003; Meyers, 2003). Typically, C/N values of below 10 signify that the organic matter is primarily comprised of matter from lacustrine algae whilst values over 20 signify that the organic matter is primarily comprised of matter from terrestrial plants washed into the lake. If C/N values sit between 10 and 25 then this would imply that the organic matter is comprised of a mix of terrestrial and lacustrine algae (Heyng *et al.*, 2012). Conroy *et al.* (2008) has also used C/N ratio alongside particle size data to reconstruct lake level and climate changes from El Junco Lake located in the Galapagos in the Eastern Pacific. They found that higher C/N ratio typically indicated a shallower lake with higher rate of terrestrial input whereas during times of high lake level C/N values would drop due to increase in algal productivity.

## 5.6.2 Carbon and Nitrogen Isotopes

### 5.6.2.1 $\delta^{13}\text{C}_{\text{organic}}$

Stable isotopes in organic sediments are frequently used as part of a suite of organic proxies that provide valuable insights into environmental changes through time. Variations in  $\delta^{13}\text{C}$ , for example, can provide information on the source of organic matter and can be used as a proxy for productivity as  $\delta^{13}\text{C}$  is preferentially taken up by algae (Meyers and Teranes, 2001). Changes in  $\delta^{13}\text{C}$  can be also used as an indicator of increased nutrient concentrations and human disturbance in the catchment (Brenner *et al.*, 1999). Changes in bulk lake sediment  $\delta^{13}\text{C}$  can be indicative of alterations to the hydrology of the lake or wider precipitation patterns through time (Heikkilä *et al.*, 2010; Hernández *et al.*, 2013).  $\delta^{13}\text{C}$  values are calculated through a ratio of  $^{13}\text{C}$  and  $^{12}\text{C}$  (Bradley, 2015). The source of organic matter is an important factor to consider when deciphering changes in  $\delta^{13}\text{C}$  as the carbon ratio in different sources are controlled by different processes. For aquatic plants, the  $\delta^{13}\text{C}$  value is controlled by the dissolved inorganic carbon (DIC) within the lake water that the plants then use for photosynthesis (Brenner *et al.*, 1999). Dissolved inorganic carbon in lake water is influenced by a range of factors including the isotopic properties of inflow to the lake,  $\text{CO}_2$  exchange with the atmosphere and photosynthesis/respiration of aquatic plants (Leng and Marshall, 2004). Whereas, for land

plants the main source of carbon exchange for photosynthesis is the atmosphere. Understanding which source of carbon is dominant will assist with deciphering which processes are controlling the  $\delta^{13}\text{C}$  values.

When the C/N ratio is used in tandem with  $\delta^{13}\text{C}$ , the data sets allow you to distinguish between the main sources of organic matter, as algae,  $\text{C}_3$  and  $\text{C}_4$  land plants have different isotopic and C/N characteristics as shown in Figure 5.6.  $\text{C}_3$  (e.g. Trees) and  $\text{C}_4$  (e.g. Grass) plants are both terrestrial plants but have different photosynthetic pathways that lead to isotopically distinct signatures (Bird *et al.*, 2020). This sits in contrast from more temperate regions where grasses tend to have  $\text{C}_3$  photosynthetic pathways but in tropical regions grasses and sedges typically have  $\text{C}_4$  synthetic pathways (Cohen, 2003). For example, the C/N value for lacustrine algae sit between 4 and 10 whilst land plants have a C/N value of over 30 enabling us to differentiate between them and identify changes in sources through time.

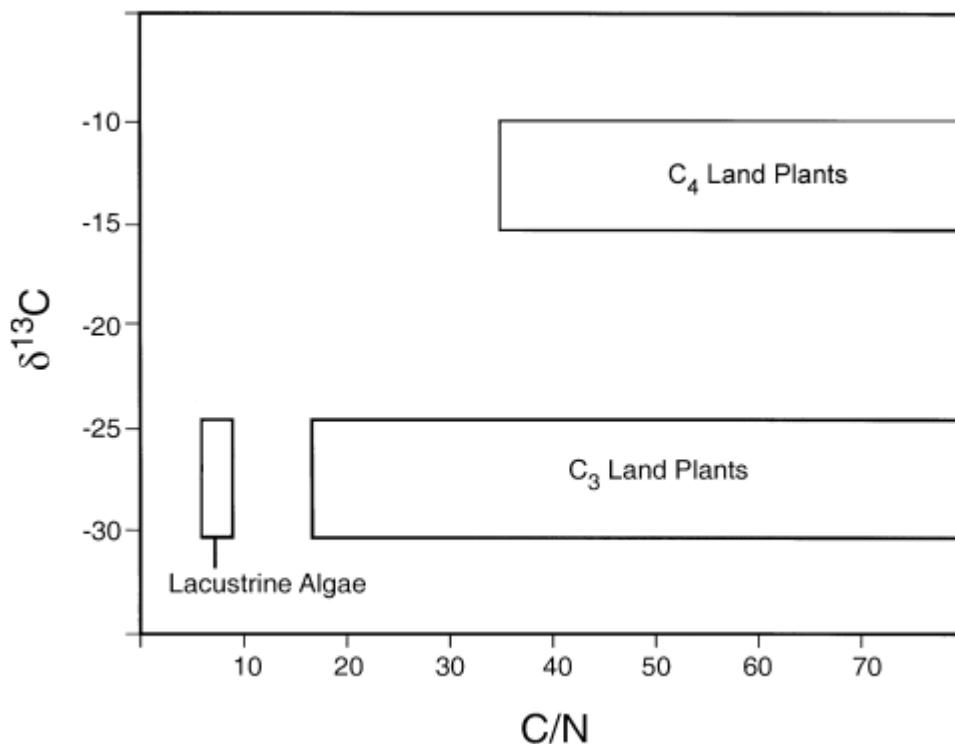


Figure 5.6: Plot of C/N ratio against  $^{13}\text{C}$  and the relative position of different types of plant organic matter (adapted from Meyer, 2003).

The  $\delta^{13}\text{C}$  samples are prepared in the same way and at the same resolution as the  $\delta^{18}\text{O}$  samples described above in section 5.5.2. except samples (approx.  $1\text{ cm}^3$ ) are acidified in

hydrochloric acid overnight - rather than sodium hypochlorite - to remove any inorganic carbon. The samples are then topped up with deionised water and rinsed three times before being dried. They are then ground and weighed into tin capsules ready for analysis.

### 5.6.2.2 $\delta^{15}\text{N}$

The main principle of nitrogen isotope geochemistry is the comparison of the relative abundance between nitrogen's two naturally occurring stable isotopes  $^{15}\text{N}$  and  $^{14}\text{N}$  (Talbot, 2001).  $\delta^{15}\text{N}$  similarly to  $\delta^{13}\text{C}$  can be used independently and in conjunction with  $\delta^{13}\text{C}$  as an indicator for organic matter source in sediments (Meyers and Lallier-Vergès, 1999; Heyng *et al.*, 2012).  $\delta^{15}\text{N}$  values do not change significantly through time due to degradation in sediments located down core when compared to surface values (Meyers and Ishiwatari, 1993).  $\delta^{15}\text{N}$  is particularly useful in conjunction with other proxies (Cohen, 2003). Comparing the  $\delta^{13}\text{C}$  and  $\delta^{15}\text{N}$  values as shown in Figure 5.7 can also assist in identifying the influences of certain processes impact on the isotopic values of autochthonous organic matter (Finlay and Kendall, 2007). N isotopes can also be used to identify changes in productivity, hypolimnion volume, water chemistry, algae, dissolved inorganic nitrogen supply and diagenetic processes (Cohen, 2003).

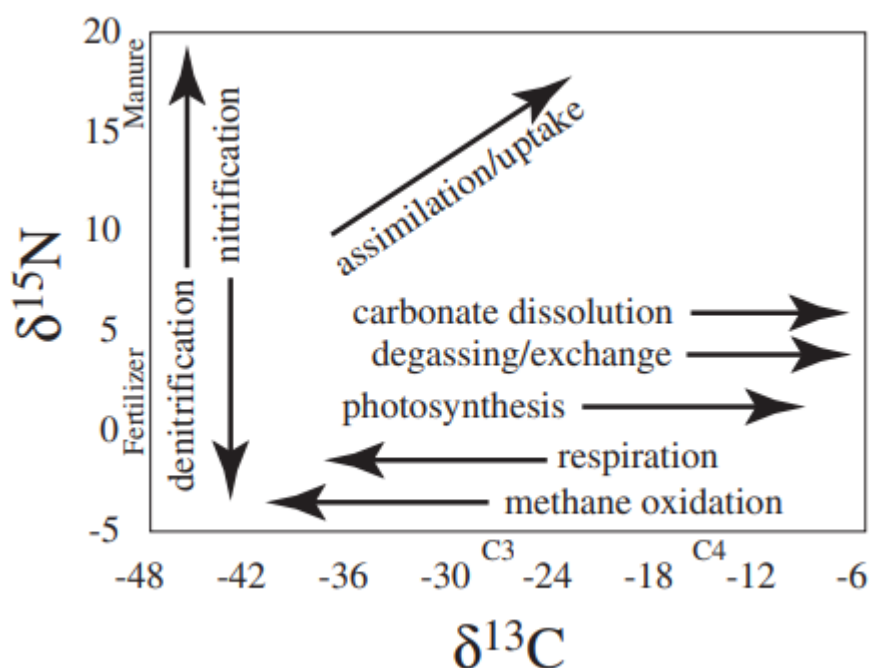


Figure 5.7: Graph denoting the different processes affecting  $^{15}\text{N}$  and  $^{13}\text{C}$  and how they impact on the isotopic values (Finlay and Kendall, 2007).

For  $\delta^{15}\text{N}$ , samples are simply freeze dried to remove water content and then weighed into tin capsules before being analysed. The material used for analysis of nitrogen content and isotopes utilises freeze dried raw sediment rather than the prepared sediment used for carbon analysis, which is acidified as the preparation of samples can remove nitrogen that already typically has relatively low values in lake sediments (Meyers, 2003). Therefore, nitrogen values presented will represent total nitrogen rather than just organic nitrogen alone. All samples were analysed at the BGS in Keyworth using the Isoprime precision with an Elementar elemental analyser. Results are reported as per mil, ‰ VPDB (Vienna Pee Dee Belemnite) for  $\delta^{13}\text{C}$  and per mil, ‰ AIR (atmospheric air  $\text{N}_2$ ) for  $\delta^{15}\text{N}$ . All organic carbon and total nitrogen samples were calibrated using in-house BROCC3 and Spirulina standards. The C/N ratio is simply calculated using the total percentage organic carbon and total nitrogen, which is reported during analysis along with the isotope values.

## 5.7 Diatom analysis

To account for periods where the potential intrusion of ocean (relatively saline) water may be a significant control on the oxygen isotope record for Lake Tiriara, diatoms were used to reconstruct salinity during the same period. Many species of diatom have a salinity tolerance that varies between species to an extent whereby the presence and absence of species can be used to infer past salinity changes in particular environments (Fritz *et al.*, 2010). Diatom species are globally distributed and their environmental preferences are relatively well understood (Stoermer and Smol, 2010), which allows the use of diatoms to reconstruct relative salinity changes in Pacific records. Diatoms have been studied in and around both Emaotfer Swamp and Lake Tiriara. Work by Chague-Goff *et al* (2016) on the peat swamp that borders Lake Tiriara looked at shifts in marine and freshwater diatoms in relation to potential tsunami and cyclone events through the Holocene showing there have been shifts in the relative presence of marine species over the past three thousand years. Similarly, work by Wirmann *et al* (2011) identified changing diatom community structure over the past 4,000 years and how it relates to hydrological changes.

Where samples were taken for the pilot oxygen isotope analysis from the Mangaia sequence, additional samples were also taken from the same section to test for presence of diatoms. As we know there is a connection between Lake Tiriara and the ocean (Ellison, 1994; Chagué-Goff *et al.*, 2016) it was important to check whether the lake was saline in the past as it may impact on the interpretation of the stable isotope data sets. Previous studies of the Emaotfer Swamp included diatom analysis and did not indicate salt water influence at this site (Wirrmann *et al.*, 2011) so further diatom analysis was not required. Samples were prepared according to an adapted method described by Batarbee *et al.* (2002). Slides were mounted using Naphrax and diatoms were identified using a high-powered light microscope. Microspheres were not added so instead of diatom concentrations, for each slide, 300 diatom valves were counted where possible and values are expressed as relative abundance percentage. Diatoms were identified using a combination of standard diatom taxonomy floras (Krammer and Lange-Bertalot, 1991; Sims, 1996) and a diatom guide from the nearby Lake Teroto on Atiu in the Cook Islands from Parkes (1994).

## 5.8 Chronology

### 5.8.1 $^{210}\text{Pb}$ & $^{137}\text{Cs}$

For younger sediments (<150 years), alternative methods need to be used to develop a chronology as radiocarbon dating becomes unreliable. Short-lived radionuclides such as lead-210 ( $^{210}\text{Pb}$ ) and caesium-137 ( $^{137}\text{Cs}$ ) have proven to be a useful tool - due to their different half-lives - in creating a robust chronology in more modern sediments (Foucher *et al.*, 2021).

The radioactive unstable isotope lead-210 ( $^{210}\text{Pb}$ ) has a half-life of 22 years and can be used to date sediments and calculate sedimentation rates over the past 100-150 years (Dinsley, Gowing and Marriott, 2019).  $^{210}\text{Pb}$  is a naturally occurring isotope as part of the decay of the  $^{238}\text{U}$  chain that enters sediment archives in two ways. The first is described as supported where  $^{226}\text{Ra}$  in sediments decays to  $^{210}\text{Pb}$  and can be accounted for through precursor isotopes present in the sediment archive. The second is described as unsupported where  $^{222}\text{Rn}$  in the atmosphere decays to  $^{210}\text{Pb}$  that then attaches to aerosols and is consequently washed out of the atmosphere through precipitation back

into the terrestrial environment where it can be deposited into lakes and peatlands. However, unlike the supported  $^{210}\text{Pb}$  the unsupported  $^{210}\text{Pb}$  cannot be attributed to a parent isotope as they are not present in the terrestrial archive (Dinsley, Gowing and Marriott, 2019) – see Figure 5.8.

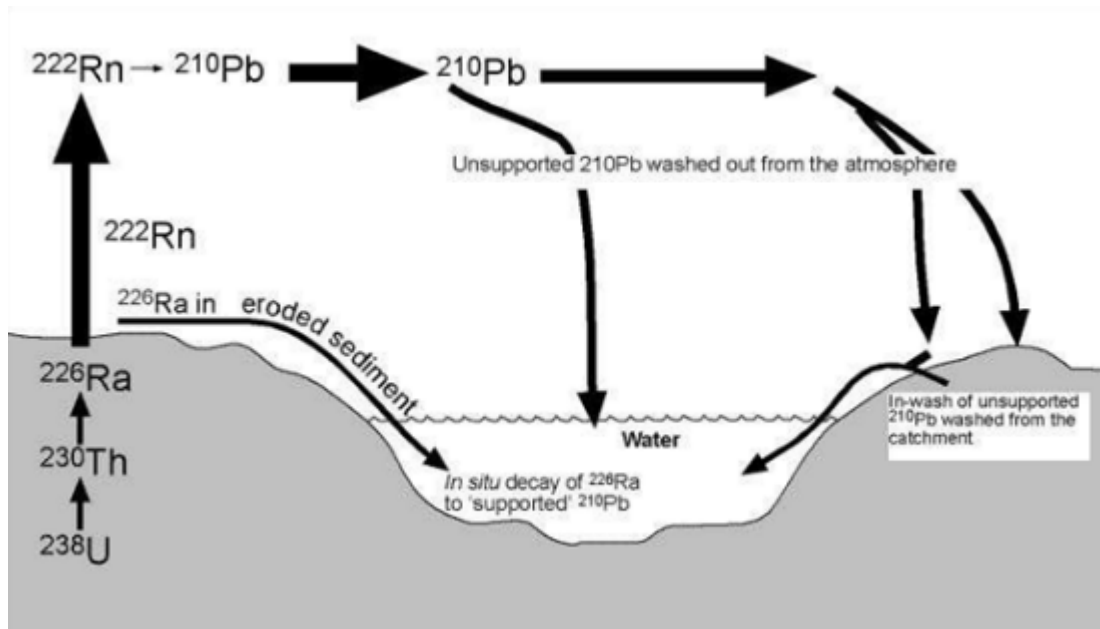


Figure 5.8: Diagram showing the different pathways of  $^{210}\text{Pb}$  into a depositional environment such as a lake (Taken from Dinsley, Gowing and Marriott (2019), original source Oldfield and Appleyby (1984).

Where  $^{210}\text{Pb}$  measurements are low, its granddaughter isotope Polonium-210 ( $^{210}\text{Po}$ ) can be used to determine  $^{210}\text{Pb}$  values in sediment (El-Daoushy, Olsson and Garcia-Tenorio, 1991). The core top sediments of Lake Tiriara had low  $^{210}\text{Pb}$  measurements so the determination of  $^{210}\text{Po}$  was used as a proxy for  $^{210}\text{Pb}$ . When the current  $^{210}\text{Pb}$  activity has been established the data needs to be analysed using an appropriate model to determine the initial  $^{210}\text{Pb}$  activity at deposition (Dinsley, Gowing and Marriott, 2019). A number of models are available but each comes with a set of assumptions about the deposition rate of  $^{210}\text{Pb}$  into the sediment archive and about the accumulation rate of the archive itself (Dinsley, Gowing and Marriott, 2019). The constant rate of supply (CRS) model assumes, as the name suggests, a constant rate of supply of unsupported  $^{210}\text{Pb}$  being deposited from the atmosphere to the depositional environment where it becomes preserved in the sediments. This constant rate is assumed even if the accumulation rates change through time at the site of deposition (Appleyby and Oldfield, 1978). The CRS model has been used by Conroy *et al.* (2008), Sachs *et al.* (2009) and Hassall (2017) for their  $^{210}\text{Pb}$  data

generated from lake sediments in the tropical South Pacific and therefore is considered appropriate for the sites studied in this thesis.

For  $^{210}\text{Po}$ , samples were prepared as per the method provided by the Geoscience Advisory Unit - which is detailed in Croudace (2010) - at the Geography and Environmental Science laboratories at the University of Southampton. This method requires 1-2 g of dry powdered sediment, which is placed into a 250ml beaker. 1 ml of *aqua regia* is added at a time to the beaker until 20 ml total has been added. The sample is left to react for 30 minutes, the beaker is then placed onto a hotplate with a stirrer for 2 hours at 70 °C. The beaker is removed from the heat and left to settle. The supernatant liquid is then decanted into a centrifuge tube and 20ml *aqua regia* is added to the beaker, which is then covered and put back onto heat for another 4 hours. Once the beaker has cooled down, the contents are then transferred to the centrifuge tube. The tube should then be put into a centrifuge and spun at 3000 rpm for 5 minutes. The supernatant liquid is then poured off and 10 ml of hydrochloric acid is added, the tube is centrifuged and then washed twice more with distilled water. The remaining sample is dried at 80 °C until all liquid has been evaporated. 5 ml of hydrochloric acid is added to the sample and then dried again until the acid has fully evaporated. This process is completed three more times but using 0.5 ml of hydrochloric acid on the repeats to ensure any nitrates are disintegrated. The evaporated samples were then transferred to the Geoscience Advisory Unit at the National Oceanography Centre in Southampton. The samples were spiked with ~0.01 Bq of  $^{209}\text{Po}$  tracer, dissolved in 8 ml of hydrochloric acid and then poured into a 250 ml beaker, which was then topped up with deionised water to 100 ml. 1.5g of Ascorbic acid was then added to the beaker and stirred. A silver disc was placed into the solution to plate the sample.  $^{210}\text{Po}$  activity is determined using alpha spectrometry.

The unstable radioactive isotope Caesium-137 ( $^{137}\text{Cs}$ ) is often used in conjunction with  $^{210}\text{Pb}$  as it provides an independent chronostratigraphic marker points from the 1950s onwards (Foucher *et al.*, 2021) with which we can test the  $^{210}\text{Pb}$  chronology.  $^{137}\text{Cs}$  is a man-made product and it was primarily produced during thermonuclear bomb testing between the 1950s and the 1980s with a fallout peak in 1963. Studies conducted in the Southern Hemisphere typically find a single peak in the  $^{137}\text{Cs}$  record which has been associated with the thermonuclear weapon tests peak though there is some debate as to the exact timing (Foucher *et al.*, 2021). Several palaeoenvironmental studies from the

tropical Pacific have used  $^{137}\text{Cs}$  as a chronological tool and accept that the peak in the  $^{137}\text{Cs}$  record occurs at AD 1964  $\pm$  1 (Terry, Kostaschuk and Garimella, 2006; Conroy *et al.*, 2008; Hassall, 2017). For  $^{137}\text{Cs}$ , samples were freeze-dried and  $^{137}\text{Cs}$  activity is determined using gamma spectrometry at the Geoscience Advisory Unit at the National Oceanography Centre in Southampton.

### 5.8.2 Radiocarbon/ $^{14}\text{C}$

Radiocarbon ( $^{14}\text{C}$ ) has been used as a chronological tool since the 1950s and can be used on a range of materials - including lake sediments - dating back to 55,000 years old, covering key periods of environmental change and human evolution (Bradley, 2015; Heaton *et al.*, 2021).  $^{14}\text{C}$  is created as part of a natural process where neutrons from cosmic rays collide with nitrogen atoms in the upper atmosphere, the product of which then oxidises and eventually reaches the carbon cycle in the form of  $^{14}\text{CO}_2$  (Bradley, 2015; Hajdas *et al.*, 2021).  $^{14}\text{C}$  is transported through the carbon cycle remaining at equilibrium with the atmosphere. At the death of any carbon containing lifeform, the  $^{14}\text{C}$  retained within the organism becomes locked within the material, as it is unable to continue an exchange with the carbon cycle. This provides a type of stop clock in that moment as through time the  $^{14}\text{C}$  will deteriorate as it is unstable and we can analyse this to determine the age of the associated material (Bradley, 2015; Hajdas *et al.*, 2021; Heaton *et al.*, 2021).

Twenty-one new AMS  $^{14}\text{C}$  dates were produced for Emaotfer and Tiriara – eleven dates for Emaotfer and ten dates for Tiriara - using a combination of bulk sediment and picked plant macrofossil samples. Samples were collected at the Geography and Environmental Science laboratories at the University of Southampton from the core material stored there. Picked samples were wet sieved to separate out the organic material and any suitable material was placed into a glass vial. Bulk samples were collected directly from the cores into glass vials. Both bulk and picked samples were freeze dried to remove any water and then all vials were sealed with a tin foil cap and labelled. They were then sent to Scottish Universities Environment Research Centre (SUERC) in Glasgow for analysis.

At SUERC the samples were subjected to an acid-base-acid protocol in order to remove any carbon not attributed to the organic samples. Prior to analysis, samples were digested in hydrochloric acid for two hours whilst being heated to 80 °C. The acid was

rinsed from the sample using deionised water and then placed in Sodium hydroxide for two hours whilst being heated to 80 °C. This process is repeated until all humic elements were removed and the sample is clear. Finally, the remaining sample was rinsed, placed again in hydrochloric acid for one hour at 80°C then rinsed and dried (Dunbar *et al*, 2016). Total carbon was calculated based on the weight change once pre-treated samples were converted to CO<sub>2</sub>, which is accomplished by heating the sample in a sealed quartz tube with Copper Oxide. Graphitisation was achieved by using a Fe/Zn reduction to convert the sample to gas.

Developments over the past six decades have meant that now dates can be produced using only a tiny amount of material (<3mg), thanks to accelerator mass spectrometry (AMS) (Dunbar *et al.*, 2016; Ascough, pers comm, March 2022). For samples processed by AMS, analysis was done at a low current. To account for modern carbon contamination in the AMS samples the data was corrected using the method presented by Santos *et al.* (2007). Additionally, for the smallest samples (<100 µgC) a further correction was required to elucidate any effect from old carbon which due to the size of the samples can become an important factor.

Radiocarbon ages are reported as the number of years before present with present referring to the year 1950 AD. Ages are reported alongside the  $\pm 2\sigma$  level for overall analytical confidence. The uncertainty values represent the overall analytical uncertainty, which accounts for any corrections and observed scatter. <sup>14</sup>C data was background corrected where possible and normalised to  $\delta^{13}\text{C-VPDB}\text{‰} = -25$ .

All age models were generated using Bayesian age-depth modelling via the Rbacon package available for use in RStudio. The <sup>14</sup>C ages were calibrated using the SHCal13 post bomb and atmospheric curves.

### 5.8.3 Tephrochronology

Tephrochronology has proven to be an important field in palaeoenvironmental studies offering an independent geochronological tool from <sup>14</sup>C. It has been widely used in Europe to the point at which researchers have developed a tephra network that is able to robustly date and link ice core, terrestrial, marine and archaeological records across the continent (Blockley *et al.*, 2014; Lowe *et al.*, 2015). The development of tephrochronology

in the tropical Pacific is not as advanced and it is still a growing field in this region but it can still be used successfully to derive known eruption dates from palaeoenvironmental and archaeological archives (e.g. Bedford, Spriggs and Regenvanu, 2006; Wirrmann *et al.*, 2011). The fundamental principle of tephrochronology is that during a volcanic eruption, a large ash plume may be produced and within that cloud is a range of airborne pyroclastic material that is ejected some distance from the volcano (R. Bradley, 2015). The smallest component of this material are microscopic glass shards that can travel up to thousands of kilometres on the wind before they are deposited. Where glass shards are deposited in a lake or a peat bog for example they become part of the environmental archive at that site (Lowe, 2011). The glass shards have a unique chemical fingerprint that can be analysed and then matched to known eruptions providing a chronological marker for that sequence.

Within the Emaotfer Swamp sediments, a potential tephra layer was identified at 26 cm depth using XRF, LOI and magnetic susceptibility data. This section of the core was sampled and sent off to the University of Auckland where the coarsest glass shards (~63–125  $\mu\text{m}$ ) were cleaned in deionised water, extracted from the sediment and mounted in an epoxy resin. The epoxy block is then ground and polished to reveal the surface of the shards, which is then sputter-coated in carbon. The shards were analysed using the JXA8530F Hyperprobe to identify the chemical fingerprint of the tephra layer in order to identify its origin. Parameters for analysis are presented in Table 5.2. To reduce Na loss, typically the electron beam size used for analysis was 10  $\mu\text{m}$  but this was dropped down to 5  $\mu\text{m}$  to accommodate for smaller shards. Secondary glass standards - ATHO-G (MPI-DING), BCR-2G, (USGS) and VG-568 (NMNH 72854) - were used for calibration purposes and to test accuracy of data output.

Table 5.2: Summary of parameters used in tephra glass shard analysis

<b>Parameter</b>	<b>Setting</b>
Beam size (defocussed)	10 $\mu\text{m}$ / 5 $\mu\text{m}$
Accelerating voltage	15 kV
Electron beam current	2 nA
Peak dwell time	1510 seconds
Total background dwell time	10 seconds

## Chapter 6 Environmental Change in Vanuatu

### 6.1 Introduction

Following from the site description in Chapter 4 and methods described in Chapter 5, this chapter presents the results from the Emaotfer Swamp sequence from Efate, Vanuatu. The sediments of Emaotfer Swamp were extracted in 1 metre sections down to a maximum depth of 294cm and consist of organic-rich peat from the surface to around 30cm depth and there is then a sharp transition to marl sediments which continue to the base of the cores. This chapter presents the chronology, sedimentology, geochemistry and stable isotope from Emaotfer Swamp. After the results, a full interpretation of the sequence is introduced followed by a more detailed examination of particular sections of interest. The chapter will conclude with a summary of the key results from Emaotfer Swamp.

### 6.2 Chronology

#### 6.2.1 Radiocarbon/ $^{14}\text{C}$

The age model for Emaotfer Swamp is based on eleven  $^{14}\text{C}$  AMS dates using a mix of plant macrofossil and bulk sediment material shown in Table 6.1. Bulk sediment was used in place of plant macrofossils when there was not sufficient macrofossil material available. It was not possible to identify whether the macrofossils were terrestrial or not due to the small size of the material. Where possible, material was picked in close pairs (one bulk, one macrofossil), where available material allowed, to account for potential reservoir effects as a majority of the Emaotfer sequence is made up of marl with a high carbonate content. It is clear from the age model shown in Figure 6.2 that there is a significant offset between some of the pairs which is likely to be due to in part to in-wash of old carbon from the limestone terrace that Emaotfer sits upon and also in part by freshwater reservoir effect which is where aquatic plants incorporates carbon from the lake water which typically has lower  $^{14}\text{C}$  values than the atmosphere producing older measured ages (Philippsen, 2013) particularly when bulk sediment is used and aquatic plant matter may be present.

Table 6.1:  $^{14}\text{C}$  dates from Emaotfer Swamp, Vanuatu.

Sample depth from surface (cm)	Dated material	$\delta^{13}\text{C}$ (VPDB‰)	Conventional radiocarbon age	2-sigma calibration (cal yr BP)
28	Peat	-25.8	303 ± 37	543
41	Bulk Sediment	-20.0	2181 ± 37	2128
43	Plant macrofossil	N/A	2315 ± 30	2261
79	Bulk Sediment	-20.2	4037 ± 37	4414
81	Plant macrofossil	N/A	2195 ± 30	4508
119	Bulk Sediment	-17.1	5321 ± 38	6043
123	Plant macrofossil	N/A	6210 ± 35	6154
216	Bulk Sediment	-26.9	7079 ± 39	7789
220	Plant macrofossil	N/A	6055 ± 30	7843
282	Bulk Sediment	-22.2	5011 ± 38	8926
284	Plant macrofossil	N/A	3360 ± 30	8962

$^{13}\text{C}/^{12}\text{C}$  ratio was measured for the smaller picked AMS dates during analysis and that value is used to correct for isotopic fractionation (as per Stuiver and Polach (1977)) but it is not appropriate to use as a  $\delta^{13}\text{C}$  value for the sample due to the method used for small AMS samples so these values are not included in Table 6.1. The dates from the base of the core were considerably younger than dates produced from shallower sediments. This is likely due to contamination of material during collection as the end of the core may have come into contact with younger material as the core was pulled out of the ground and subsampled from the Russian corer.

### 6.2.2 Tephrochronology

A potential tephra layer was identified at 26-27 cm within the Emaotfer Sequence from XRF and magnetic susceptibility. Figure 6.1 shows multiple panels with different elements of the identified tephra layer from Emaotfer Swamp along with the Kuwae tephra's chemical fingerprint. It's clear that the Emaotfer shards (EMB in Figure 6.1) share a very similar chemical makeup with other confirmed Kuwae deposits. The Kuwae eruption occurred approximately 1452 AD providing a chronological marker in the lower part of

the peat section of this sequence. The caldera of Kuwae is located north of Efate between the islands of Epi and Tongoa only around 60 miles away. The Kuwae eruption has been estimated to have an explosive index of VEI 6 (Nemeth, Cronin and White, 2007). A limited number of shards were found within the Emaotfer sequence perhaps explaining the slight discrepancies between data sets and there is one outlying data point. A potential tephra layer was identified at 225-233 cm within the Emaotfer Sequence from XRF and magnetic susceptibility similar to that of the layer identified at 26-27cm. The sample from 225-233 cm had some reworked brown platy tephra shards present but there was no evidence of a primary tephra layer and a vast majority of the material was terrestrial material (A. Monteath, Pers Comm, May 2023).

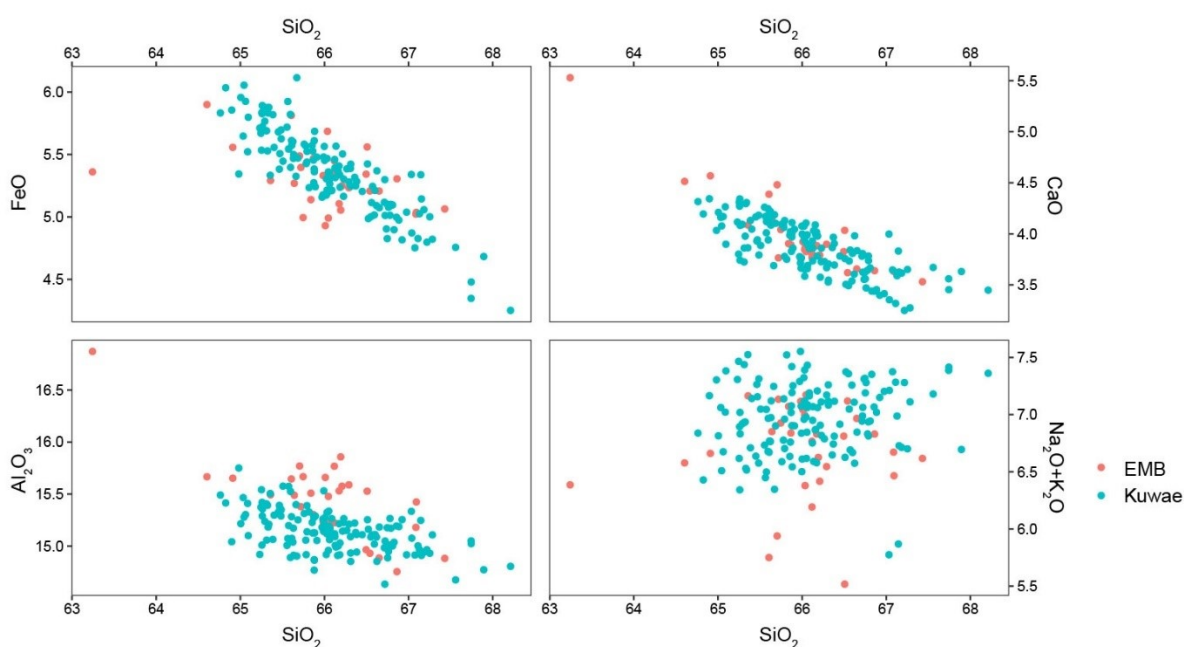


Figure 6.1: Panels show different elements of the chemical fingerprint of tephra shards for the identified tephra layer at Emaotfer compared to known Kuwae deposits.

### 6.2.3 Rbacon Age Model

The <sup>14</sup>C ages, tephra layer and surface age – taken as a minimum age based on the date of core extraction - were used as a data input for the Rbacon package to produce an age model using the southern hemisphere post-bomb curve. The maximum age of the sequence presented in this thesis is 9182 yr cal BP at 294 cm depth and 58% of the dates fell within the age model produced using the Rbacon package. The sedimentation rate for Emaotfer based on this age model is 20 years per centimetre and the rate of

sedimentation appears to decrease around 6000 yr cal BP to present and becomes significantly slower from around 2000 yr cal BP. The rate of sedimentation increases again in the uppermost part of the sequence as the site transitions into a peat bog from around 30 cm to the top of the record. There are large uncertainties in these age models and so a series of age models were run to generate the most robust age model possible. Figure 6.2 and Figure 6.3 show two of the best model outcomes. The age model presented in Figure 6.2 has all the ages weighted equally. The age model in Figure 6.3, to counter the old carbon effect of the marl sediments, put a higher weighting was placed on picked macrofossil dates within the age model as they would not be heavily influenced by reservoir effects.

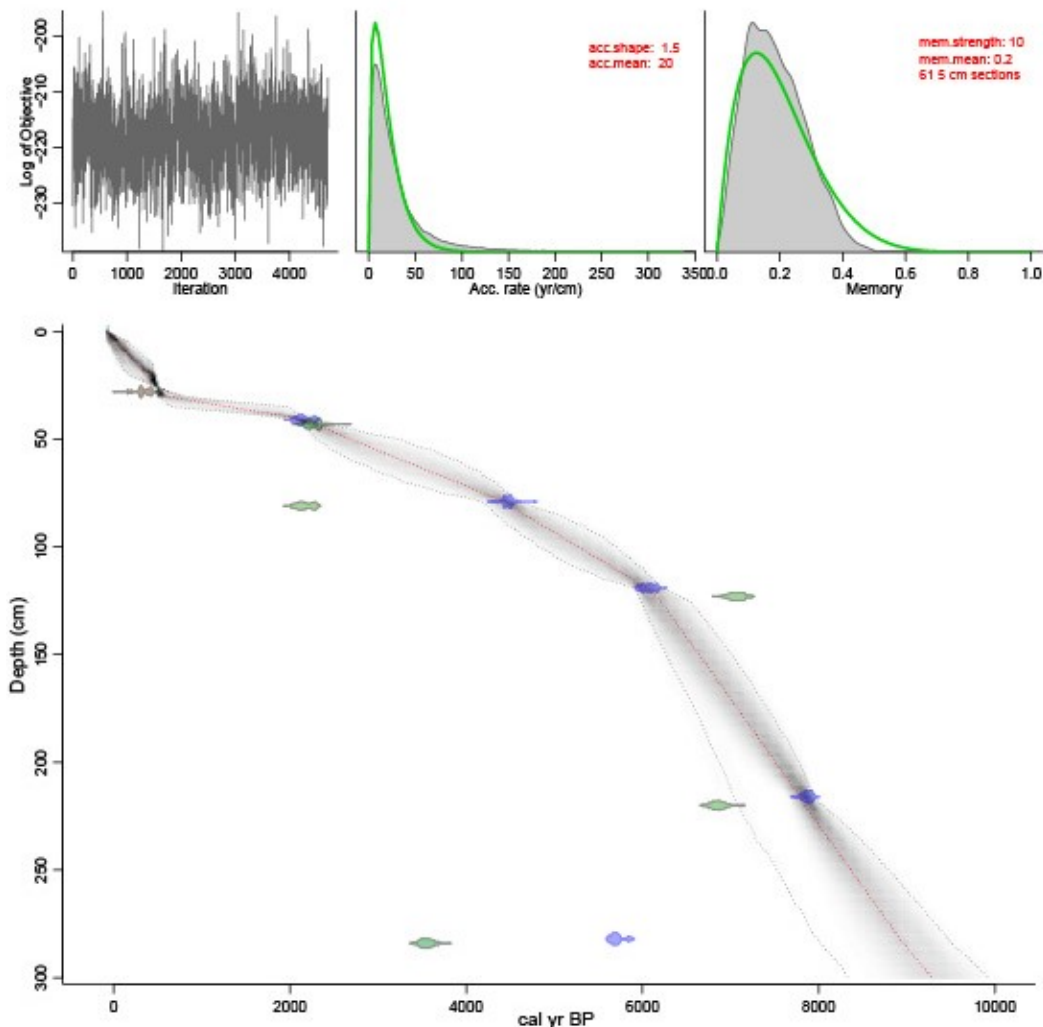


Figure 6.2: Age model generated by the Rbacon package for Emaotfer Swamp. This is the unweighted age model and colours denote the material used for each date. Green = Plant macrofossil, Blue = Bulk sediment and Brown = Peat.

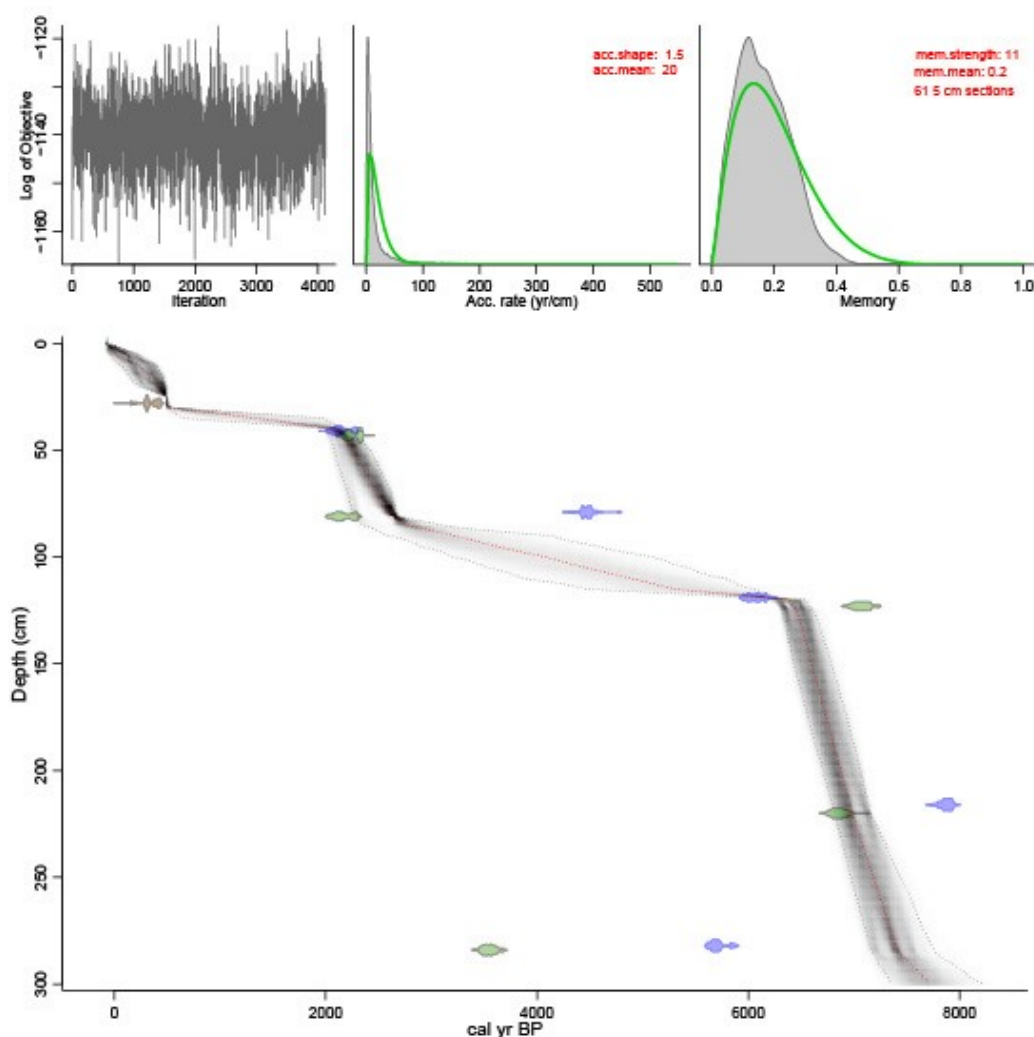


Figure 6.3: Age model generated by the Rbacon package for Emaotfer Swamp. This is the weighted age model and colours denote the material used for each date. Green = Plant macrofossil, Blue = Bulk sediment and Brown = Peat.

For the purposes of this thesis, the age model in Figure 6.2 was used as the age model for the Emaotfer sequence. The second weighted age model in Figure 6.3 suggested a sequence of potential hiatuses or at least a major slowing in sedimentation, which is not supported by the evidence from the sequence. Whereas, the age model in Figure 6.2 just suggests a slowing down in sedimentation just prior to the transition to a swamp, which is supported by evidence in the sequence (this is discussed further in section 6.8.4) and seen in other cores from the same site (N. Dabais, Pers Comm, April 2023).

### 6.3 Magnetic Susceptibility

Looking at the record as a whole in Figure 6.4, the top third of the sequence from 100 cm to the surface – which covers approximately 5000 yr BP to present - has a higher level of magnetic susceptibility and a greater degree of variability compared to the deeper sediments. Prior to 5000 yr BP the magnetic susceptibility levels are very low and show only some small peaks from around 7500 – 8000 yr BP. There is a large magnetic susceptibility peak of 3.4776 SI at 26 cm depth just as the sequence transitions into peat. This is likely to be due to an increase in the deposition of volcanic material from the Kuwae eruption in 1452 AD (498 yr BP) as a sample was taken from this depth and tephra shards from Kuwae were identified as discussed in the chronology section of this chapter. There is a series of small peaks in magnetic susceptibility from around 200 cm down to 235 cm.

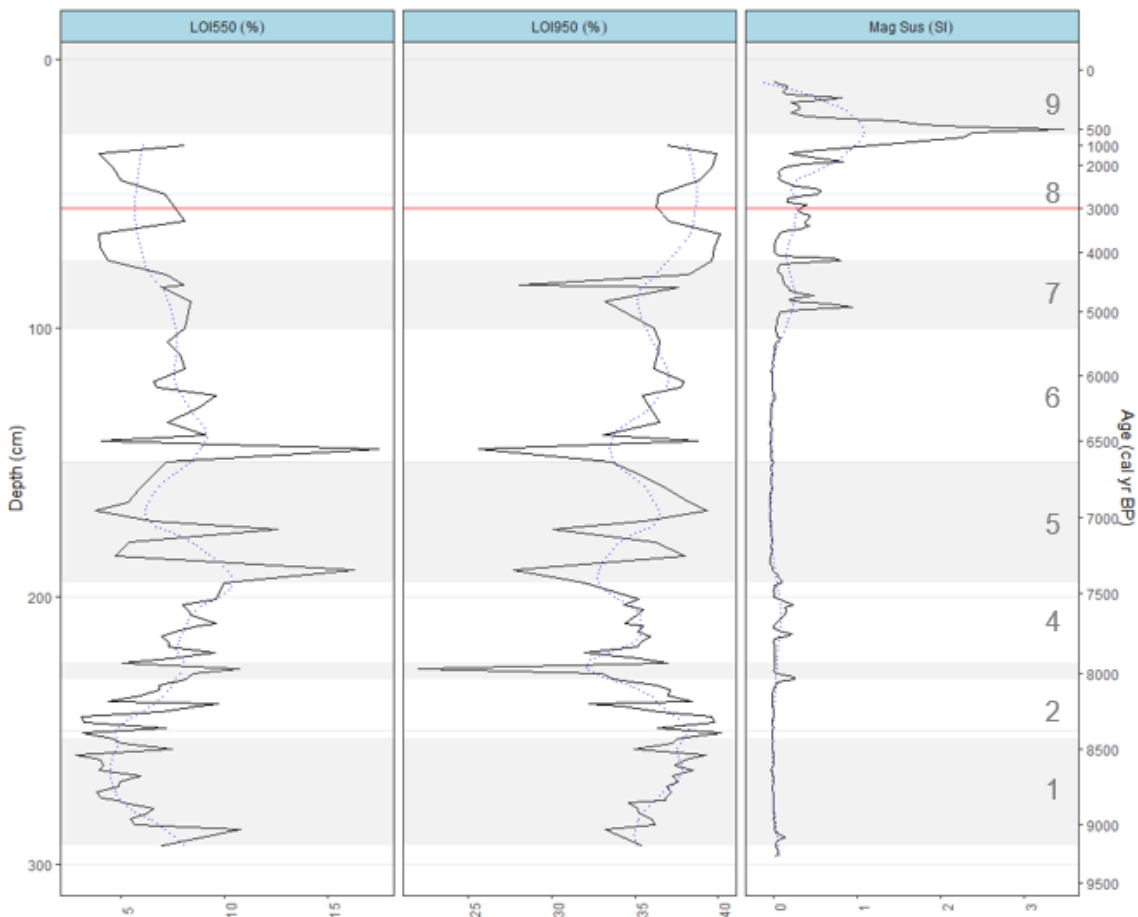


Figure 6.4: Plots of the loss-on-ignition at 550 and 950 °C along with the magnetic susceptibility data for the Emaotfer core sequence. Red line denotes the start of the first wave of human migration into Remote Oceania. Blue line is loess smoothed.

## 6.4 Loss-On-Ignition

Due to limited availability of material, the sampling strategy for the LOI record matches the isotopic samples where a sample is taken every 5 cm for the first 197 cm and following this every 2 cm producing 84 measurements. From Figure 6.4, it is clear that LOI<sub>550</sub> and LOI<sub>950</sub> are inversely related. LOI<sub>550</sub> values were relatively low in the Emaotfer sequence with a minimum value of 3% at 259 cm and a maximum value of 17% at 145 cm. LOI<sub>550</sub> typically remain below 10% throughout the sequence. There is initially a downturn in LOI<sub>550</sub> values in zone 1 but following this LOI<sub>550</sub> values gradually increase through zones 2-4. There is a higher degree of variability through zone 5. From zone 6 onwards values stabilise and show a lower rate of variation.

LOI<sub>950</sub> values were higher than LOI<sub>550</sub> in the Emaotfer sequence with a minimum value of 22% at 227 cm and a maximum value of 40% at 251 cm. LOI<sub>950</sub> values show little variability across zone 1 though values increase gradually throughout from 35 to 38% as they move into zone 2 which shows a slightly higher degree of variability in zone 2 with values varying between 32 and 40%. There is a trough in zone 3 where LOI<sub>950</sub> values dip to 22% at 227 cm. LOI<sub>950</sub> then return back up to around 34-35% through zone 4. In zone 5 there is a higher rate of variability compared to earlier in the record. This variability stabilises through zone 6 with values only varying between 35 and 37%. There is a slight dip in zone 7 to 28% before values increase into zone 8 with LOI<sub>950</sub> varying between 36 and 40% up to the peat boundary.

## 6.5 $\mu$ XRF Geochemistry

Itrax  $\mu$ XRF data originally had a resolution of 200 $\mu$ m but here it has been averaged to a 1 cm resolution to enable comparison between all datasets. When presented individually as opposed to a ratio, elements have been normalised using the molybdenum incoherent scatter signal to correct for water content (Boyle, Chiverrell and Schillereff, 2015). For the correlation matrix and the PCA, the data was transformed using a centred log-ratio to account for dilution effects (Weltje *et al.*, 2015). Zones were designated based on trends in the  $\mu$ XRF and stable isotope data.

For Emaotfer the  $\mu$ XRF data was delineated into eight zones:

Table 6.2: Breakdown of XRF zones for Emaotfer Swamp sequence and a description of major changes in elemental profiles.

Zone	Depth (cm)	Age (cal yr BP)	Description of XRF
E-1	253 – 293	8417-9137 ± 958	There is a high degree of variability in both Ca and S in this part of the sequence but overall, there is an increase in Ca and a slight decrease in S across the zone. Ti, Fe and Si remain relatively stable.
E-2	231 – 253	8031-8417 ± 879	This zone sees an increase in Ti, Fe and Si across this section and relatively constant level of S. Contrastingly, there is a decrease in Ca in this part of the core.
E-3	225 – 231	7926-8031 ± 809	The three terrestrial indicators – Fe, Ti and Si – all peak sharply in this zone indicating a higher level of in-wash into the lake. There is also a peak in S and a drop in the Ca signal within this section. Possible event layer as it is notably different from the zones either side.
E-4	195 – 225	7424-7926 ± 799	S and Si both decrease across this zone whilst other elements show a stabilisation in values but at a higher overall average compared to zone E-1.
E-5	150 – 195	6644-7424 ± 623	This zone sees an increase in the relative variability in the terrestrial proxies, Ti, Fe and Si along with Ca. S does not show the same behaviour and instead dips down to lower average values across this zone.
E-6	100 – 150	5262-6644 ± 455	S increases rapidly in this zone to peak whilst Ca remains relatively stable with a decreasing variability across the section. Terrestrial indicators all decrease gradually across this part of the sequence though Fe does start to rise again towards the end of zone 6.
E-7	75 – 100	4196-5262 ± 478	There is a slight decrease in Fe but a slight increase in values in Ti compared to the zone prior. Si shows a gradual increase in values with Ca also showing an increase in values through this zone. S shows a relatively rapid decrease in values through this zone.
E-8	30 – 75	564-4196 ± 478	Ca values remain variable but on average relatively constant through this zone and similarly Ti, Fe and Si also show stabilisation in values in this section though with a lower rate of variability. This zone sees S drop to very low levels, which continues into the next section.
E-9	0 - 30	564 ± 196 to present	There is a peak in Ti and Fe at the start of this zone along with Si, which is the location of the tephra layer, identified as the Kuwae eruption of 1452. In this section, the sediments change from marl to peat, which is why there is a sudden drop in the amount of Ca present in this section. S remains very low as per the zone E-8.

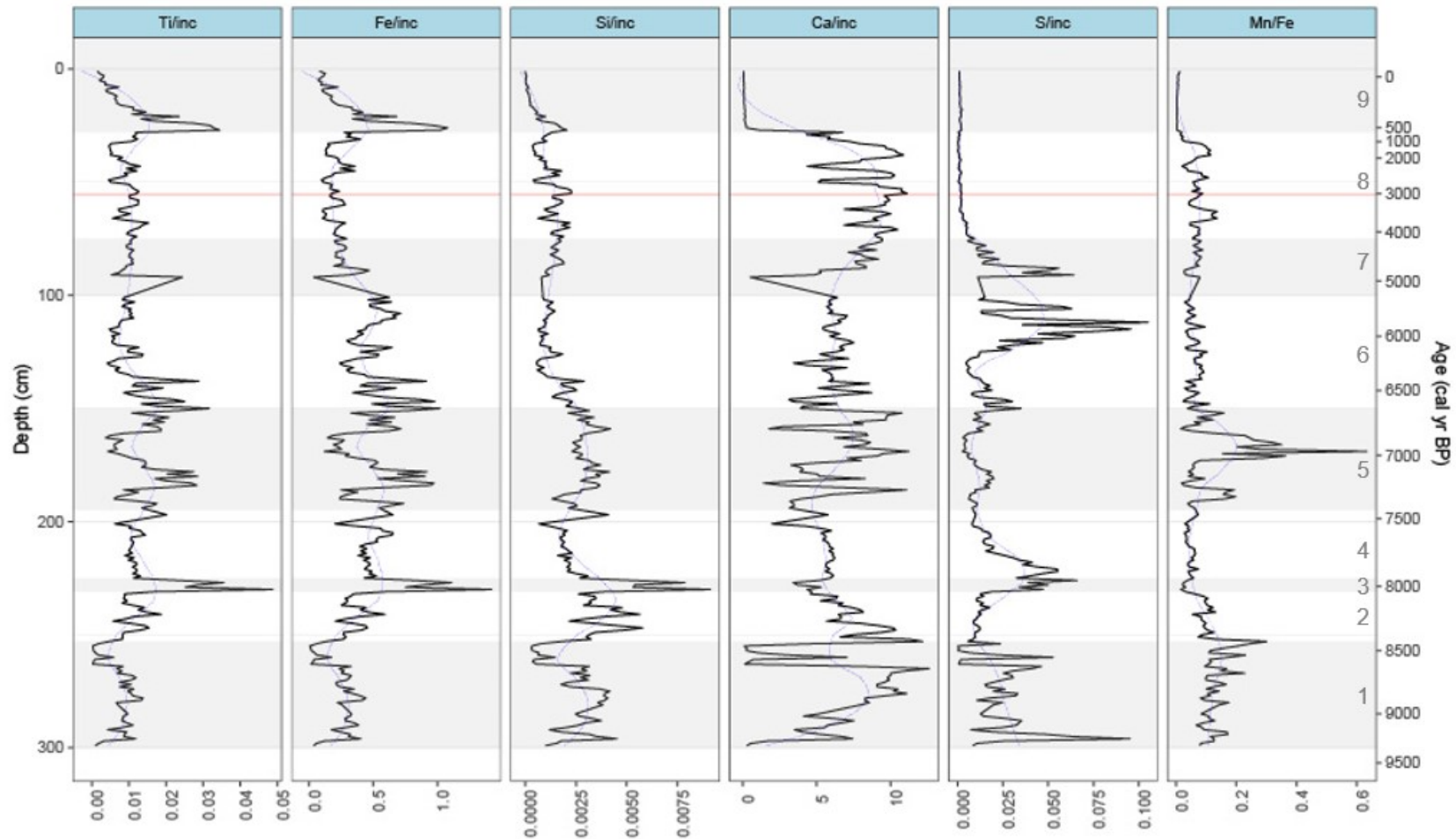


Figure 6.5: Plots of XRF geochemistry data for the Emaotfer core sequence. Grey zones relate to the XRF zones described in Table 6.2. Red line denotes the start of the first wave of human migration into Remote Oceania. Blue line is loess smoothed.

Ca has a strong positive relationship with Sr with an r-squared value of 0.636 ( $n= 281$ ,  $p < 0.01$ ) but neither element has a strong relationship with Ti (Figure 6.6). This suggests that despite being located within a calcium carbonate catchment the calcium in this system is not being transported via in-wash which is indicated by the presence of Ti. Instead it is being produced in the lake which is supported by the strong relationship between Sr and Ca throughout the sequence which are indicative of authigenic carbonate precipitation in the form of aragonite ( $\text{SrCO}_3$ ) (Burn and Palmer, 2014) and it is expected that this has not changed throughout the record.

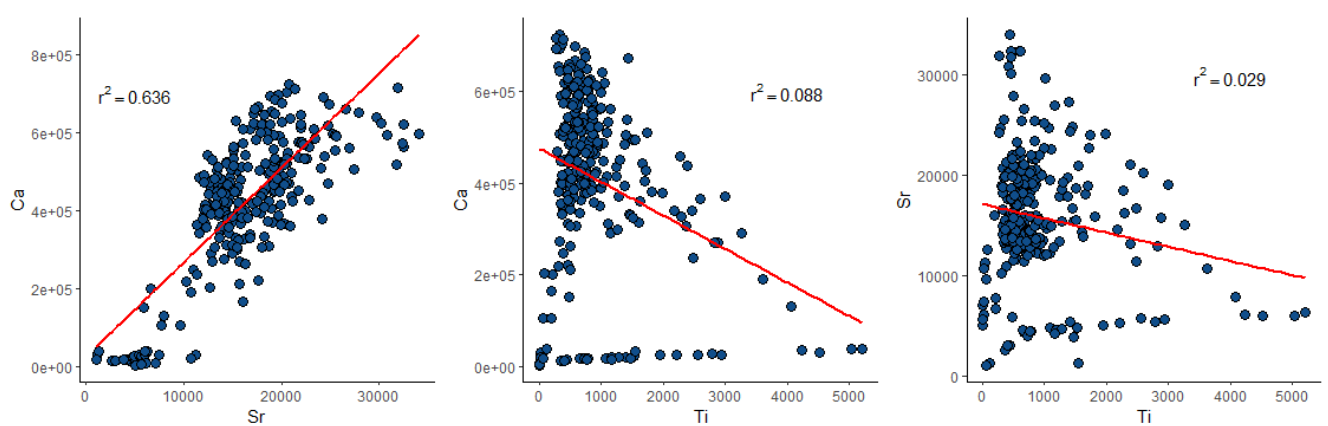


Figure 6.6: Plots showing the relationship between Sr, Ti and Ca in the Emaotfer core sequence.

### 6.5.1 Principal Component Analysis

Figure 6.7 and Figure 6.8 show the Principal Component Analysis (PCA) and correlation matrix for the Itrax  $\mu$ XRF data for Emaotfer Swamp. Here the data have been split into groups based on the depth and distance along the PCA axes indicates the weighting of each depth in the first two principal components. Axis 1 explains most of the variance (61.9%) and shows key zones spread mainly along this axis. Overall, PCA1 and 2 combined accounts for 79.6% of the data variance.

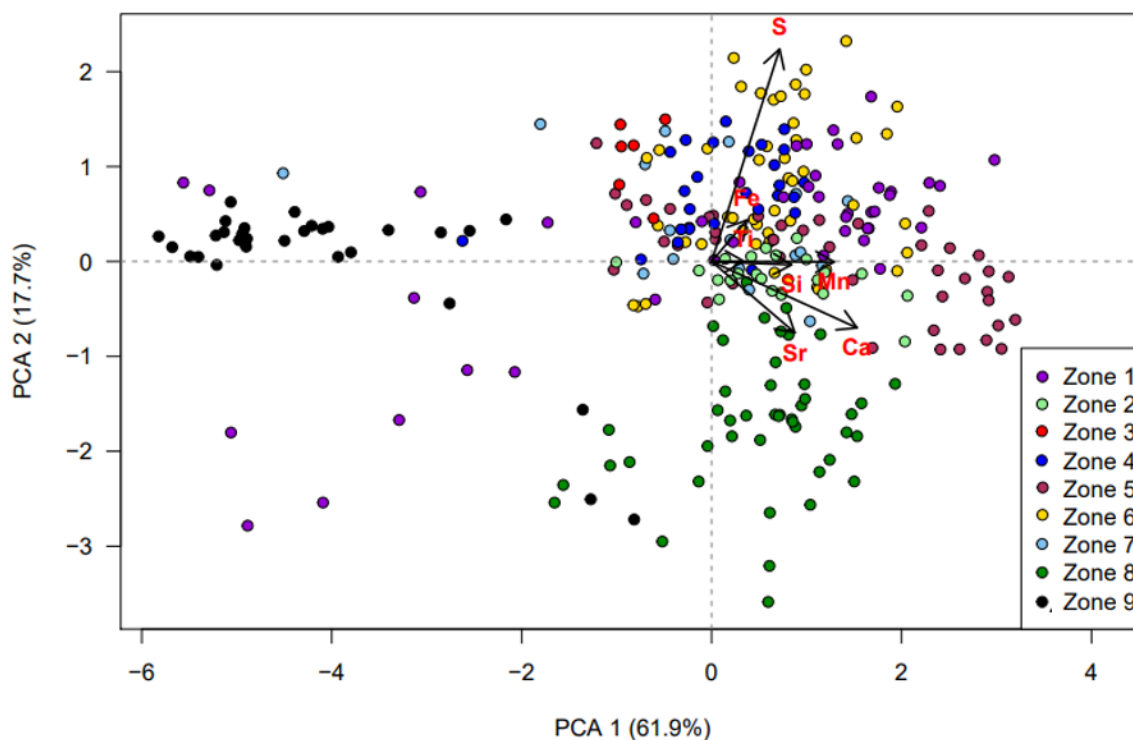


Figure 6.7: Principal component analysis for the Emaotfer Swamp sequence with data point colour denoting the zones laid out in the XRF section.

In the first principal component, it is clear that zone E-9 is strongly negatively loaded whilst a majority of the Emaotfer sequence is positively loaded. This will be due to the compositional differences between zone E-9 and the rest of the Emaotfer sequence as this section of the core is where peat accumulation begins whereas zone E-1 through E-8 are comprised of carbonate rich lake sediments. PCA 1 represents the inorganic/organic components of the sediment sequence. The loading of the second principal component appears to be the terrestrial indicators in the positive loading and freshwater indicators in the negative loading. Both Sr and Ca are loaded positively in PCA 1 and negatively in PCA 2 and have a strong positive correlation with one another with a value of 0.86, which fits with the strong  $r$ -squared value in the linear regression for these elements. This suggests that the carbonate precipitating in the lake is aragonite ( $\text{SrCO}_3$ ). Similarly, Ti and Fe are positively loaded in PCA 1 and PCA 2 and are strongly positively correlated with a value of 0.84, validating their use as a terrestrial indicators.



## 6.6 Organic Proxies

### 6.6.1 Total Organic Carbon

Total organic carbon (TOC) values range between 10.04 and 40% across the Emaotfer sequence – see Figure 6.10. There is initially a decrease in TOC values through zone 1 from 29 to 17%. TOC then increases in zone 2 typically staying between 30 and 38% but with a relatively high rate of variability. There is a decrease in TOC values from 33% at 233cm in zone 2 down to 10% at 227 cm through zone 3 but they gradually increase through zone 4 and then become relatively steady through zone 5 varying between 24 and 33%. There is a jump in values as it moves into zone 6 where TOC varies between 30-40% before another significant drop in TOC values appears in zone 7 down to 10 % at 86 cm before values rise quickly again and return to the average values seen in zone 6 which continue up to the top of the sequence.

#### 6.6.1.1 TOC vs LOI<sub>550</sub>

As discussed in the methods chapter, typically there is a strong relationship between TOC and LOI<sub>550</sub> as they both are indicators of the presence of organic matter within sediment. For the Emaotfer sediments however, this relationship does not hold true. Figure 6.9 shows that the data points are widely spread and have an  $r^2$  value of 0.0184 indicating there is no relationship between these two data sets. Normally the LOI<sub>550</sub> values should be double the value of TOC as typically organic matter is made up of around 50% carbon (Meyers and Teranes, 2001). For the total organic carbon measurement the carbonate component of the sediment has to be removed to prevent any inorganic carbon from being measured alongside the organic component – the methodology relating to this was described in Chapter 5. The discrepancy between LOI<sub>550</sub> and TOC for the Emaotfer sediments could be due in part to the high carbonate fraction present in the lake section of Emaotfer sediments. The TOC values are reflecting the total carbon of the organic component of the sediments only. The LOI<sub>550</sub> values, on the other hand, are generated from raw sediment from the cores without any pre-treatment so represents the total organic content of the bulk sediment sections as the sediment is initially combusted at 550 °C, which would remove the organic content and leave the inorganic carbon in place as that only combusts at a higher temperature of 950 °C. Therefore, based on the three

data sets it would seem appropriate to consider LOI<sub>550</sub> values as the most representative data set in relation to organic content.

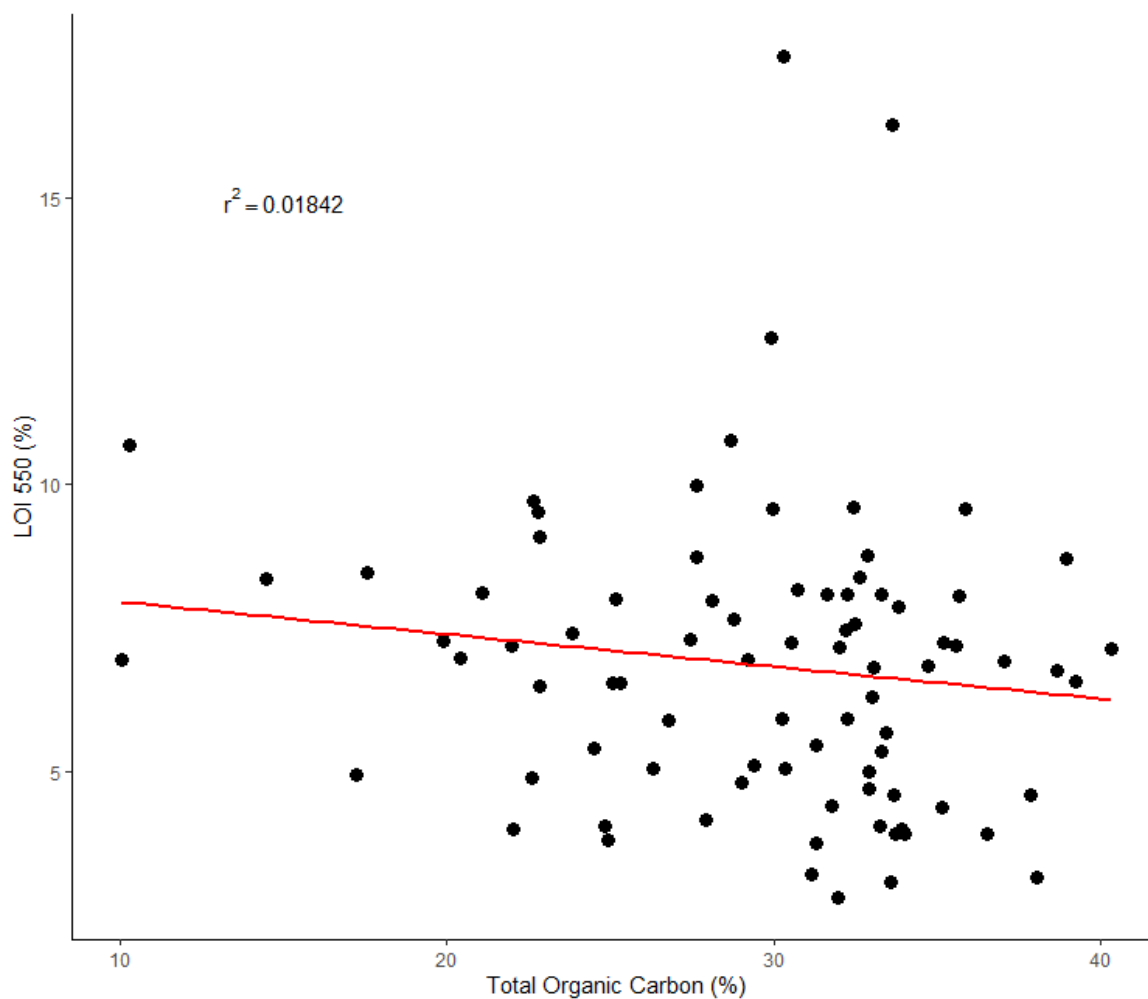


Figure 6.9: Scatterplot showing the relationship between TOC and LOI550 for Emaotfer Swamp.

### 6.6.2 Total Nitrogen

Total Nitrogen remains relatively steady throughout the sequence, fluctuating primarily between 1-2% with a minimum value of 0.4% at 227 cm and a maximum value of 2.8% at 50 cm. There is a steady decrease down to 0.4% at 227 cm but values gradually recover back up to around 1%. There is a slight increase in the overall average from 86cm towards the top of the sequence following the dip in values to 0.46% at this depth. There is a brief peak from 1.4% at 55cm up to 2.8% at 50 cm before dropping back to 1.4% at 45 cm.

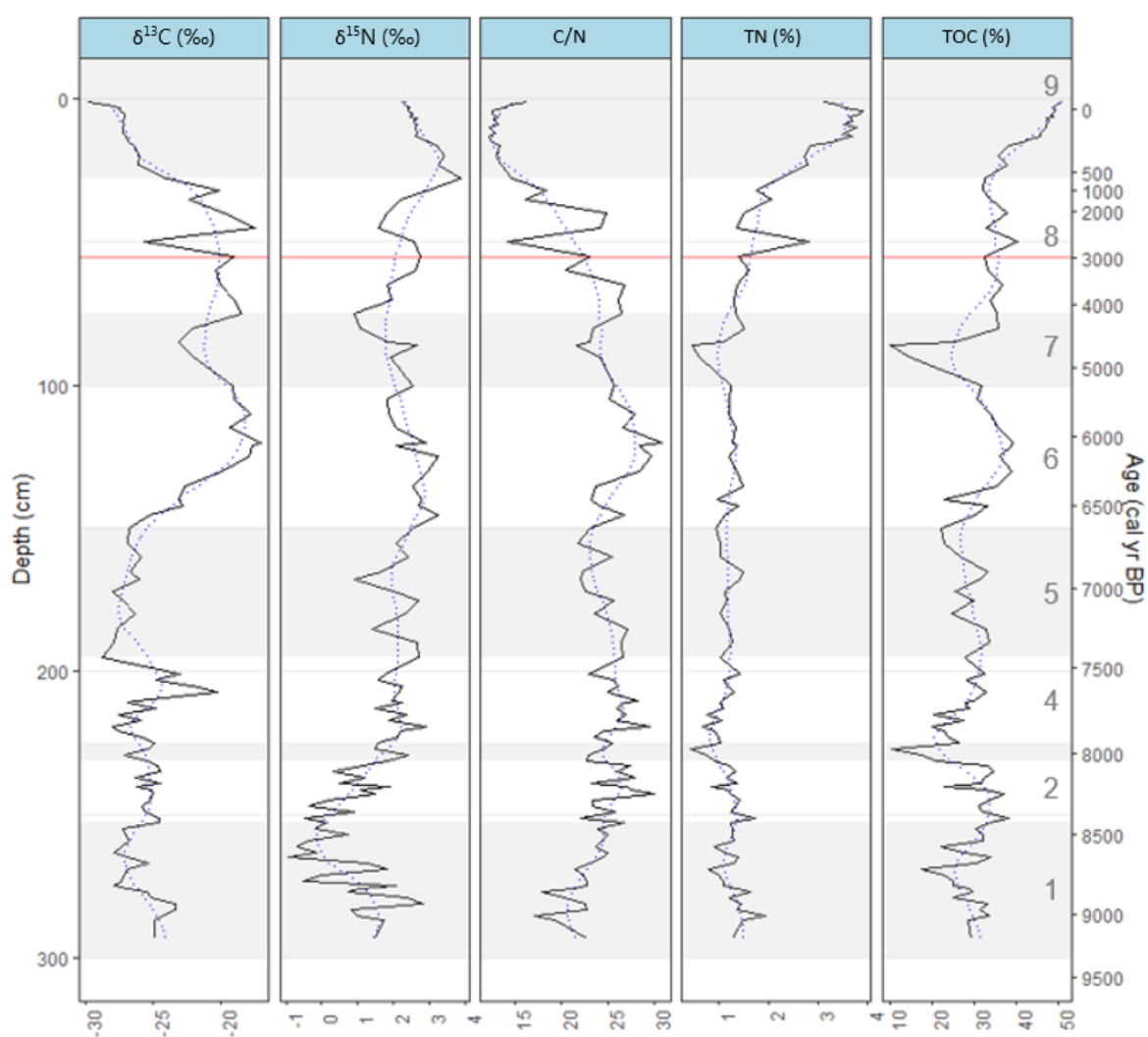


Figure 6.10: TOC, TN,  $\delta^{13}\text{C}$  (‰ VPDB),  $\delta^{15}\text{N}$  (‰ Air) and C/N for Emaotfer Swamp. Red line denotes the start of the first wave of human migration into Remote Oceania. Blue line is loess smoothed.

### 6.6.3 C/N ratio

C/N values fluctuate throughout the sequence but particularly in the latter half of the profile, with a minimum value of 14.57 at 50 cm to a maximum value of 30.81 at 120 cm. In zone 1, there is a gradual increase in C/N values. From zone 2 through to the end of zone 5, C/N values remain relatively similar on average, fluctuating between 21 and 29 through this part of the sequence. There is a rise and peak in the C/N values in zone 6 of 30.81 at 120 cm. Following this there is a continuous decline of C/N values through to the peat boundary.

#### 6.6.4 Organic $\delta^{13}\text{C}$ and $\delta^{15}\text{N}$

The  $\delta^{13}\text{C}$  record for Emaotfer has a minimum value of  $-28.73\text{‰}$  at 195 cm and a maximum value of  $-17\text{‰}$  at 120 cm depth. The  $\delta^{13}\text{C}$  record starts with values around  $-24\text{‰}$  with a downward shift at 275 cm to more negative values through to the end of zone 1.  $\delta^{13}\text{C}$  rises in zone 2 and through zone 3 with values between  $-27$  and  $-24\text{‰}$ . There is a sharp peak in  $\delta^{13}\text{C}$  of  $-20.20\text{‰}$  at 207 cm depth. Immediately after this, there is a pronounced decrease in  $\delta^{13}\text{C}$  at 195cm back down to  $-28.73\text{‰}$  to similar levels seen in zones 1-3, showing little variation with values between  $-28$  and  $-25\text{‰}$ . From 150cm the values start to steadily increase peaking at  $-17\text{‰}$  at 121 cm before levelling out mid-way through zone 6 and then remaining at an overall more enriched level varying between  $-25$  and  $-17\text{‰}$  though typically remaining at around  $-19\text{‰}$  on average but with higher rate of variability through to the peat boundary.

The  $\delta^{15}\text{N}$  record has a lower range of values with a minimum value of  $-0.93\text{‰}$  at 265 cm and a maximum value of  $3.24\text{‰}$  at 145 cm. In zone 1, there is a very high degree of variability in  $\delta^{15}\text{N}$  values relative to the rest of the sequence, with values ranging from  $-0.93$  to  $2.82\text{‰}$ . Overall, through this zone  $\delta^{15}\text{N}$  values are decreasing. In zone 2, from 265 cm,  $\delta^{15}\text{N}$  starts to become enriched and this continues through to zone 3. From zone 4 up to the peat boundary the  $\delta^{15}\text{N}$  values level out. Values vary between  $0.89$  and  $3.24\text{‰}$  so there is a relatively high rate of variability, but the overall average remains relatively constant through this part of the record.

A comparison of C/N against organic  $\delta^{13}\text{C}$  can provide insights into the source of organic matter in the sediment sequence through time. In Figure 6.11 it is clear that through time there is a shift from  $\text{C}_3$  plants to  $\text{C}_4$  plants at Emaotfer. As deeper sediments in zones 1 to 5 are predominantly in the  $\text{C}_3$  plants section but the data migrates towards  $\text{C}_4$  plants in the younger zones 6 to 7 indicating that the source of organic matter for this sequence changes through time.

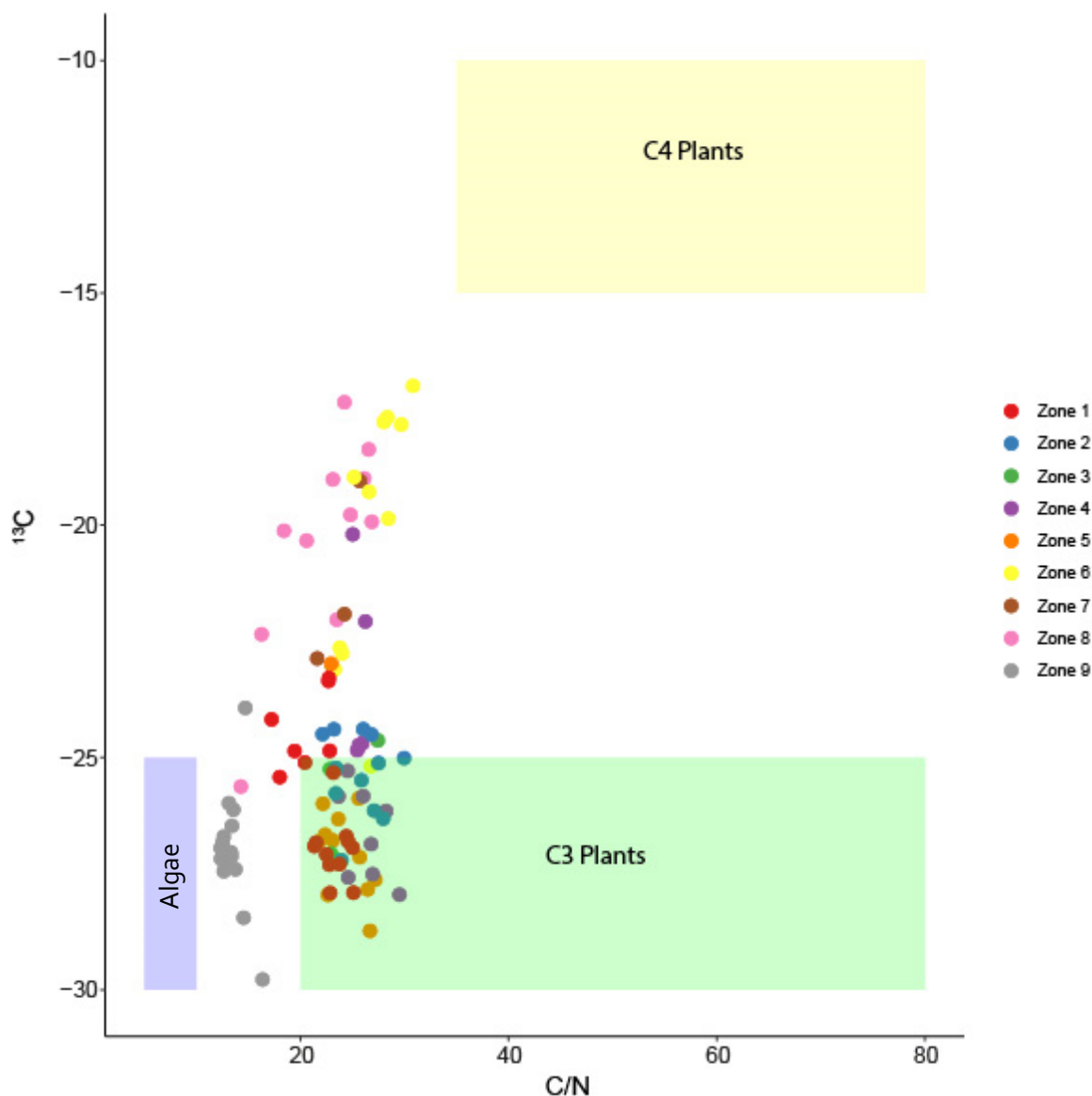


Figure 6.11: Plot showing the C/N and  $\delta^{13}\text{C}$  (‰ VPDB) data for Emaotfer Swamp and how it relates to typical algae,  $\text{C}_3$  and  $\text{C}_4$  plant values. Colours denote the zone.

## 6.7 Inorganic Proxies

### 6.7.1 $\delta^{18}\text{O}$ and $\delta^{13}\text{C}$

Figure 6.12 shows the  $\delta^{18}\text{O}$  and  $\delta^{13}\text{C}$ , Ca/in and  $\text{CO}_2$  yield data for Emaotfer Swamp. In the oldest part of this record in zones E-1 and E-2 which cover the period from 9137 to 8031  $\pm$  958 cal yr BP, the  $\delta^{18}\text{O}$  values are relatively stable and fluctuate around 4-4.5‰. In zone E-3, from 237 cm,  $\delta^{18}\text{O}$  values start to rapidly drop and reaches -6.13‰ at 227cm before sharply rising again up to -4.40 at 225 cm. Values then remain relatively steady through zone E-6 at around 4‰ again. In zone E-5, the values fluctuate and show a greater degree

of variability, declining after 203 cm down to -5.17‰ at 172 cm before rising again. In zone E-6, from 155 cm there is a steady increase in  $\delta^{18}\text{O}$  values from -4.65 up to a peak of -2.79‰ at 122 cm – the highest value in the data set. Following this the values drop again to -4.07‰ but remain relatively stable though there is a gradual decrease in values up to the peat boundary.

Through the deepest part of the Emaotfer sequence in zone E-1 to E-2, the inorganic  $\delta^{13}\text{C}$  values remain relatively steady. There are dramatic changes in inorganic  $\delta^{13}\text{C}$  through zones E3-5. There is a dip in zone E-3 down to -4.12‰ at 227 cm, which is also reflected in the  $\delta^{18}\text{O}$  and  $\text{CO}_2$  yield. The  $\delta^{13}\text{C}$  then increases through into zone E-4 reaching a peak of 2.98 at 203 cm. In the inorganic  $\delta^{13}\text{C}$  record, there is a similar drop in isotope values between 6644-7424  $\pm$  623 (~150 – 195 cm) in zone E-5 that was observed in the organic  $\delta^{13}\text{C}$  record. From 203 to 195cm there is a 6.88‰ decrease in values to -2.16‰ at 195cm. After 150cm/6644  $\pm$  623 cal yr BP, the values shift upwards by 3.23‰ and continue to steadily increase to 3.84‰ at 125cm before a small step down in values at 115 cm to 2.57‰ where it remains relatively steady until 80cm. From 80cm/4470  $\pm$  262 cal yr BP, the inorganic  $\delta^{13}\text{C}$  start to decrease down to -0.09‰ at 60cm before briefly rising and peaking again at 2.47 at 38cm before dropping off to -0.21‰ at 32cm near to the start of the peat sediments.

The  $\text{CO}_2$  yields from the Emaotfer sediments were consistently high throughout the record, typically producing over 10mb of gas indicating high carbonate content as expected with the marly composition of the lake sediments. The only exception is the slightly lower yield of 7.5mb at 227 cm, which corresponds with drops in the  $\delta^{18}\text{O}$  and  $\delta^{13}\text{C}$  values as well as TOC, TN and  $\text{LOI}_{950}$ .

The Ca record shows that the overall average pattern for calcium levels in the core are relatively stable throughout the record. There is slight increase in the average value mid-way through zone E-5 at around 185 cm and again in zone E-8 before calcium values decline as the sediments transition from marl to peat.

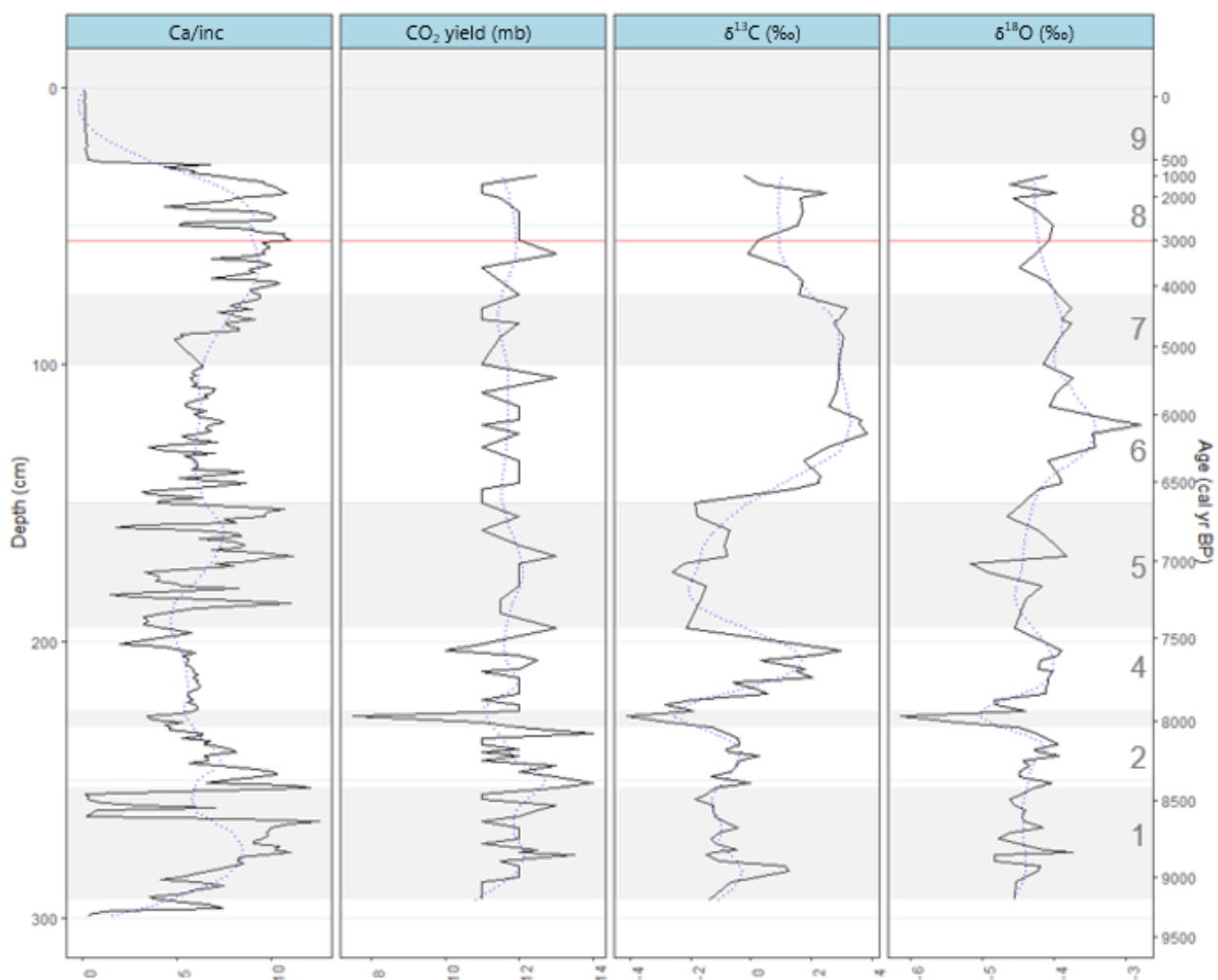


Figure 6.12: Plot showing the Ca/inc, CO<sub>2</sub> yield data,  $\delta^{13}\text{C}_{\text{inorganic}}$  (‰ VPDB) and  $\delta^{18}\text{O}$  (‰ VPDB) for the Emaotfer Swamp core sequence. Red line denotes the start of the first wave of human migration into Remote Oceania. Blue line is loess smoothed.

Figure 6.13 shows that within the Emaotfer sediments the  $\delta^{18}\text{O}$  and  $\delta^{13}\text{C}$  values do covary with all data points providing an  $r^2$  value of 0.59 ( $p < 0.01$ ,  $n = 82$ ). The strength of the covariation of the two values varies throughout the core with the section covering 150-200cm providing the strongest  $r^2$  value of 0.75 ( $p = 0.001262$ ,  $n = 10$ ). The data point that sits on the negative end of the covariant trend is from 227 cm depth.

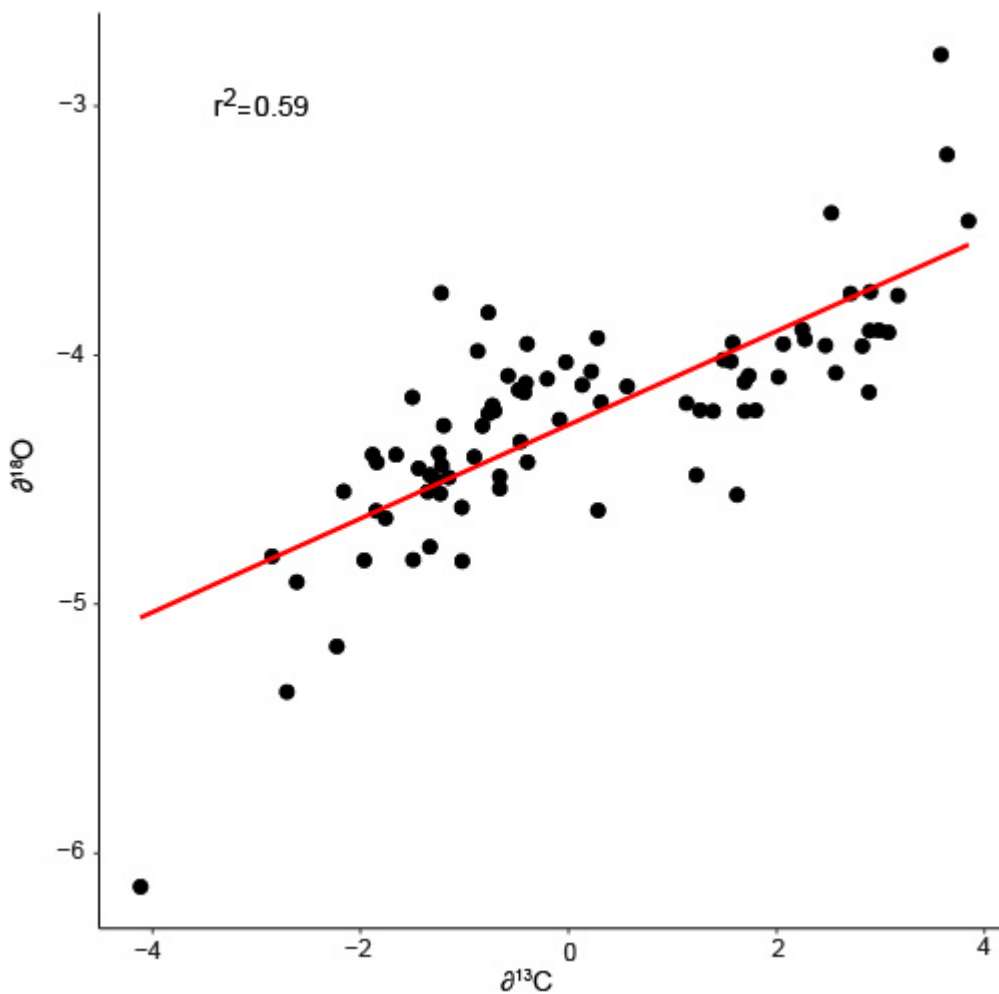


Figure 6.13: Plot showing the relationship between inorganic  $\delta^{13}\text{C}$  (‰ VPDB) and  $\delta^{18}\text{O}$  (‰ VPDB) from Emaotfer Swamp with a line of best fit and displaying the r-squared value.

## 6.8 Palaeoenvironmental change in Vanuatu during the Holocene

### 6.8.1 Interpretation of the Emaotfer Swamp sequence

Isotopic covariance between  $\delta^{18}\text{O}$  and  $\delta^{13}\text{C}$  is common for closed-lake systems (Talbot, 1990) and the trend from Emaotfer swamp does indicate that this represents such a system. The oldest part of the Emaotfer sequence is in **Zone E-1** (253-293 cm, 8417-9137 cal yr BP  $\pm$  958). The  $\delta^{18}\text{O}$  values vary slightly between -3.75 and -4.83 ‰ but the overall pattern is fairly steady through this zone and into the next, indicating no major shift in average precipitation patterns. There is a slight decrease in  $\delta^{13}\text{C}_{\text{inorg}}$  values through this zone but there is a relatively high degree of variability with a range of -1.49 to 1.26 ‰. This zone has a low level of terrestrial input, evidenced by the relatively low level of XRF indicators Ti and Fe. Both TOC and TN values in this zone gradually decrease and dip

down until around 269 cm before rising again. Similarly, there is also a decreasing LOI<sub>550</sub> to reflect the TOC values and conversely an increase in LOI<sub>950</sub>. The organic  $\delta^{15}\text{N}$  and  $\delta^{13}\text{C}$  however, show a continuous decrease in values throughout this zone. There appears to be an increase in the amount of carbonate precipitation in this zone as the Ca/inc values rise quickly in this zone, which accounts for the rise in LOI<sub>950</sub>. This likely represents a temporary shallowing where plant productivity is decreasing, indicated by the drop in TOC and LOI<sub>550</sub> (Burnett *et al.*, 2011) and carbonate is precipitating as the ions become concentrated in the lower lake level (Hassall, 2017; Thompson *et al.*, 2017).

Based on the current age model, **Zone E-2** (231-253 cm, 8031-8417 cal yr BP  $\pm$  879) fits with the timing of the 8.2 kyr event but considering the relative proxy changes and age model error it seems likely that the next zone corresponds to this event. There is a lower degree of variability in  $\delta^{13}\text{C}_{\text{inorg}}$  with a rise in values across this zone. Slight increase in  $\delta^{18}\text{O}$  values but relatively low variability. This zone sees a steady input of terrestrial material across this zone though still relatively low in comparison to other zones – this represents a shift upward in the average values for terrestrial indicators such as Ti and Fe. However, there is an increase in LOI<sub>550</sub> along with decreasing LOI<sub>950</sub>, which would indicate lower terrestrial in-wash and greater level of organic material, which is supported by the increase of TOC (Langdon *et al.*, 2010). The proxy records from this zone show a continuation of relatively stable lake conditions with increase in terrestrial plant productivity with stable C/N values but an enrichment of organic  $\delta^{13}\text{C}$  indicating an increase in C<sub>4</sub> plant matter (Burnett *et al.*, 2011).

**Zone E-3** (225-231 cm, 7926-8031 cal yr BP  $\pm$  809) shows a considerable departure from the proxy signals present across zone E-1 and E-2. This section shows a rapid drop in  $\delta^{13}\text{C}_{\text{inorg}}$  and  $\delta^{18}\text{O}$  to lowest value in sequence of -4.12 ‰ and -6.13 ‰ respectively. These low values place this section of the core as an apparent outlier on the most negative end of the  $\delta^{18}\text{O}$  and  $\delta^{13}\text{C}$  covariant trend which generally indicates that conditions were wetter (Talbot, 1990). This is also supported by a peak in the magnetic susceptibility, which comes along with a notable shift upward in all terrestrial indicators - Ti, Fe and Si. This would indicate a significantly higher rate of in-wash into the lake (Chagué-Goff *et al.*, 2016). There is also a gradual increase in C/N, perhaps suggesting a shift from algae to terrestrial plant sources for organic material, terrestrial material is dominating over in-lake productivity due to the increased amount of in-wash. As mentioned, given the error

associated with the age model it seems likely that this zone represents the 8.2kyr event, given the signals from the proxies and taking into consideration the errors associated with this sequence. The 8.2 event signal has been found in other records in the tropical Pacific including Lake Lanoto'o in Samoa (Hassall, 2017) and possibly also in Spooky Lake in Palau that sees large shifts in hydroclimate proxies around this time (Smittenberg *et al.*, 2011). Further discussion surrounding the evidence for a wet event in this zone is covered in section 6.8.2. Whilst this may not add to the discussion on changing hydroclimate during periods of migration, it does lend support for the dates provided by the current age model as this 8.2 kyr feature in the record does fit with the current age model, taking into consideration the associated error. As peaks in Ti, Fe and Si can also be associated with tephra layers (Kylander *et al.*, 2012) and tephra layers have been found in other sequences from Emaotfer Swamp (Wirrmann, Eagar, *et al.*, 2011), this horizon was tested for tephra presence but only reworked material was found and a majority of the material was terrestrial in-wash (A. Monteath, Pers Comm, May 2023).

The  $\delta^{18}\text{O}$  values return to similar levels seen in zone E-1 and E-2 in **Zone E-4** (195-225 cm, 7424-7926 cal yr BP  $\pm$  799), though values are slightly enriched indicating slightly drier conditions that are similar to earlier zones in the sequence or at least a shift back to typical lake sediment composition following the zone-E3 proxy departure. Through this zone, there is a relatively slow rise in  $\text{LOI}_{550}$  and fall in  $\text{LOI}_{950}$ , though the major change in this section is a peak in  $\delta^{13}\text{C}$  organic and inorganic values and a gradual rise in TOC. This could be a possible shift in vegetation to  $\text{C}_4$  from  $\text{C}_3$  and potentially a higher rate of productivity in the area leading to a rise in the amount of organic content preserved in the lake sediments (Burnett *et al.*, 2011).

The  $\delta^{18}\text{O}$  values in **Zone E-5** (150-195 cm, 6644-7424 cal yr BP  $\pm$  623) have a slight drop in average values though there is a higher degree of variability in this zone compared to zones E1-2 and zone E-4. This zone sees a notable drop in  $\delta^{13}\text{C}_{\text{inorg}}$  values compared to the zone before, but these values are closer to those in zone E-1 to 2 though the average value is lower. Similar patterns are also seen in the  $\delta^{13}\text{C}_{\text{org}}$  implying that the change has caused similar changes in both the inorganic and organic  $\delta^{13}\text{C}$ . TOC, TN and C/N all remain relatively constant through this zone. This could indicate a change in organic matter likely representing an increase in primary productivity particularly of  $\text{C}_3$  plants based on the C/N and the  $\delta^{13}\text{C}_{\text{org}}$  values (Langdon *et al.*, 2010; Maxson *et al.*, 2021). This zone also sees

significant variation in the LOI<sub>550</sub> and LOI<sub>950</sub> record – highest rate of variability in the whole Emaotfer sequence. Initially there is a drop in LOI<sub>550</sub> that starts to recover towards the end of the zone but with large spikes through this zone and into the next with an accompanying rise in LOI<sub>950</sub> and slight fall in values towards the end of the zone. There is a substantial rise in the Mn/Fe ratio in this part of the sequence that could indicate a drop in water levels, increased mixing thus creating oxic conditions throughout the water column which would produce an increase in the Mn/Fe ratio as seen in other tropical lake records (Burn and Palmer, 2014). This could represent drier conditions compared to earlier zones with a lowering of the water level, causing the lake water to mix and become oxic and allowing C<sub>3</sub> macrophytes to develop as seen in the present day (Bruhl and Wilson, 2007; Kalfatak and Jaensch, 2014; Cadd *et al.*, 2018). Zhang et al (2014) found that the period from 9200 to 5600 yr BP was characterised by notable variations in El Niño incidence at the multi-centennial scale, which could explain some of the large variations seen in the proxies from Emaotfer Swamp through this zone.

In **Zone E-6** (100-150 cm, 5262-6644 cal yr BP  $\pm$  455) from 150 cm, the  $\delta^{13}\text{C}$  organic and inorganic values become substantially enriched compared to the previous zone with values remaining positive with a range of 1.73 to 3.84 ‰ – more similar to that of zone 4. The inorganic and organic  $\delta^{13}\text{C}$  remain high through several zones indicating a permanent change in the surrounding vegetation from C<sub>3</sub> to C<sub>4</sub> plants. This could be caused by a reduction in arboreal species that are typically C<sub>3</sub> and the development of more open landscapes and grasses that tend to be C<sub>4</sub> (Bird *et al.*, 2020). The relationship between organic  $\delta^{13}\text{C}$  and C/N show that the zones following zone E-5 all plot towards C<sub>4</sub> values. There is a significant enrichment in  $\delta^{18}\text{O}$ , with the highest values in the sequence at - 2.97 ‰, which would suggest a drier period (Leng and Marshall, 2004; Langdon *et al.*, 2010). This zone represents a major dry period in the Emaotfer Swamp record from 6644 to 5262 cal yr BP  $\pm$  455 that potentially has also influenced vegetation on the island too. This interpretation is corroborated by records from Lake Teroto in the Cook Islands and Lake Lanoto'o in Samoa, which both indicate that there was a drying phase across the central Pacific in the mid-Holocene which is rounded to around 6,900-5,700 cal yr BP (Hassall, 2017) and the Emaotfer sequence suggests this drying phase may have extended further west in this region.

For **Zone E-7** (75-100 cm, 4196-5262 cal yr BP  $\pm$  478), the data presents a mix of signals. The magnetic susceptibility record remains relatively low through zones E-1 to E-6, however, in this zone there are some small peaks in the magnetic susceptibility indicating an input of ferromagnetic material possible due to an increase in in-wash of inner volcanic materials. This is not supported by the Ti or Fe records that show both low values and low-level variability across this zone. However, there is a drop in a number of proxies including TN, TOC, and  $\delta^{13}\text{C}_{\text{org}}$  along with  $\text{LOI}_{950}$  at around 84-86 cm whereas  $\text{LOI}_{550}$  remains relatively steady throughout this section. There is also a decrease in C/N, which along with decreasing  $\delta^{13}\text{C}_{\text{org}}$  could indicate a shift to higher aquatic algae productivity (Langdon *et al.*, 2010). This perhaps could also be a possible tephra layer as there are peaks in Ti and Si but not Fe, which would indicate not a terrestrial source but Ti and Fe have been used as indicators of tephra layers in the past (Kylander *et al.*, 2012) and multiple tephra layers have been identified at Emaotfer Swamp (Wirrmann, Eagar, *et al.*, 2011). Another explanation could be wetter conditions, but this idea is not supported by  $\delta^{18}\text{O}$  that dip slightly moving into this zone or the terrestrial in-wash indicators. Proxies recover back to similar values seen in zone E-6 so proves to be a temporary shift. Wirrmann *et al.* (2011) suggest that from 5000 cal yr BP there was a rise in the ENSO events, which bring drier conditions based on their sequence from the same site. This could explain the mix of signals through this zone with an increase in variability due to a rise in ENSO events.

Based on the current age model, **Zone E-8** (30-75 cm, 564-4196 cal yr BP  $\pm$  478) covers the arrival of humans into Vanuatu and the subsequent colonisation of Efate as well as the second wave of migration into Eastern Polynesia. This zone sees a substantial drop in the sedimentation rate, especially between 30 and 46 cm. There is also a higher degree of variability in  $\delta^{13}\text{C}_{\text{org}}$ ,  $\delta^{15}\text{N}$  sees a slight increase but overall, there is a rise in the TN to the highest levels seen within the lake sediments. Similarly, there are slightly more variable  $\text{LOI}_{550}$  and  $\text{LOI}_{950}$ , with a small dip and rise in values respectively. There is also a slight decrease in  $\delta^{13}\text{C}_{\text{inorg}}$  from the higher levels sustained through the previous two zones. The  $\delta^{18}\text{O}$  values remains relatively steady through this zone. It still shows a slightly higher average value compared to the older half of the Emaotfer sequence indicating a shift towards slightly drier conditions in this part of the record. There is a temporary enrichment in the  $\delta^{18}\text{O}$  values along with Ti and Fe record at 50 cm, which is also seen in

Ca/inc, C/N, organic  $\delta^{13}\text{C}$  but this is not reflected in the inorganic  $\delta^{13}\text{C}$  or  $\delta^{15}\text{N}$  and there is a rise in TN and TOC values. This zone could be indicative of a period of shallowing in the lake level – more evaporation leads to a deepening of the mixed layer and concentration of nutrients for algae within the water column (Gagliardi *et al.*, 2019). This occurs immediately following the start of the first wave of human migration at approximately 3000 yr BP. The Emaotfer sequence provided by Wirmann *et al.* (2011) also found that water levels around 3100-2140 yr BP were shallow based on ecological indicators such as pollen, diatoms and ostracods, rather than geochemical proxies. This shows that multiple lines of evidence are providing confidence in the interpretation of changes during this period.

**Zone E-9** (0-30cm, 564 cal yr BP  $\pm$  196 to present) covers the top sedimentary unit, which comprises of organic rich peat. This zone sees an increase in the TOC and TN percentages. It also sees a drop in the organic  $\delta^{13}\text{C}$  in this zone. This could be due to the dominance of  $\text{C}_3$  sedges such as *Cyperus difformis*, *Lepironia articulate* and *Gahnia sp.* that are able to dominant the swamp landscape once water levels had dropped and are present on the site today (Bruhl and Wilson, 2007; Kalfatak and Jaensch, 2014; Cadd *et al.*, 2018). Based on the current age model, the transition from lake to swamp occurred around 531  $\pm$  98 cal yr BP. There is, however, a potential hiatus at the lake-peat sediment boundary. This is evidenced by a substantial jump in age from the radiocarbon date at end of the peat section which is dated to approximately 531  $\pm$  98 cal yr BP at 28-29 cm up to 2131  $\pm$  157 cal yr BP at 41 cm, the first radiocarbon date in the marl section, a jump of 1600 years in approximately 12 cm of sediment. This jump is supported by a second date from plant macrofossils from 43 cm depth which has a similar but slightly older date of 2255  $\pm$  142 cal yr BP, suggesting that these first marl dates are relatively accurate. This indicates either a potential hiatus or at least a significant drop in the rate of sedimentation in that part of the core. This zone has an identified tephra layer which is attributed to the Kuwae eruption from 1453 AD. The tephra layer corresponds with the largest spike in the magnetic susceptibility record as well as peaks in the XRF data for Ti, Fe and Si, which as mentioned can be indicators of tephra layers (Kylander *et al.*, 2012) but slightly different signal from that of the peaks in zone E-7. The peat sediments continue up to the top of this record and in the present day the site is still a freshwater swamp with standing water present (Kalfatak and Jaensch, 2014; Sear pers comm, Aug 2019). There was a period of

higher levels of sustained El Niño events from 1400 through to 300 yr BP (Wirrmann, Eagar, *et al.*, 2011), which would typically present as drier conditions in Vanuatu that could explain this reduction in sedimentation in the lead up to this zone and the drying out of the basin and formation of swamp.

Overall, the Emaotfer sequence sees shifts between wet and dry conditions over the past 9,200 years as well as major shifts in vegetation. The next sections will examine some of the key findings in more detail.

### **6.8.2 Evidence for a Wet event in zone E-3 – 8031-7926 cal yr BP ± 809**

As discussed in section 6.8.1, despite the age suggestions from the age model, the errors associated with it mean it is likely that this zone represents the 8.2 kyr event. This is supported by similarities between this record and others from the tropical South Pacific.

The key indicators of a wet event include a spike in Fe/inc, Ti/inc and magnetic susceptibility at 227 cm (c. 7159 - 8250 cal yr BP). These are all indicators of an increase in terrestrial in-wash into the system that occurs typically during periods of higher or more frequent precipitation (Davies, Lamb and Roberts, 2015; Sear *et al.*, 2020; Maloney *et al.*, 2022). These peaks also all coincide with a drop in  $\delta^{13}\text{C}_{\text{inorg}}$ ,  $\delta^{18}\text{O}$ , TOC, TN and  $\text{LOI}_{950}$ , which suggests that terrigenous in-wash from the surrounding catchment is dominating the sediment composition during this time. Furthermore, the  $\delta^{18}\text{O}$  and  $\delta^{13}\text{C}_{\text{inorg}}$  data from this zone sit at the negative end of the covariant trend as an outlier, which signals a shift to wetter conditions (Talbot, 1990).

However, a study by Rohling and Pälike (2005) cautioned against making broad assumptions about connections between the North Atlantic meltwater pulse thus named the 8.2 ka event and other far-field climate anomalies around the same period. They asserted that it is difficult to resolutely link climatic changes in regions outside of the Atlantic basin to the 8.2 ka meltwater pulse. Therefore, care must be taken when attributing changes in the Pacific basin to the 8.2 ka event. However, work on identifying the possible impacts of the 8.2 ka event in the tropical Pacific has begun. Atwood (2015) found that the meltwater pulse in the North Atlantic likely led to a southward shift in the ITCZ and a heightened period of rainfall within the tropical Pacific alongside weakened ENSO variability. Further to this, in John Hassall's (2017) work, the Lanoto'o upland lake

site in Samoa presents with an increase in precipitation between ca.8200-7900 cal yr BP, which is similar to timing of 8.2ka event in Greenland ice cores. He suggests either an expansion of the SPCZ or a shift in its location towards the southeast at 8175 cal yr BP, which is then followed by contraction or shift northwest at 8070 cal yr BP. Hassall (2017) postulates that the 8.2ka event was expressed in the southwest Pacific. There are similarities in the results between Hassall's Lake Lanoto'o record and the record from Emaotfer Swamp. Both present with a peak in the Ti/inc record and a drop in TOC alongside a drop in  $\delta^{18}\text{O}$  values within the Emaotfer Swamp sequence which indicate wetter conditions which is paralleled in the drop in  $\delta^2\text{H}_{\text{C}_{26}}$  from Lanoto'o. It is a challenge to confirm whether this was an event expressed in the southwest Pacific based on existing records. However, an updated age model for the Lanoto'o record means that the potential wet event identified may have occurred 1000 years earlier, around 9200 yr BP. The only other records that date back that far come from Palau in the North Pacific (Smittenberg *et al.*, 2011) and the Galapagos (Conroy *et al.*, 2008) and Easter Island (Sáez *et al.*, 2009; Margalef *et al.*, 2014; Horrocks *et al.*, 2015) in the far eastern South Pacific. Smittenberg *et al.* (2011) note that the inundation of Spooky Lake took place between 9.3 and 8.7 kyr BP due to sea level rise. This caused the lake to shift from holomictic to meromictic state with preservation of organic in anoxic layer occurred 8.7 to 8.2 kyr BP. It is difficult to pick out climatic record during this period due to the overwhelming impact of sea level rise on this system. Whilst it is still remains unclear whether or how the 8.2 ka event presents in South Pacific, this record from Emaotfer Swamp along with the records from Lake Lanoto'o in Samoa (Hassall, 2017) and El Junco in the Galapagos (Atwood, 2015) do suggest a heightened period of precipitation in this region around the accepted timing of the 8.2 ka event (Rohling and Palike, 2005; Hassall, 2017) but further work would need to be conducted on the connections between the Atlantic Ocean and Pacific climate to resolutely tie these events together.

### **6.8.3 Evidence for drought event in zone E-5 - 6644-7424 $\pm$ 623 cal yr BP**

There are three lines of evidence in this zone to support the interpretation of a shift to dry conditions through zone E-5 - approximately 6736-6121  $\pm$  415 cal yr BP. Firstly, in the XRF data there are peaks in the Ca/inc values through this zone along with a small peak in S/inc. Peaks in Ca, Sr and S alongside decreases in organic carbon similar to Zone 2 in lake

Tiriara have been seen in coastal lake sequences in the Caribbean (Burn and Palmer, 2014). There is also a spike in the Mn/Fe ratio, which only occurs in this zone indicating a shift to oxic lake conditions as the lake level drops (Burn and Palmer, 2014). Secondly, there is also a notable downward shift in both  $\delta^{13}\text{C}_{\text{inorg}}$  and  $\delta^{13}\text{C}_{\text{org}}$  in this zone. The C/N data does not show the same downward shift and could indicate a change in organic matter likely representing an increase in primary productivity (Langdon *et al.*, 2010; Maxson *et al.*, 2021). The same signals are also seen in the sub-tropical Blue Lake in North Stradbroke Island just off the east coast of Australia which are potentially linked to a change to a drier climate that occurred at the same time (Maxson *et al.*, 2021). Similarly, in Emaotfer, we see an enrichment in  $\delta^{18}\text{O}$ , which also typically signals a shift to drier conditions as evaporation outweighs precipitation leading to a build-up of the heavier  $\delta^{18}\text{O}$  isotope. Thirdly and finally, this is also supported by a dip in terrestrial input 162-175 cm within this zone. This can also indicate drier conditions as a reduction in rainfall would cause a drop in the amount of in-wash into the system as there is not a transport mechanism to move that material into the lake (Davies, Lamb and Roberts, 2015; Maloney *et al.*, 2022). All this evidence points towards an overall shift toward dry conditions through zone E-5 which covers the period  $6644-7424 \pm 623$  cal yr BP.

#### **6.8.4 Evidence for drought event at the transition between zone E-7 and E-8**

The transition between zone E-7 and E-8 represents a sharp transition within the sediments where there is a change from a lake environment to peatland. This occurs around 499 - 629 cal yr BP based on the current age model which has a date from the base of the peat but in the Wirrmann sequence from the same site, this change occurs around 1500 yr BP.

Similar changes whereby a site transitions from lake to wetland conditions are seen in a study of the sub-tropical Welsby Lagoon in Australia. The record from Welsby sees a decrease in water depth along with an increase in organic matter and higher  $\delta^{13}\text{C}$  as rooted macrophytes start to dominate the wetland. It is likely that this change occurred here at Emaotfer as well which have persisted through to the modern day. The site does currently have standing water but is dominated by C3 sedges (Kalfatak and Jaensch, 2014; Cadd *et al.*, 2018). However, there is a reduction in  $\delta^{13}\text{C}$  in the Emaotfer sequence

whereas Cadd et al (2018) find the  $\delta^{13}\text{C}$  due to the emergent aquatic plants. In the  $\delta^{13}\text{C}$ -C/N plot the peat section from Emaotfer plots between Lacustrine Algae and  $\text{C}_3$  plants suggesting that algae still a significant proportion of the organic matter make up which is supported by the presence of diatoms throughout the peat section of the Wirmann (2011) Emaotfer sequence.

As discussed in section 6.2.3, the radiocarbon date from the bottom of the peat section puts the start of peat accumulation at 498-563 cal yr BP. Due to the presence of the Kuwae tephra at 26-27cm depth that occurred at approximately 1452 AD, it seems likely that the base date of the peat sits somewhere between the mean value of 514 cal yr BP and the older end of the estimate. The peat accumulation rate at that part of the core is estimated to be 17 years per cm of sediment. The youngest date from the marl part of the sequence is at 41 cm with an approximate age of 2012-2288 cal yr BP. Over 13 cm of sediment there is nearly 1,500 years' worth of sediment accumulation. This represents either a significant decrease in the accumulation rate or perhaps a hiatus in the sequence that has not at this stage been refined in terms of chronology. Either represents a notable change in the sediment sequence that can be interpreted as a consequence of a shift to drier conditions. A similar pattern is seen in multiple cores taken from Easter Island/Rapa Nui, where there is a large sedimentation hiatus from 4,500 yr BP to 800 yr BP. The hiatus is caused by a change to dry conditions during this time and when conditions become wetter and more conducive to peat accumulation, sedimentation resumes (Mann *et al.*, 2008; Sáez *et al.*, 2009; Cañellas-Boltà *et al.*, 2012; Margalef *et al.*, 2014). Potentially continuous sedimentation at Emaotfer could be explained by the difference in the precipitation regimes between Vanuatu and Easter Island. Vanuatu is located in the much wetter SPCZ dominated tropical Pacific region (precipitation range of 1000 and 3000 mm (Wirmann, Eagar, *et al.*, 2011)). Whereas, Easter Island is located in the drier and more variable sub-tropical region which has much lower precipitation (precipitation range of 500 and 2000 mm (Cañellas-Boltà *et al.*, 2012)). The lower precipitation range during drier conditions could lead to hiatuses in sedimentation as seen in the records from Rano Aroi and Rano Raraku (Mann *et al.*, 2008; Sáez *et al.*, 2009; Cañellas-Boltà *et al.*, 2012; Margalef *et al.*, 2014).

The peat section from the Wirmann cores is approximately 150cm long with the Kuwae tephra sitting at 42-43 cm down. There is a significant difference in the stratigraphy

between the Wirrmann Emaotfer sequence and the sequence presented in this thesis. The study conducted by Wirrmann (2011) estimated that peat accumulation began at approximately 1500 cal yr BP within their sequence. Almost 1000 years earlier than the base date on the EMB sequence. This could be due to the location within the site the sequence was taken from. The cores presented in this thesis were taken from the edge of the Emaotfer Swamp due to the height of standing water. A more marginal sequence of cores could mean that the sediments in that area are some of the first to dry out when the swamp waters recede in dry conditions and some of the last to become wet when waters rise during wetter periods.

Other local records from Efate including two studies from the nearby Lake Emaotul, located approximately 6 km north of Emaotfer Swamp support the hypothesis of dry conditions at the onset of the MCA. The first from Maloney et al (2022), uses  $\delta^2\text{H}$  dinosterol as a proxy, the lake record shows a large downward shift in the mean precipitation rates at approximately 1000 AD, which then persists through to the modern day. This includes two downward spikes, one at the onset of the MCA and another in the MCA-LIA transition.

The second study from Lake Emaotul looked at the ecological changes in relation to the precipitation changes identified by Maloney et al (2022). They found that a shift to dry conditions around 1000 cal yr BP saw a change in vegetation toward a sedge, grass and fern dominated environment and a decline in all main taxa of chironomid (Strandberg et al., 2023). Strandberg et al (2023) found that both vegetation and chironomid communities recovered in approximately 80 years.

The agreement of the evidence from Emaotfer swamp with other local records from Lake Emaotul (Maloney et al., 2022; Strandberg et al., 2023) provides confidence in the interpretation of this change as a response to hydrological change at the onset of the MCA.

## 6.9 Summary

This chapter presents the palaeo results for the Emaotfer Swamp sequence. The key finds from this are that the  $\delta^{18}\text{O}$ ,  $\delta^{13}\text{C}_{\text{inorganic}}$  and Ti/inc records in the Emaotfer Swamp sequence all suggest a relatively short-lived wet event around 8.2kyr event - c. 7159 -

8250 cal yr BP. The same wet signal is also seen in the record from Lake Lanoto'o in Samoa in proxies such as TOC and Ti/inc (Hassall, 2017) supporting Hassall's (2017) suggestion that the 8.2kyr event resulted in an expansion or SW shift of the SPCZ as Vanuatu sits just south of the SPCZ zone. This provides confidence that our age model is relatively robust as it matches with the timing of the 8.2 kyr event within error. However, an updated age model for Lanoto'o (D. Sear, pers comm, June 2023) now draws the timing of this into question. The  $\delta^{18}\text{O}$  and terrestrial XRF proxies in the Emaotfer Swamp record all indicate a move toward drier conditions around approximately 6736-6121  $\pm$  415 cal yr BP. There is a paucity of records from the tropical South Pacific that date back beyond the Common Era. Two records that cover this time period show agreement on this change in hydroclimate from records in Samoa and the Cook Islands (Hassall, 2017). Hassall (2017) suggests that this dry period is due to a contraction or north-west migration of the SPCZ between 6,900-5,700 cal yr BP. Finally, the results suggest that another dry period occurred no earlier than 2012-2288 cal yr BP and likely ended approximately 499 - 629 cal yr BP with the initiation of peat growth in the basin, indicating a shift back to wetter conditions. In the lead up to the transition of Emaotfer Swamp from a marl lake to a peatland, there was a considerable decrease in the rate of accumulation that represents either a hiatus in the sediments that requires further refinement in terms of chronology or a significant slowdown in productivity. Other records from Efate support this interpretation as they also indicate that there was a shift to dry conditions around 1000 AD that saw changes in rainfall, vegetation and ecology (Maloney et al., 2022; Strandberg et al., 2023).



## Chapter 7 Environmental Change in the Southern Cook Islands

### 7.1 Introduction

As noted in Chapter 4, the Southern Cook Islands sit in an SPCZ sensitive area and played an important role in the second wave of human migration into Eastern Polynesia acting as “gateway islands” for migration into the remotest parts of the Polynesian triangle (Allen and Wallace, 2007). Lake Tiriara is also located locally to the Tangatatau Rockshelter (Kirch, 2017b), a key archaeological site. Following from the site description in Chapter 4 and methods described in Chapter 5, this chapter presents the results from the Lake Tiriara sequence from the island of Mangaia located in the Southern Cook Islands. The sediments from Lake Tiriara, Mangaia went down to a maximum depth of 840 cm and are mainly composed of gyttja, silty/clay lake sediments. This chapter presents the chronology, sedimentology, geochemistry, stable isotope and diatom results from Lake Tiriara. After the results, a full interpretation of the sequence is introduced followed by a more detailed examination of particular sections of interest. The chapter will conclude with a summary of the results from Lake Tiriara.

### 7.2 Chronology

#### 7.2.1 <sup>14</sup>C

The age model for Tiriara is based on ten <sup>14</sup>C AMS dates using a mix of plant macrofossil and bulk sediment material. Bulk sediment was used in place of plant macrofossils when there was insufficient macrofossil material available. It was not possible to identify whether the macrofossils were terrestrial or not due to the small size of the material.

<sup>13</sup>C/<sup>12</sup>C ratio was measured for the smaller sample AMS dates during analysis and that value is used to correct for isotopic fractionation (as per Stuiver and Polach (1977)) but it is not appropriate to use as a  $\delta^{13}\text{C}$  value for the sample so these values are not included in Table 7.1.

Table 7.1:  $^{14}\text{C}$  dates from Lake Tiriara, Mangaia.

Sample depth from surface (cm)	Dated material	$\delta^{13}\text{C}$ (VPDB‰)	Conventional radiocarbon age	2-sigma calibration (cal yr BP)
107	Plant Macrofossil	-15.7	151 ± 35	248
190	Plant Macrofossil	-27.8	309 ± 37	540
191	Bulk Sediment	---	650 ± 30	545
221	Bulk Sediment	---	890 ± 30	676
290	Bulk Sediment	-28.0	983 ± 37	889
310	Bulk Sediment	-27.9	880 ± 37	968
374	Bulk Sediment	---	1,575 ± 30	1368
451	Bulk Sediment	---	1,650 ± 30	1748
475	Bulk Sediment	-30.6	1,999 ± 35	1914
544	Bulk Sediment	-23.7	2,509 ± 37	2398

### 7.2.2 $^{210}\text{Po}/^{210}\text{Pb}$ and $^{137}\text{Cs}$

The Po-210 data from the top 30 cm of the Tiriara sediment sequence are, within measurement uncertainties, uniform as seen in Figure 7.1. This indicates that the sediments from 30 cm depth up to the top of the core have been subject to mixing. This makes the sediments unsuitable for Pb-210 decay-based sedimentation rate determination. Similarly, the two data points from 100 cm and 115 cm analysis showed the same Pb-210 activity concentrations (within counting uncertainties) but are overall lower than the upper sediments, which indicates that Pb-210 is being constantly supported by the radioactive decay of Ra-226 (and eventually U-238) in the sediment. This is the background Pb-210 concentration and that uniform Pb-210 activity makes this unsuitable for sedimentation rate determination. Therefore, only the five data points between 66cm and 100cm can be used for this purpose. Calculating a natural logarithm from Po-210 activities for these points, and plotting the values against depth, generates a linear trend as shown in Figure 7.2, which can be used for sedimentation rate determination.

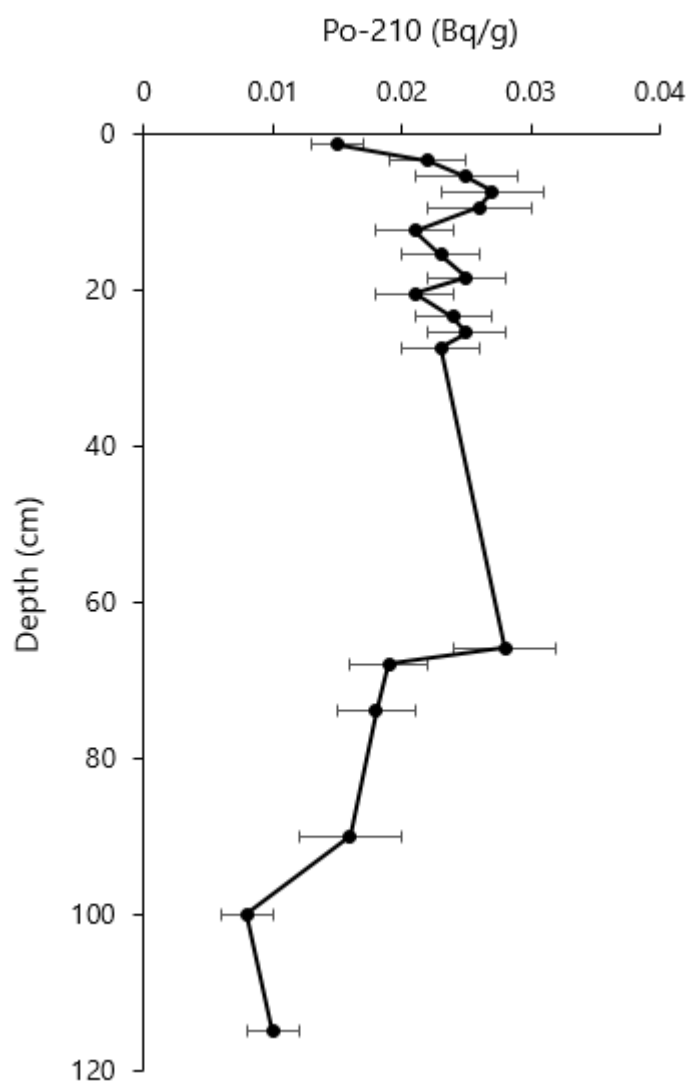


Figure 7.1: Plot of Po-210 activity going down through the Lake Tiriara core top sequence.

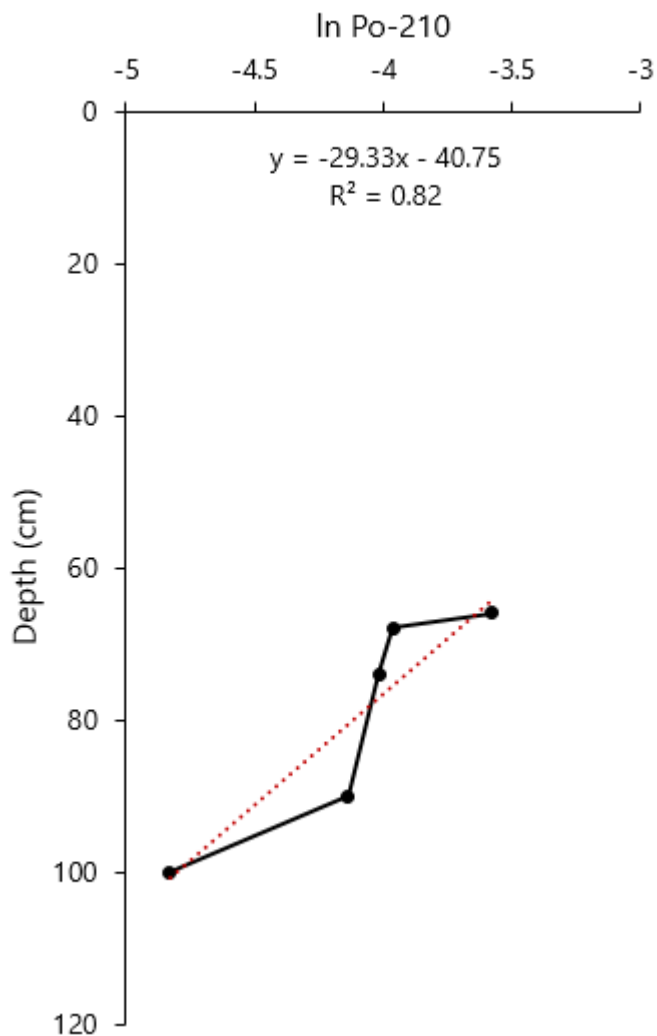


Figure 7.2: Plot of the linear regression of the natural logarithm of the Po-210 data from 66-100 cm down through Lake Tiriara core sequence with the linear regression equation and r-squared value reported.

Figure 7.2 shows that the linear fit is not perfect, but the correlation coefficient is strong with a  $R^2 = 0.82$ . The sedimentation rate is calculated by multiplying the slope of the line of best fit and the decay constant for Pb-210 (ca.  $0.03118071 \text{ y}^{-1}$ ). For the Mangaia cores, the sedimentation rate is calculated at ca.  $0.9 \text{ cm/year}$ . However, the resolution of the data for this 66-100 cm region is much lower than in the upper region and there are not enough data points to confirm that the lower two data points represent the supported Pb-210 layer. Therefore, Po-210 in this case is not suitable for chronological dating of the core top sediments.

The Cs-137 levels for Lake Tiriara sediments were below the detection capability of the mass spectrometer so it is not possible to utilise this as an independent test for the Po-210 results.

### 7.2.3 Rbacon Age Model

The age model is based only upon the  $^{14}\text{C}$  dates due to the issue with mixing and uncertainty around background values of Po-210 and the Cs-137 being below detectable levels. Figure 7.3 shows the age model for the Mangaia sequence. The maximum mean age of the sequence presented in this thesis is 2481 yr cal BP at 560 cm depth and 100% of the dates overlapped with the age model produced using the Rbacon package. The sedimentation rate for Tiriara based on this age model is 5 years per centimetre and the rate of sedimentation appears to be relatively stable through the record with a slight increase around 2000 yr cal BP to present.

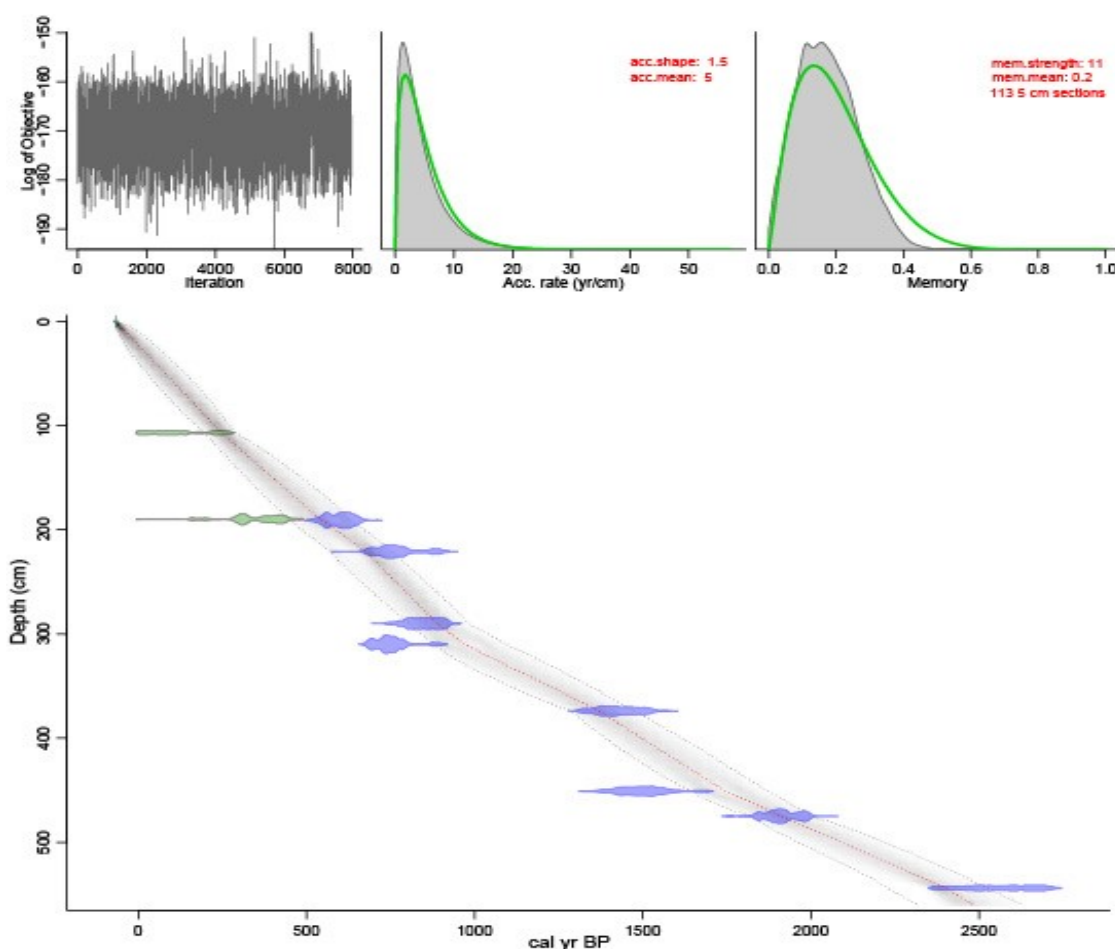


Figure 7.3: Age model generated by the Rbacon package for Lake Tiriara. This is an unweighted age model and colours denote the material used for each date. Green = Plant macrofossil and Blue = Bulk sediment.

### 7.3 Magnetic Susceptibility

Magnetic susceptibility in this study is used as a measure of erosional activity in the catchment and associated in wash (Sear et al., 2020). Peaks are interpreted as evidence for catchment soil erosion and runoff, augmented by changes in sediment availability due to catchment disturbance such as clearance following the arrival of humans. Lower values are interpreted as periods of limited catchment disturbance or dilution by organic matter. There is clearly an inverse relationship between magnetic susceptibility and the LOI data, particularly LOI<sub>950</sub> as seen in Figure 7.4. There are three large peaks in magnetic susceptibility within the Lake Tiriara record located in zones M-2, 5 and 7. The first is located in zone M-2 and represents the largest peak in magnetic susceptibility in this record with a value of 0.0017095 SI at 427 cm. The second peak is in zone M-5 with a value of 0.0015295 SI at 192 cm. The final third peak is located in zone M-7 where magnetic susceptibility rises to 0.0012464 SI. These three peaks all correspond with large drops in the LOI values. After all three of these larger peaks, the values return to lower base values which typically happens relatively quickly with a rapid rise and fall in magnetic susceptibility values but for the second larger peak in zone M-5 the values increase relatively quickly but fall more gradually back to those lower base values. There is also an overall increase in magnetic susceptibility and variability in values through both zone M-3 and 4, from 345 cm onwards, with three smaller peaks before the second larger peak in zone M-5.

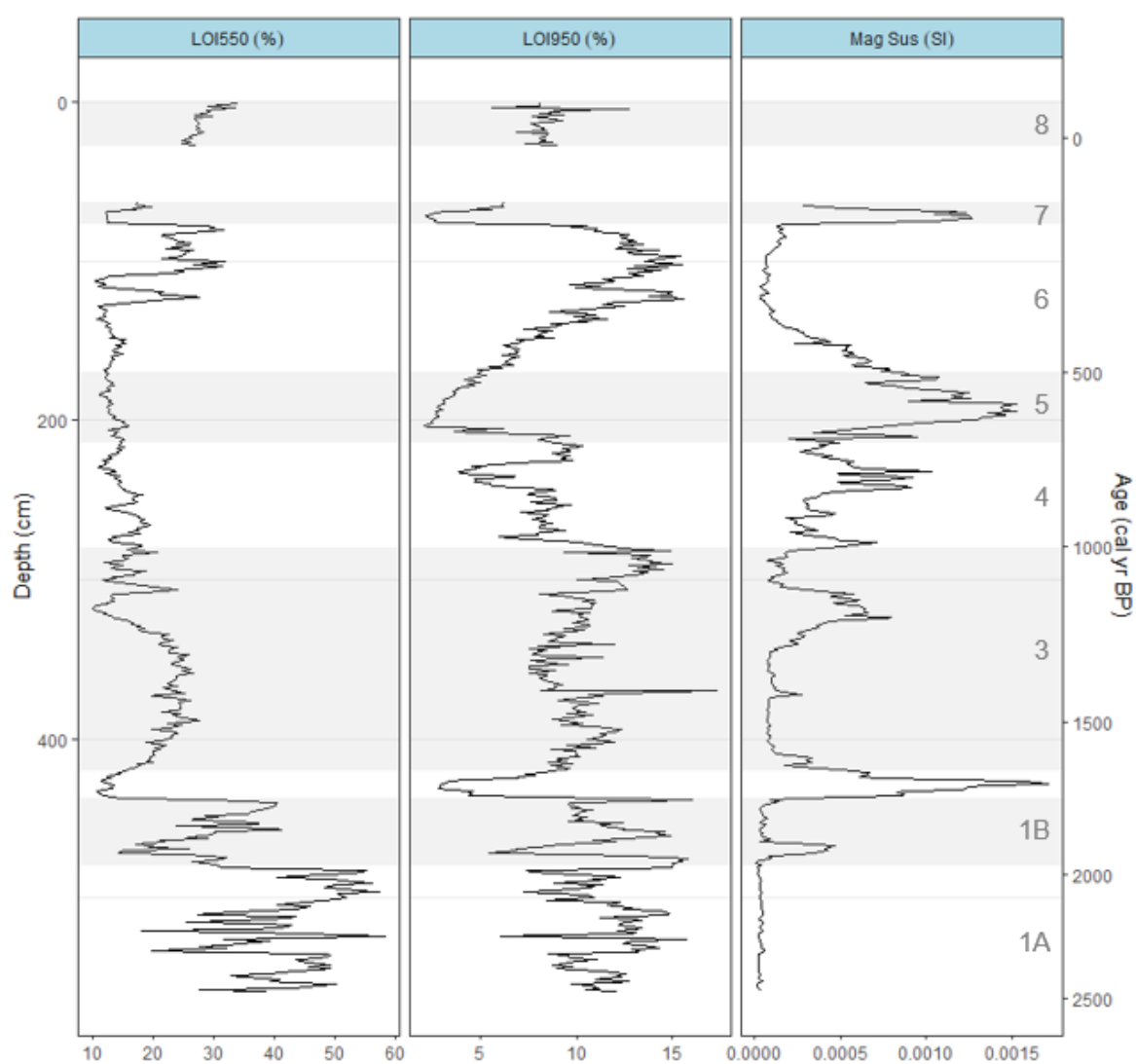


Figure 7.4: Plots showing the LOI<sub>550</sub>, LOI<sub>950</sub> and magnetic susceptibility data for the Mangaia sequence.

## 7.4 Loss-On-Ignition

Figure 7.4 shows the LOI results for Lake Tiriara at 550°C and 950 °C alongside the magnetic susceptibility data. LOI<sub>550</sub> percentage varies between 10-58% with the highest LOI<sub>550</sub> measurement of 58.2% at 524.4 cm depth and the lowest LOI<sub>550</sub> measurement of 10.12% at 317.66 cm depth. Unlike the Emaotfer sequence, the LOI<sub>550</sub> and LOI<sub>950</sub> do not display an inverse relationship but show more resemblance in their behaviour down core.

There is a higher rate of variability in the deepest sediments of the Tiriara sequence, particularly in zone M-1A which continues into M-1B though the latter zone sees a drop in the overall LOI<sub>550</sub> percentage. There is a clear and large drop in both LOI<sub>550</sub> and LOI<sub>950</sub> from 437 cm, which also sees the start of a peak in the magnetic susceptibility data.

Following this, the LOI<sub>550</sub> values increase gradually before stabilising with only a small degree of variation across zone M-3. At the end of this zone as it transitions into zone M-4 the organic percentage becomes depressed relative to the earlier sediments as it starts to gradually drop until it reaches around 12% at 320cm. The LOI<sub>550</sub> percentage remains fairly stable through the rest of zone M-4 and this continues throughout zone M-5. In zone M-6, the LOI<sub>550</sub> percentage rises rapidly, peaking at 27.8% at 122 cm before dropping quickly to 12.54% at 71 cm.

LOI<sub>950</sub> percentage typically varies between 5-12% with the lowest LOI<sub>950</sub> measurement at 1.48% at 79 cm depth and the highest LOI<sub>950</sub> measurement at 12.3% at 287 cm depth. The Lake Tiriara record has relatively stable levels of LOI<sub>950</sub> in the oldest part of the record but there are three periods where LOI<sub>950</sub> drops. The first occurs between 420-438 cm, with a dip from 15.99% at 438 cm down to 2.85% at 431 cm, the second is at 158-243 cm (c. 775 – 1124 cal yr BP) with a dip to 2.09% and finally the third is between 63-83 cm (c. 272 – 379 cal yr BP) with a low value of 2.12%. Other than these two periods, the rest of the record shows variability but a similar mean state throughout.

## 7.5 $\mu$ XRF Geochemistry

Itrax  $\mu$ XRF data originally had a resolution of 200 $\mu$ m but here it has been averaged to a 1 cm resolution to enable comparison between all datasets. When presented individually as opposed to a ratio, elements have been normalised using the molybdenum incoherent scatter signal to correct for water content (Boyle, Chiverrell and Schillereff, 2015). For the correlation matrix and the PCA, the data was transformed using a centred log-ratio to account for dilution effects (Weltje *et al.*, 2015). Zones were designated based on trends in the  $\mu$ XRF data and later refined using the stable isotope and diatom composition of samples.

The terrestrial indicators show peaks and troughs throughout the record though there is no clear shift in the average level of terrestrial records. There does appear to be an overall decrease in marine indicators especially in the first half of the record, but the latter half do not show a continuation of this trend.

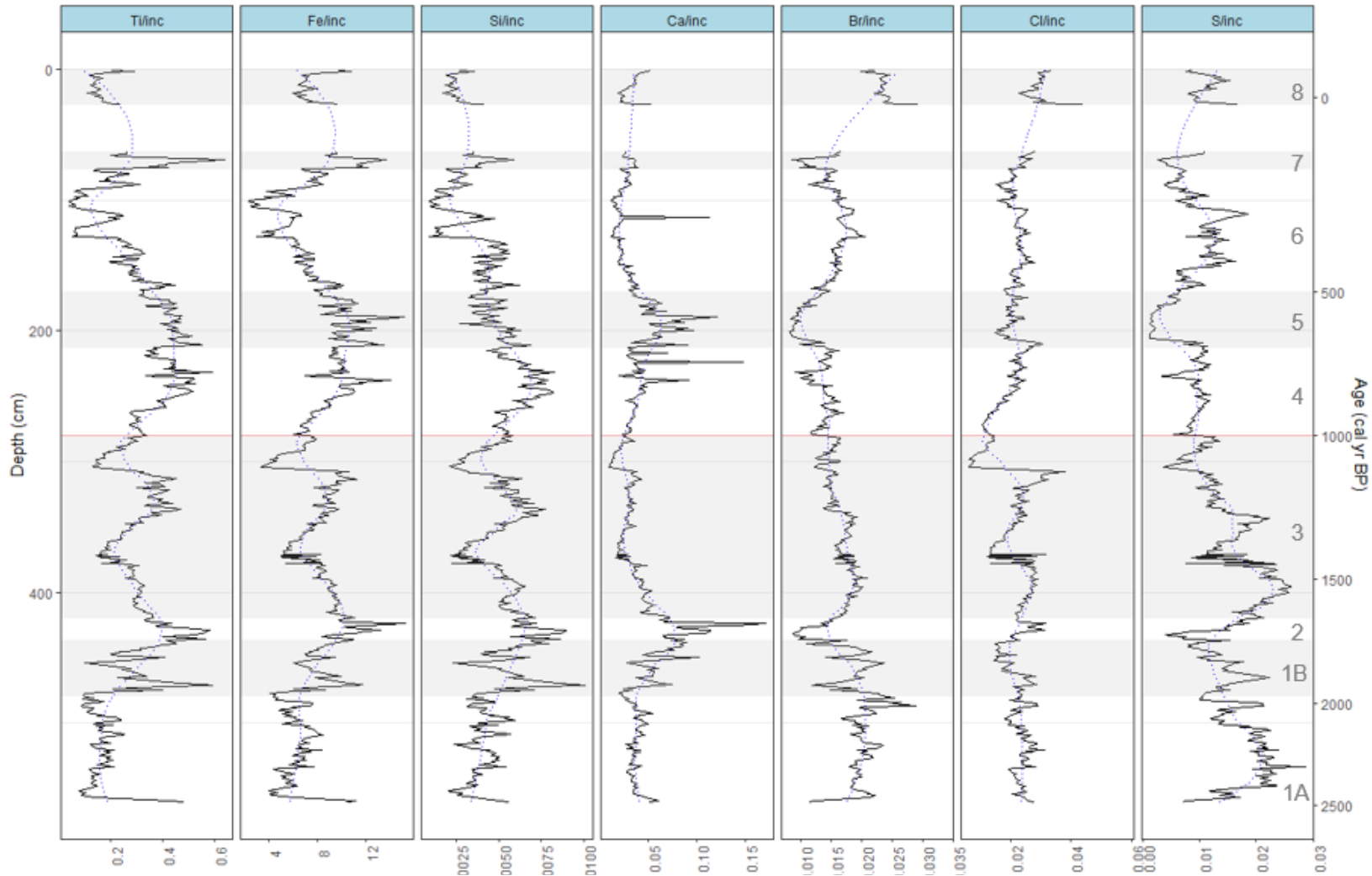


Figure 7.5: Plots showing the XRF geochemistry data for the Mangaia sequence. Red line denotes the start of the second wave of human migration into eastern Polynesia.

For Mangaia the  $\mu$ XRF data was delineated into eight zones:

Table 7.2: Breakdown of XRF zones for Lake Tiriara sequence and a description of major changes in elemental profiles.

Zone	Depth (cm)	Age (cal yr BP)	Description of XRF
<b>M-1A</b>	480-560	2481 to 1950 $\pm$ 174	This zone shows relatively low levels of terrestrial input from Ti, Fe and Si in comparison to the rest of the sequence. There are high levels of S in this section and relatively high levels of Br but low levels of Ca.
<b>M-1B</b>	437-480	1950-1678 $\pm$ 124	The levels of Br and S decrease through this zone whilst Cl remains relatively level. There is an increase in Ti, Fe, Si and Ca though there is a higher rate of variability in these elements compared to the previous zone.
<b>M-2</b>	420-437	1678-1594 $\pm$ 126	This section appears to sit in contrast to the zones either side indicating the presence of an event layer potentially. We see peaks in terrestrial proxies such as Ti, Fe and Si as well as Ca, which typically indicates the presence of carbonate in this system. For the marine indicators both Br and S drop in this zone but there is a small peak in Cl.
<b>M-3</b>	280 – 420	1594-859 $\pm$ 126	Terrestrial indicators drop following the peak from the zone prior but start to rise again halfway through the zone, peaking just before a dip in values around 300 cm. Ca remains low throughout this section. Br shows a lower level of variability through this section and remains relatively steady. S peaks at around 400 cm then gradually decreases through the zone whilst Cl has a small rise in the first half of the zone before a drop in values, but this peaks again towards the end of this section.
<b>M-4</b>	214-280	859-647 $\pm$ 104	This section shows a rise in the terrestrial indicators as well as Ca and Cl. S and Br values remain relatively stable throughout.
<b>M-5</b>	170-214	647-470 $\pm$ 102	This zone sees a peak in the terrestrial proxies and in Ca. The values for Br and S see values drop in this zone but Cl remains relatively stable with a subtle drop in values.
<b>M-6</b>	77-170	470-160 $\pm$ 95	All the terrestrial proxies decrease across this zone and Ca returns to relatively low values. Both Br and S have a gradual increase and stabilisation of values through this section whilst Cl values remain relatively constant throughout.
<b>M-7</b>	63 - 77	160-119 $\pm$ 60	This section sees a rapid peak in the terrestrial proxies and a small peak in Ca. The Br and S values drop and Cl values gradually increase through this zone.

<b>M-8</b>	0 - 28	16 ± 54 - present	This section has the highest levels of Br of the entire sequence. All proxies show an initial drop in values from 28cm. Terrestrial proxies all decrease following this then level out but have a small peak at the top of the sequence. Ca and Cl gradually increase across this zone whilst Br stabilises then drops again at the top of the section. S has a peak in this zone, which drops off at the top of the sequence.
------------	--------	-------------------	--

Ca has a moderate positive relationship with Sr with an r-squared value of 0.44 ( $n = 500$ ,  $p < 2.2e-16$ ) but a weaker relationship with Ti (Figure 7.6). This suggests authigenic carbonate precipitation is being produced in the lake rather than being transported via in-wash which is indicated by the presence of Ti (Evans *et al.*, 2019). However, unlike Emaotfer Swamp, the Lake Tiriara sediment is not dominated by calcium carbonate and it is likely that carbonate is only precipitated in certain parts of the core, so these relationships need to be used with caution as for a majority of the sequence carbonate is not the key driver of Ca and Sr levels. With no strong correlation with S or Sr, it is likely that the carbonate being precipitated in the sequence is calcium carbonate ( $\text{CaCO}_3$ ) and it is expected that this has not changed throughout the record.

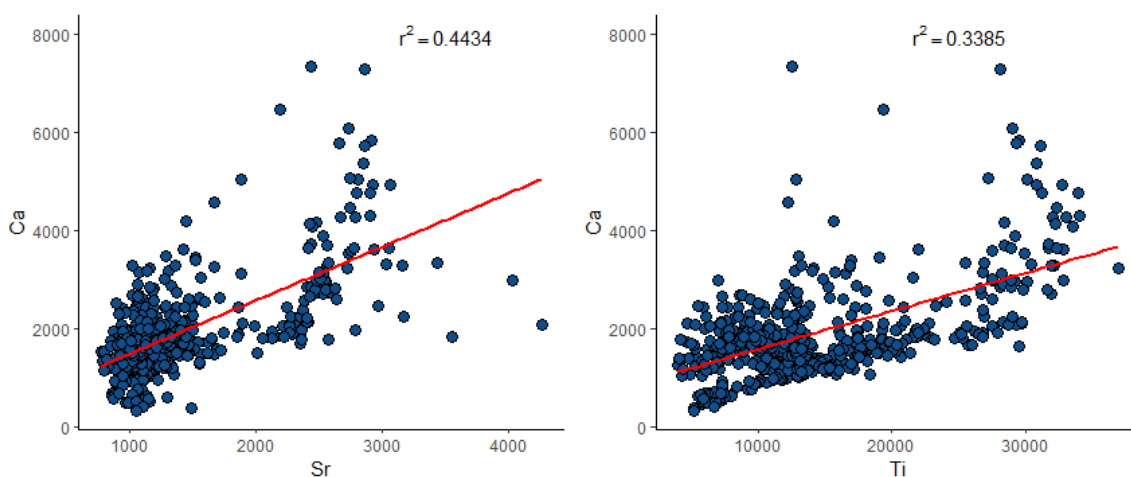


Figure 7.6: Plots showing the relationship between Sr, and Ti against Ca in the Tiriara core sequence.

### 7.5.1 Principal Component Analysis

Figure 7.7 and Figure 7.8 show the Principal Component Analysis (PCA) and correlation matrix for the Itrax  $\mu$ XRF data for Lake Tiriara. Here the data has been split into groups

based on the zones dictated in section 7.5 and distance along the PCA axes indicates the weighting of each depth in the first two principal components. Axis 1 explains most of the variance (62.2%) and shows key zones spread mainly along this axis. Overall, PCA1 and 2 combined accounts for 76.5% of the data variance. Br and Cl marine indicators have a strong correlation to one another and a strong negative correlation to the terrestrial indicators. Br and Cl track negatively in PCA1 and positively in PCA2. The biplot shows that sections from the youngest and oldest parts of the Tiriara cores are mostly strongly associated with these elements. The terrestrial indicators generally have a strong positive correlation to one another though this correlation is weak where indicators are positively or negatively loaded on PCA2. They are all positively loaded on PCA1 but are split with Ti and Si sitting negatively on PCA2 whilst Fe, Rb are positively loaded in PCA2. These indicators are most strongly associated with zone M-4 and M-5. The sections of the core that associate strongly with S are within zone M-3 that cluster most tightly around the S axis. Further to this, the other freshwater biogenic indicators do not show a strong correlation with other indicators though Ca shows a moderate correlation of 0.47 with Sr. Whilst Si, which can be either a freshwater or terrestrial indicator, here appears to have no significant correlation with the terrestrial elements and a weak correlation with Ca of 0.27.

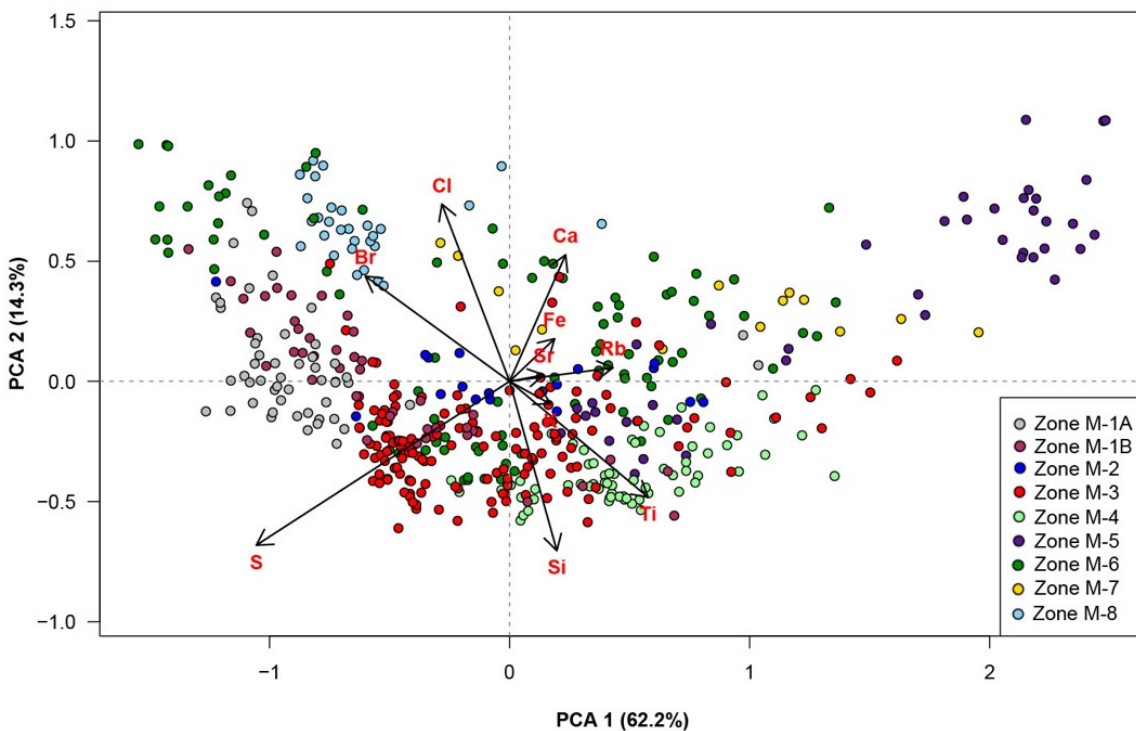


Figure 7.7: Principal component analysis plot for PCA 1 and PCA2 of the Mangaian sediments.



## 7.6 Organic Proxies

### 7.6.1 Total Organic Carbon and Nitrogen

There is a relatively large range of values for total organic carbon in this sequence with a minimum value of 0.91% and a maximum value of 34.5% - see Figure 7.9. Zone M-1A shows the highest TOC values for the Mangaiian sequence with maximum values of 34.5% at 500 cm and this zone also has the overall highest average TOC with values ranging between 13.02 and 34.49%. This average drops as the sequence transitions into zone 1B though the rate of variability remains relatively high. However, the TOC plummets in zone M-2 to 0.91% at 428 cm - the lowest values observed in the sequence. The values gradually increase through the start of zone M-3 up to a maximum value of 12.43% though these values start to decrease through to the end of zone M-3 and into zone M-4. From 323 cm onwards the TOC becomes relatively suppressed through zones M-4 and 5 with values only varying between 1.6 and 5.92%. In zone M-6, the rate of variability increases with values ranging between 3.67 and 17.92%. Zone M-7 shows a drop in the TOC to 3.81% though throughout zone M-8 the TOC values gradually increase.

Total Nitrogen values generally mirror the pattern of the TOC values through the whole sequence. Values are low, ranging from a minimum of 0.11% to a maximum value of 2.58%. Total nitrogen sequence starts with relatively high and variable values across zones M-1A and 1B, which are moving gradually to lower values. In zone M-2 the values plummet to the lowest value of 0.11% between 426 and 428 cm, a pattern that was also observed in the TOC record at this depth. Following this, values remain low (<1%) with a low rate of variability compared to that of zones M-1A and 1B. There is a small peak at 96 cm with a value of 1.24% before values drop again. The topmost sediments show an increase in the total nitrogen value across the section rising from 0.8% at 28 cm up to 1.06% at the top of the core.

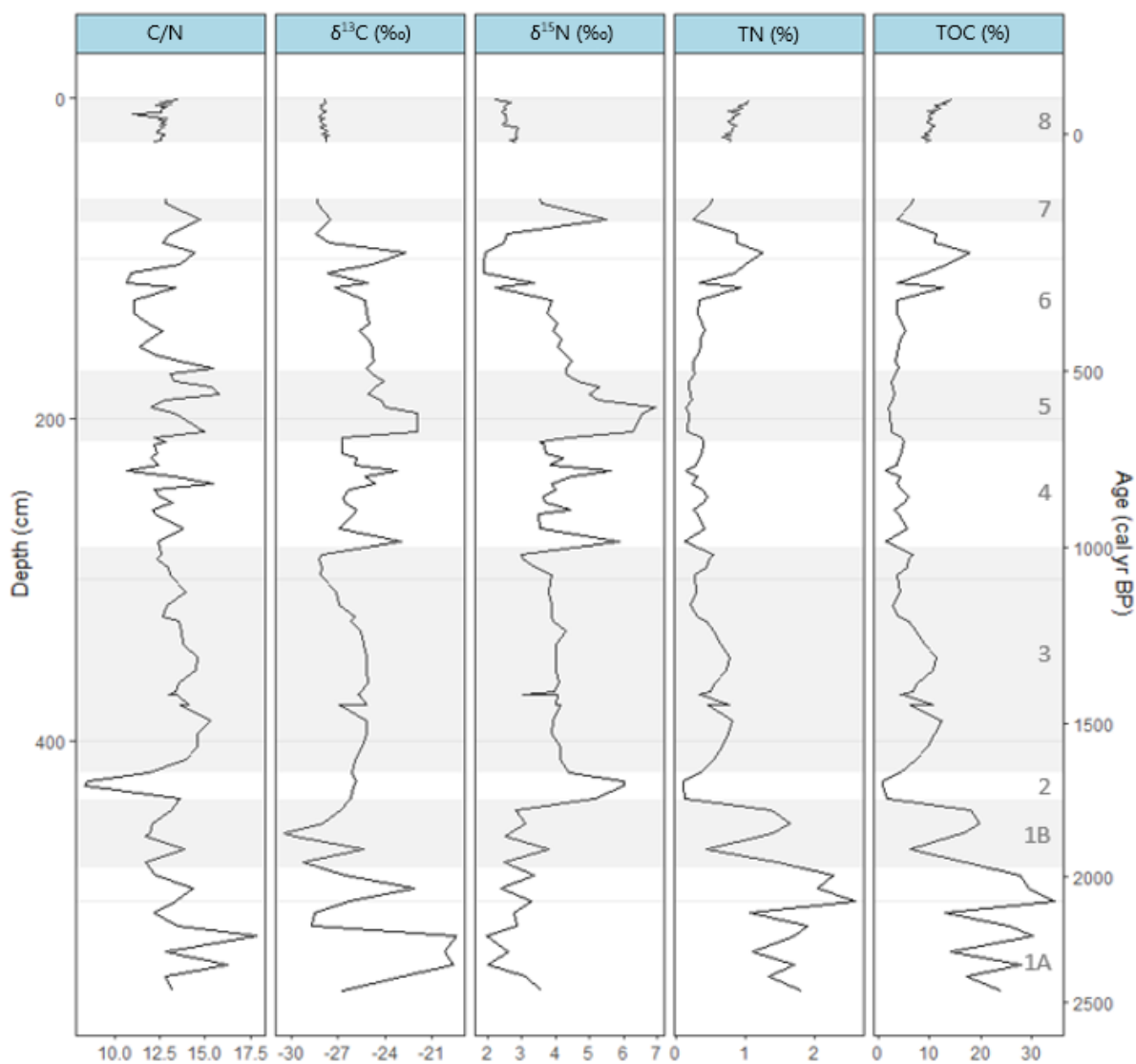


Figure 7.9: Plots showing the C/N,  $\delta^{13}\text{C}_{\text{org}}$  (‰ VPDB),  $\delta^{15}\text{N}$  (‰ Air), TN and TOC data from the Mangaia sequence.

### 7.6.2 C/N ratio

The C/N values range from a minimum value of 8.34 at 428 cm to a maximum of 17.82 at 522 cm. The C/N record starts with relatively high values and a high rate of variability across zones M-1A and 1B though with an overall decrease in values across these zones. There is a large drop in the C/N ratio to 8.34 at 428 cm where there are also considerable drops in TOC and TN. This likely represents a high proportion of algal material in this section of the core. This event is relatively short-lived and C/N values rise and show a relatively steady decline across zones M-3 to 4 but generally fluctuate between 12 and 14. From mid-way through

zone M-4 and into zone 5 the C/N values start to show a higher rate of variability and overall slightly higher values, particularly in zone M-5. There is a drop in values as the sequence moves into zone M-6 but they recover towards the end of the section. The core top sediments show very little variation in values with a few exceptions but C/N values in this section typically fall between 12 and 13.

### 7.6.3 Organic $\delta^{13}\text{C}$ and $\delta^{15}\text{N}$

The  $\delta^{13}\text{C}$  record shown in Figure 7.9 similarly to the LOI<sub>550</sub> record shown in Figure 7.4 shows a high degree of variability in the deepest zones, M-1A and 1B. In the latter half of zone M-1B the isotope values start to gradually rise and then in zones 2-3 the  $\delta^{13}\text{C}$  values remain relatively stable varying between -25‰ and -27‰. The  $\delta^{13}\text{C}$  values start to slowly decline in the beginning of zone M-4 and then similar to the  $\delta^{15}\text{N}$  record the values start to show a larger degree of variability, fluctuating between -28.5 and -22.94‰. In the start of zone M-5 there is a large upward shift in the  $\delta^{13}\text{C}$  to -21.93‰ though this drops to -23.94‰ and then very slightly declines through to the end of this zone. In zone M-6 again there is a larger degree of variability in values before dropping to -27.54‰ in zone M-7. In zone M-8 the values are more tightly constrained relative to the rest of the record and vary between only -27.87 and -28.17‰.

The lowest values of  $\delta^{15}\text{N}$  are found primarily in the deepest sections of the Manganian sequence. In zones M-1A to 1B values vary between around 2 and 4‰. At zone M-2, there is a relatively large spike in  $\delta^{15}\text{N}$  values up to 6‰. Values then drop through zone M-3 where they remain stable throughout at around 4‰ or slightly below. This continues into zone M-4 but from 284cm ( $871 \pm 93$  cal yr BP) the values start to show a large degree of variability with values ranging from 3‰ to 5.87‰. In zone M-5, there is a big shift upwards in the  $\delta^{15}\text{N}$  isotope values up to 6.94‰ - the highest value in the record – though this drops down to 5.22‰ and then gradually declines through the rest of the zone and drops to 1.88‰ in zone 6 before spiking again in zone M-7 to 5.50‰. The  $\delta^{15}\text{N}$  values in zone M-8 are relatively stable in comparison to the rest of the record, only varying between 2 and 3‰.

A comparison of C/N against organic  $\delta^{13}\text{C}$  is shown in Figure 7.10. The points that represent zone 2 show that the event layer in that zone sits neatly within the algae section of the plot

indicating the main source of organic matter for that event layer was from lacustrine algae. Otherwise, the rest of the Mangaia sequence seems to show that the organic matter is likely sourced from a mix of sources as many of the data points sit between C<sub>3</sub> plants and algae.

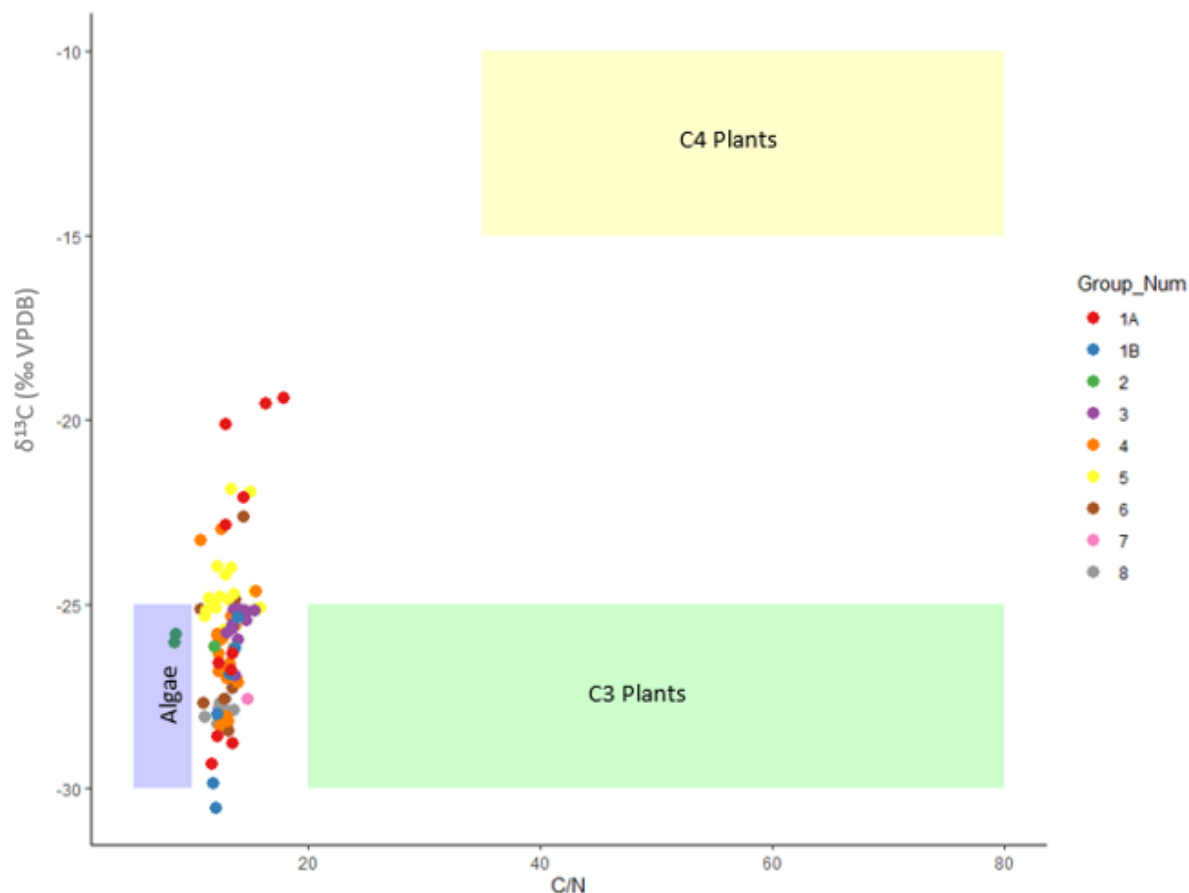


Figure 7.10: Plot showing the C/N against the  $\delta^{13}\text{C}$  (‰ VPDB) values for each zone of the Mangaia sequence. Boxes denote typical values for lacustrine algae (purple box), C<sub>3</sub> (green box) and C<sub>4</sub> plants (yellow box).

## 7.7 Inorganic Proxies

### 7.7.1 $\delta^2\text{H}$ and $\delta^{18}\text{O}$ in modern water

Figure 7.11 shows the results of the modern lake water isotopic content for Lake Tiriara in relation to other freshwater lakes and local rainfall. The pink regression line represents the local evaporation line and the isotopic data for freshwater lakes comes from data published by Maloney et al (2019) on lakes across the South Pacific islands. The blue regression line

represents the local meteoric water line and the isotopic data for rainfall events is derived again from data published by Maloney et al (2019) along with rainfall data from Rarotonga – the geographically closest available record - taken from the Global Network of Isotopes in Precipitation database (IAEA/WMO, 2020).

Lake Tiriara sits very close to the local meteoric water line indicating that at the time of sampling in 2016 it was not evaporative and likely represents the isotopic composition of local rainfall (Leng and Marshall, 2004).

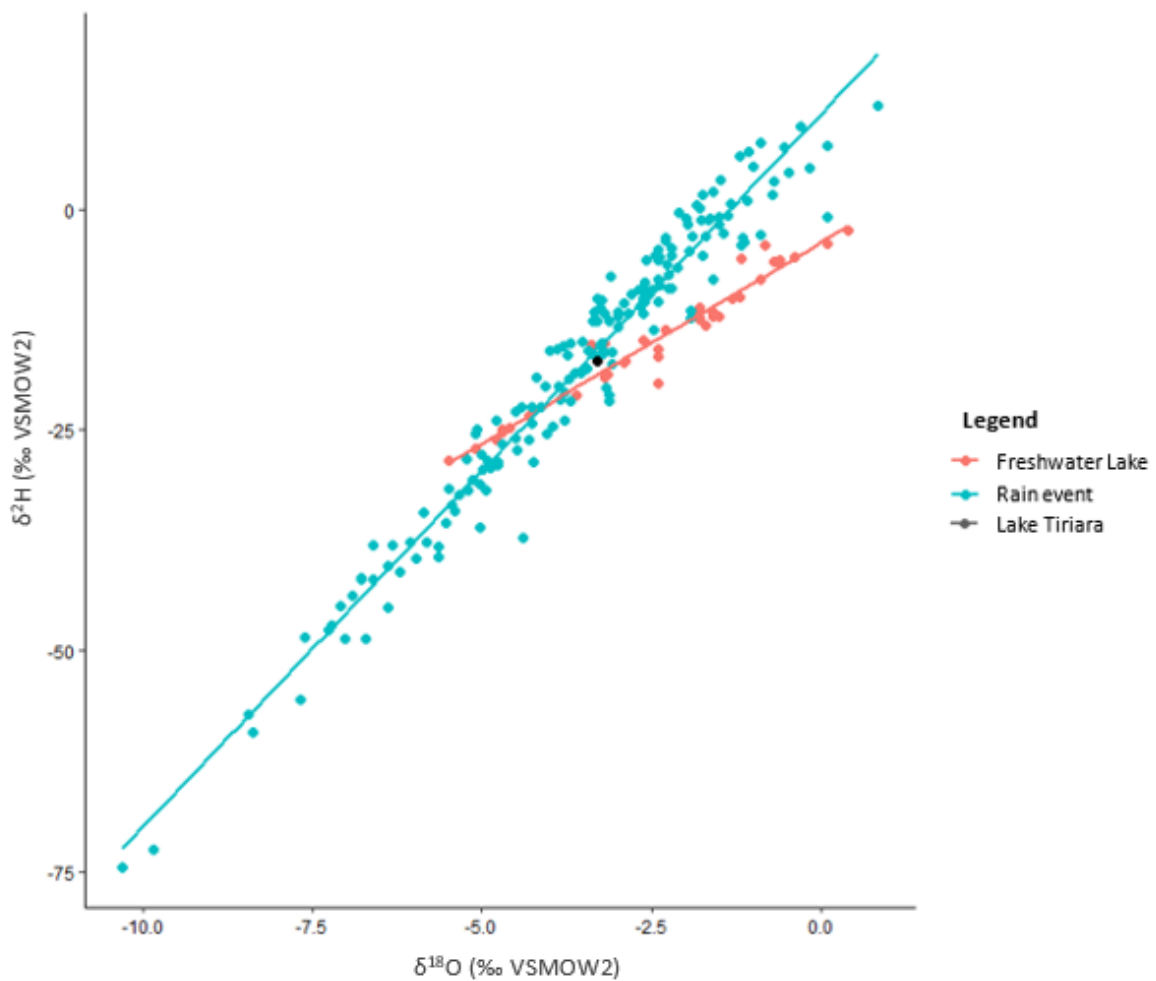


Figure 7.11: Plot showing the <sup>2</sup>H and <sup>18</sup>O for rain events in the tropical Pacific, freshwater lakes taken from Maloney *et al* (2019) and Lake Tiriara.

### 7.7.2 Inorganic $\delta^{18}\text{O}$ and $\delta^{13}\text{C}$ record

Figure 7.12 shows the results for inorganic  $\delta^{18}\text{O}$  and  $\delta^{13}\text{C}$  for Lake Tiriara alongside the Ca/Inc ratio from the Itrax XRF data and the  $\text{CO}_2$  yield data produced during sample preparation for oxygen isotope analysis.

$\delta^{18}\text{O}$  values for the Lake Tiriara sequence vary between -10.8 and 0.94‰. No data points were recoverable from zones M-1A and M-1B. The first data points come from zone M-2 with values close to 1‰. The  $\delta^{18}\text{O}$  record then goes through a series of peaks and troughs through zone M-3 and M-4, levelling out at 252 cm to 228 cm. The largest cluster of data points are found in zone M-5, which begins with the largest peak in  $\delta^{18}\text{O}$  with a value of 0.94 at 211 cm. The values then drop slightly and vary between -0.94 and -4.42‰ within this cluster. The  $\delta^{18}\text{O}$  record then drops down to -9.28‰ towards the end of zone M-5 before rising again to -2.85‰ in zone M-6. The second cluster of data points are located in zone M-8 within the core top sediments from 25 cm upward. Values in this section range from -6.78 to -2.40‰.

$\delta^{13}\text{C}_{\text{inorg}}$  values across the sequence vary between -23.97 and 3.48‰. The first data points come from zone M-2, which represents the highest peak in values with 3.48‰ at 428 cm. The  $\delta^{13}\text{C}$  then drops down and remains relatively steady through zone M-3, varying between -7 and -12‰. There is a small dip in values -16.94‰ at 236 cm before a notable step up in values between 140-211 cm where values vary between -4.52 and 2.80‰. Following this, the  $\delta^{13}\text{C}_{\text{inorg}}$  values from the core top sediments were markedly lower than those measured down the sediment sequence.  $\delta^{13}\text{C}_{\text{inorg}}$  values for sediments from 30 cm to the surface were all -19.72‰ or lower.

The Ca/Inc ratio remains consistently low with values below 0.05 throughout the record. There are two exceptions to this. The first occurs from 1929 to 1450 yr BP, covering 379-475 cm, spread across zones M-1B through to M-3. There is a steady increase in the Ca/Inc ratio through zone M-1B from 475 cm. The calcium peaks in zone M-2 at 424 cm with a value of 0.17, which occurs at 1655 yr BP, before steadily decreasing through into zone M-3. The second occurs from 1092 to 340 yr BP, covering 129-300 cm, and spread across zone M4-M5. The rise in calcium is gradual across the whole of zone M4. There are several individual data point spikes but the peak in the calcium based on the smoothed data is in zone M5 at

## Chapter 7

189 cm with a value of 0.12, which occurs at 547 yr BP. The calcium record did not correlate well with the LOI<sub>950</sub> record - with a Pearson's correlation value of -0.37 - that is understood to typically be indicative of carbonates, inferring that LOI<sub>950</sub> is not an ideal proxy for identification of carbonate in the Mangaia sequence.

There is a change in the relationship between  $\delta^{18}\text{O}$  and  $\delta^{13}\text{C}$  following zone M-5. Earlier in the sequence the  $\delta^{18}\text{O}$  and  $\delta^{13}\text{C}$  both show a similar pattern and direction of change. However, the data points that succeed zone-M5 start to show opposite direction of change between the two variables. This indicates that the relationship between  $\delta^{18}\text{O}$  and  $\delta^{13}\text{C}$  changes in the younger sections of the core.

These peaks in the Ca/Inc also coincide with the peaks observed in the yield data. Samples from 180-208 cm and 428 cm all produced higher levels of CO<sub>2</sub> on reaction to phosphoric acid. Overall, CO<sub>2</sub> yields were low across most of the sequence with values below 4mb. Despite the limited nature of these datasets, -  $\delta^{18}\text{O}$  and  $\delta^{13}\text{C}$  in particular - the presence of carbonate in certain sections of the core can tell us something about this environment which typically is not conducive to precipitating carbonate.

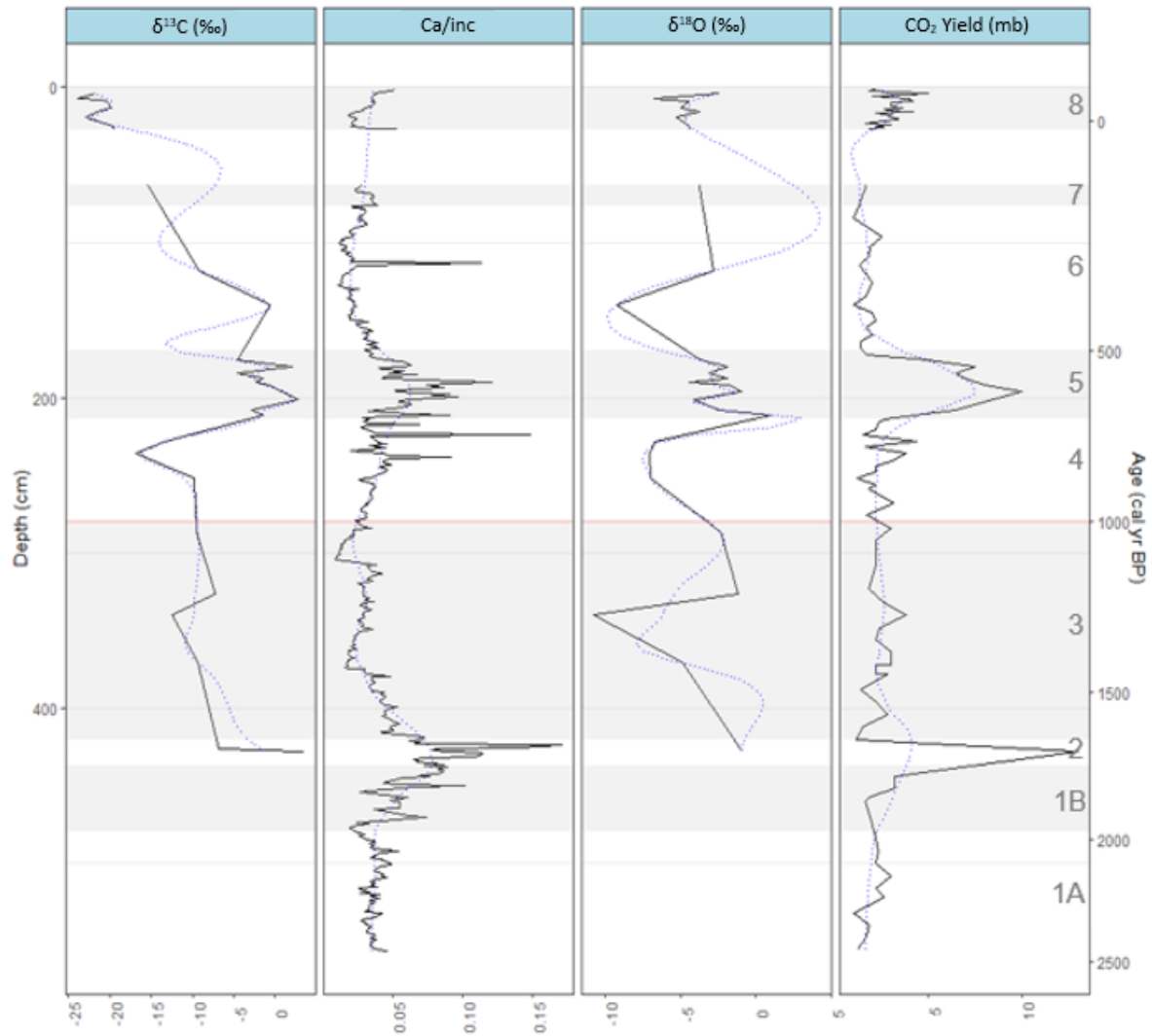


Figure 7.12: Plots showing the inorganic  $\delta^{13}\text{C}$  (‰ VPBD),  $\delta^{18}\text{O}$  (‰ VPBD), Ca/inc XRF and  $\text{CO}_2$  yield data from the Mangaia sequence. Blue line is loess smoothed.

In contrast to the Emaotfer record, the  $\delta^{18}\text{O}$  and  $\delta^{13}\text{C}$  for Lake Tiriara do not covary. Figure 7.13 shows that the Tiriara sediments  $\delta^{18}\text{O}$  and  $\delta^{13}\text{C}$  values provide an  $r^2$  value of 0.18 ( $p=0.02168$ ,  $n=27$ ) indicating a weak relationship between the two variables.

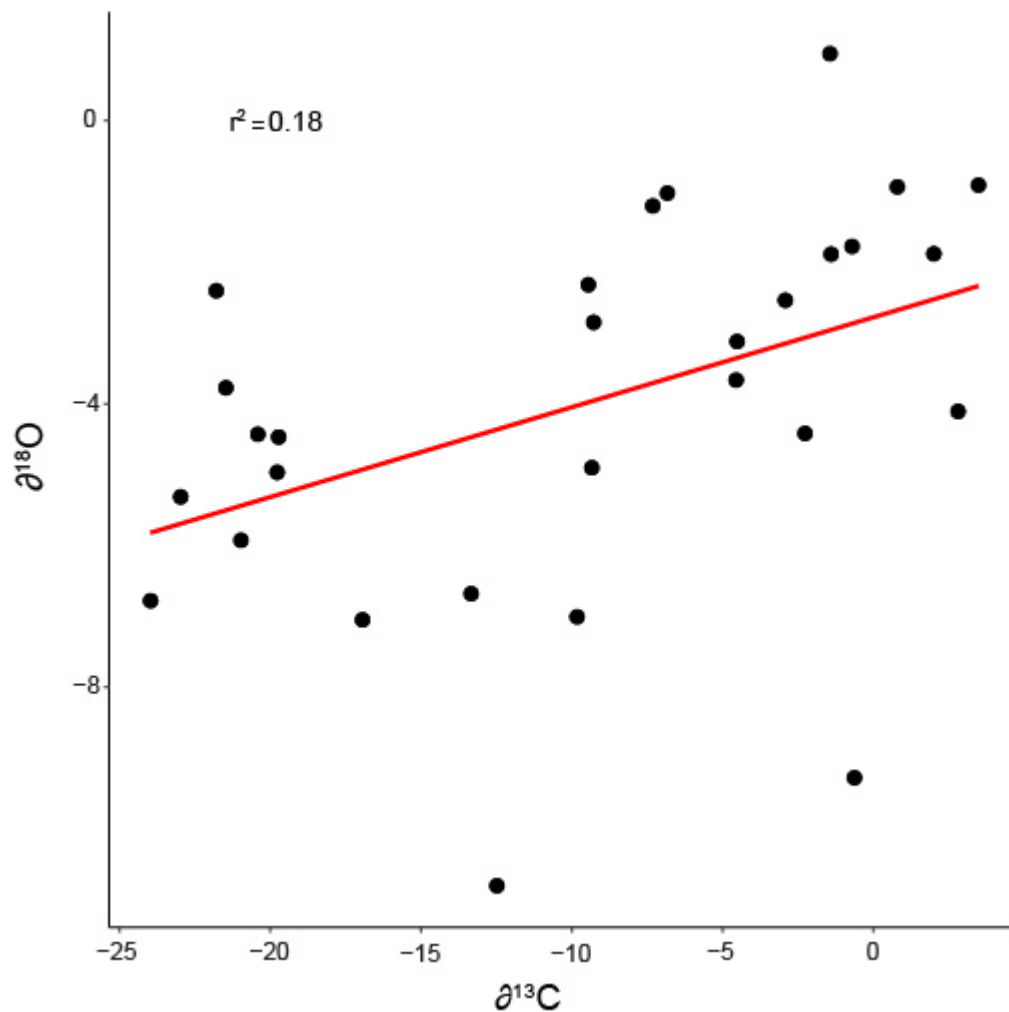


Figure 7.13: Plot showing the relationship between inorganic  $\delta^{13}\text{C}$  (‰ VPBD) and  $\delta^{18}\text{O}$  (‰ VPBD) from Lake Tiriara, Mangaia with a line of best fit and displaying the r-squared value.

## 7.8 Diatoms

For every sample taken for pilot oxygen isotope analysis – which were spread across the Mangaia sequence to test for carbonate - another sub-sample was taken to determine diatom content, providing twelve samples across the sequence.

The diatom record for Lake Tiriara (Figure 7.14) shows variation between the high and the low  $\text{LOI}_{950}$  values, which were used to choose the location of subsamples. Diatoms in Tiriara show shifts back and forth between high and low  $\text{LOI}_{950}$  values. Where samples were taken in the low-mid  $\text{LOI}_{950}$  readings, the concentration of diatoms was much lower than the samples taken at the high  $\text{LOI}_{950}$  measurements. At 533 cm we see that *Navicula spp.* is dominating the assemblage at Tiriara making up over 89% of the total relative abundance. In

the next sample at 513 cm there is a drastic drop in *Navicula spp.* to just over 1% and instead *Pseudostaurosira brevistriata* dominates making up 94.67% of the total diatom assemblage. From this stratigraphic sequence, the most unusual sample was at 477.4 cm in zone M-1B, where the concentration of diatoms was very high and dominated by *Pseudostaurosira brevistriata* though there were a low number of *Navicula spp.* present as well. This sample may be representative of an algal bloom or a high level of productivity in the lake. Where the concentration is high enough to get an idea of the assemblage, we see that at 370 cm in zone M-3 the assemblage becomes quite diverse and no single species dominates. Later in zone M-3, at 287 cm we see a return to a *Navicula sp.* dominated assemblage which is also seen at 118 cm too though the diversity of species increases in the earlier sediments. Overall, the oldest part of this record shows a shift from an assemblage dominated by *Navicula spp.* at 533 cm to one dominated by *Pseudostaurosira brevistriata* at 477 and 513 cm in zone M1A and 1B. After this the low LOI<sub>950</sub> values have low counts and poor preservation of diatoms but the samples at 370 and 287 cm in zone M-3 and 118 cm in zone M-6 show a shift from a more diverse and balanced assemblage at 370 cm to assemblages dominated by *Navicula spp.* again. The samples taken at 63, 211, 326 and 426 cm which were identified as having low LOI<sub>950</sub> values, we see very low total diatom counts possible due to poor preservation. The key change in the stratigraphy is the shift from *Pseudostaurosira brevistriata* dominance prior to 300 cm to a *Rhoplodia gibberula* and *Navicula spp* dominance in the top half of the sequence.

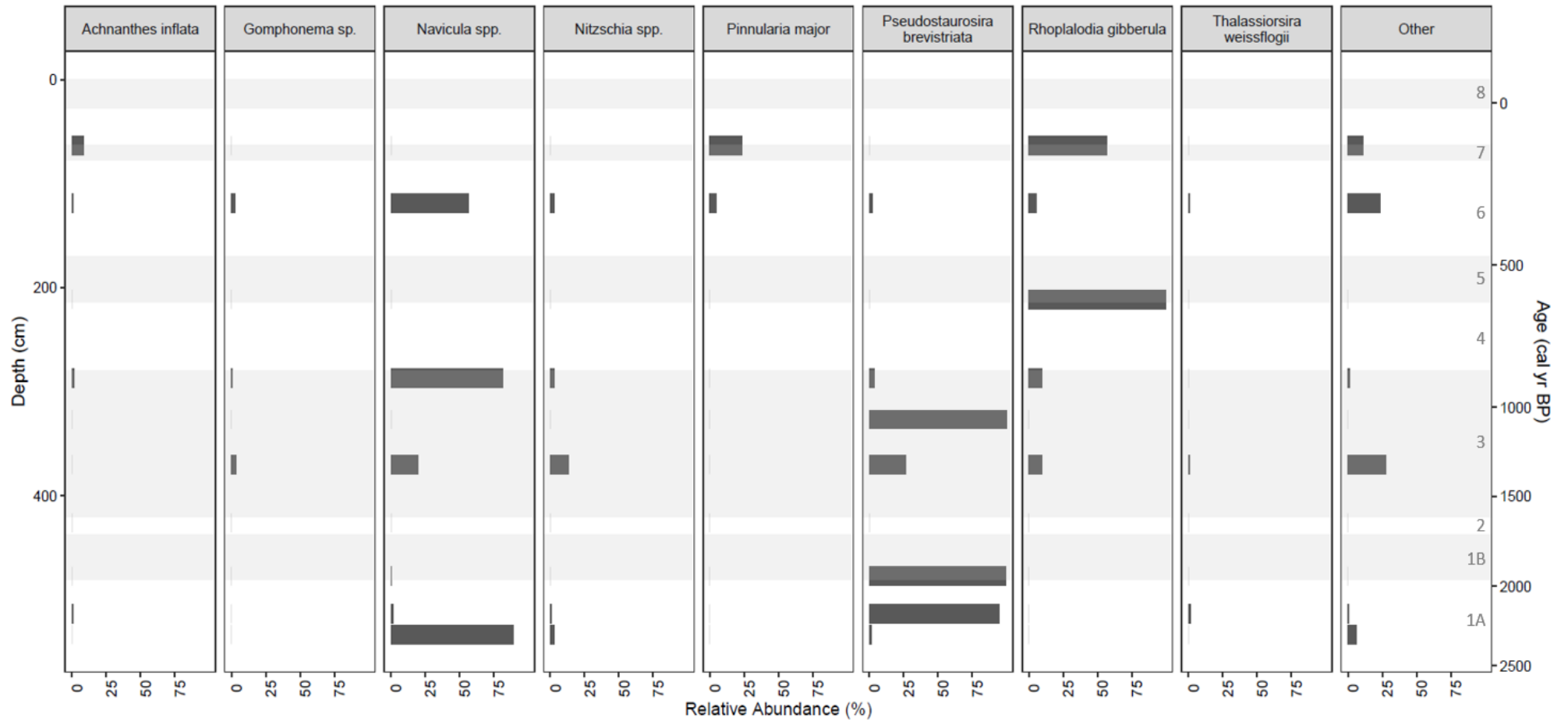


Figure 7.14: Stratigraphic plot for the relative abundance of diatom types from Lake Tiriara.

## 7.9 Palaeoenvironmental change in the Cook Islands during the Late Holocene

The palaeoenvironmental history of Mangaia can be split into two halves, the first covering the period prior to human arrival (2500 - 950 yr BP) and the second post human arrival (950 yr BP to present). Following this section, several subsections will delve into particular zones of interest.

### 7.9.1 Interpretation of the Lake Tiriara Sequence

#### 7.9.1.1 Pre-human arrival – 2500 – 950 yr BP

In Lake Tiriara, the oldest part of the record presented starts in Zone M-1 which is split into **M-IA** (480 – 560 cm, 2481 to 1950 cal yr BP  $\pm$  174) and **zone M-IB** (437-480 cm, 1950-1678  $\pm$  124 cal yr BP). The ages suggest that this record begins prior to human arrival in the Southern Cook Islands around 1000 AD (Kirch, 2017b; Sear *et al.*, 2020). The  $\mu$ XRF record shows relative stability in most indicators though both Br/inc and S/inc show some of the highest levels in this zone. Whilst they can both be indicative of increased marine influence (Davies *et al.* 2015) but when considered in conjunction with the enriched  $\delta^{13}\text{C}$  and high TOC values it likely indicates an increase in organic material relative to the rest of the sequence. These values do drop in zone M-1B but are still relatively high compared to the rest of the Mangaia sequence. This zone likely represents a swampy or marshy environment. There are diatoms present in these sediments, indicating that there is likely to be standing water on the site during this time. This is seen in other records as after the transition from lake to swamp in the Emaotfer swamp site in Vanuatu, diatoms were still present (Wirrmann, Eagar, *et al.*, 2011). The two diatom samples from zone M-1A, the first at 533 cm shows a dominance in type B – an unknown *Navicula* spp. (89%) - whilst the sample at 513 cm shows an assemblage dominance by *Pseudostaurosira brevistriata* (94%), a freshwater species. Whilst the diatom samples in zone M-1B at 477 cm found the diatom assemblage is dominated by *Pseudostaurosira brevistriata* (99%), the same freshwater species found in zone M-1A and the relative abundance of frustules in the sample is very high indicating favourable conditions for this species.

In **zone M-2** (420-437 cm, 1678-1594 ± 126 cal yr BP) the proxy signals in this section sit in stark contrast to the zones to either side and the signals in subsequent zones are notably different from those prior to zone M-2, indicating a major and relatively rapid change in the system. This zone is characterised by enriched inorganic  $\delta^{13}\text{C}$  to positive values, which would indicate a marine source of inorganic carbon (Clayton and Degens, 1959). This zone is also one of only two areas within the core sequence with a peak in calcium  $\mu\text{XRF}$ , this is also reflected in the high  $\text{CO}_2$  yield collected during carbonate analysis. Alongside this, in the organic geochemistry there are notable drops in the C/N, TN and TOC, which again is reflected in the  $\text{LOI}_{550}$  and  $\text{LOI}_{950}$ . This suggests a significant input into this system of non-organic material that is suppressing the relative amount of TOC and TN. From the XRF data, there are peaks in the terrestrial proxies – Ti, Fe, Si – along with a peak in the magnetic susceptibility in this zone, indicating terrestrial in-wash into the system (Davies *et al*, 2015). The diatom sample from this zone has a dramatic drop in the concentration, with no diatom frustules present in the sample. This could be due either to an overwhelming input that reduced overall diatom concentration in the sediment or poor preservation of diatom frustules during this time. There are a few possible interpretations of this data so the evidence for both a possible drought event and a potential tsunami event will be covered in more detail later in this chapter in section 7.9.2.1 and 7.9.3.

Following the possible tsunami/drought event, the proxy signals in **zone M-3** (280 – 420 cm, 1594-859 ± 126 cal yr BP) show a much lower rate of variability, but particularly those relating to organic geochemistry. Initially, there is a steady decline in terrestrial indicators along with a substantial drop off in the Ca/inc in this zone. During this time there is also a rapid increase in S/inc and Br/inc following notable dips during zone M-2. A ratio of Br/Cl and S have been used collectively as a marine indicator in New Zealand lake sediments (Evans *et al*, 2019). This could signal an increase in marine influence on the lake over this period and results from the PCA show sediments between 300-55 cm depth strongly associate with both Br and S. However, in other tropical lake systems, S is used as a signal for gypsum precipitation that occurs during dry periods (Burnett *et al*, 2011). The diatom record at 370 cm shows a relatively diverse assemblage for this record and whilst *Rhoplalodia gibberula* - which can tolerate a range of salinity conditions having been found in brackish river mouths in Micronesia (Navarro and Lobban, 2009), freshwater swamps in Kenya (Owen *et al.*, 2004) and even adapted to live in hypersaline lakes in

Brazil if in low quantities (Laut *et al.*, 2019) - or *Thalassiosira weissflogii* could suggest either a fresh or saline environment, however, other freshwater species such as *Pseudostaurosira brevistriata* imply a freshwater environment. In remote regions, isolation and its associated lack of competition can make many diatom species appear more generalist in their tolerances (M.A. Harper, pers comm, Nov 2022). Nevertheless, the presence of all these species point to a freshwater system that perhaps is slightly brackish. The oxygen isotope record at this point indicates wetter conditions at the start of zone M-3 and drier conditions from 326 cm (ca.  $1067 \pm 135$  cal yr BP), which corresponds with a drop in the concentration of diatoms at the same point in time. This shift to a drier period aligns with the start of the MCA and the second wave of migration into Eastern Polynesia, although there is a limited amount of data for this section of the sequence in terms of  $\delta^{18}\text{O}$ . The organic geochemistry during this period has a very low variability and remains relatively steady throughout zone M-3, indicating no major change in vegetation or organic material. Lake Tiriara is mentioned within the traditional tales from Mangaia's ethnohistory, in which it is described as being a freshwater lake (Reilly, 2009). This zone could represent a change in the ontogeny of the system and the evolution from a swamp/wetland to a lake system – as it presents almost as the reverse of the Welsby Lagoon sequence in Australia (Cadd *et al.*, 2018), which transformed from a lake to a swamp, though perhaps with the addition of brackish in-wash from the makatea tunnels.

#### 7.9.1.2 Post-human arrival – 950 yr BP to present

There is initially a drop in terrestrial indicators at the start of **Zone M-4** (214-315 cm,  $859-647 \pm 104$  cal yr BP) but they increase throughout this period and represent the start of a sustained high level of terrestrial input, which is reflected in the peaks in the magnetic susceptibility record in this zone. This coincides with a reduction in the TOC and TN during this period but sees an increase in the  $\delta^{13}\text{C}_{\text{org}}$  and  $\delta^{15}\text{N}$  values and their rate of variability. Coinciding with this increase in terrestrial input there is also an increase in variability in a number of proxies such as  $\text{LOI}_{550}$ , magnetic susceptibility, organic  $\delta^{13}\text{C}$  and  $\delta^{15}\text{N}$ . Higher organic  $\delta^{13}\text{C}$  could be indicative of a shift towards high algal productivity as the overall C/N is gradually dropping in this zone but perhaps in combination with changing vegetation as there are also spikes in the C/N, which would indicate more  $\text{C}_4$  plants in the area (Burnett *et al.*, 2011). There is an increase in Ca/inc record through this zone but the

variability in this proxy increases significantly approximately halfway into this zone and there is a small pickup in the CO<sub>2</sub> yields, which suggest a low level of carbonate is being precipitated during this time. This sits in contrast with  $\delta^{18}\text{O}$  and  $\delta^{13}\text{C}_{\text{inorg}}$  both show initial downturn in zone M-4 before rapidly increasing just before the boundary for M-3, which typically would indicate slightly wetter conditions (Tiwari, Singh and Sinha, 2015). The presence of freshwater mollusc (D. Sear, pers comm, April 2023) found at 224 and 272 cm during sub-sampling indicates a freshwater environment through this zone. Zone M-4 covers human arrival in Mangaia and the MCA and likely reflects a start in changing landscape dynamics due to human activity. According to the age model human arrival is at around 305 cm within the Lake Tiriara sequence. Furthermore, the diatom stratigraphy shows a major change around 300 cm, which prior to human arrival was dominated by *Pseudostaurosira brevistriata* but after human arrival was dominated by *Rhoplalia gibberula* and *Navicula spp* indicating there was a change in the lake system around this time. *Pseudostaurosira brevistriata* is typically a fresh or fresh-brackish diatom but noted to have a “low salinity optima” (Tibby *et al.*, 2007, p. 214) but otherwise is known to be a cosmopolitan species that can endure a wide range of environmental conditions which makes its utility as an environmental indicator limited (Bennion, Appleby and Phillips, 2001; Tibby *et al.*, 2007; Cantonati *et al.*, 2021). Whereas *Rhoplalia gibberula* also known as *Epithemia gibberula* is a diatom species, as mentioned previously has a wide salinity tolerance. It has also been identified as a species that is found in shallow lakes that experiences recurrent mixing, which enables the typically epiphytic species to dwell in the water column (Gasse and Fontes, 1989; Cocquyt and De Wever, 2002). Furthermore, it has been identified within swamp sequences in Kenya with shallow surface water (Owen *et al.*, 2004), within the littoral zone in Bolivia (Sylvestre *et al.*, 1995) and has also been linked to periods of “hydrological deficit” in records (Yacobaccio and Morales, 2005, p. 7). The ecology of this species indicates that this species may be a useful indicator of shallowing of the lake and the start of the presence of peat at the fringes of Lake Tiriara as conditions become drier and it starts its transition to a swamp as other lake systems on Tiriara have done (Ellison, 1994).

**Zone M-5** (170 – 214 cm, 647-470 ± 102 cal yr BP) represents the MCA-LIA transition.

There is some evidence to suggest that this MCA-LIA transition zone represented some of the driest conditions in the sequence. The  $\delta^{18}\text{O}$  is relatively enriched due to evaporation

but not high enough to reflect a marine input, which indicates drier conditions (Tiwari, Singh and Sinha, 2015). The presence of a freshwater environment is also supported by the presence of freshwater molluscs in this zone (D. Sear, Pers Comm, April 2023), found in the sediment at 190 cm during sub-sampling. The presence of calcium in the record due to in wash from the makatea escarpment can be ruled out based on the  $\delta^{13}\text{C}_{\text{inorg}}$  values, as the values for marine typically sit at around 0‰ whereas freshwater values vary more widely (Cuna, Pop and Hosu, 2001; Oehlert and Swart, 2014) and the  $\delta^{13}\text{C}_{\text{inorg}}$  values from this section sit at around -4 to 2 ‰. Also due to the increased rate of terrestrial in wash that typically would mute signals from other inputs into the system but here Ca/inc also increases, which indicates that there is a different process in play in this zone. The makatea escarpment is poor agricultural land so there is not the same utilisation of the land and increase of material as the inner valleys and slopes of the island. Here the increase in the Ca/inc signal is interpreted as a drier period that reduced the lake level, concentrating the ions enough to produce a higher rate of carbonate precipitation (Conroy *et al.*, 2008; Hassall, 2017; Thompson *et al.*, 2017). A potential dry period at this time is also supported by the lack of diatoms from this zone, as only a small number of frustules were present in the sample from this zone. It has been suggested that diatom frustules can be poorly preserved in the sediments when sections of the lake dry out and the frustules are exposed to the atmosphere (Conroy *et al.*, 2008). This zone represents not only a potential climatic change but also a human signal. This zone represents the start of the Tangatatau phase where people had started to live permanently in the island's interior and were developing the agricultural cultigens in the lowland swamp areas (Kirch, 2017b). This is evidenced by the increase in the  $\delta^{13}\text{C}_{\text{organic}}$  which indicates a change in the type of vegetation present likely brought about by the intensification of agriculture during this time. The theory of intensification is also supported by charcoal data from the same Tiriara sequence presented by Temple-Brown (2018) that shows that the peak in the charcoal data occurs at 200 cm within the Mangaia sequence (Figure 7.15) dating to  $500 \pm 92$  yr BP based on the age model from this thesis, which can be attributed to an increase in human activity in relation to slash and burn agriculture.

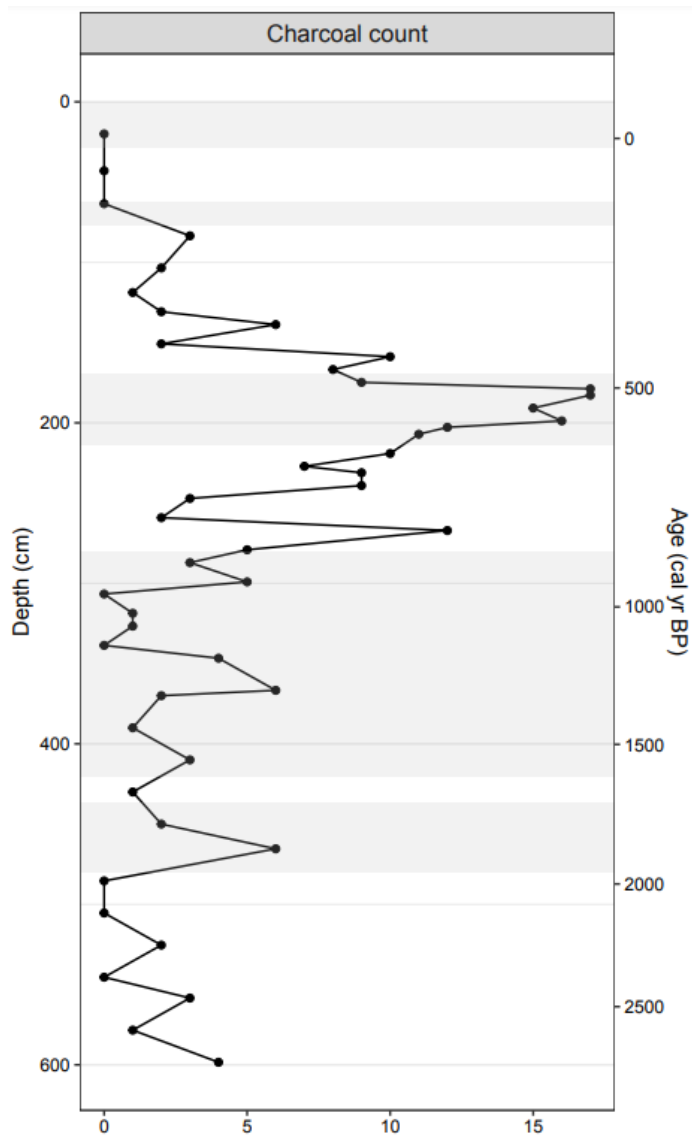


Figure 7.15: Charcoal count data from the Lake Tiriara sequence plotted against the age model presented in section 7.2.3. - data from Temple-Brown (2018).

The increase in the terrestrial signal that continues through this zone from the previous zone M-4 would typically be attributed to an increase in in-wash due to an increase in precipitation. However, even when conditions are drier, the tropical Pacific is still relatively wet in comparison to more temperate regions and this could instead be indicating an increase in the amount of available material, which has risen due to humans altering the landscape to make way for agriculture causing an increase in the amount of erosion taking place (Sear *et al.*, 2020; Maloney *et al.*, 2022). It is clear that in zone M-5, the human population has grown to such an extent that it is now having a major impact on the proxy signals in Lake Tiriara. The difference of this section of the core in comparison to other parts of the sequence is apparent in how it plots on the PCA, positively loaded in PCA 1 and 2 but completely separate from other zones.

**Zone M-6** (77-170 cm, 470-160 ± 95 cal yr BP) covers the LIA period. This zone shows a drop in all terrestrial indicators as well as calcium, which are slightly conflicting, as a drop in terrestrial indicators would signify a reduction of in-wash and thus a drop in rainfall whereas the drop in calcium would likely be due to dilution of ions due to higher water level. There is also an increase in Br and S along with the TOC and TN. The  $\delta^{15}\text{N}$  gradually drops over this zone before a notable dip, which coincides with those increases in TOC and TN. Perhaps signifying gradually wetter conditions that allow for algal productivity and eventually a burst of organic productivity. The  $\delta^{18}\text{O}$  values dip down in this zone before returning to mid-range value of -2.85 ‰ whilst the  $\delta^{13}\text{C}_{\text{inorg}}$  initially stays high in this zone before decreasing through the latter half. The diatom sample from this period shows that diatom concentrations had recovered following zone M-5 and there was a relatively high level of diversity in the assemblage with more than 10 different species though still an overall dominance by *Navicula* spp. (56%). There are a mix of signals here in terms of a drop in in-wash signal but overall, the proxies indicate a shift back to wetter conditions following the MCA-LIA transition. Other records from across the Pacific including Vanuatu, Samoa and Wallis, find that there are mixed signals during the LIA period between records indicating that conditions were variable across the region during this time but typically wetter following the MCA-LIA transition (Maloney *et al.*, 2022) as suggested by the Tiriara sequence.

**Zone M-7** (63 – 77 cm, 160-118 ± 60 cal yr BP), likely represents another event layer as it shares similarities with zone M-2 and sits in stark contrast to the overall pattern of change in the sequence. There is a big shift upward in magnetic susceptibility to rival the levels seen in zone M-2 and M-5 paired with notable drops in the LOI values. This zone also sees an increase in the terrestrial in-wash signal but has no peak in the Ca/inc or any of the other XRF proxies. Along with this, the inorganic geochemistry shows low  $\delta^{13}\text{C}_{\text{inorg}}$  values, with mid-low  $\delta^{18}\text{O}$  value with low  $\text{CO}_2$  yield whilst the organic geochemistry has relatively high values on  $\delta^{15}\text{N}$  though low on TOC, TN and  $\delta^{13}\text{C}_{\text{org}}$ . This zone is different to zone M-2 as the C/N remains relatively high so perhaps this section represents a wet event with the associated in-wash. This is supported by the fact that unlike zone M-2, this zone does have diatoms present in the sediments. A diatom sample from 63 cm (ca. 118 ± 59 cal yr BP) shows a higher proportion of *Rhoplodia Gibberula* (56%) but also includes *Achnanthes inflata* (8%) and *Pinnularia major* (23%) which are freshwater species so

perhaps signals a continuation of fresh to potentially brackish conditions. There is a gap in the data between zone M-7 and M-8 from 29 to 64 cm where sediment was lost during extraction.

**Zone M-8** (0-28 cm,  $16 \pm 54$  cal yr BP - present) has quite a different set of characteristics compared with the deeper parts of the sequence. Overall, there is a much lower rate of variation across all proxies in this zone. This highlights the importance of palaeoenvironmental studies to portray the true degree of variation occurring at sites such as Lake Tiriara. There is evidence for some remineralisation of organic carbon and an increase in CO<sub>2</sub> from catchment. This could be due to wash in from lake edges when they are exposed during dry period as the lake is shallow with low gradient sloping sides (Shanahan *et al.*, 2007; Maloney *et al.*, 2022). Both the inorganic and organic  $\delta^{13}\text{C}$  in the core top sediments show lower values in comparison to the rest of the Mangaia sequence. This could be due to the rapid infilling of the lake, causing it to shallow out which leads to oxidation of the lake bottom allowing  $^{12}\text{C}$  to escape, drawing down TDIC values (Leng and Marshall, 2004). The modern lake is less than two metres deep and many other lakes across the island have completely been filled in (Ellison, 1994). This interpretation is also supported by the findings of the Po-210 analysis, which indicates that there has been mixing of the core top sediments. The sampling area may have been subjected to processes that caused the bottom sediments to be disrupted and mixed altering the typical Po-210 curve (Zaborska *et al.*, 2007), this potentially could have been caused by bioturbation due to presence of freshwater eels in this shallow lake (Kirch *et al.*, 1995). This zone also sees the highest Br/inc levels in the sequence, likely due to shallowing of the lake and the development of peat at its edges (Chagué-Goff *et al.*, 2016).

## **7.9.2 Evidence for drought events within the Tiriara sequence**

### **7.9.2.1 Zone M-2 - $1678-1594 \pm 126$ cal yr BP**

There are several interpretations of the proxy signals presented in zone M-2 ( $1678-1594 \pm 126$  cal yr BP). The first possible explanation is that these shifts represent a drought event. One line of evidence towards this explanation is that whilst the overall profile presents that impression of an event layer as it sits in stark contrast to the preceding and subsequent proxy profiles, one aspect of the Ca/inc signal does suggest a build up to zone

M-2 instead of the rapid shift of an event layer. Rather than a rapid increase at the start of the zone, the Ca/inc signal does slowly increase in the section prior to M-2. A palaeo record from a coastal Caribbean lake picks out drought events and the elemental signature included peaks in Ca, Sr and a small peak in S along with a large dip in organic carbon, very similar to the signal seen in zone 2 in the Tiriara sequence (Burn and Palmer, 2014). Conroy et al (2008) found that there were higher rates of calcium carbonate precipitation at Genovesa Crater Lake in the Galapagos, when two consecutive rainy seasons failed. Other studies from within the Pacific and other regions also suggested that dry conditions could result in the precipitation of authigenic carbonate where lake levels drop, concentrating the levels of carbonates in the water column (Johnson *et al.*, 2016; Hassall, 2017; Thompson *et al.*, 2017). Furthermore, as discussed earlier, Conroy et al (2008) suggested that diatom frustules can be poorly preserved due to dry conditions and no diatom frustules were found in this section of the core. Similarly, samples taken from zone-M2 did not have any diatoms present whereas they are abundant in other parts of the sediments suggesting that the conditions during this time were not conducive toward the preservation of diatom frustules. The poor preservation of diatoms within lake sediment could be due to a range of factors, including temperature (Kamatani, 1982), turbidity (Reed, 1998), high pH (Dong *et al.*, 2008), high salinity (Reed, 1998; Ryves *et al.*, 2006), carbonate concentration (Ryves *et al.*, 2006) and exposure to the atmosphere when water bodies dry out (Conroy *et al.*, 2008). As discussed, a number of these factors can be directly linked to the effects of a dry period on a water body.

Earlier work conducted on Lake Tiriara by Ellison (1994) found that there was major forest clearance at approximately 1650 cal yr BP, which would correspond to this zone.

However, there are some inconsistencies in terms of the timing of certain changes between Ellison's record and the record presented in this thesis that draws the Ellison (1994) age model into question. The Tiriara sequence presented here has ten AMS <sup>14</sup>C dates covering the past 2,500 years whereas the Ellison sequence has seven <sup>14</sup>C dates covering more than 7000 years. In addition, <sup>14</sup>C samples from this study covered 1cm sections rather than the 10cm sections used in the Ellison paper, which would provide an average age over a larger section of sediment. The sequence presented here from Lake Tiriara has a more robust age model and so further work needs to be conducted to

constrain the timing of this forest clearance as it is likely that it was much later than Ellison (1994) suggests.

Further to this, the study by Toomey et al (2016) looked at the Ti/Ca ratio that they interpret as higher levels of precipitation in the Society Islands. For the time period that covers zone M-2 in the Tiriara sequence, the Ti/Ca ratio shows a large but rapid drop in values. This indicates a notable drop in the amount of terrestrial material being washed into the bay via erosion. This could in part be due to a reduction in precipitation so available material does not have a mechanism for being transported through to the bay from the island interior. This shows that other records in the same region may also indicate a temporary shift to drier conditions. However, the Ti/inc values in zone M-2 of the Tiriara sequence shows the opposite trend, with the largest peaks in terrestrial signals (Ti, Fe, Si) seen in this section of the core. This potential event layer occurs before the arrival of humans (Kirch, 2017b; Sear *et al.*, 2020) so the changes are not human-derived.

There are some similarities between the signals observed in this section of the Tiriara sequence and drought events identified in other studies from tropical islands. However, there are also several anomalies making it difficult to provide a conclusive interpretation. For example, within the event layer the  $\delta^{13}\text{C}_{\text{inorg}}$  show a mix of values, of which one is relatively enriched at 3.48‰, perhaps indicating a marine source whereas the other value is almost 9‰ lower at -6.83‰ suggesting a mix of sources in this zone. An alternative explanation for these changes could be a large tsunami; this will be examined in more detail in section 7.9.3.

#### **7.9.2.2 End of Zone M-3 - 1594-859 ± 126 cal yr BP**

Towards the end of Zone M-3 (1594-859 ± 126 cal yr BP) represents the second potential drought event in the Tiriara sequence that occurs just prior to the onset of the MCA at around 1000 AD (approx. 1067-881 ± 135 cal yr BP). Unlike the other two key zones picked out in this section, there are no major changes in C/N,  $\delta^{13}\text{C}$ ,  $\delta^{15}\text{N}$  or many of the XRF profiles. There is a depression in the Fe/inc and Ti/inc along with the magnetic susceptibility that suggests a decrease in in-wash around the time of human arrival indicating perhaps a drier period but there are no significant changes in any other proxy. Another record from Lake Tiriara, but taken from the peat at the edge of the lake, also found that around 1200 yr BP there was a shift toward drier conditions (Chagué-Goff *et*

*al.*, 2016). However, that study also inferred the start of wetter conditions from 1016 – 839 cal yr BP due to an increase in terrigenous in-wash XRF signal. Instead, this thesis suggests that this signal is in fact is the start of a major alteration of the landscape by humans leading to an increase in the amount of erodible material available, with the increase in human activity evidenced by an increase in charcoal from 300 cm (Temple-Brown, 2018) or  $929 \pm 113$  yr BP, that notably increases and peaks at approximately 500  $\pm 92$  yr BP. Overall, due to the low resolution of  $\delta^{18}\text{O}$  across this section, further work would need to be conducted to pick out the hydroclimate signal in the lead up to the MCA on Mangaia and refine the timings of these changes.

### 7.9.2.3 Zone M-5 - $647\text{-}470 \pm 102$ cal yr BP

Zone M-5 ( $647\text{-}470 \pm 102$  cal yr BP) represents the third potential drought event in the Tiriara sequence and it covers the MCA-LIA transition. It becomes more difficult to untangle the different signals in this part of the core, as there is the addition of another source of disturbance, humans. Nevertheless, this zone is the second of two sections within the Tiriara sequence that has carbonate present. As discussed in the previous section, the presence of carbonate in this part of the sequence and not elsewhere suggests a change in conditions that is favourable for carbonate precipitation such as shift toward drier conditions (Hassall, 2017; Thompson *et al.*, 2017).

The primary source of evidence for a dry period through zone M-5 is the oxygen isotope data. The most enriched values of the  $\delta^{18}\text{O}$  Tiriara record are in this section of the sequence. A majority of the data points sit above the modern lake water value of  $-3.3\text{‰}$  and well above the average  $\delta^{18}\text{O}$  value for the sequence of  $-3.98\text{‰}$  indicating that this section of the core represents some of the driest conditions of the sequence.

Interestingly, the  $\delta^2\text{H}_{\text{dinosterol}}$  record from Efate in Vanuatu also shows an extreme shift toward drier conditions during the MCA-LIA transition and similarly has peaks in the magnetic susceptibility record during the same period (Maloney *et al.*, 2022) just like the Tiriara sequence. In the Pacific islands, human activity has altered the Ti records in palaeo archives due to slash and burn techniques used to clear the land for agriculture. The clearing of the land destabilises the surface soils and generates an increase in available material for transport when it rains. A record from Lake Teroto in the Southern Cook Islands showed that following human arrival there was an upward shift in the average of

the Ti record, which is linked to soil erosion (Sear *et al.*, 2020). However, as the Maloney (2022) record is taken from Vanuatu, this would suggest that perhaps these changes are not necessarily human-related as Efate was colonised during the first wave of human migration into the Pacific almost 2000 years before Mangaia. The increase in magnetic susceptibility is unlikely to be a signal relating to landscape change due to the intensification of agriculture as this would have occurred much earlier in the sequence. However, the second larger peak in magnetic susceptibility in the MCA-LIA transition is attributed to the Kuwae tephra. Whereas, the signal in the Tiriara sequence is much more drawn out rather than a sharp peak and drop off and occurs in time with the peak in the charcoal record (Temple-Brown, 2018) indicating that the magnetic susceptibility and in turn, the terrestrial XRF signals relate to human activity in this sequence. Both records suggest a drying trend during the MCA-LIA transition and both show this increase in magnetic susceptibility and Ti record despite being at different stages in the colonisation process suggesting an alternative driver. Interestingly, in the Tiriara sequence produced by Ellison (1994), the charcoal record starts from around  $2480 \pm 60$  cal yr BP and peaks shortly after. However, in the Tiriara sequence charcoal data from Temple-Brown (2018) shows the charcoal starts to rise from background levels around  $929 \pm 113$  cal yr BP as discussed in the previous section and peaks around  $500 \pm 92$  cal yr BP, which fits with the archaeological sequence of intensification of agriculture around this time on Mangaia (Kirch, 2017b). If there are errors in the age model used by Ellison *et al* this would also push the date of major forest clearance - currently assigned to zone M-2- forward if the age model presented in this thesis is correct.

Maloney *et al* (2022) found that the Ti record for Lake Lanoto'o in Samoa showed a similar pattern of change to the magnetic susceptibility record and in turn both records matched the  $\delta^2\text{H}$  dinosterol changes through the sequence with the exception of the MCA. This is because the dry conditions that dominated during that time caused the water levels to drop resulting in an alteration to the physical characteristics of the lake morphology. Exposing the shallower margins of the lake provides an additional source of material during rainfall events. These changes resulted in a disconnection between the Ti and magnetic data erosion record and the dinosterol hydroclimate records. The drivers of Ti in-wash often change in arid environments where climate change can alter the typical watershed features (Davies *et al*, 2015). A study from Lake Bosumtwi in Ghana similarly

found that terrestrial input into the lake was controlled by how much of the catchment was erodible. The levels of terrestrial input were higher when the water level in the lake was lower, e.g. during drier periods, as more of the lake bed is exposed, increasing the erodible catchment area (Shanahan *et al.*, 2009). It is important to consider the local catchment processes when using Ti/inc as a proxy as the drivers of Ti input into a lake can change through time. As we have seen in the tropical Pacific, the Ti signal can be altered due to human activity, changes in the basin catchment during dry periods and due to increased precipitation through time. The use of a multi-proxy approach allows for more robust interpretation of the Ti/inc signal.

### 7.9.3 Evidence for a palaeotsunami within the Tiriara sequence

As outlined in section 7.9.1.1, there is a notable shift in a number of proxies from 437 cm ( $1677 \pm 127$  cal yr BP) including peaks in the magnetic susceptibility,  $\delta^{18}\text{O}$ ,  $\delta^{13}\text{C}_{\text{inorg}}$ ,  $\delta^{15}\text{N}$  and Ca/inc alongside drops in the LOI<sub>550</sub>, LOI<sub>950</sub>, C/N. There is a notable shift in the characteristics of the Tiriara lake sediments from before to after this short section, indicating that it represents some kind of major event in the sedimentary sequence. This event layer could potentially be an example of a palaeotsunami deposit. A palaeotsunami is simply a tsunami event that took place before the advent of historical record so there are not any written observations of the events and the only record of them is typically within sedimentary archives (Goff, Chagué-Goff, *et al.*, 2012). The identification of prehistoric tsunami deposits and their sedimentary indicators has come about through the study of both modern and historic tsunami events (Goff, Chagué-Goff, *et al.*, 2012). A substantial list of proxies that can be used to identify palaeotsunami deposits is available in Goff *et al.* (2012) but include a range of sedimentological, geochemical and palaeoecological indicators.

Magnetic susceptibility has been suggested as a possible proxy for palaeotsunamis, though there are no examples of this proxy being utilised in the study of palaeotsunami deposits yet (Goff, Chagué-Goff, *et al.*, 2012). However, research conducted in Portugal on the historic 1755 Lisbon tsunami found that the magnetic susceptibility dropped within the identified tsunami deposit (Font *et al.*, 2010). In the Tiriara sediments, there is a large spike in magnetic susceptibility during this event layer indicating an increase in the amount of ferro-magnetic sediments which are typically terrestrial and the volcanic

sediments on Mangaia are iron-rich indicating that the source of these sediments are terrestrial rather than marine. There are spikes in the XRF data for Fe/inc and Ti/inc – both terrestrial indicators. Tsunami signals usually do not come with increased input of terrestrial elements such as Fe or Ti (Chagué-Goff *et al.*, 2016). However, with the Tiriara sequence, we have to consider the impact of the barrier of the makatea. The makatea is made up of an ancient upraised coral that surrounds the older volcanic core standing up to 70 metres tall and forms a barrier of at least 600 metres wide between Lake Tiriara and the ocean (Wood, 1967). There are some small openings within the makatea and tunnels that transport water between the lake and the ocean (Ellison, 1993). This would block or filter any material coming from the ocean and when the wave returns it would drag terrestrial material back, which is then blocked by makatea on its return to the ocean and then could have theoretically been deposited in the lake. The possible presence of a tsunami event in the Tiriara record also indicates that the tsunami wave would have to have been relatively significant in size to either breach or push through the makatea boundary of Mangaia. Several studies have noted the deposition of terrestrial material within tsunami deposits due to the backwash of the wave (Kokociński *et al.*, 2009; Chagué-Goff *et al.*, 2011; Riou *et al.*, 2020). A study from Samoa studied off-shore deposits and found a terrestrial signal in the XRF geochemical data in the shallow marine sediments due to backwash from two tsunamis (Riou *et al.*, 2020). In Mangaia, the terrestrial sediments are prevented from moving into the shallow marine environment by the makatea escarpment, so those sediments are instead held within this lake sequence.

Other XRF geochemical data peaks of note are Ca/inc and Sr/inc. A peak in Ca can be indicative of either increased calcite precipitation (Chagué-Goff *et al.*, 2016) or increased marine influence (Cuven, Francus and Lamoureux, 2011) though typically in conjunction with a peak in Sr/inc will indicate carbonate precipitation (Chagué-Goff *et al.*, 2016). There is a small peak in Cl but a drop in Br, both elements have been used as indicators of marine input (Chagué-Goff *et al.*, 2016). However, Br can also be indicative of organic content (Davies, Lamb and Roberts, 2015) which would decrease with the input of tsunami material and this is evident in the Tiriara sediments from other proxies with the drop of TOC and LOI<sub>550</sub> values. The Ca/inc ratio and the CO<sub>2</sub> yield from the samples taken from this event layer indicate that carbonate is present and at the highest rate within the entire sequence. This section represents one of only two places in the sequence where

carbonate appeared in high enough concentrations to collect  $\delta^{18}\text{O}$  and  $\delta^{13}\text{C}_{\text{inorg}}$ . This indicates that these two sections represent conditions different to the norm – for this section the theory is that this is potentially due to tsunami inundation. Precipitation of carbonate within the water column assumes the presence of enough standing water. Data from the sections prior to zone M-2 indicate that the site was likely a wetland rather than a lake so there would be little water on the site for carbonate to precipitate from thus indicating a different mechanism for the presence of carbonate in the system. Conroy et al (2008) found that during periods of higher salinity at Genovesa Crater Lake, there were higher rates of calcium carbonate precipitation. The  $\delta^{13}\text{C}_{\text{inorg}}$  data from zone 2 are quite different, one at  $-6.83\text{‰}$  indicating freshwater source and the other at  $3.48\text{‰}$  indicating marine carbon sources (Clayton and Degens, 1959), which could be due to the mixing of marine and terrestrial sediments in this section.

Diatoms, as discussed in Chapter 5, are useful as indicators of environmental change as different species have different environmental tolerances. The application of diatoms in the study of palaeotsunamis is particularly useful in freshwater environments where inputs of marine diatoms due to saltwater inundation are easily recognisable as different to the normal species distribution. For the zone 2 event layer in the Tiriara lake sediments, there are no diatoms present. This is possibly due to dilution in deposited material or destroyed at some point either by power of tsunami breaking up frustules, changes in water chemistry being poor for diatom preservation or exposure to the elements. This is not uncommon, typically there are three common findings in relation to the diatom record in palaeotsunami layers; 1) good preservation of marine and brackish diatoms, 2) poor preservation of full diatom frustules along with a high proportion of broken frustules or 3) poor preservation of any diatoms (Goff, Chagué-Goff, *et al.*, 2012). As discussed earlier, factors such as temperature (Kamatani, 1982), turbidity (Reed, 1998), high salinity (Reed, 1998; Ryves *et al.*, 2006) and exposure to the atmosphere (Conroy *et al.*, 2008) can lead to the poor preservation of diatoms within a sediment archive. In a study looking at predecessors to the 2004 Boxing Day Tsunami found that the 2004 event layer did have both brackish and marine diatoms present whilst deposits relating to earlier tsunamis in the region - similar to the Lake Tiriara sediments - did not have any diatoms preserved within the sediments (Jankaew *et al.*, 2008).

A study conducted on Mangaia attempted to pick out past cyclone and tsunami events from a peat sequence taken from the edge of Lake Tiriara, close to the opening into the makatea (Chagué-Goff *et al.*, 2016). The results suggest three possible tsunami events based on a mix of sedimentological, geochemical and diatom data. The first potential tsunami event is dated to around 2250-1900 cal yr BP and it is suggested that it was likely generated along Tonga-Kermadec Trench. The second is dated to 667-576 cal yr BP and similarly is tied to a fault rupture of Tonga-Kermadec trench and the final possible event is dated to 348-303 cal yr BP but is thought to be due to a local submarine slope failure. Based on the age model for the Tiriara lake sediments, the most likely candidate is the tsunami dated to 2250-1900 cal yr BP. However, with only three dates for the Tiriara peat sequence and no age model presented, there is a level of uncertainty surrounding the dates from this sequence. From the Wallis and Futuna record, the chronology for the trench sections that are used to identify the two tsunami events (Goff, Lamarche, *et al.*, 2011) are also not tightly constrained. The new ages introduced in section 7.2.3 for the lake sediments provide a more robust chronology for Tiriara and suggest an earlier date of  $1572-1678 \pm 129$  cal yr BP for a possible tsunami event. Evidence for this tsunami has been identified in sediments from Wallis and Futuna (Goff, Lamarche, *et al.*, 2011) with a lower estimated age of 1860-2000 yr BP and citing a possible Tonga-Kermadec Trench origin. It has also potentially been identified in sediments from Hawkes Bay (Goff, 2008) and the Bay of Plenty in New Zealand (Bell *et al.*, 2004), though the authors of both reports state that they think the tsunami was likely a local-impact event for these records. The provenance of the tsunami in the Tiriara sequence is likely to be from the Tonga-Kermadec Trench, which is the primary source of earthquakes that generate tsunamis that can reach the Cook Islands (Thomas and Burbidge, 2009).

Interestingly, in a study by Toomey *et al.* (2016), their Ti/Ca XRF record has a large downward shift at approximately 1666 yr BP that coincides with zone M-2. The drop in their record indicates a large increase of marine derived material over terrestrial and it was rapidly deposited in their near-shore record. Similar to Lake Tiriara, Apu Bay is located on the southern side of Tahaa in the Society Islands. The sediments were taken just offshore but within the bay area. This spike is the largest downward shift in the record and appears to be short-lived. Toomey *et al.* (2016) assume that any changes in

their record are storm related rather than tsunami generated due to Apu Bay being on the southern side of the island, offering some level of shelter from tsunami events.

Furthermore, tephra shards were found in three locations within the sedimentary sequence from Lake Tiriara. Shard concentrations in these sections were particularly low with only the layer located at 380-385 cm depth providing a substantial enough quantity of shards to be considered a credible tephra layer with 23 shards of tephra per gram of sediment (A. Bourne, Pers Comm, February 2023). In zone M-2, the spike in magnetic susceptibility, Ti, Si, Ca and Fe alongside drop in organic content observed in this section could be indicative of the presence of a tephra layer. However, this zone has been analysed to identify any potential tephra layers and no shards were found (A. Bourne, Pers Comm, February 2023). The low concentration of shards accounts for the lack of response in any of the proxies from the sediment sequence. Importantly, no tephra shards were found in zone M-2, ruling out an alternative tephra layer theory for these proxy changes and backing the interpretation of a tsunami event in this part of the sequence.

#### 7.9.4 Use of Ti/inc as a precipitation proxy

Other studies have identified Titanium  $\mu$ XRF data as a possible precipitation proxy in lake systems and have used it alongside proxies such as hydrogen isotopes to identify changes in hydroclimate in the Pacific region (Hassall, 2017; Sear *et al.*, 2020). The Lake Tiriara carbonate  $\delta^{18}\text{O}$  results presented in this thesis appear to mimic the Ti/inc changes despite suggestions that there may be a delay in the preservation of the  $\delta^{18}\text{O}$  signal due to the time it takes to alter and then preserve the isotopic signature of the lake water, whereas the terrigenous in-wash signal is entered into the sedimentary sequence immediately (Hernández *et al.*, 2010). However, a comparison between Mangaia's Lake Tiriara and Atiu's Lake Teroto Ti/inc records (from Sear *et al.* (2020)) show a mix of correspondence and deviation through time (Figure 7.16). Lake Teroto represents the closest palaeo sequence geographically to Mangaia and also sits within the Southern Cook Islands. There is a similar pattern of change in the Ti/inc records for both Teroto and Tiriara from around 1000-1100 yr BP till 438 yr BP. However, outside of this section there is not a clear relationship between the two titanium records from these sites.

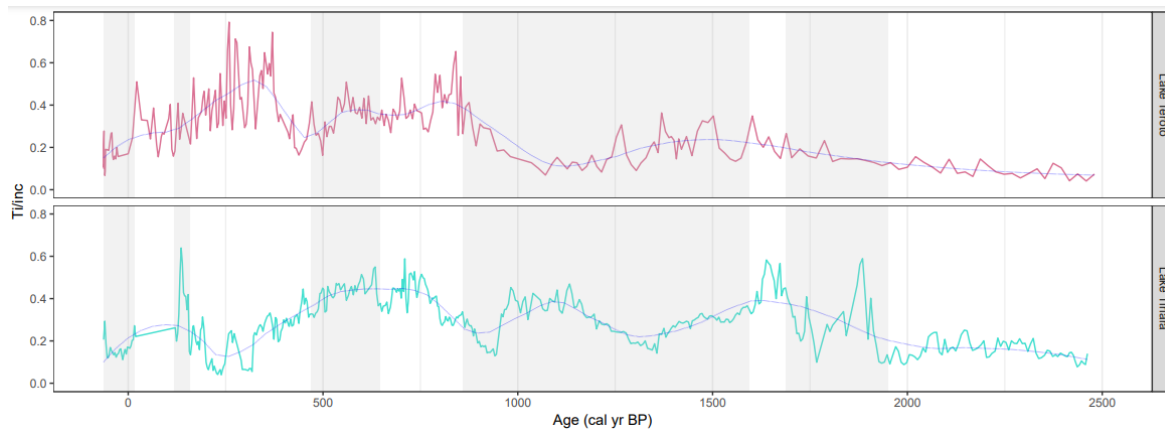


Figure 7.16: Plot showing the Ti/inc XRF data from Lake Teroto (Sear et al, 2020) (top) and Lake Tiriara (this thesis) over the past 2,500 years. Blue line is loess smoothed.

Hassall (2017) showed a relationship between Atiu and Rarotongan rainfall and Figure 7.17 shows that there is also a relationship between Mangaian and Rarotongan rainfall with an  $R^2$  of 0.51 and a correlation coefficient of 0.71 ( $p < 0.01$ ). There is not sufficient data overlap in the Atiu and Mangaia rainfall records to be able to definitively (dis)prove a relationship between the rainfall patterns on the two islands. However, there is clearly a connection between the rainfall patterns of the islands in the Southern Cooks. The islands of Mangaia and Atiu are relatively close to each other by Pacific standards, only 215 km between them, so they should present a similar rainfall pattern over time. An assumed similarity in rainfall patterns should then assume a similar Ti/inc record if Ti/inc is a proxy indicative of rainfall. This is puzzling as typically increases in Ti/inc have been associated

with increases in precipitation when it is seen that more soil is washed into the lake (Chagué-Goff *et al.*, 2016; Evans *et al.*, 2019; Sear *et al.*, 2020).

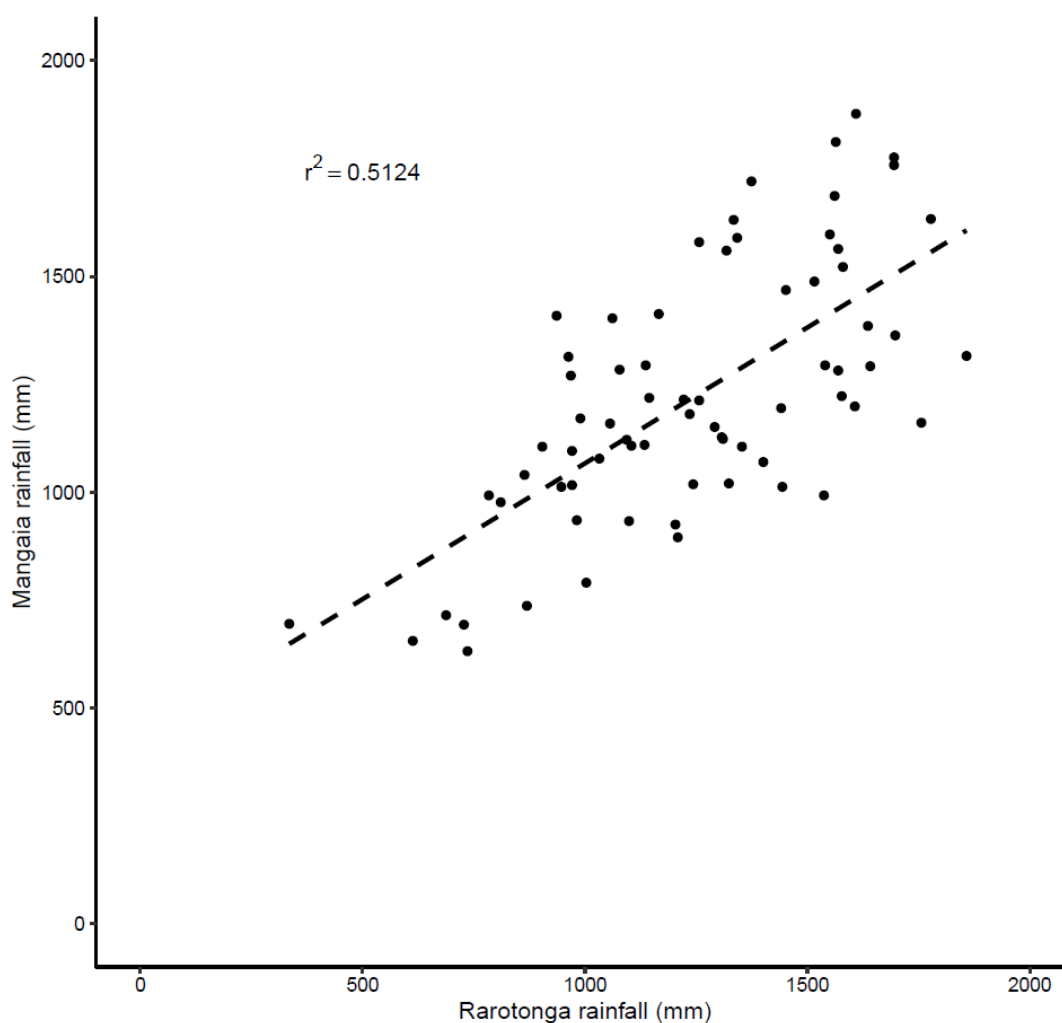


Figure 7.17: Plot of wet season (Nov-Apr) rainfall data from Rarotonga and Mangaia with linear regression value – data from KNMI climate explorer (2023).

Drivers and mechanisms of Ti may vary change through time and for lake systems that are very similar, their physical characteristics may offer some additional insight into the differences observed in the palaeoenvironmental records. Teroto has a smaller surface area of 0.03 km<sup>2</sup>, a sharp bed gradient and is also notably deeper overall at 8.4 m (Parkes, 1994; Hassall, 2017). Whereas, Lake Tiriara has a larger surface area of 0.2km<sup>2</sup> but is shallow (1.2 m), sits at an elevation of 5 masl (Schabetsberger *et al.*, 2009) and has a low gradient bed. These characteristics make this a system that is feasibly more reactive to dry periods and thus the biota of this lake are more heavily impacted during dry conditions. This idea is supported by evidence from modern changes in the area of the study lake (Figure 7.18) which shows that the surface area of Lake Tiriara fluctuates over

the 14 year period, with Tiriara experiencing 13,195 m<sup>2</sup> change in surface area.

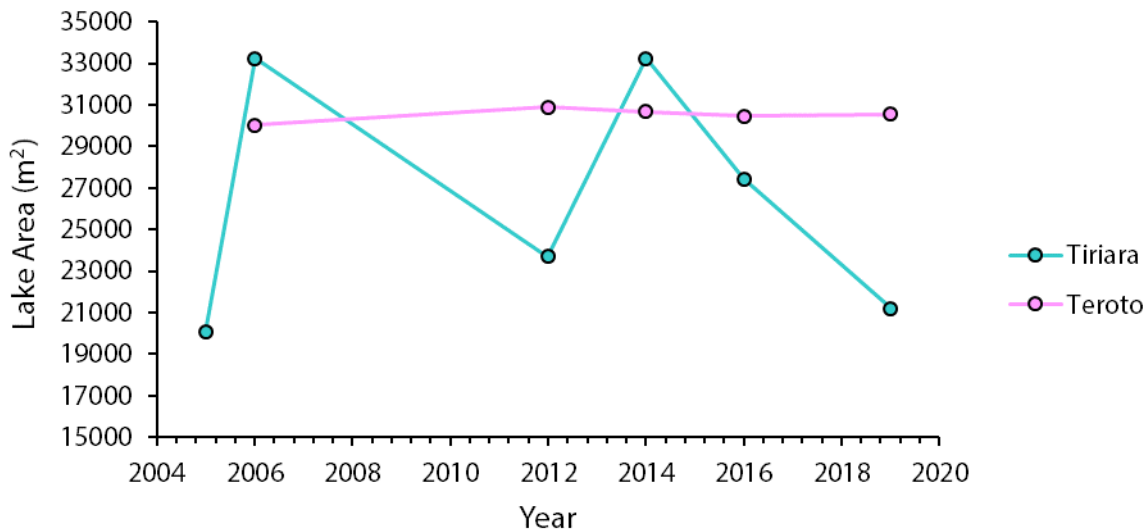


Figure 7.18: Changes in the lake area between 2005 and 2019 for both Lake Tiriara and Lake Teroto calculated using satellite images in google earth.

There are several interpretations of these results. Firstly, Ti/inc in this system may not be indicative of wet conditions but dry conditions. As the lake dries out more material becomes available for erosion and transport at the lake margins and is readily washed into the lake when it rains (Shanahan *et al.*, 2009; Hassall, 2017; Maloney *et al.*, 2022). This is contrary to the findings reported by Sear *et al* (2020) that saw that Ti/inc and hydrogen isotope records used to reconstruct precipitation were shifting in concert. This highlights the importance of evaluating the Ti/inc within the local context as drivers of this signal change site-to-site. However, it is apparent in Figure 7.18 that the Ti/inc records from Tiriara are not responding the same way through time as the study conducted by Sear *et al* (2020), particularly around 1000 cal yr BP where it is suggested there was a significant dry period in the Southern Cook Islands indicating that in the Tiriara record Ti/inc may not be tied to the hydroclimate record in the same way as other records in the Southern Cook Islands. The mismatch could be due to errors in the age models, to line up the changes at 1000 yr BP, both records would have to match at their maximum error, but it is still within the associated age model errors for both records. Additional work would need to be conducted to assess and potentially combine the age models of the two records to establish whether the timing of these changes is asynchronous for these islands or not. Secondly, in wetter conditions, the area of Lake Tiriara likely increases substantially, generating a larger evaporative surface area resulting

in higher  $\delta^{18}\text{O}$  evaporative signal – this idea is supported by modern lake surface area changes (Figure 7.18) but not by the modern isotopic data presented in section 7.7.1, which indicates that Tiriara is not an evaporative system but rather reflects the isotopic composition of local rainfall. Alternatively, it could be that the  $\delta^{18}\text{O}$  is not an indicator of isotopic fractionation in this system but instead is indicative of a rainfall amount effect, which negates fractionation signal. The concept behind this is that the precipitation rate in the Pacific region is high so when there is a wetter period the sheer volume of rainfall being inputted into the system means that both  $^{18}\text{O}$  and  $^{16}\text{O}$  levels increase and exceed the  $^{18}\text{O}$  enriched levels during drier periods. This amount effect is observed in stalagmite records in the Pacific (Maupin *et al.*, 2014) but this is because these records are preserving an archive of the precipitation amount changes and there are not the same fractionation pathways as there are in lakes. Further to this, Hassall (2017) showed that modern precipitation in Rarotonga becomes more  $^{18}\text{O}$  depleted the higher the rate of precipitation. There is limited evidence for changes in air mass source and Hassall (2017) highlights that such changes may be evident during El Niño and La Niña episodes when water sources change. Though several records from the tropical South Pacific found that based on the reconstructed  $\delta^{18}\text{O}$  rainfall values through the Holocene, there has been no significant change in the source of water vapour in this region (Stott *et al* 2004; Maupin *et al* 2014). Furthermore, as discussed earlier, in the diatom record for Lake Tiriara samples that corresponded with the higher  $\delta^{18}\text{O}$  measurements also presented with low counts and poor preservation of frustules. A study done by Conroy *et al* (2008) on El Junco lake in the Galapagos found that diatoms were only well preserved in their record during a period when the lake became more stable and theorised that dry periods could have led to the poor preservation of frustules when the lake dried up. Considering this evidence and the three conceptual models from the isotopic results, it would seem as though in Lake Tiriara at least perhaps Ti/inc is not a proxy for precipitation, though further work would need to be conducted in order to verify this.

## 7.10 Summary

In summary, the key findings from the Mangaia sequence are two shifts towards dry conditions around  $1067-881 \pm 135$  cal yr BP, which coincides with the arrival of humans to Mangaia (Kirch, 2017b) and  $647-470 \pm 102$  cal yr BP, which coincides with

the postulated 1300 AD event hypothesised by Nunn and colleagues (Nunn, 2000b, 2000a; Nunn and Britton, 2001; Goff and Nunn, 2016). These dry periods are evidenced by the  $\delta^{18}\text{O}$  and Ca/inc records. Within the Tiriara sequence, there is also a relatively short-lived event showing a major change in a range of proxy signals, which has been interpreted as a palaeotsunami layer in zone M-2. This event layer is dated to  $1572-1678 \pm 129$  cal yr BP, which considering the age model error could correspond to palaeo-tsunami deposits found on Mangaia (Chagué-Goff *et al.*, 2016) and in Wallis and Futuna (Goff, Chagué-Goff, *et al.*, 2011) that cite the potential source as the Tonga-Kermadec Trench. Finally, the XRF proxy Ti/inc should be utilised carefully as the relationship between rainfall and terrestrial input as measured by Ti/inc can change through time. Local changes within the basin can dominate over wider regional climate signals. This could be due to changes in sediment availability because of human activity or natural land cover change or, during dry conditions, the exposure of additional sediment as water levels drop.

## Chapter 8 Modelling Prehistoric Polynesian Island Life

### 8.1 Introduction

The reconstruction of ancient environments and the associated climates have provided us with insights into the changing environmental context that past societies have had to navigate (e.g. Kirch *et al.*, 2012; Brandt and Merico, 2015; Kuil *et al.*, 2016; Sear *et al.*, 2020). However, whilst palaeoenvironmental and palaeoclimate studies may discuss the potential impacts of environmental or climatic change on the systems and societies in their region of study they do not consider those connections in any tangible way (Kirch, 1984, 1994; Nunn, 2000a; Duprey *et al.*, 2014; Cochrane, 2018). As discussed in section 2.6, socio-ecological models can be a useful tool in making these connections, by reconstructing the dynamics of past societies and testing hypotheses around changes to these systems, including the influence of climate change (Barton *et al.*, 2012). To date, there are no socio-ecological studies utilising models that deal with climate as a potential driver of change to prehistoric island life in the tropical South Pacific. There are existing studies that look at other drivers (e.g. conflict, societal change, ecological degradation), which do have relevance here - just not about climate change (e.g. Brander and Taylor, 1998; Field, 2004; Brandt and Merico, 2015). The aim of this chapter is to understand how climate impacted population dynamics and food security in prehistoric Polynesia. To that end, a conceptual model will be presented that represents the current understanding of the relationships between climate, food security and South Pacific island population. These relationships will then be represented mathematically in a system dynamics model, which is applied to the island of Mangaia as a case study of the impact of climate change on prehistoric Polynesian island life. The overall aim is to test the hypothesis that drought could have been a driver of prehistoric human migration - or at least had a significant impact on population numbers that may have instigated migration - within the tropical South Pacific (Sear *et al.*, 2020). This chapter begins by introducing the conceptualisation of the socio-ecological system of prehistoric Polynesia using the island of Mangaia case study. The subsequent subsections in this first section will discuss various aspects of the Mangaian socio-ecological system based on the current understanding of this island's

prehistory with a view to incorporation into the model. This is followed by a description of the development of the systems dynamics model, the software implementation and a detailed explanation of the model components, feedbacks, parameters and set up. Next, the results from the model and several scenarios will be presented with a brief interpretation. The scenarios offer a range of precipitation and drought characteristics that are used to test the response of the Mangaian island system and also includes a palaeo precipitation scenario. This chapter will end with a discussion of the limitations of the model and suggestions for further development.

## **8.2 Socio-ecological system of the Prehistoric Polynesians**

The islands of the Pacific often vary from one another physically, ecologically and socially and so the socio-ecological system is relatively unique island to island. The model presented in this chapter was developed around the composite island of Mangaia for four reasons; 1) It is one of the study sites in this research, 2) The archaeology of Mangaia is relatively well understood and provides good dating for human arrival and subsequent societal changes (Kirch, 2017b), 3) Mangaia was one of the most densely populated islands in Polynesia (Kirch, 2017b) – and therefore offers insight into an island system at its limit, and 4) Southern Cook Islands are considered the gateway islands from which the rest of Eastern Polynesia was colonised and therefore it offers insight into the Pacific human migration story, particularly the start of the second wave into Eastern Polynesia. A general model for all Pacific islands would likely be limited in how it could represent reality, as it would not capture the key characteristics of the socio-ecological system of the particular islands. For example, a more general model would understate the diversity of islands across the Pacific in terms of climate, geology and hydrology (as per Nunn *et al.*, 2016) so it would be difficult to understand the implications of changing hydroclimate on these island systems. Key sources from the first Europeans to visit and document the island offer information on the socio-hydrological system of prehistoric Mangaia. Some insight comes from the first European contact made by Captain Cook in 1777, although he never made landfall so only provides a passing first impression with comments on the geomorphology of the island, the resources offered by the island and observations of the population. The first written account of a visit to the island comes from John Williams (1837), an English missionary who visited Mangaia on four occasions.

The first was in 1823 when a small group of missionaries and their wives landed on the island but were attacked by the Māngaians and so they retreated back to the ship. Later in 1824, William's ship passed by Mangaia again and they left two missionaries behind on the island to convert the Māngaians to Christianity. Williams returned to Mangaia a third and fourth time in 1830 and 1831 respectively during which he spent time amongst the people and travelled across the island offering observations of his interactions and findings. One of the primary ethnohistoric texts of Māngaian prehistory comes from William Wyatt Gill, another English missionary who lived on the island for twenty years from 1852. He published a number of books over the years including the story of Mangaia and its mythology (Gill, 1894). He achieved this through collaboration with Mamae, a Māngaian pastor and member of the Ngati Vara clan who was Gill's friend and colleague. Finally, Peter Buck also known as Te Rangi Hīroa, a half English, half Māori doctor and anthropologist resided on Mangaia between December 1929 and April 1930. During his time on the island, he conducted the first modern ethnographic study of Mangaia including both contemporary measurements of the population and documenting the island's history and culture (Hiroa, 1934). These reports and observations from the first missionaries and visitors offer the closest representation of the prehistoric Pacific society available as no other written records are available – only archaeology and palaeoenvironmental studies can provide any further insight. The rest of this section will explore the different aspects of the prehistoric Māngaian socio-ecological system as understood from contemporary observation as well as ethnohistorical, archaeological and palaeoenvironmental sources.

### **8.2.1 Hydrology**

As discussed in Chapter 4, Mangaia receives approximately 1900-2050 mm of rainfall annually and like most tropical South Pacific islands has two seasons; a dry season running from June through to November and a wet that runs from December through to May, with a majority of rainfall falling within the wet season – see section 4.3.2. There are a number of rain-fed streams present on Mangaia that run from the higher inner volcanic cone out into the lowland swamp valleys – see Figure 4.6. In the past, water gathered against the makatea escarpment forming lakes from which the water then drains through the makatea tunnels and into the ocean. There is only one permanent freshwater lake on Mangaia in the present day, Lake Tiriara, but during the mid-Holocene

there were five lakes where the rainwater streams met the makatea rim of the island, though current data suggest the other four filled in prior to human arrival (Ellison, 1994). Due to the volcanic geology of Mangaia's interior it is possible that there are perched pockets of water that permeate through the rock (United Nations, 1983) and in the present day, islanders utilise boreholes as a water supply (National Environment Service Government of Cook Islands, 2021), which indicates that there is groundwater present on the island. However, there is no evidence that suggests that groundwater was utilised as a major source of water during Mangaia's prehistory. Therefore, surface water from streams and lakes was likely the only source of freshwater in prehistory.

### **8.2.2 Demography**

Mangaia is split into six political districts – Kei'a, Tava'enga, Karanga, Ivirua, Tamarua and Veitatei – which also mirror geographic borders with the boundaries between each district reaching radially from the highlands to the ocean, offering each district a section of highlands, lowland swamp and makatea – see Figure 4.7 and Figure 4.8. The population primarily resided close to the streams and productive "puna" lands in each of the districts during times of peace, whereas during periods of war people moved either toward highland hiding places or toward the makatea caves to avoid conflict (Hiroa, 1934). Warfare is not considered in the model as these would be short temporary changes and the aim to keep the model in its simplest form and focused on the environmental drivers in this instance. Though there are now three villages on the island of Mangaia, there were never any villages or settlements within any of the districts prior to European contact (Hiroa, 1934). Cook's observations in 1777 described the islanders as "numerous and well fed" (Cook, 1821). Following the arrival of Europeans onto the island in 1833, the missionary John Williams estimated that there were around 2000-3000 people living on the island but this number was given some time after European arrival so it is assumed that the population was likely much larger previously, but decreased due to introduced diseases (Williams, 1837). A later population study conducted in 1929-1930 by Te Rangi Hiroa (1934) found the population had then dropped by around half again to 1,241 within 100 years. It has been suggested that Mangaia held the highest population density in Polynesia with up to 150 people per km<sup>2</sup> of arable land even when using the first missionary evaluation of population size (Kirch, 2017b). To date, there has been no estimation of the maximum population that existed on Mangaia during its prehistory.

### 8.2.3 Land and water management

Reilly (2009) provides a range of interpretations for the different land divisions of Mangaia from a mix of anthropological (Mark, 1976), geographical (Allen, 1969) and Hiroa's (1934) account and from an interview with a contemporary Mangaian. These interpretations break Mangaia up into five to six different ecological zones, which are synthesised below - starting from the coast and travelling landward to the highlands - and illustrated in the cross-section shown in Figure 4.8. The zones are representative of all of the six districts of Mangaia:

The first zone - "Tai" - is made up of the coastal strip outside of the Makatea escarpment and includes the beach "Pae Tai" along with the lagoon "Pi'aki" and the reef "roroka", which are utilised for fishing.

The second zone - "Rau-tuitui" - is devoted to the Makatea escarpment and named for the candlenut tree, which is known locally as Tuitui. This zone is primarily made up of two sections. The first consists of small patches of soil on the makatea known as "kavava" that, despite poor soils, can be used to grow sweet potato, trees and other dryland crops (Hiroa, 1934; Mark, 1976; Kirch, 2017b). Within this zone, a second section comprises the "rāei", which are areas of relative desert-like conditions where nothing grows (Allen, 1969; Mark, 1976). The combination of the first coastal zone and the makatea makes up 56% of the total land area of Mangaia.

The third zone - "Puna" lands - comprises the lowlands that lie between the outer makatea escarpment and the inner volcanic valleys and highlands and are the primary taro growing areas on the island. The streams on Mangaia flow from the central volcanic core radially out into the lowlands, offering large swaths of land suitable for agriculture. These puna lands were the prime location for the building of irrigation terraces and pondfields for taro cultivation (Kirch, 1994, 2017b). Men built and maintained the taro pondfield systems whilst women were responsible for growing and harvesting crops (Hiroa, 1934). The fertility of the soils is maintained by allowing alluvial soils to flood onto the pondfields, which are so fertile that no additional fertilisers are required (Allen, 1971; Kirch, 2017b). This zone is the "single most productive and valued" of all the regions of Mangaia (Kirch, 2017b, p. 23). Despite its value, this zone makes up only 2% of the total land area of Mangaia.

The fourth zone – “Rau-tuanu’e” – named for the anu’e fern that is abundant on the highland volcanic core, includes the highly eroded volcanic slopes and the Rangimoti’a, the “Crown of Mangaia” – central high volcanic plateau (Hiroa, 1934, p. 4). This zone also includes forests within the narrow valleys that produce fruit, which are utilised during difficult times. The highland areas above the valley and central plateau were of little agricultural use and little grows there beyond the anu’e fern (Kirch, 2017b). The combination of the highlands and the valleys is approximately 42% of the total land area of Mangaia.

The primary zone of interest for this chapter is the fertile Puna lands where a majority of the taro cultivation on the island takes place. It is widely agreed that taro (also known locally on Mangaia as mamai) was an important staple food of Mangaia during its prehistory (Hiroa, 1934; Allen, 1969; Kirch, 1994, 2017b). The importance of the crop is illustrated in the mythology of Mangaia that intimately ties together plant and human growth within its stories (Hiroa, 1934) and as Mangaian society developed, the status of the taro producing lands grew too (Kirch, 1994). It is also illustrated in the use of the word “Puna” for both the districts and the irrigated taro lands (Allen, 1969; Reilly, 2009). Many Marae – a traditional temple or place of worship - and other archaeological sites have been found around the irrigated taro lands of Mangaia (Kirch, 2017b). The development of taro pondfields was not unique to Mangaia; many other islands across the Pacific had developed taro pondfields including islands in the Solomon Islands (Kirch, 1994; Bayliss-Smith and Hviding, 2015), French Polynesia (Kennett *et al.*, 2006) and Hawai’i (Kirch, 1994, 2007; Leppard, 2019), to name a few. Nevertheless, taro was a vital crop for the Mangaians and played a role in the development of the complex society on the island (Hiroa, 1934; Kirch, 2017b). Ethnohistoric accounts of conflict between groups on the island primarily occur over the fertile puna lands with victors awarded these revered fertile areas from the fallen and the vanquished are then assigned the agriculturally-poor makatea land (Hiroa, 1934).

Taro requires wet and humid conditions and it is not drought resistant (Food and Agriculture Organization, 2010). In a visit by missionary John Williams in 1833, he observed the terrace infrastructure for the taro pondfields, finding it present in most of the valleys around the island with approximately thirty to fifty acres of plantation per valley. He found that the islanders had created an effective irrigation infrastructure that

utilised wooden pipes made from hollow trees to transport water from the streams to the pondfield (Williams, 1837). The islanders also dug irrigation channels known as “aravai” to connect the streams and the pondfields though the exact timing of the development of these irrigation strategies are currently unknown (Kirch, 2017b). There is commonality between prehistoric Polynesia and the Maya civilisation. Both developed agricultural systems, which were vulnerable to rainfall changes and perhaps were reaching the limit of population carrying capacity (Dunning *et al.*, 2002; Chase and Scarborough, 2014; Kuil *et al.*, 2016). Where the two diverge somewhat is over water management. The Maya developed a system of reservoirs (Lucero, Gunn and Scarborough, 2011; Kuil *et al.*, 2016) whilst the Polynesians did not. Instead, they developed irrigation systems for the taro wetfields resulting in a level of water management within both systems. However, even with the development of irrigation infrastructure, the vital puna lands are still vulnerable to drought. In 1926, Hiroa observed that a drought event could possibly impact on the puna lands causing the irrigation pondfields to dry up (Hiroa, 1934, p. 125). This is confirmed by contemporary accounts from Mangaia that also describe how the taro pondfields can dry up during drought periods when there is not enough water in the streams to irrigate the land leading to crop losses (Kirch, 2017b). The value of water is cemented in Polynesian culture as evidenced in language. The Hawaiian word for wealth is “waiwai” which is the word for water – “wai” – repeated twice and is synonymous to the Mangaian word for water “vai”. However, there is little evidence for water management from Mangaia’s ethnohistory, beyond the development of irrigation channels, that they could utilise during times of drought.

There was a level of understanding within Mangaian society of land management and there is evidence of this from ethnographic studies. When certain resources - including agricultural and marine stocks - came under pressure or became depleted a meeting of the district and sub-district chiefs was called and a closed season or ra’ui was declared by the “Ruler of Food” that affects the whole island until the season is reopened once the relevant stocks have replenished (Hiroa, 1934, p. 141). The existence of a Ruler of Food known fully as “te ariki i te ua i te tapora kai (the high chief presiding at the head of the food baskets)” (Hiroa, 1934, p. 117) and the use of ra’ui shows that land management was integrated into the fabric of Mangaian society. However, despite this, there is evidence of environmental degradation on the island as the population grew and

developed (Ellison, 1994; Kirch, 2017b). This was primarily caused by the deforestation of the island's interior – typical of many South Pacific islands histories - but specifically the volcanic highlands and associated slopes leading to soil erosion. Agriculture on Mangaia started with shifting-cultivation that primarily would have utilised these inner highland areas, cutting down the native vegetation, burning the land and introducing the cultigens brought with the first settlers (Kirch, 2017b). In Mangaia, high population density during the pre-contact period placed strong pressure on people to extract maximum yields (Kirch, 1994). An increasing rate of shifting-cultivation and the associated method of slash and burn would have exposed large areas of land to the elements leading to the soils being gradually eroded away until the land was no longer suitable for cultivation (Kirch, 2017b). This deposition of alluvial material made the lowland valleys and swamps suitable for taro pondfields and enabled the intensification of agriculture required to sustain the growing population (Allen, 1969; Kirch, 2017b). The erosion caused by human activity is evidenced by the rise of Ti/inc and Fe/inc XRF ratios presented in Chapter 5, which are used as indicators of erosion or in-wash into the lake. The rapid infilling of lakes around the island is believed to have occurred prior to human arrival based on current ages (Ellison, 1994) though the dating on those changes is contentious. However, in the ethnohistory of Mangaia, Lake Tiriara alone is mentioned (Reilly, 2009) perhaps indicating it was the only remaining lake at the moment of human occupation. Currently, Lake Tiriara is the only remaining lake left and it too is succumbing to rapid infilling and is likely only still present due to its low elevation (Ellison, 1994).

### 8.3 Conceptual Model

Figure 8.1 illustrates the socio-ecological conceptual model for prehistoric Pacific islands. This model is split into three main groups and a unit area for the model is one individual island. On the left are the external environmental components, which include key environmental drivers that are external to an island i.e., are regional rather than a local control that can influence water and food resources on an island. Sea level change has been included within this group as it is an external environmental component that impacts water resources in Pacific islands through salinization of groundwater lenses (Dixon-Jain *et al.*, 2014). Similarly, short-lived extreme events are included in this group as the Pacific is a tectonically active region and experiences tsunamis as well as cyclones,

which can impact food and water resources on an island through either overtopping events that pollute freshwater sources with salt water or destruction of valuable crops. This in turn would lead to a drop in population due to the decline in food and water availability. Finally, the last component of this group is climate. Whilst this encompasses all aspects of climate, the key element for this model component are changes in precipitation that led to drought conditions. The Pacific region is characterised by its highly variable rainfall and both water and food resources (including taro) are very highly reliant on rainfall (Palanisamy *et al.*, 2018).

The central part of the model is the socio-environmental interface where the external environmental and internal social elements converge. This group includes physical environmental components that are internal and local and are impacted upon or driven by the external environmental and internal social components (e.g. Kuil *et al.*, 2016). Here environmental degradation is classed as a decline in the relative environmental condition of the island in comparison to the island's condition just prior to the arrival of humans. An example would be the deforestation of primary forest taxa by humans as seen in Upolu, Efate, Rapa, Mangaia and many other islands across the Pacific (Ellison, 1994; Kennett *et al.*, 2006; Gosling *et al.*, 2020; Strandberg *et al.*, 2023). This is displayed in a different colour as this component is a process rather than a physical component of the island. The water component here refers to any potable water resource including but not limited to groundwater, rivers and lakes. The food resources component includes marine, wild and agricultural resources - but for the purposes of the scenarios examined below it is assumed that the island community is well established and they depend heavily on subsistence farming and some marine resources for a majority of their food requirements.

On the right are the social components. The main physical parameter within this group is the people component which represents the total population of the island and the interaction with other components in the model are based on changing population size. Within this there are also components of memory/indigenous knowledge, vulnerability and adaptive capacity. Adaptive capacity here refers to a community's ability to adapt to adverse conditions, such as an extreme event. Whilst it is appreciated that memory/indigenous knowledge and adaptive capacity are inter-related, here they are expressed separately. This is because there is a scenario in which an island community

has a high-level of indigenous knowledge, but other variables may impact on their ability to utilise that knowledge to adapt to a changing environment, though a high level of indigenous knowledge would increase their chances of doing so. For example, knowledge of food storage techniques such as fermenting crops like breadfruit and banana (Kahn *et al*, 2014) would make populations more resilient to drought events. Finally, the vulnerability component is included so as to represent how changes in water and food resources due to either external environmental factors or internal human activity impacts upon the vulnerability of the community through time. For example, vulnerability would increase with environmental degradation as this would bring about declines in food and water availability that leads to population decline as there is less food and water available per person, which makes the population more vulnerable to future extreme events or climate variability.

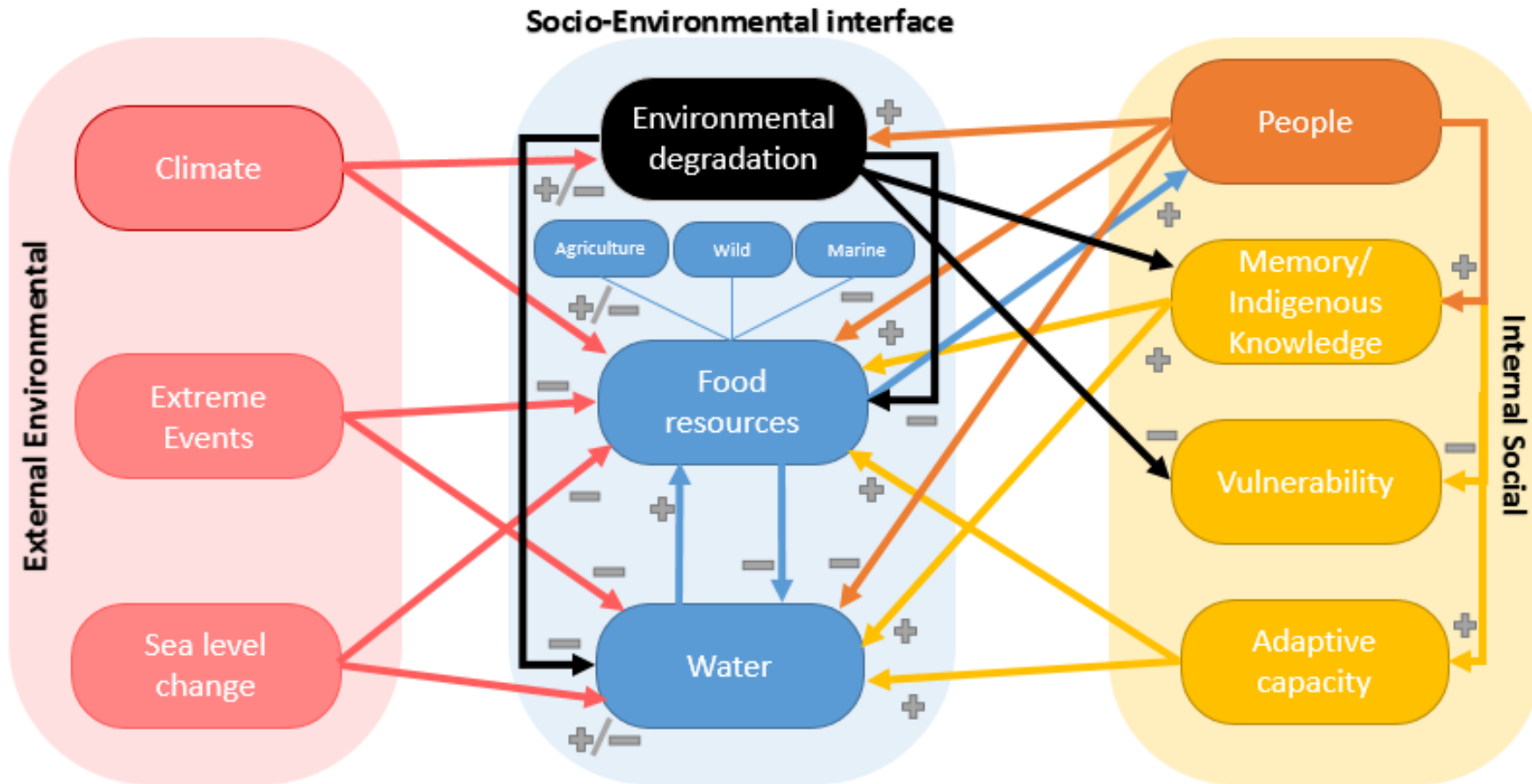


Figure 8.1: Conceptual model of the Mangaia socio-ecological system split into external environmental, internal social and the socio-environmental interface.

## 8.4 Model Development

### 8.4.1 Vensim

Vensim was the software chosen for building a model to represent the prehistoric Polynesian socio-ecological system. It is a system dynamics software that offers a user-friendly interface that is free to use for research purposes (Ventana Systems, 2015). It provides a graphical output of a model that illustrates the connections between different elements of the model visually and in an easily communicable way (El Sawah *et al.*, 2017). Users are able to build visual representations of systems primarily through a series of stocks and flows, levels and variables, each represented by a differential equation or constant value. Licenced versions also offer additional features including monte carlo sensitivity analysis which is useful for model evaluation (El Sawah *et al.*, 2017). An overview of some of the system dynamics software available were briefly compared in the paper by El Sawah *et al.* (2017). These alternative available software can require the payment of significant licence fees (e.g., Stella), specialist programming skills and/or knowledge of coding languages (e.g. Geonamica, R). Vensim offers similar proficiency to Stella, but users are able to test a lower capability software for free if the programme is being used for research purposes before upgrading to a licence for additional capabilities. The ability to represent island socio-ecological systems in Vensim was tested by reproducing an ordinary differential equation model developed by Brandt and Merico (2015) to investigate the collapse of Easter Island. Using Vensim it was possible to reproduce the results of the model offering confidence that the software was appropriate to use for developing a model looking at environmental change.

### 8.4.2 Creating the Model

The focus of the model is on the climatic, agricultural and population dynamics of the Mangaian island socio-ecological system. The conceptual model in Figure 8.1 covers more components but with model building there are trade-offs between generality, precision and realism – see Figure 8.2 (Troy, Pavao-Zuckerman and Evans, 2015). The aim is to focus on the vital components in the first instance to represent the impact of hydroclimate change on island life. It is considered good practice to start with a model in

its simplest form, selecting the key variables and functions of the system to reflect its fundamental behaviours (El Sawah *et al.*, 2012; Brandt and Merico, 2015).

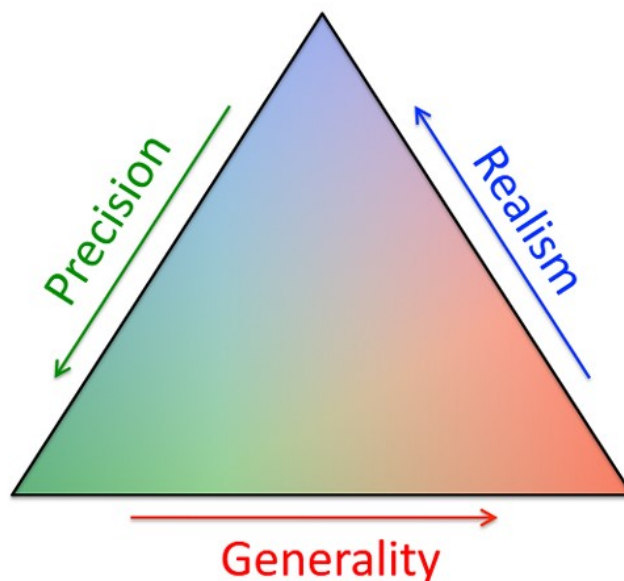


Figure 8.2: “Tradeoffs in model building between generality, precision and realism.”

Taken from Troy et al 2015

This could potentially be built upon later but the more complex a model becomes, the less precise the outputs (Brandt and Merico, 2015) and as discussed in Chapter 2, system dynamics models have the capacity to easily become overly complex (Kelly *et al.*, 2013; El Sawah *et al.*, 2017) and difficult to interpret. An overly complex model would introduce additional uncertainty – particularly in a prehistoric system where data is not complete – and its outputs would not be truly “realistic” or testable (Brandt and Merico, 2015) and the model may become intractable. Figure 8.3 shows a revised conceptual model with the essential components in colour and the additional non-essential components in grey.

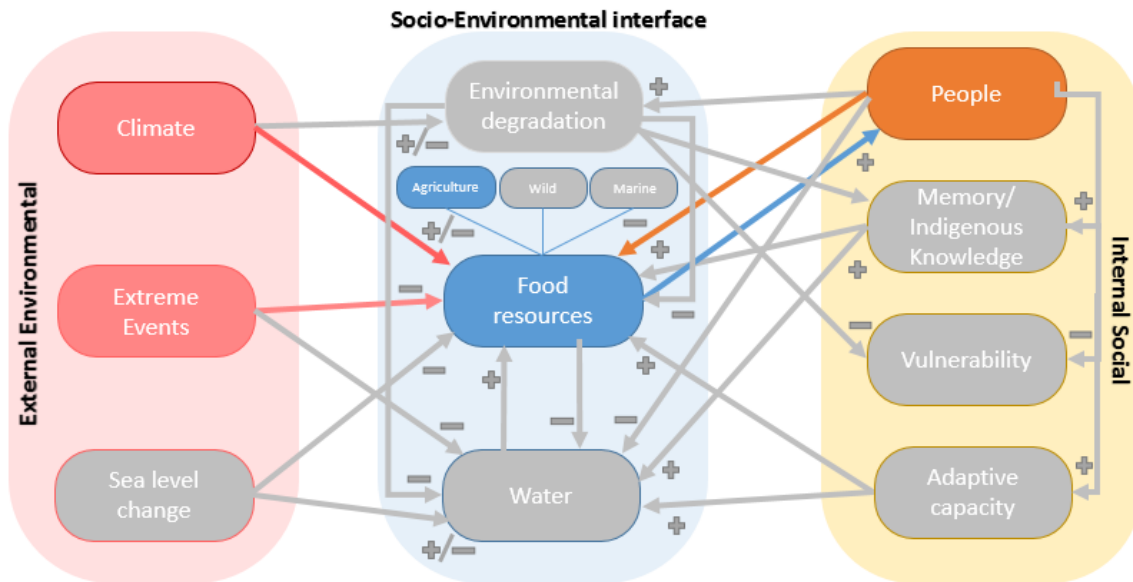


Figure 8.3: Conceptual model of the Mangaia socio-ecological system split into external environmental, internal social and the socio-environmental interface. This version denotes the components that were selected as part of the final socio-ecological model.

The key components in this model are: 1) climate, specifically rainfall which as discussed in Chapter 2 played an important part in many aspects of the prehistoric Pacific island life, 2) population as we are interested in how environmental factors impacted on the population dynamics and finally, 3) agriculture or more specifically food availability, was dominated by the taro pondfields, which became an important resource and staple food crop that became entangled in Manganian society. Based on the ethnohistoric and archaeological evidence examined in section 8.2, these four aspects were chosen to capture the fundamental aspects of the Manganian prehistoric socio-ecological system.

Following the development of the conceptual model and the identification of the fundamental components required to represent the system, the theoretical relationship between the chosen variables were plotted on xy plots. Next, the lines representing the relationships between two components were formalised into differential equations to quantify these relationships. A visual representation of the socio-ecological system and the differential equations defining the relationship between different components and their variables were combined and the model developed in Vensim.

## 8.5 Model parameterisation

This model is adapted from and inspired by both the Brandt and Merico (2015) model and the Kuil et al (2016) Maya socio-hydrological model. As such it also uses ordinary differential equations to replicate the relationship between Precipitation ( $P$ ), population ( $N$ ) and food availability ( $FA$ ). The aim is to simulate the impacts of changing climate on prehistoric Polynesian islands, specifically food availability and the repercussions this has on the growth of the initial settling population. Parameters used within the differential equations are listed in Table 8.1 below. The origin of these values is discussed within subsequent subsections. The symbols for every variable and parameter of the equations are also listed.

Table 8.1: List of parameters, stocks and outputs used within the Mangaia socio-ecological model.

Symbol	Name	Starting or constant value	Units
<b>Parameters</b>			
$\mu_N$	Max human growth rate	0.03/0.0228	Year <sup>-1</sup>
$\delta_N$	Labour required	106	People/km <sup>2</sup>
$F_N$	Food requirement per person	912,500	Kcal/year
$C_{max}$	Maximum crop yield	100	%
$\theta_c$	Adjustment parameter	2.0e+5/200000	-
$\delta_c$	Adjustment speed	0.007	-
$\gamma_c$	Crop calorie availability	1664510400	Kcal/km <sup>2</sup>
$m_c$	Crop mortality rate	10	%
$L_t$	Total available land	19.9	Km <sup>2</sup>
<b>Stocks</b>			
$N$	Population	50	N <sup>-1</sup>
<b>Outputs</b>			
$\Theta_N$	Available Labour	-	N <sup>-1</sup>
$\gamma_N$	Population food requirement	-	Kcal <sup>-1</sup>
$r_N$	Population growth rate	-	-
$K_A$	Agricultural Carrying Capacity	-	N <sup>-1</sup>
$C$	Total crop calorie production	-	Kcal/year
$FA$	Food Availability	-	Kcal <sup>-1</sup>
$L$	Available land	-	Km <sup>2</sup>

External Data			
<b>P</b>	Precipitation	-	mm/year

Figure 8.4 shows the structure of the Vensim model showing how the variables relate to each other. Population is represented as a stock within the model with population growth provided as an input into that stock. The colours denote the different components of the system, with purple representing the human population, orange denoting variables related to land availability, green for agricultural variables and blue for the rainfall input that drives the model. The subsequent subsections will describe each of these components, their constituent variables and how the relationships are represented in the model.

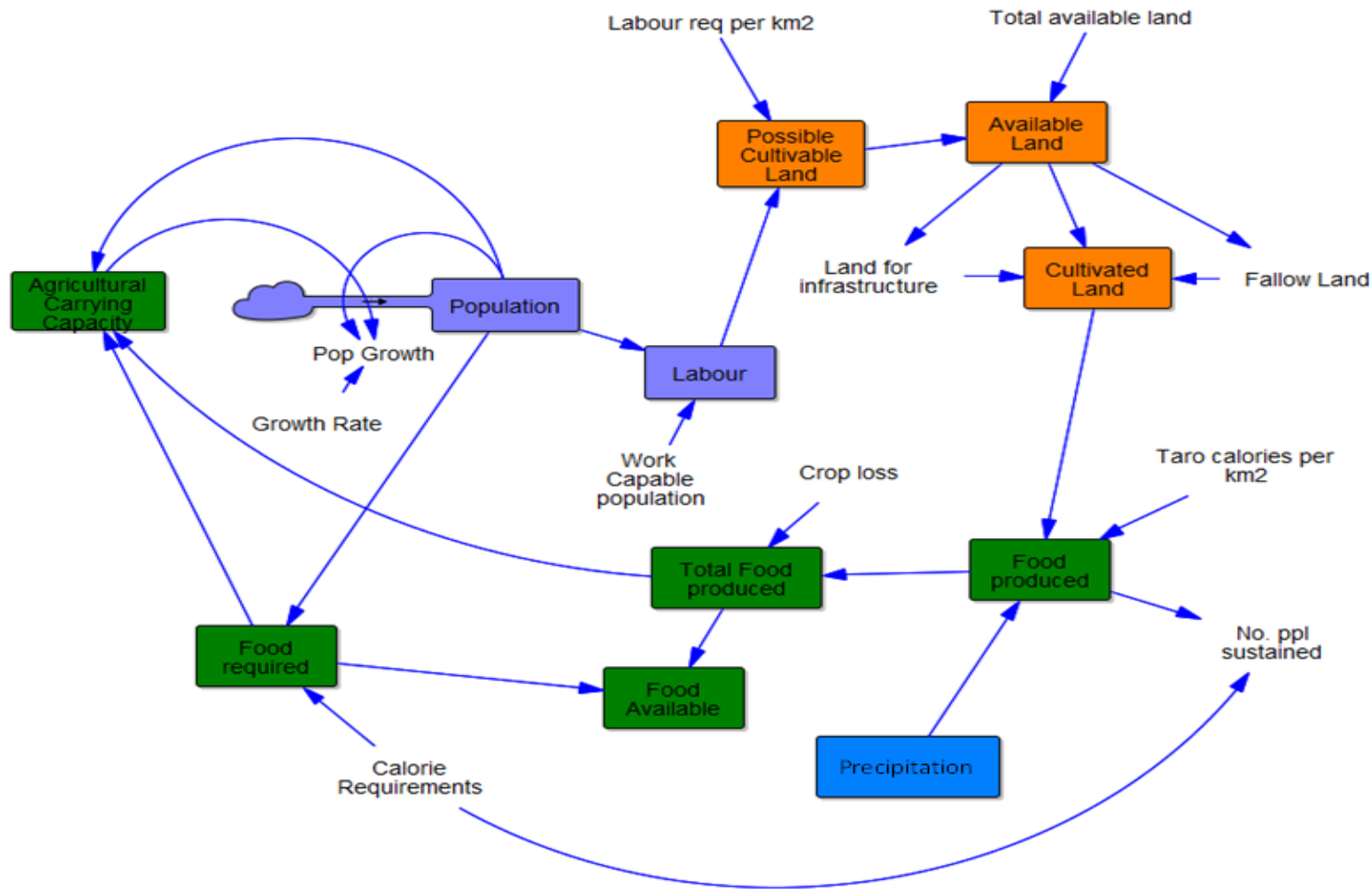


Figure 8.4: Visualisation of the Vensim model structure

### 8.5.1 Population

Population ( $N$ ) is calculated as the current population multiplied by the population growth rate ( $r_N$ ). The population growth rate is determined by multiplying the maximum human growth rate by the ratio of the population over agricultural carrying capacity. The growth rate is constrained by how close the population is to the agricultural carrying capacity, such that it decreases as resources become strained. This equation is adapted from the Brandt and Merico (2015) model and uses their suggested value of 0.03 for the maximum growth rate, which was originally proposed by Birdsell (1957) for ancient societies. The model was given an initial starting population of 50 people as per existing models of Pacific societies (Brandt and Merico, 2015), which is the assumed size of a migrating community. The earliest population estimate of 2000-3000 people was provided by Williams (1837) in 1832 though this estimate followed an epidemic caused by diseases introduced by the first missionaries to the island that was “exceedingly fatal” (Williams, 1837, p. 81). There is currently no estimate of the absolute maximum population size or population dynamics pre-contact, only the post-contact value. This model offers the opportunity to explore the possible population dynamics on pre-contact Mangaia. The change in population of a time step,  $t$ , is:

$$\frac{N}{t} = (r_N N) + N \quad (1)$$

Where  $N$  is the total population and  $r_N$  is the population growth rate, which in turn is calculated as:

$$r_N = \mu_N \left(1 - \left(\frac{N}{K_A}\right)\right) \quad (2)$$

Where  $\mu_N$  is the maximum population growth rate and  $K_A$  is the total agricultural carrying capacity, which is described in more detail in the next section.

### 8.5.2 Carrying Capacity

Similar to the model created by Hamilton and Kahn (2007) the agricultural carrying capacity value is a function of the amount of food available (specifically staple starch, i.e. Taro) from the cultivable land and the population size that could be sustained by this, taking into account the food required by the population. The carrying capacity of the island is determined by the availability of food and is limited by the amount of land available for cultivation. The equation is derived from the carrying capacity component of Brandt and Merico's (2017) population equation but adapted to represent agricultural carrying capacity:

$$K_A = N\left(1 - \frac{Y_N - C}{Y_N}\right) \quad (3)$$

Where  $Y_N$  is the population food requirement, which is measured as the number of calories required per year for the total island population and  $C$  is the total crop calorie production, which is a calculation of the total calories produced by the amount of land being cultivated for crops.

### 8.5.3 Food Availability

Food availability is modelled as the ratio between food produced ( $C$ ) and food required by the population of the island ( $\gamma N$ ) both measured in calories per year. This is expressed as:

$$FA = \frac{C}{\gamma N} \quad (4)$$

How much food is produced is calculated by taking the crop yield per km<sup>2</sup> multiplied by the amount of land cleared. The amount of available land is initially controlled by labour availability to physically clear and work the land and later is limited by the total available land on the island suitable for taro, which is estimated at 19.9 km<sup>2</sup> by Kirch (2017). This is noted as an important factor especially in the early stages of colonisation where limited population dictates the amount of land that can be cleared and worked for agricultural

purposes (Kirch, 2017b). The food required is calculated by multiplying the total current population ( $N$ ) by the food calorie requirement per person ( $F_N$ ), which is expressed as:

$$\gamma N = NF_N \quad (5)$$

The values for available labour and the number of people required to work the land are both taken from Lee and Tuljapurkar (2008) and Puleston and Tuljapurkar (2008) who assume that 50% of the population is available for agricultural work. They suggest that a single adult can manage 0.9443 ha of agricultural land over a year, which equates to 0.009443 km<sup>2</sup> when utilising traditional methods over the course of a traditional working day. Available land is calculated as the fraction of the available labour ( $\theta_N$ ) over the labour required per km<sup>2</sup> ( $\delta_N$ ) up to a maximum value of 19.9 km<sup>2</sup>, which is the total amount of available land that is suitable for taro production ( $L_t$ ). This is expressed as:

$$L = \text{MIN}\left(\frac{\theta_N}{\delta_N}\right), L_t \quad (6)$$

Pondfield systems require some fallowing to maintain soil fertility (Kirch, 1994) with both Kirch (1994) and Hamilton and Kahn (2007) suggesting that approximately 20% of land is left fallow at any one time.  $\gamma_c$  represents the calorie production per km<sup>2</sup> of taro. There are a number of values suggested for the yield of wetland taro based on modern observations of pondfield systems using traditional methods of cultivation. These values range from 13.3-20 t/ha/yr based off Futunan pondfield systems (Kirch, 1994), mid-range values of 20.22 t/ha/yr based off modern Hawaiian values (Huang, 1979) to high range of 25.1-58.1 t/ha/yr based off traditional pondfield techniques in Maewo, Vanuatu (Spriggs, 1984). For this model, this value is constant and is taken from Huang's (1979) estimation of 20.22 t/ha/year and the calculation of calories/hectare/year which was then adapted to reflect values per km<sup>2</sup> as this represented the middle range of values suggested. Alternative yields were considered as part of the sensitivity analysis. Hamilton and Kahn (2007) similarly adopted a mid-range value of 25 t/ha/yr for their model based on values from Kirch (1994) and Spriggs (1984) and so a comparable approach is adopted here too. To calculate changing crop yields in response to precipitation a logistic growth equation was used to reflect the conditions required for the production of taro as per the values provided by the FAO (1996). Total crop calorie production is calculated as:

$$C_c = C - m_c \quad (7)$$

Where  $C_c$  is total crop calorie production,  $C$  is maximum crop calorie production and  $m_c$  is crop mortality. Total crop calorie production in turn is calculated as:

$$C = L(\gamma_c \frac{C_{max}}{1 + \theta_c e^{-\delta_c P}}) \quad (8)$$

Where  $L$  is the available cultivable land,  $\gamma_c$  is the crop calorie availability,  $C_{max}$  is the maximum crop yield and  $P$  represents precipitation, which is the external driver and uses a set data set. The next section goes into more detail about the precipitation values used for this. Finally,  $\theta_c$  and  $\delta_c$  represent mathematical constants that define the shape of the logistic growth curve, which represents the relationship between rainfall and taro yields. This relationship was defined by the minimum (1000 mm/yr) and optimum rainfall values (1800-2700 mm/yr) for taro, which were taken from the FAO (1996) published values.

#### 8.5.4 Precipitation

To test the behaviour of the model and understand the reaction of the Manganian socio-ecological system to changing hydrological conditions a series of precipitation data sets mimicking the rainfall of Mangaia were created. Precipitation data sets of 1000 years were generated from R code using a first order autoregressive model, often termed an AR(1) model that utilised the statistical characteristics of the observed rainfall from Mangaia over the past century to create as representative a data set as possible. Table 8.2, shows the four rainfall scenarios and their characteristics. The rationale for using these values is that Scenario 1 and 2 are based on the range of observed rainfall data from Mangaia with different Rho values that alter the duration and frequency of drought events. A lower value of Rho corresponds to lower autocorrelation between one data point and the next generating a more random series of numbers and therefore drought events are frequent but short-lived. A higher Rho value increases the autocorrelation and generates a lower frequency of drought events but a longer duration. The available rainfall data for Mangaia only covers approximately 40 years and likely does not

represent the true range of values so to account for an increased range of variability through time scenarios 3 and 4 had the same statistical values but an increased range of precipitation values to test the models behaviour. For each scenario, 10 rainfall time series were generated to represent the variability in the stochastic generation of rainfall data in the AR(1) model to test the sensitivity to drought events at different stages of the 1000-year sequence.

Table 8.2: The statistical and drought characteristics of the different rainfall scenarios

Scenario	Magnitude	Duration	Frequency	Rho (-1 to 1)	Range (mm)
1	Low	Low	Low	0.4	1000-2800
2	Low	High	High	0.9	1000-2800
3	High	Low	Low	0.4	250-3000
4	High	High	High	0.90	250-3000

Based on the rainfall data sets and the model outputs from each scenario, the R package ‘drought’ was used to calculate the drought duration, frequency and severity. The impact of drought events upon population dynamics was calculated as per Kuil *et al* (2019) using two metrics. The first is the rate of recovery, which measures the time it takes for the population value to return to its pre-drought value – see Figure 8.5. The second is maximum population change - referred to as impact in Figure 8.5 - which identifies the percentage drop in the population from the start of the drought to the lowest population value within the duration of the drought. Drought duration is calculated in a similar manner to that of McGree *et al* (2016) with the drought starting when it sinks below the drought threshold which is typically done using z-scores. Drought severity is the sum of the rainfall deficit below the threshold for every year of the drought duration (Hao and Yu, 2022). The end of the drought period is when the precipitation returns to above the drought threshold, which is set for a total rainfall value of 1000 mm/year. Typically, a threshold for drought is set at the lowest 20% of rainfall values for the scenario data as per Kuil *et al* (2019) and is used within the hydrology literature (Sheffield and Wood, 2008; Van Loon *et al.*, 2014; Van Loon, 2015). However, as there is no quantitative

reconstruction for precipitation, the modern data for Mangaia has only 40 years of complete data and the rainfall datasets generated have different ranges and characteristics, a statistically based threshold for meteorological drought is not appropriate. Instead, an absolute drought threshold is used based on the level of rainfall (1000 mm/year) at which the model starts to exhibit impacts upon the agricultural carrying capacity and the population, specifically on the yields of taro. The threshold is physically based (i.e., it relates to agricultural impacts) but is based on the parameters of the model, which are uncertain. This could be improved in the future with the use of quantitative palaeo data sets that allow for a better understanding of meteorological drought locally.

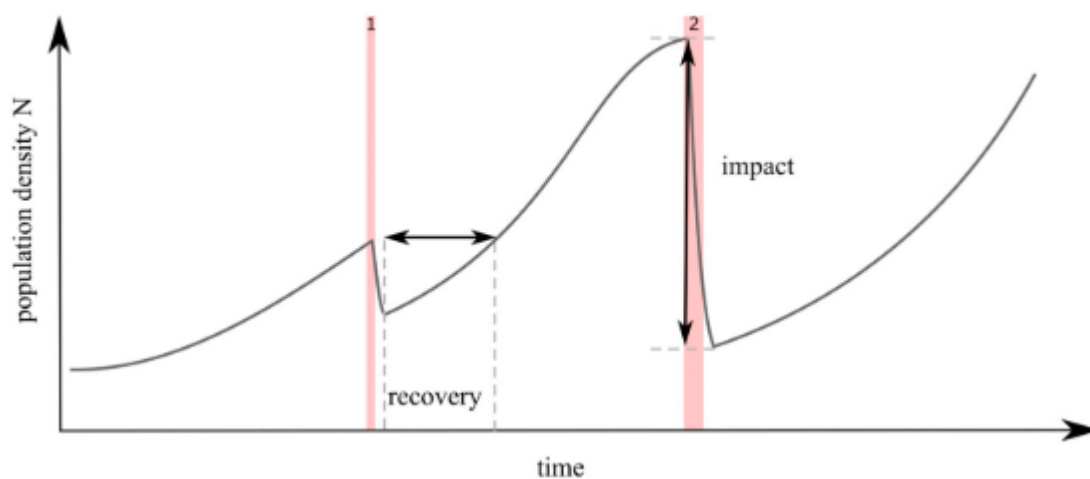


Figure 8.5: Graph identifying how the metrics of impact and recovery are measured. Red lines denote drought events. Taken from Kuil et al 2019.

#### 8.5.4.1 Palaeo Reconstruction Rainfall Data Set

As noted, no previous study on understanding agricultural and population dynamics in the tropical Pacific has utilised a palaeo data set for rainfall. This study, just like the Kuil et al (2016) Maya model study, uses palaeoclimatological precipitation reconstructions for the Late Holocene. Currently, there are not annually resolved precipitation records that go back c.1000 years in the Pacific. The Toomey (2016) record from Apu Bay in the Society Islands has a sub-annually resolved and continuous 3,000 year record, but this record is clearly impacted by humans with the upward shift in mean values at the start of the MCA around Polynesian expansion. Furthermore,  $Ti$  is an erosion proxy rather than a direct precipitation proxy. Alternatively, a number of biomarker and dinosterol hydrogen isotope records have been developed across the Pacific region (Smittenberg *et al.*, 2011;

Atwood and Sachs, 2014; Hassall, 2017; Sachs *et al.*, 2018; Sear *et al.*, 2020; Maloney *et al.*, 2022) - including one from Samoa and another from the Southern Cook Islands (Hassall, 2017; Sear *et al.*, 2020). The dinosterol data from Samoa is a more direct precipitation proxy and can be converted into mm/day values using a calibration set developed from tropical South Pacific sediments (Maloney *et al.*, 2019). However, these records are not annually resolved. Instead, they represent the rate of change over long time periods with snapshots of values that cover approximately a decade of sedimentation. To generate a precipitation record that represents palaeoclimatic change in the tropical Pacific that can be utilised within the model, a simulated data set is generated based on characteristics of the historical observations of Mangaia, but which matches the changing “mean value” provided by the dinosterol data set over time. As with most palaeo records, there is uncertainty in the values, but this will still offer some insight into changing hydrological patterns over this period and how it may have impacted on agriculture and population dynamics in the region.

The best data available is the record from Lake Lanoto’o located on the island of ‘Upolu in Samoa, which is shown in Figure 8.6 – it is the closest quantitatively reconstructed rainfall record, thanks to the calibration set developed by Maloney *et al.* (2019). The resolution of the data set varies between 21 and 368 years. The available data was smoothed using a loess smoother to generate a mean precipitation dataset over the past 2000 years – see Figure 8.6. It is clear from this figure that these rainfall values typically sit above the threshold of 1000 mm/year required for taro production.

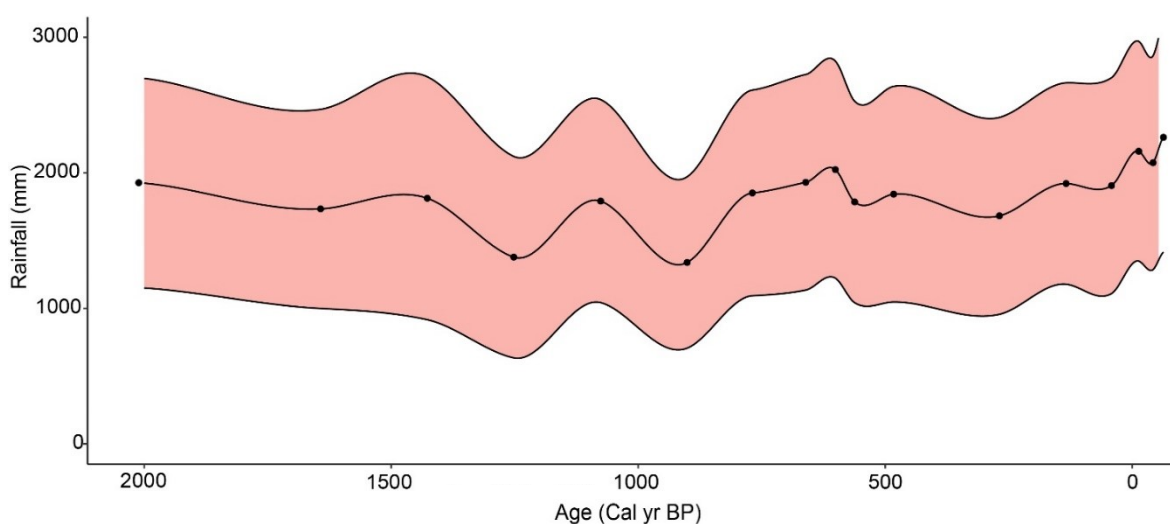


Figure 8.6: The quantitative precipitation reconstruction covering the past 2,000 years from Lake Lanoto'o in Samoa - taken from Sear et al (2020) with a loess smoother running through the points giving the running mean precipitation value. The red area denotes the minimum and maximum error associated with the dinosterol reconstruction.

The two islands of 'Upolu and Mangaia are quite different in terms of elevation and location in relation to the SPCZ which in turn influences the level of rainfall each island receives. Lake Lanoto'o is a highland site that sits at 760 masl. (Sear *et al.*, 2020) whereas the island of Mangaia has a maximum elevation of 168m (Ellison, 1994). Historical measured data shows that there is a difference of approximately 1000 mm/year between the average for modern precipitation from Samoa and Mangaia. As the model is designed to represent the Mangaian island system – the reconstruction was corrected to account for the difference between the precipitation profiles for the two islands to provide a more representative rainfall profile for Mangaia for this period. To account for the error associated with the dinosterol reconstruction, a set of scenarios within the boundaries of the error were used to represent the range of possible precipitation profiles. Two versions of the palaeo data sets were created; the first covered the full dinosterol reconstruction providing a 2000-year reconstruction. It assumes human arrival 2000 yr BP which while factually incorrect it does allow us to test how the model behaves under a longer time period with two notable dry periods. The second palaeo data set was a 1000-year subset that starts at the arrival of humans to Mangaia in approx. 1000 AD (Kirch, 2017b; Sear *et al.*, 2020) to the year 2000 AD. This second version of the data set is most representative of conditions at the time of human arrival in Mangaia.

The first round of model outputs using the values for palaeo scenarios P1 through P5 (Table 8.3) based on the data from Sear et al (2020), did not fit what we know about Mangaia from the archaeological record in terms of the timing of agricultural intensification and a known period of food stress around 1400 AD. Therefore, several iterations between the mean value and the mean plus 25% of the error were run through the model to see if a scenario that fit the archaeological findings would emerge. The palaeo rainfall datasets were generated using the same method described in section 8.5.4. using time-varying mean values from the dinosterol reconstruction in order to mimic the reconstructed variability of rainfall over time. The standard deviation value is taken from the modern observed data from Mangaia. Table 8.3 lists the palaeo scenarios, the dinosterol values used and other statistical values for each scenario.

Table 8.3: Palaeo rainfall scenarios, the associated dinosterol iteration values

Palaeo Scenario	Mean Value	Rho (-1 to 1)	Standard Deviation
<b>P1</b>	Mean	0.9	436.07
<b>P2</b>	Mean - 50% Error	0.9	436.07
<b>P3</b>	Mean – 100 % Error	0.9	436.07
<b>P4</b>	Mean + 50% Error	0.9	436.07
<b>P5</b>	Mean + 100 % Error	0.9	436.07
<b>P6</b>	Mean + 25% error	0.9	436.07
<b>P7</b>	Mean + 20% error	0.9	436.07
<b>P8</b>	Mean + 15% error	0.9	436.07
<b>P9</b>	Mean + 10% error	0.9	436.07
<b>P10</b>	Mean + 5% error	0.9	436.07

## 8.6 Sensitivity Analysis and Model Validation

There is uncertainty surrounding the parameters of the model as they are not directly measurable for an archaeological system (Brandt and Merico, 2017) or there is not necessarily a modern-day equivalent system that the parameters can be built around. Once a model has been developed, built and produced results, it is important to evaluate its performance and outputs through model testing and evaluation. For SD models this

can include the use of Monte Carlo sensitivity analysis as well as behavioural and structural evaluation, which can be used to evaluate how plausible the model results are and compare against existing models from the literature (El Sawah *et al.*, 2017).

### 8.6.1 Sensitivity Testing

To gauge the potential ramifications of parameter uncertainties on the model outputs, parameters including maximum human growth rate ( $\mu_N$ ), labour required ( $\delta_N$ ) and crop calorie availability ( $\gamma_c$ ) were evaluated using sensitivity tests. The values of these parameters were altered by +/- 10, 25 and 50% and run through the model to show the impact of changes to these parameters on the model outputs. The sensitivity ranges are reasonable as there are uncertainties in these values as discussed in section 8.5, changes of 10 or 25% would encompass some of the uncertainty suggested within the wider literature. A change of 50% would indicate that there are large uncertainties in the parameter values and this allows us to test whether significant uncertainties would result in changes in the model behaviour. Figure 8.7 shows the results from the sensitivity testing of maximum human growth rate ( $\mu_N$ ), labour required ( $\delta_N$ ) and crop calorie availability ( $\gamma_c$ ). Parameters such as food requirement per person ( $F_N$ ) and total available land ( $L_t$ ) are not considered as part of the analysis as these are known fixed values. The sensitivity of the model to the rainfall external data input is tested as part of the model scenarios presented within the results section below, so is not included here. Figure 8.7 shows the food availability output as this is influenced by each of the parameters tested. The sensitivity tests show that despite the alterations to parameter values, the model still displays the same behaviour over time, but the speed of those changes increases or decreases in reaction to the different parameter values, as would be expected. This offers confidence that the model is not producing certain behaviours because of a particular parameter value choice, providing confidence in the robustness of the model formulation and its outputs.

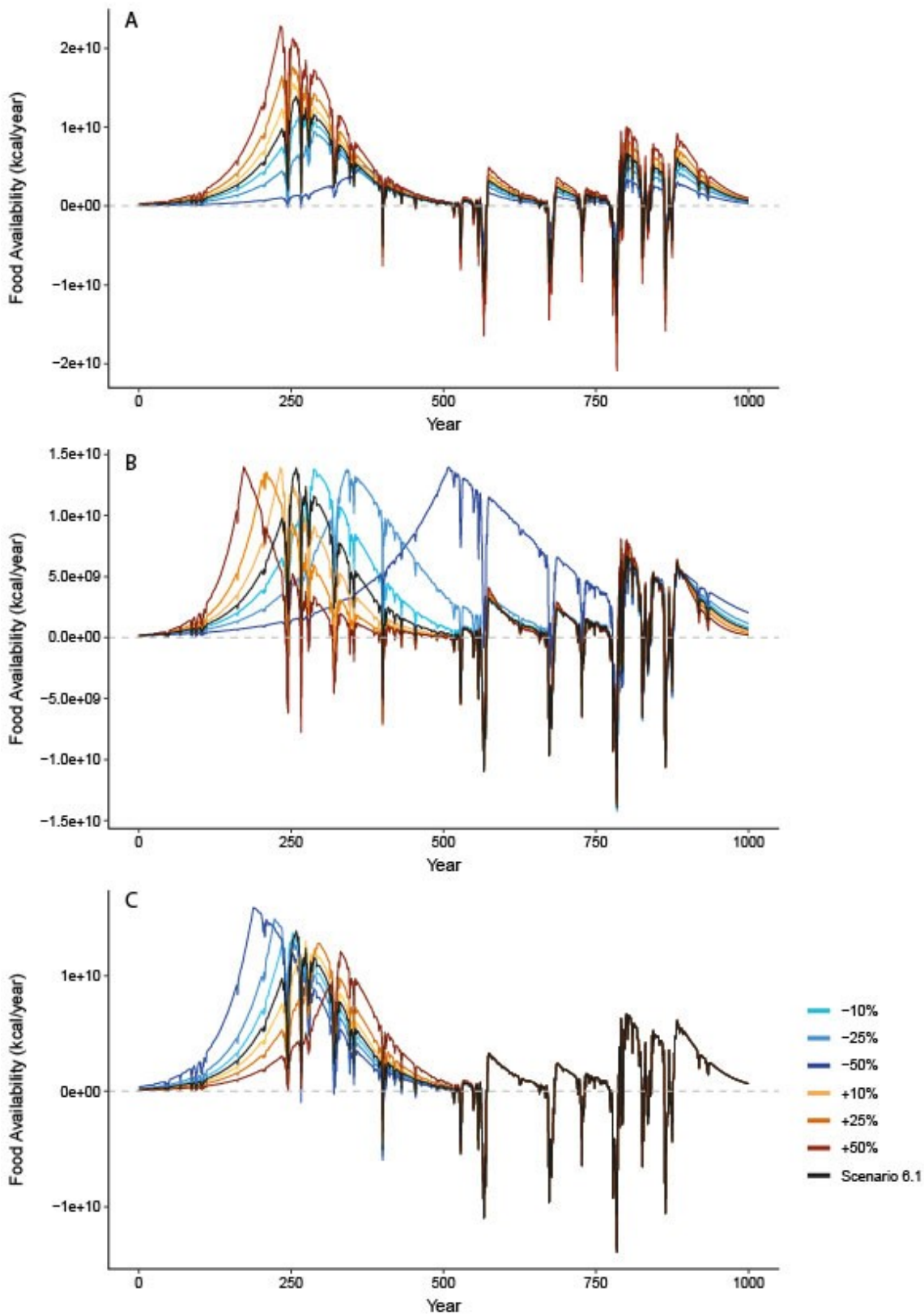


Figure 8.7: Sensitivity test outputs for A - crop calorie availability, B - maximum population growth and C - Labour required plotted against the baseline of food availability output from Scenario 6.1.

## 8.7 Results

### 8.7.1 Scenario model outputs

Table 8.4 and figure 8.8, shows some of the key outputs – drought characteristics, population and agricultural carrying capacity of the socio-ecological Vensim model of Mangaia as well as the rainfall input for each iteration of each scenario.

For the first set of data from scenario 1, there are very few fluctuations in the population curve, indicating that very little change occurs under this scenario. This is due to the low magnitude and duration of drought events in this series. The droughts are more frequent than in scenario 2 as per Table 8.4, but this clearly does not have a notable impact on agricultural and population dynamics if the drought events are low in magnitude and duration.

Table 8.4: Drought characteristics of the model scenarios

	<b>Scenario 1</b>	<b>Scenario 2</b>	<b>Scenario 3</b>	<b>Scenario 4</b>
Drought Frequency (per 1000 years)	106.80	47.10	107.20	43.80
Drought Intensity - Average	0.78	1.72	0.78	1.91
Drought Intensity - Maximum	4.31	20.88	4.61	13.80
Drought Duration – Average (Years)	1.49	3.39	1.47	3.79
Drought Duration – Maximum (Years)	5.00	19.70	5.50	17.30

In scenario 2, the dips in population numbers and in the agricultural carrying capacity are noticeably larger than in scenario 1. The length of time that the agricultural carrying capacity remains below the maximum capacity is also longer in scenario 2 due to the longer duration of droughts due to the higher autocorrelation compared to

scenario 1 (Table 8.2 and Table 8.4). This implies that a longer duration is a more influential factor than more frequent shorter duration events in terms of their impact upon agricultural carrying capacity and population dynamics.

As described in Table 8.2 and shown in figure 8.8, scenario 3 and 4 have a larger range of rainfall than scenarios 1 & 2. This allows us to test the reaction of the model to a higher value of precipitation variability as it is unlikely that 40 years of recorded rainfall is representative of the full range of Manganian precipitation. This range of rainfall also introduces droughts that significantly affect the taro yields and in turn agricultural carrying capacity.

In scenarios 3 and 4, there are clearly larger fluctuations in the agricultural carrying capacity and population in comparison to scenarios 1 and 2 due to the increase in the magnitude of change. The biggest fluctuations in the population and agricultural carrying capacity occur following a relatively stable and smooth initial growth period for approximately 300 years. There is, however, a wider spread in the initial exponential growth of the population in both scenarios 3 and 4. This indicates that whilst drought events may not cause a notable decrease in population, it does slow the rate of growth in those early stages of colonisation. The fluctuations in population become larger as it grows closer to the absolute maximum carrying capacity of the island. The number of people needing to be supported per km<sup>2</sup> of taro pondfields increases to the point at which no excess food is produced. Therefore, when a reduction in rainfall occurs there is no redundancy for crop loss and so there is a greater impact on the population. It is clear from figure 8.8 that the rainfall dataset for scenario 4 - which has less frequent but more severe droughts than scenario 3- has the biggest impact on the yield and thus population out of all of the scenarios.

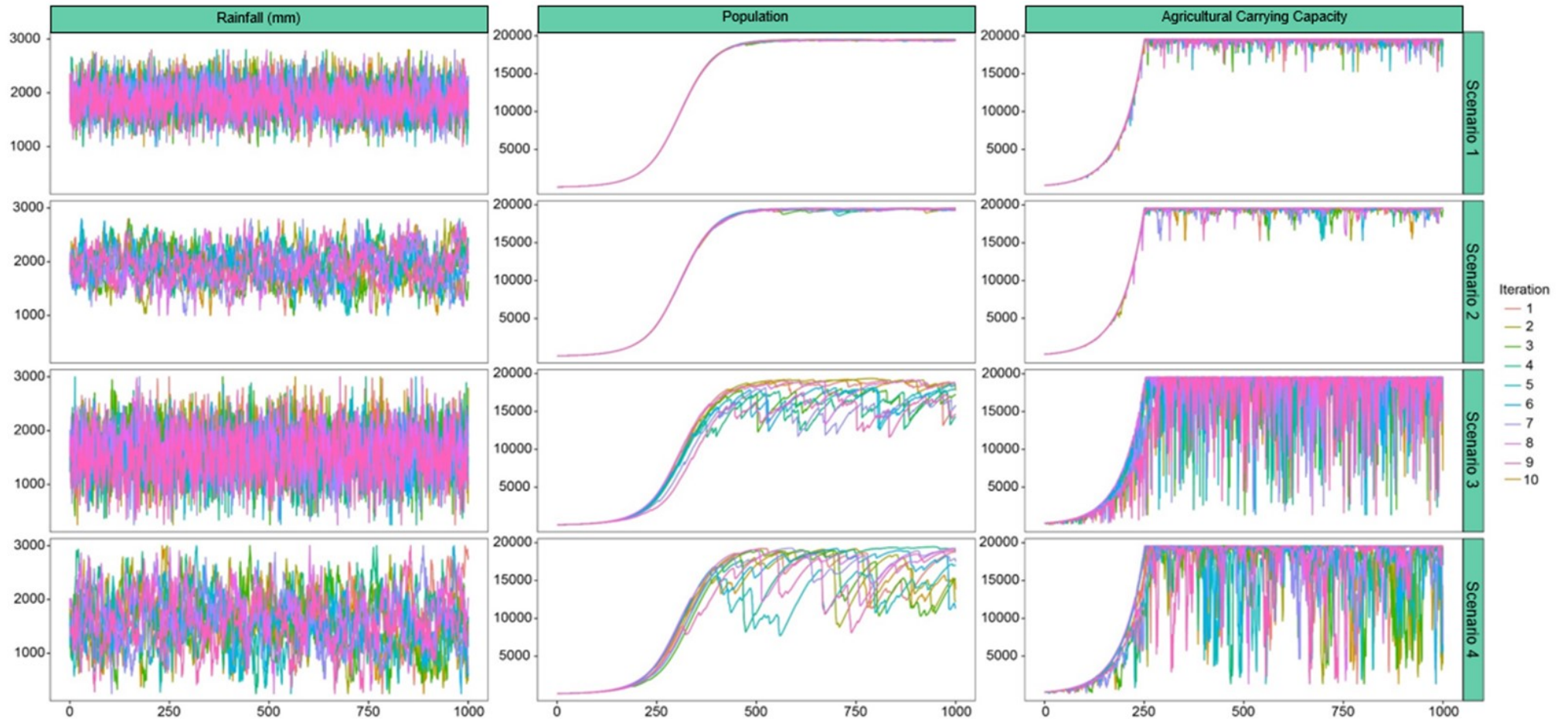


Figure 8.8: Outputs from the system dynamics Vensim model for Mangaia. The outputs are broken down into the four scenarios run as per Table 8.2. Within each panel the colours represent the 10 iterations of each scenario.

### 8.7.2 Scenario drought and population metrics

Figure 8.9 presents the results from scenario 3 and 4, which shows the population density against the maximum population change for each individual drought event for the two scenarios. As the lower rainfall limit for scenarios 1 and 2 was 1000 mm, which is the drought threshold, these scenarios were removed from the drought and population dynamic metric analysis.

The severity of each drought event is calculated using a combination of the intensity and duration and then indicated by the colour of the individual event point. It was clear from the scenario data presented in the previous section that the population density and the drought duration both play a role in the impact of droughts on population dynamics. This plot clearly shows that with population density values below approximately 100 people/km<sup>2</sup> typically droughts will not drive a negative population change, indicating that droughts have a lower impact on smaller populations. This is because there is more food available per person when there is a lower population density, which creates a buffer in times of drought. However, there are drought events that occur in times of lower population density values, but which do result in negative population change if severe enough. Over time, the average population change that occurs with low-level severity droughts drops. Initially, the population change remains positive, that is, population growth continues as the more frequent but lower severity droughts have a low level of impact on agricultural carrying capacity and thus population dynamics. As the population density increases so does the impact of the drought as measured by maximum population change during each drought event. The population density threshold where drought events start to have a notable impact is different for each scenario. For scenario 3 the threshold is about 250 people/km<sup>2</sup>. For scenario 4 the threshold is about 150 people/km<sup>2</sup>. The difference between these two scenarios is the longer duration of droughts in scenario 4 indicated by overall higher severity drought events as illustrated in Figure 8.9.

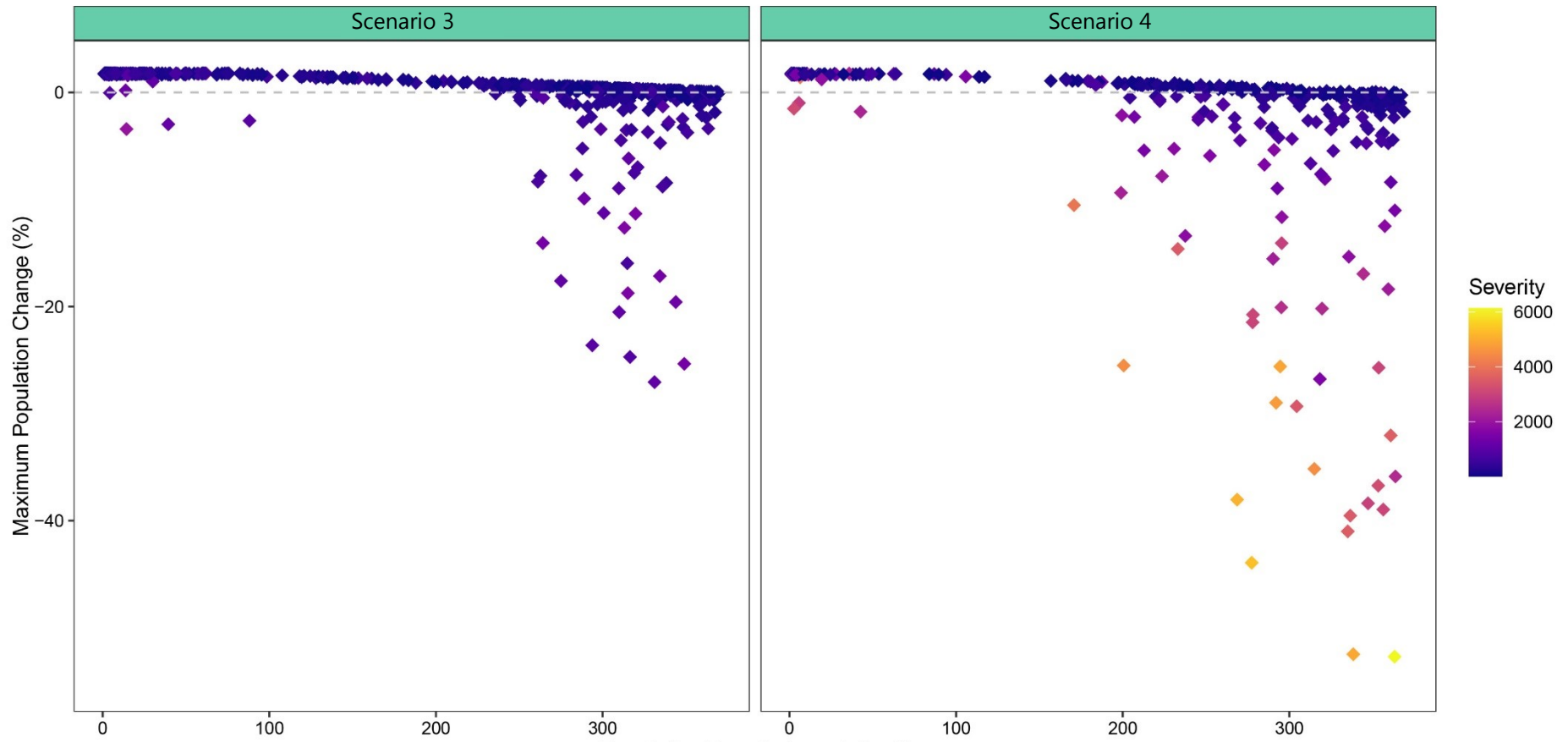


Figure 8.9: Graph showing the outputs from the drought and population metrics produced for the rainfall data for scenarios 3 and 4.

### **8.7.3 Palaeo Scenario**

#### **8.7.3.1 1000-year palaeo sequence**

This sequence represents the likely climatic changes that occurred on Mangaia as humans arrived on the island in 1000 AD. The time series was cropped so human arrival coincides with the precipitation record at 1000 AD. Figure 8.10 shows some of the key outputs – population and agricultural carrying capacity - of the socio-ecological Vensim model of Mangaia as well as the rainfall input for each scenario.

The results for rainfall palaeo scenario P1, which was based on the mean value of the dinosterol records corrected to represent conditions on Mangaia (Table 8.3), indicate that Mangaia would not have been able to sustain a population using taro for at least 500 years following initial human arrival. The population does not reach maximum carrying capacity before the end of the time sequence. The low levels of rainfall as humans arrive stalls the population growth such that a permanent population would not have been able to be supported until around 1500 AD.

It is clear that similar to the 2000-year sequence, scenarios P2 and P3 have rainfall series that are not high enough to grow taro in sufficient yields needed to support a population. Each successive scenario above the mean value for which the rainfall amount is increased, shows a decrease in the period between arrival and rapid population growth.

There is a noticeable step up in values between scenario P1 and scenario P9, which represents the mean plus 5% of the error. This represents a threshold change between a rainfall scenario that can produce a good taro yield and a rainfall scenario that sees notable slowdown in the growth of the population due to lower taro yields.

Palaeo scenario P5, which is at the upper limit of the dinosterol error, shows a similar pattern to the model scenarios with precipitation levels higher than 1000 mm so there is little to no stress on the population through time. The scenario data in section 8.7.1 shows that by 250 years into the sequence the population is shifting toward exponential growth. This is reflected in the palaeo scenario P5. Scenario P4 similarly shows rapid population growth and supports a population throughout, although the time to exponential growth is

slowed and there are fluctuations in population once it reaches close to its maximum carrying capacity as the rainfall varies affecting crop yields.

For palaeo scenarios P6 through P10, the start of exponential population growth is delayed by several hundred years. After 1500 AD, population growth slowed due to a downward shift in the rainfall records at around 1400 AD that persisted for around 300 years. Towards the end of the series, rainfall values start to rise again and this is shown in the slow but steadily growing population values through the latter half of the record. Some of the model outputs show intersecting lines between scenarios despite the difference in mean value. This is due to the randomness in the generation of the annual rainfall data - which may cause very large droughts to be generated.

The model suggests that the initial drought or dry period that potentially occurred concurrently with the second wave of human migration in the tropical Pacific (1000 yr BP) would have slowed the growth of the population of Mangaia following initial colonisation. This is evident in Figure 8.10 from the flattening of the population curves as the precipitation drops incrementally through the scenarios. The lower the precipitation values, the slower the population grows and the agricultural carrying capacity shows a similar pattern as people are required to clear the land for agriculture and keep it productive.

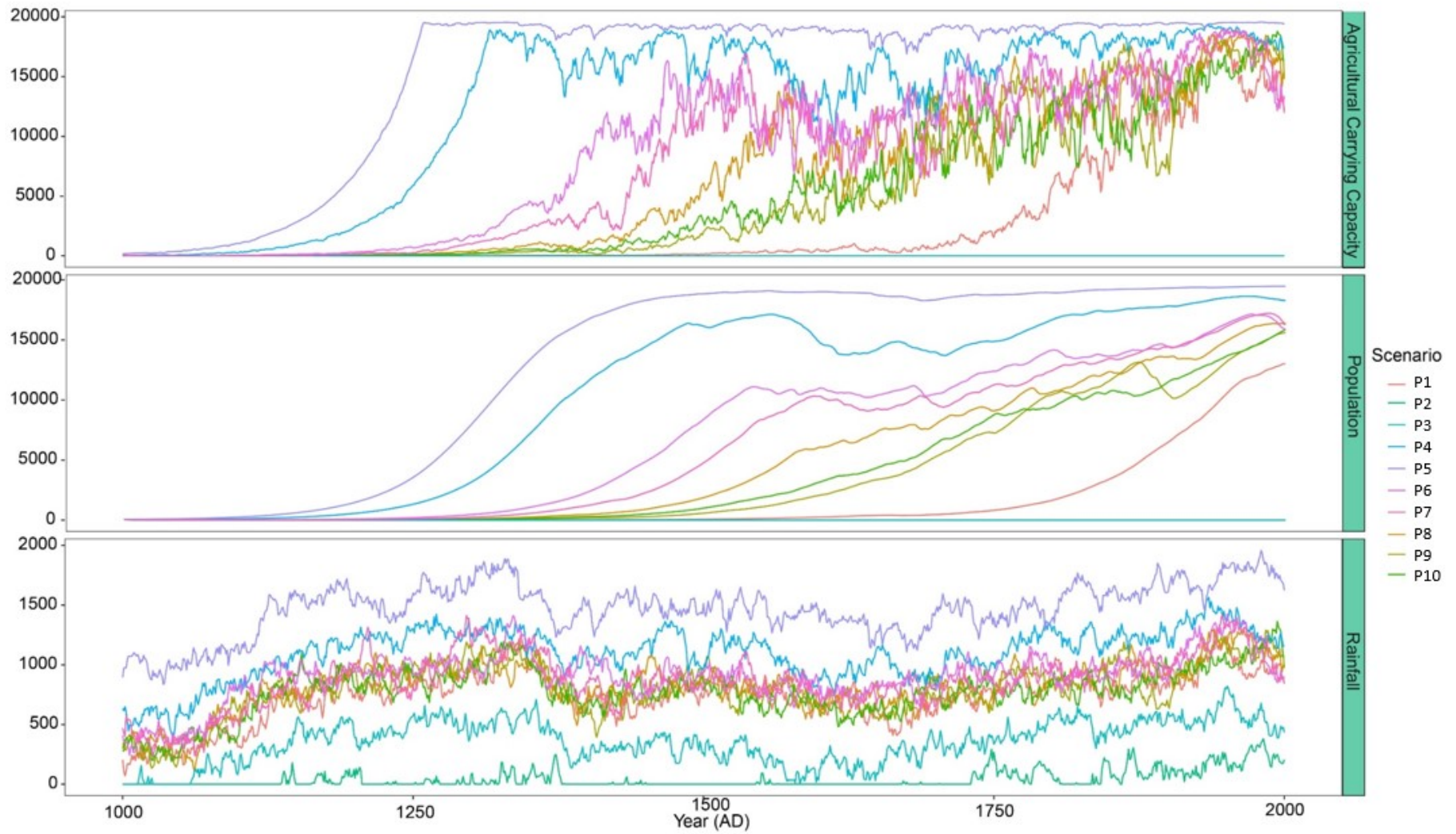


Figure 8.10: Model outputs for the 1000-year palaeo scenario showing the agricultural carrying capacity, population and rainfall outputs

### 8.7.3.2 2000-year palaeo sequence

Figure 8.11 shows the model outputs based on the full 2000-year palaeo sequence from Lanoto'o and assumes humans arrived 2000 years ago. Whilst factually incorrect, the outputs allow some insights into the reaction of a small island socio-ecological system to the longer-term hydrological change in the tropical Pacific. The patterns seen in this sequence are similar to those in the 1000-year sequence in terms of delay in growth and the overlap in some of the model outputs. However, over the 2000-year sequence that includes the two shifts to drier conditions, there is a divergence in these overlapping scenarios. Only scenarios P6 through P8 show a similar pattern of change. Scenarios P1, P9 and P10 show a notable departure during the recovery period following the first dry period and the impact of the second dry period. Running the model using the full 2000-year sequence shows the behaviour of the system to the two drying periods that occur relatively quickly one after the other. The model shows significant periods of stress upon island resources and island life around 700 AD and 1000 AD. The key finding to note is that the populations essentially collapsed in the second period of drought under scenarios P1, P9 and P10. As seen in the 1000-year sequence, scenarios P2 and P3 do not reflect precipitation series that are able to sustain a population as the precipitation is not high enough to provide adequate yields of taro.

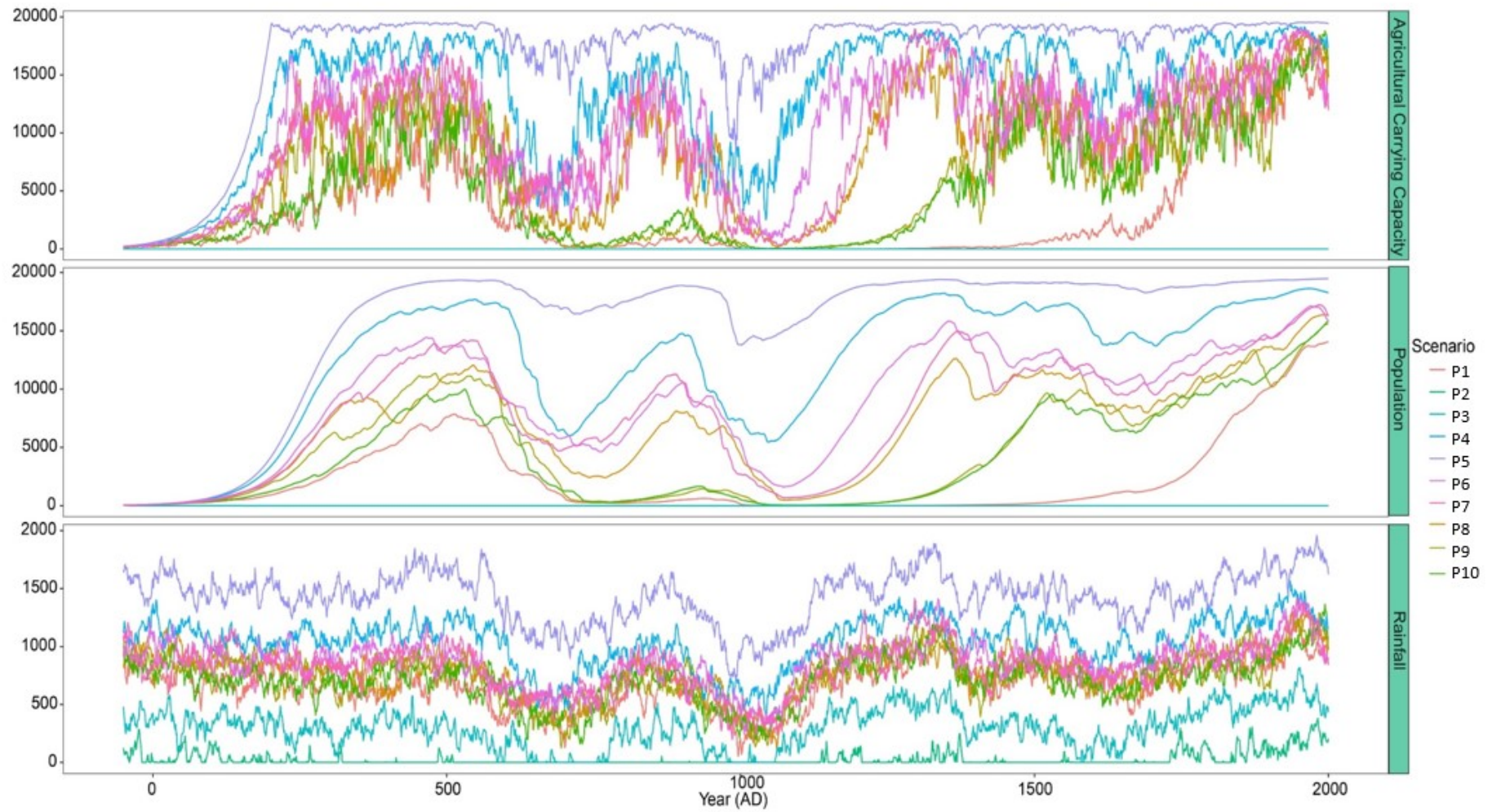


Figure 8.11: Model outputs for the 2000-year palaeo scenario showing the agricultural carrying capacity, population and rainfall outputs.

#### 8.7.4 Palaeo drought and population metrics

Figure 8.12 and Figure 8.13 show the drought and population metrics for each of the palaeo scenarios. For scenarios P2 and P3 in both the 1000-year and 2000-year sequences, the whole rainfall sequence is characterised as one large drought event as the rainfall sequence does not reach above 1000 mm and the population collapses almost immediately after arrival. All the other palaeo scenarios include this large drought event that has a large impact on the population early on when the population density is very low. This indicates how prominent this drought period likely was and the impact it would have had on island populations.

Palaeo scenarios P4, P6, P7 and P8 which represents the +50%, +25%, +20% and +15% of the error range for the dinosterol values show more of a similar pattern to the drought metrics from the earlier model scenario outputs particularly in Figure 8.12, which shows the outputs from the 2000-year sequence. Whereby, once the population density is high enough drought events start to have a bigger impact on population dynamics. The data from the 1000-year sequence shows the same drop in maximum population change through time with the low severity droughts. However, as population density increases, the impact of low severity drought events causes the population growth to drop until the start of a decline in population numbers from around 150 people/km<sup>2</sup> for scenario P6, around 200 people/km<sup>2</sup> for scenario P7 and P8. Scenario P4 with the highest rainfall levels has a higher population density of close to 300 people per km<sup>2</sup> due to the good taro yield provided by higher and more consistent rainfall.

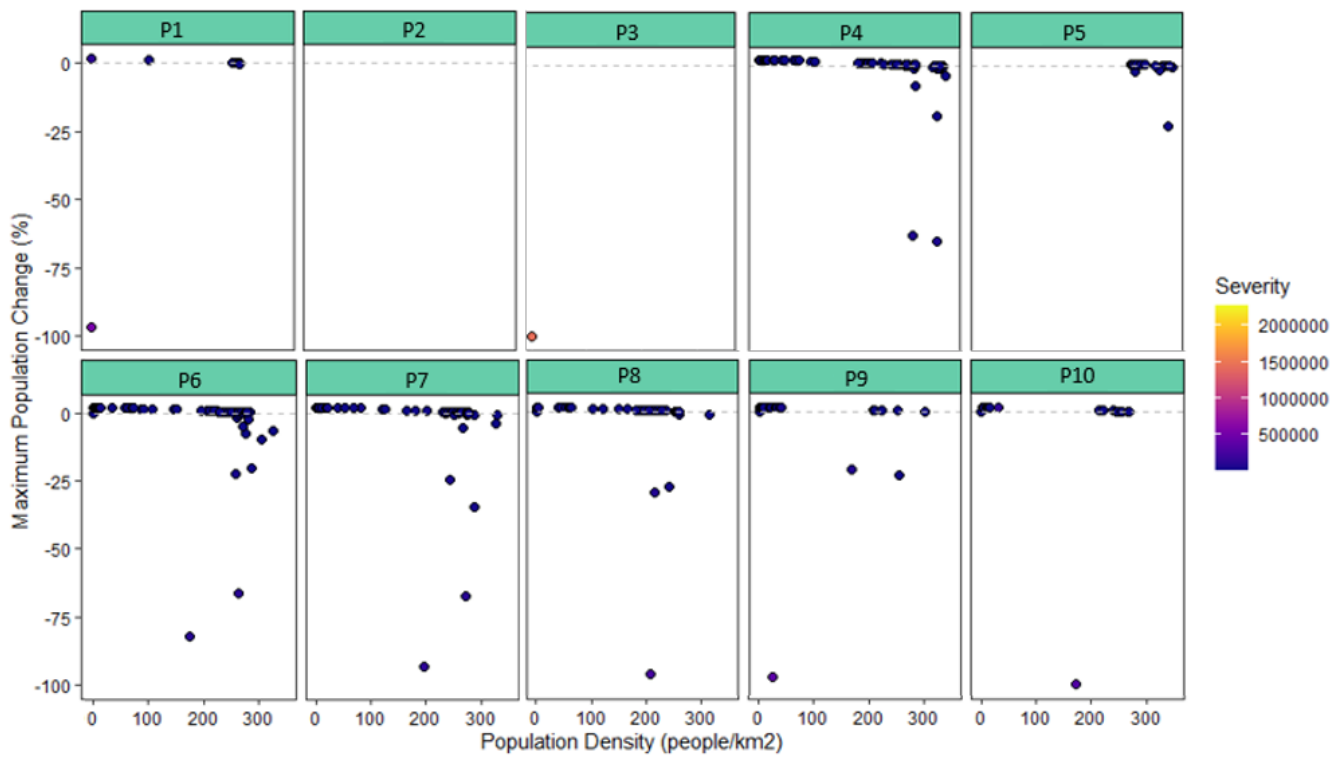


Figure 8.12: Graph showing the outputs from the drought and population metrics produced for the 2000-year palaeo scenario

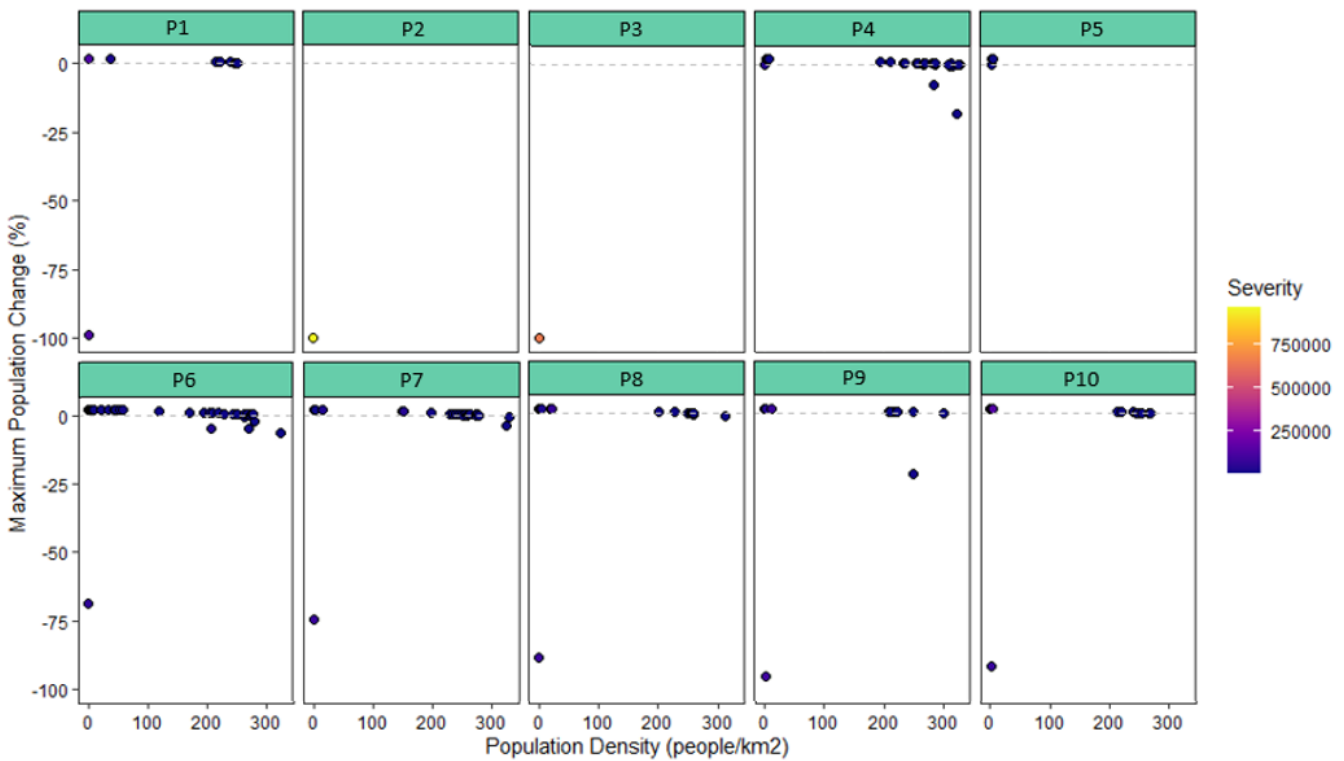


Figure 8.13: Graph showing the outputs from the drought and population metrics produced for the 1000-year palaeo scenario

### 8.7.5 Model Evaluation and Interpretation

Behavioural and structural testing involves determining whether the model adequately represents the observed system behaviour and to understand whether the model provides a reasonable representation of the real system (El Sawah *et al.*, 2017). This is difficult to do when modelling a prehistoric system, as there is no observed data available to compare with the model outputs and the modern-day system itself likely no longer functions in the same way. To evaluate the structure and outputs of this model, the alternative is to compare with existing palaeo and archaeological records. Another way to evaluate the model is to compare it to other models from the literature to see whether it produces similar behaviours. This will allow us to see whether the outputs are plausible and how useful the model is for understanding the socio-ecological system of Mangaia.

A comparison to Kuil *et al* (2016) is difficult as the climate, system and adaptations (the use of reservoirs) are quite different to Polynesian island life during the late Holocene. However, some models focus on agriculture and population dynamics in the tropical Pacific that provide a more useful comparison.

Kirch (2017) looked at the relationship between population and food availability in Hawaii and states that there are parallels to be drawn between the Hawaiian and Mangaian examples. From this, he postulated several theories on the population and agricultural dynamics:

- 1) Initially the limits on food production following colonisation was a shortage in available labour.
- 2) Over time, the population of the island would have rapidly increased and eventually reached the total carrying capacity of the island causing a negative shift in food availability. The drop in food availability would have limited fertility and increased mortality leading to an overall decline or upper limit on population numbers.
- 3) Environmental degradation – specifically deforestation and the associated erosion - would impact on the agricultural productivity of the island and the amount of suitable land
- 4) The shift from agricultural productivity being limited by labour to being limited by land availability would have taken approximately 250 years.

He drew parallels between the socio-ecological dynamics of Mangaia and the outputs of his 2012 paper which used a model to reconstruct the impact of agricultural intensification in Hawai'i (Kirch *et al.*, 2012). However, these observations were not followed through with an attempt to model the Mangaian system. The model presented in this chapter offers an opportunity to test some of the hypotheses Kirch set out in his 2017 monograph on Mangaian archaeology.

As discussed in section 8.5.3 the availability of labour was written into the model and this controls the amount of food that can be produced following initial colonisation as per Kirch's theory. As the population grows, so does the amount of food produced until the population hits the maximum amount of land that is able to be cultivated for wetland taro. In this instance, Kirch's theory was written into the model to reflect the most up to date knowledge of the Mangaian agricultural system.

When compared to the Kohala model created by Kirch *et al* (2012) (see Figure 8.14), the outputs of the model scenarios 3 and 4 in section 8.7.1 show a similar pattern of population growth with the smoother exponential rise following initial colonisation before levelling out when the population reaches the carrying capacity of the island or area, after which, the population fluctuates based on environmental factors. The fluctuations in the model scenarios 3 and 4 are notably larger than those in the Kohala outputs as the Hawai'i model takes into account other food sources. The Mangaia model focuses specifically on taro production and if other food sources were considered then the outputs would likely be more similar in terms of the lower rate of variability in the population numbers once they plateau at around the carrying capacity.

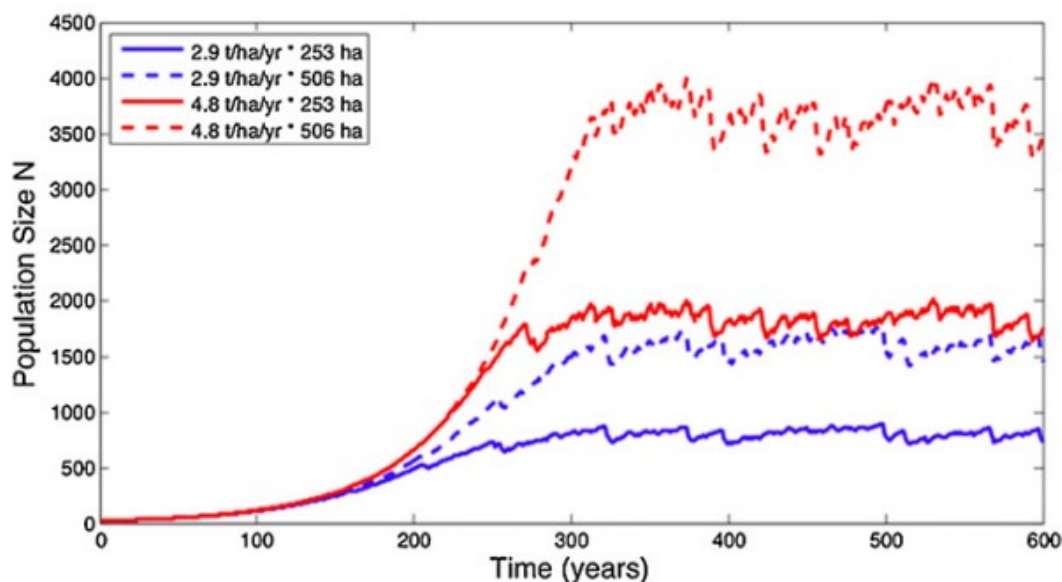


Figure 8.14: Model output from Kohala model showing population change over time taken from Kirch et al (2012).

Figure 8.15 shows the modelled total available food for scenario 4. After approximately 250 years, the amount of food available per person starts to decrease. If this graph is compared to the model output graphs in section 8.7.1 it is clear that the reason for this is that the population reaches the agricultural carrying capacity at around 250 years post-arrival. This is consistent with Kirch's theories on population growth and food availability and the timeline for reaching those thresholds. The model developed by Kirch et al (2012) utilised a modified nutrient cycling model, a demographic model and was more complex as it included marine resources, hierarchical social organisation and a more diverse agricultural system. Despite the two models being significantly different and representing different levels of complexity, they both show similar outputs, providing confidence in the model outputs and also indicates that this simplified model has likely still managed to capture the major dynamics of the system.

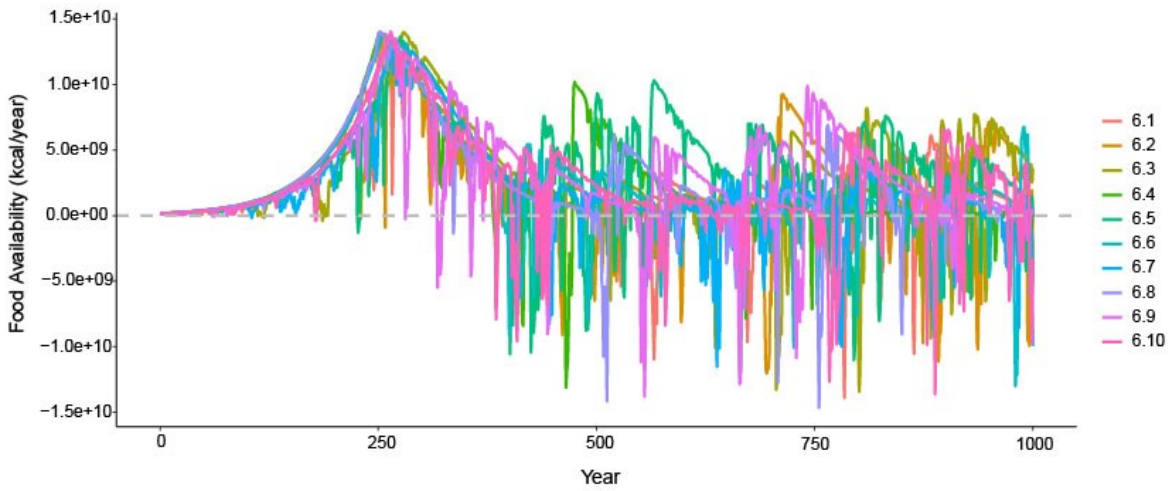


Figure 8.15: Total food availability model output from the model scenario 4.

Figure 8.16 shows the food availability for each of the palaeo scenarios run based on a corrected version of the Lanoto’o dinosterol precipitation reconstruction. It is clear that a majority of the palaeo scenarios indicate a much later peak in food availability than Kirch (2017b) has suggested and they peak much lower than those in the model scenario outputs with the exception of the palaeo scenarios P4 and P5.

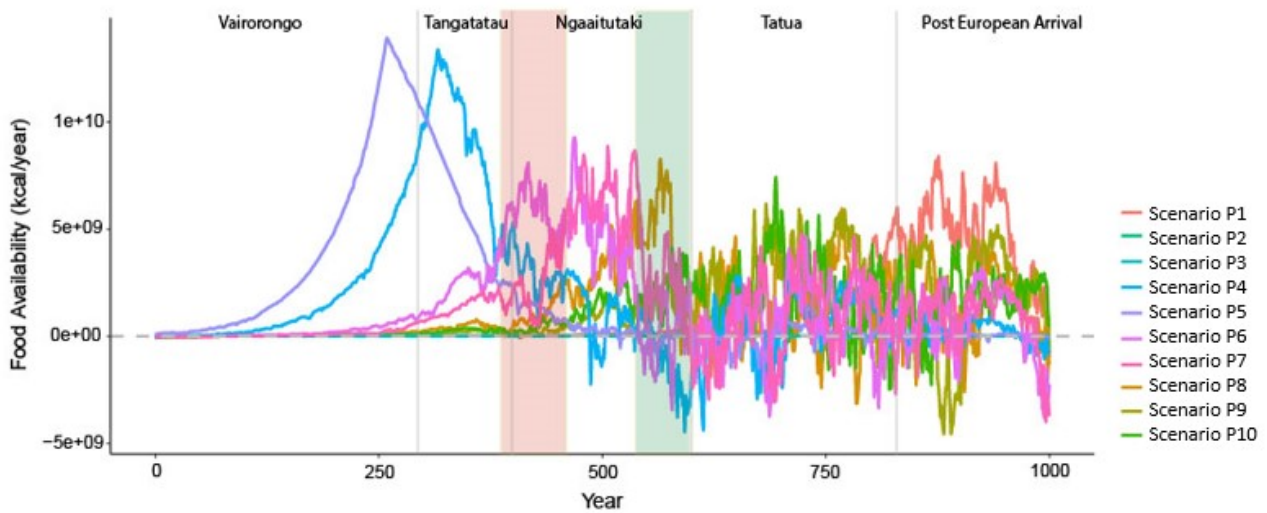


Figure 8.16: Total food availability model output from the palaeo scenarios. Red box highlights a period of conflict in Manganian history and the green box highlights a period where food production improved as per Kirch (2017). Grey lines denote the breaks between different periods of Manganian history with the name of each period labelled as per Kirch (2017).

Only the palaeo scenarios P4 and P5, which sit at the higher end of the dinosterol error, show a similar peak height to the model scenario data. Palaeo scenario P5, which reflects the absolute dinosterol error maximum, hits the peak in food availability at around 250 years. Whereas the food availability peak in scenario P4 comes in at least 50 years later. The next scenario to peak in scenario P6 which occurs at around 400 years post-colonisation and other palaeo scenarios subsequently peak after this point. This suggests that on Mangaia the food availability in relation to the key horticultural crop taro occurred later than normal due to adverse climatic conditions. The dinosterol mean value, represented by scenario P1, does not peak until 500 years post-human arrival.

Kirch (2017b) suggests that there was a period of stress on Mangaia toward the end of the Tangatatau phase (1300 – 1400 AD) between approximately 1250 AD and 1450 AD. During this time, there was a rise in conflict and a decline in the number of pig bones in the archaeological horizon with evidence of cannibalism from 1390 to 1470 AD – this is highlighted by the red box in Figure 8.16. The population had started living around the wetlands and developing horticulture during this period. An explanation for this based on the model outputs is that there is a gap between the start of exponential population growth and the peak in food availability (thanks to agricultural intensification of taro production) due to unfavourable conditions for taro production in the first century or so following human arrival. The models suggest that had conditions been more favourable in the first century following human arrival then the ramp up to agricultural intensification could have occurred at least a century earlier perhaps preventing this period of stress at the end of the Tangatatau phase.

Nevertheless, conditions appeared to improve on Mangaia following this period of stress with an increase of pig bones in the archaeological sequence within the Ngaaitutaki phase (1400 – 1600 AD) – highlighted by the green box in Figure 8.16. It is believed that the population peaked in Mangaia in this phase (Kirch, 2017b). Kirch (2017b) believes this improvement in food availability conditions were likely due to the intensification of agriculture and the introduction of the Sweet Potato. Palaeo scenarios P6, P7 and P8 show food availability increasing just prior to and over this period as taro agriculture expands.

Following this, a number of animals become extirpated in this period including some that were important food sources in previous phases and there is a higher level of violence –

these indicate stress on food availability again. In the palaeo models, around 550 to 600 years post-human arrival, which would equate to approximately 1550 to 1600 AD, the food availability drops down rapidly as the population grows.

The model findings are consistent in a number of ways with what we currently know about Manganian prehistory but highlight climate as a possible driver of population stress caused by the slowing of the intensification of agriculture due to adverse climatic conditions for the growth of taro. In the palaeo scenarios, the recovery of the population in the beginning of the Ngaaitutaki phase could be due to the late blooming of the taro agricultural intensification, which was delayed due to adverse climatic conditions around the time of colonisation.

A space-limited environment model based on the 'Opunohu Valley on Moorea, French Polynesia was introduced by Hamilton and Kahn (2007). Hamilton and Kahn's (2007) model relates to the model presented in this chapter in terms of the representation of a maximum carrying capacity. The difference is that Hamilton and Kahn's (2007) carrying capacity is an absolute maximum value whereas the value in the Mangaia model is a dynamic value through time similar to the Brandt and Merico (2015) Easter Island model. Their absolute carrying capacity was a population of 58,435, which comes out at a population density of 436 people per km<sup>2</sup>. The Mangaia model gave an absolute carrying capacity of 19,548, which gives a population density of 377 people per km<sup>2</sup>. This offers some confidence that the model is providing a relatively realistic output when compared to other similar models. However, this may seem relatively coincidental considering that the Mo'orea model takes into account a wider range of agricultural crops and soil properties. Hamilton and Kahn (2007) do admit that their maximum carrying capacity value is much higher than their population estimate based on the house-count method and instead suggest that this number is potentially twice what the valley would have actually produced so it represents an absolute maximum assuming optimum outputs. Similarly, a population of 19,548 is much higher than the estimated 3,000 in 1833 even if they had been decimated by an epidemic. In a number of the palaeo scenarios however, the population does not reach the absolute maximum carrying capacity as it does in the model scenarios that perhaps represent a more optimised system whereas the palaeo scenarios do appear to present a relatively more realistic estimate.

The sensitivity tests presented in section 8.6.1 showed that despite the alterations to parameter values, the model still displayed the same behaviour over time but the speed of those changes increases or decreases in reaction to the different parameter values, as would be expected. This offers confidence that the model is not producing certain behaviours because of a particular parameter value choice, which provides confidence in the robustness of the model outputs. Even in an extreme case, illustrated with a 50% alteration in parameter values the model does not produce significantly different model behaviours, showing that the model is not that sensitive to the tested parameters suggesting the results are robust to these uncertainties. The results presented in this chapter from the model outputs in section 8.7 also provided a sensitivity test for the rainfall input. There is however evidence of thresholds of change particularly with the changes in rainfall data, as shown in palaeo scenarios P2 and P3 (Figure 8.10) suggesting the model has some sensitivities to rainfall above or below 75% of the mean where the population essentially collapses. This suggests that the scenarios showing some of the extreme ends of the possible rainfall profiles should be considered with care. However, those scenarios do suggest extreme changes in the precipitation amount. The variation in rainfall values for the palaeo scenarios is high due to the uncertainty from palaeo data sets, which is a limitation that can only be overcome with new local quantitative palaeo records with lower uncertainties in the calibration profile. The impact of uncertainty around rainfall and the other parameters should be considered when evaluating the model outputs, however the overall response of the model is likely robust.

### **8.7.6 Limitations/Further development**

As per the sentiments expressed by Brandt and Merico (2015), this model attempts not to edge into an overly complex representation of this system. The model aims to be a representation of Mangaia stripped down to its key and most important components and feedbacks. Due to this, when this model is compared to the socio-ecological system of Mangaia described in the earliest sections of this chapter, it is clear that there are some aspects of the system that have not – at this stage – been represented.

To keep the model from becoming overly complex, water resources were excluded as a component. There is information available in the archaeological and ethnohistorical record surrounding agriculture and irrigation on Mangaia, whereas there is essentially no

information on stream flows and domestic water use during this period adding additional uncertainty. Therefore, there is no justification to add further complexity given the lack of data and knowledge of how water was used.

The model represents a mono-crop society by focusing on taro as it was a key staple crop. However, Polynesians were a multi-cropping society with food adaptation strategies to deal with extreme conditions. The introduction of multi-cropping and simulating the switch between resources during times of hardship would likely reduce the magnitude of the fluctuations seen in the population outputs in scenarios 3 and 4 to become something more like the Kirch et al (2012) outputs. Further to this, early settlers to the island and founding settlements would have initially utilised wild resources as primary food sources including bats, birds, fish and wild growing vegetation. In other parts of the Pacific, isotopic studies have shown that first settlers depended on foraging and wild animals for sources of food prior to the establishment of agricultural crops (Kinaston, Buckley, *et al.*, 2014). The inclusion of wild resources would have allowed for a higher carrying capacity for the island and perhaps a buffering of the impact of drought by switching to alternative sources of food. However, it is difficult to identify and quantify the wild resources available during this time and how they were used in the early stages of settlement in Mangaia. Very little is known about the first arrival of humans and their diet on this island (Kirch, 2017b). Adding a simple representation of "resilience" that integrates these missing effects could help to reconcile and understand the model outputs with other evidence.

There was evidence of resource management within Mangaian society from ethnographic studies (e.g. Hiroa, 1934). When certain resources came under pressure including agricultural and marine stocks a meeting of the district and sub-district chiefs was called and a closed season or ra'ui was declared by the "Ruler of Food" that affects the whole island until the season is reopened once the relevant stocks have replenished (Hiroa, 1934, p. 141). Resource and land management are not included as components in this model. However, despite this example of resource management, Mangaia was also subject to poor land management and the model does not account for environmental degradation. As land is cleared for agriculture there is an increase in erosion – as seen in the palaeo record (Ellison, 1994) – which impacts on the ability of the land to cultivate crops (Ladefoged, Flaws and Stevenson, 2013). Further to this, nutrients and soil

productivity are not considered as per Kirch (2012) – instead the current model assumes that the nutrients and soil productivity are homogenous across the taro swamp. This element of the system would be more relevant if other land types were included e.g., makatea, highland valleys etc. Only one land type is represented and it is assumed in the current model that nutrient availability and soil productivity is uniform.

In terms of the population component, the model assumes a homogenous age distribution. This could be developed further to represent a realistic distribution as per Puleston and Tuljapurkar's (2008) space-limited population model. In reality, the percentage of labourers assumes a certain percentage of work capable and non-work capable population. This is partially included by selecting a percentage of the population capable of working in agriculture, but this could be developed further to understand the importance of age structure and possible feedbacks that are age dependent.

In the Easter Island model developed by Brandt and Merico (2015) they included an epidemic component to their model to represent the introduction of diseases by Europeans. In the palaeo scenarios explored in this chapter, the population continues to grow through to the year 2000 AD. Whereas, we know that the population of Mangaia was decimated by illness following the arrival of Europeans in 1824 (Williams, 1837). The focus of this model was specifically to understand the prehistoric socio-ecological system rather than reconstruct the population dynamics through to the post-contact period.

Whilst there are a number of elements in this socio-ecological system that could be introduced and built into the model, the aim was to maintain simplicity and therefore interpretability by representing the key components and feedbacks to understand the broader socio-ecological processes during the periods of human migration in the tropical South Pacific. Future work may look to develop this simple model to better represent some of the elements described here but for the purposes of this thesis the model did provide insights into how changing hydrological conditions impacted on prehistoric island life.

## **8.8 Summary**

To summarise, this chapter introduced a new systems dynamics model of the Mangaian socio-ecological system. The model and the outputs presented indicate that population

density plays a part in how droughts affect island systems. Also, drought duration rather than frequency was the key drought characteristic that brought about the largest changes in population and agricultural carrying capacity. The palaeo scenarios showed that the dry period concurrent with human arrival on Mangaia would have slowed the growth of the population as rainfall levels were low enough to impact upon taro yields during initial colonisation. In addition, the 2000-year sequence showed how the two drier periods in the Lanoto'o record would have had a major impact on island systems like Mangaia and this perhaps could be projected onto other island systems in the Pacific.

Allen (2006) suggested that it was important to understand how climate change specifically impacts upon island resources separate from other social factors such as population growth, economic intensification etc. It is difficult to disentangle population from island resources as the human population is part of the socio-ecological system. Nevertheless, whilst simple, this model does provide some useful insights into the socio-ecological system of Mangaia during the late Holocene. This is the first model of prehistoric island life that utilises rainfall palaeo data to understand how changing hydrological conditions affects agricultural and population dynamics. Future work may seek to develop this model further and represent more elements of the socio-ecological system, but this model lays the groundwork towards that endeavour.

## **Chapter 9 Discussion**

### **9.1 Introduction**

Following on from the two palaeo records presented from Emaotfer Swamp in Chapter 6 and Lake Tiriara in Chapter 7, this discussion will provide a comparison between these records and other existing records in the tropical South Pacific to identify the overarching changes in hydroclimate across the Pacific during key periods in human history for this region. The second part of this discussion will consider whether drought or changing hydroclimate was a driver for human migration and subsequent colonisation by providing a comparison between the socio-ecological model outputs presented in Chapter 8 along with archaeological and palaeoenvironmental data from the region. This chapter will conclude with a short summary identifying the main findings from this discussion.

### **9.2 Palaeoenvironmental change surrounding periods of human migration and colonisation in the tropical South Pacific**

To follow on from the interpretation of the data from Emaotfer Swamp and Lake Tiriara in Chapter 6 and Chapter 7 respectively, this section seeks to provide a comparison of these new records from Emaotfer Swamp in Vanuatu & Lake Tiriara in Mangaia, Cook Islands against other records in the Pacific to draw conclusions around climatic change during key periods of human migration.

#### **9.2.1 Palaeoenvironmental change in Early to Mid-Holocene and surrounding first wave of migration c. 3000 yr BP**

Overall, there are very few records from the tropical South Pacific that date back beyond 3,000 yr BP and the first wave of migration into the tropical Pacific, and even fewer to 9,000 yr BP that can be compared to the Emaotfer Swamp record. Figure 9.1, presents records from Samoa, Cook Islands and North-Eastern Australia that have continuous records going back beyond the first wave of migration and allow for a comparison to the Emaotfer Swamp record presented in this thesis. Where the records disagree is over the

two larger shifts in the  $\delta^{18}\text{O}$ , the first being the wetter period just after ca. 8,000  $\pm$ 780 yr BP. In other records from the tropical Pacific including Samoa, that period is presenting a slightly drier period according to the dinosterol record but other proxies such as Ti also indicate a drier period (Figure 9.1-B and C). This shows some disagreement between two of the geographically closer records over notable shifts in hydroclimate in the Emaotfer record over hydroclimate proxies. In the original data presented by Hassall (2017) the 8.2 event matched up well with the Emaotfer record, however in Figure 9.1 the Lanoto'o data is presented using an updated age model (D.Sear, pers comm, June 2023) that pushes that wet event closer to 9200 yr BP and other records from across the Pacific region do not show a wet event in their records till around 7,000 yr BP. This could be due to the large uncertainties in the Emaotfer Swamp age model that for this suggested 8.2 event could be shifted by 285 to 780 years based on the 2-sigma error meaning the synchronicity between different island records is difficult to distinguish particularly in the deeper part of the records including this wet event in zone E-3. There is concurrence in the dry signal around 6,100 yr BP that also appears in the Lake Lanoto'o record. The record from Atiu in the Cook Islands starts shortly before this shift toward drier conditions but the start of the record does indicate a considerable drop in precipitation around this time. The  $\delta^{18}\text{O}$  record from Emaotfer Swamp does not show any extreme fluctuations from around 6,000 years through to present and overall conditions appear to be getting gradually wetter during this time but are relatively constant through to the end of the lake section. However, around the start of the first wave of migration at approximately 3,000 yr BP, there is a slight dip in the  $\delta^{18}\text{O}$  values suggesting a slight drying during this time. The isotopic data from clam shells taken from New Caledonia and Vanuatu indicate that conditions around the first wave of migration (approx. 3000 yr BP) were drier than modern conditions (Duprey et al, 2014). The Australian record (Figure 9.1-E) whilst sitting at the end of the western Pacific region does provide a quantitative 7,700 year record of precipitation changes and has similar responses to larger climatic oscillations such as ENSO as the Western Pacific Islands. This record from Swallow Lagoon similarly suggests that conditions are relatively stable if not moving overall towards wetter conditions in the lead up to 3200 yr BP. This record does appear to have a notable permanent downward shift in average precipitation values around 3200 yr BP alongside an increase in variability. The record indicates that the climate mean state in the Pacific is drier overall leading to

an increase in the frequency of anomalous dry years. However, the paucity of records available to compare to the Emaotfer Swamp record makes it clear that further work needs to be carried out to improve our understanding of Holocene climate change in the tropical South Pacific.

Contrastingly, the record from Samoa (Figure 9.1-B) shows that in the lead up to the first wave of human migration conditions were becoming relatively wetter showing perhaps that these shifts to wetter conditions were occurring across the western side of the South Pacific at least, though this quickly shifts towards drier conditions following this period. This is also supported by the record from the Galapagos that shows an overall shift toward wetter conditions in the present day (Atwood and Sachs, 2014; Zhang, Leduc and Sachs, 2014). This sits in stark contrast to many records across the Pacific such as the ones presented in Figure 9.1, which point towards a shift overall toward drier conditions during the same period and that conditions in the present are wetter than in the past. This would suggest that there was some level of change towards drier conditions along with a higher level of spatial variability in precipitation around the time of the first wave of human migration. However, when viewed in concert with other records from across the SPCZ region, this notable change is not discernible in all records and in fact in some records sits in direct disagreement. Though both the leaf wax and the Ti/inc records from Lanoto'o from Hassall (2017) show a drying phase starting approximately 400 years after the start of colonisation of remote Oceania. This highlights the importance of using a range of records across the region of interest to identify the key patterns of change rather than relying on records from the periphery. This also highlights the importance of robust age models as the errors associated with the Emaotfer Swamp age model presented in section 6.2.3 means that there is a high level of uncertainty around the timing of changes but agreement with other regional records particularly with the mid-Holocene drying phase highlighted in Figure 9.1 and later the dry period around 1000 AD, which is discussed further in the next section, provides some confidence in the age model within younger parts of the Emaotfer sequence.

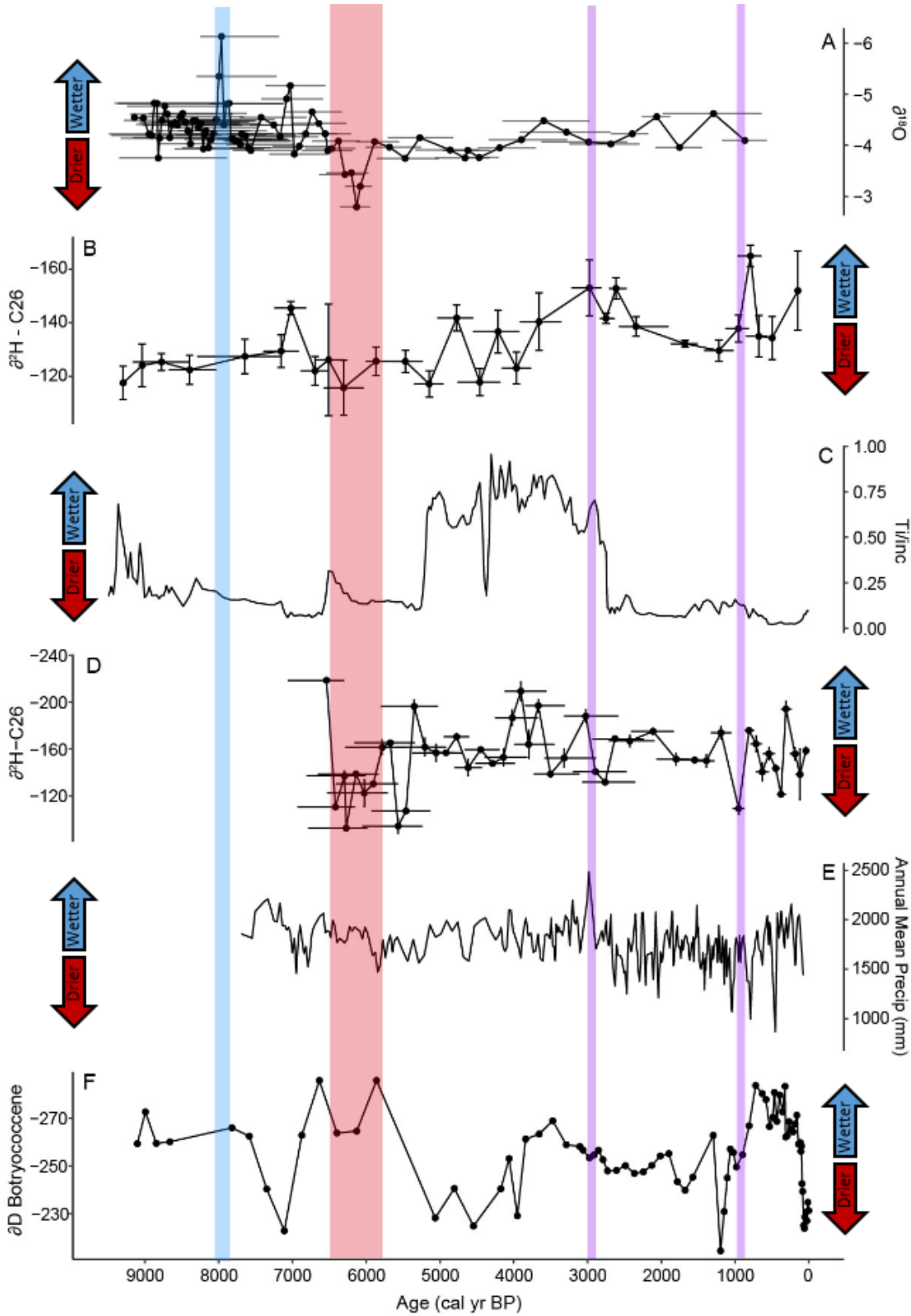


Figure 9.1: Comparison between palaeo records from Australia, Melanesia and Polynesia. A – Emaotfer Swamp  $\delta^{18}\text{O}$  (‰ VPDB) record from Efate, Vanuatu (this thesis), B –  $\delta^2\text{H-C}_{26}$  (‰ VSMOW) biomarker record from Lake Lanoto’o, Samoa (Hassall, 2017), C – Ti/inc record from Lake Lanoto’o, Samoa (Hassall, 2017), D –  $\delta^2\text{H-C}_{26}$  (‰ VSMOW) biomarker record from Lake Teroto, Atiu, Cook Islands (Hassall, 2017), E – Annual

Mean Precipitation (mm/year) derived from carbon isotope ratios from Eastern Australia (Barr et al, 2019) and F - Botryococcene (‰) from Lake Junco – Galapagos (Zhang et al, 2014). Blue box denotes the wet event identified in the Emaotfer Swamp record, red box denotes dry period identified in Emaotfer Swamp record and purple boxes denote the start of the two periods of human migration in the tropical Pacific.

### 9.2.2 Palaeoenvironmental change surrounding second wave of migration c. 1000 yr BP/MCA

Over the past few decades, a number of new records covering the Common Era have been published from the tropical South Pacific that has developed our knowledge of climate conditions around the second wave of migration across the Pacific but specifically Eastern Polynesia (Figure 9.2 and Figure 9.3).

There is consensus particularly between the new Mangaia data and the existing Atiu records. The Mangaia  $\delta^{18}\text{O}$  record has age model uncertainties that overlaps with similar trends in the Atiu  $\delta^2\text{H}$  leaf wax (Sear *et al.*, 2020) that show at the transition into the MCA conditions were relatively dry though following this both the Mangaia  $\delta^{18}\text{O}$  and Atiu  $\delta^2\text{H}$  records indicate that as the MCA progressed there was a shift to wetter conditions. As discussed in section 7.9.1.2. the shift in diatom community from one dominated by *Pseudostaurosira brevistriata* to one dominated by *Rhoplodia gibberula* could also indicate a possible shallowing of Tiriara or shift toward wetland conditions (Gasse and Fontes, 1989; Sylvestre *et al.*, 1995; Cocquyt and De Wever, 2002; Owen *et al.*, 2004; Yacobaccio and Morales, 2005) due to dry conditions occurring around human arrival to the island. This pattern is also seen in the Samoan  $\delta^2\text{H}_{\text{dinosterol}}$  record (Sear *et al.*, 2020). The Toomey (2016) record (Figure 9.3-C) shows more subtle variations. There is an overall shift upward in the average value of the Ti/Ca at around 1000 yr BP. This likely represents an increase in the amount of available material due to human activity on the island perhaps but the Mangaia and Atiu records both indicate a shift to wetter conditions within the MCA following the initial dry conditions. However, Ti/Ca is not a direct precipitation proxy, as it can be influenced by erosion and marine processes. Discounting the Toomey record, the other hydroclimate records from this region indicate that there

was likely a shift to drier conditions in the lead up to the second wave of human migration across the Pacific into Eastern Polynesia. Furthermore, several records from Melanesia also indicate a shift to drier conditions during this time indicating that this was a climatic shift that impacted large areas of the tropical South Pacific. For example, a  $\delta^2\text{H}$  dinosterol record from Efate on Vanuatu – the same island as the Emaotfer Swamp – found that there was a notable shift toward drier conditions at the start of the MCA, which fits with the potential hiatus, drying of the basin and later development of peat at Emaotfer also located on Efate (Sear *et al.*, 2020; Maloney *et al.*, 2022). The Samoan  $\delta^2\text{H}$ -C<sub>26</sub> leaf wax record (see Figure 9.1-D) from Hassall (2017) and the  $\delta^2\text{H}$  dinosterol record (see Figure 9.3-E) from Maloney *et al* (2022) show a period of drying leading up to the second wave of migration. This fits with the hypothesis that there was potentially a hiatus in the Emaotfer record just prior to the start of the peat sequence. In the Samoan record there is a large spike just following the second wave of migration that would have allowed for the development of a swamp in the dried up Emaotfer basin following human arrival in Eastern Polynesia. This would account for the decrease in the accumulation rate leading up to this point and the development of peat in the top part of the sequence.

Based on this evidence, a dry period that occurred around approximately 1000 AD appears in records in both Melanesia and Polynesia. This indicates that this shift in the hydroclimate was felt across multiple regions in the tropical South Pacific and the timing coincides with the second wave of migration into Eastern Polynesia.

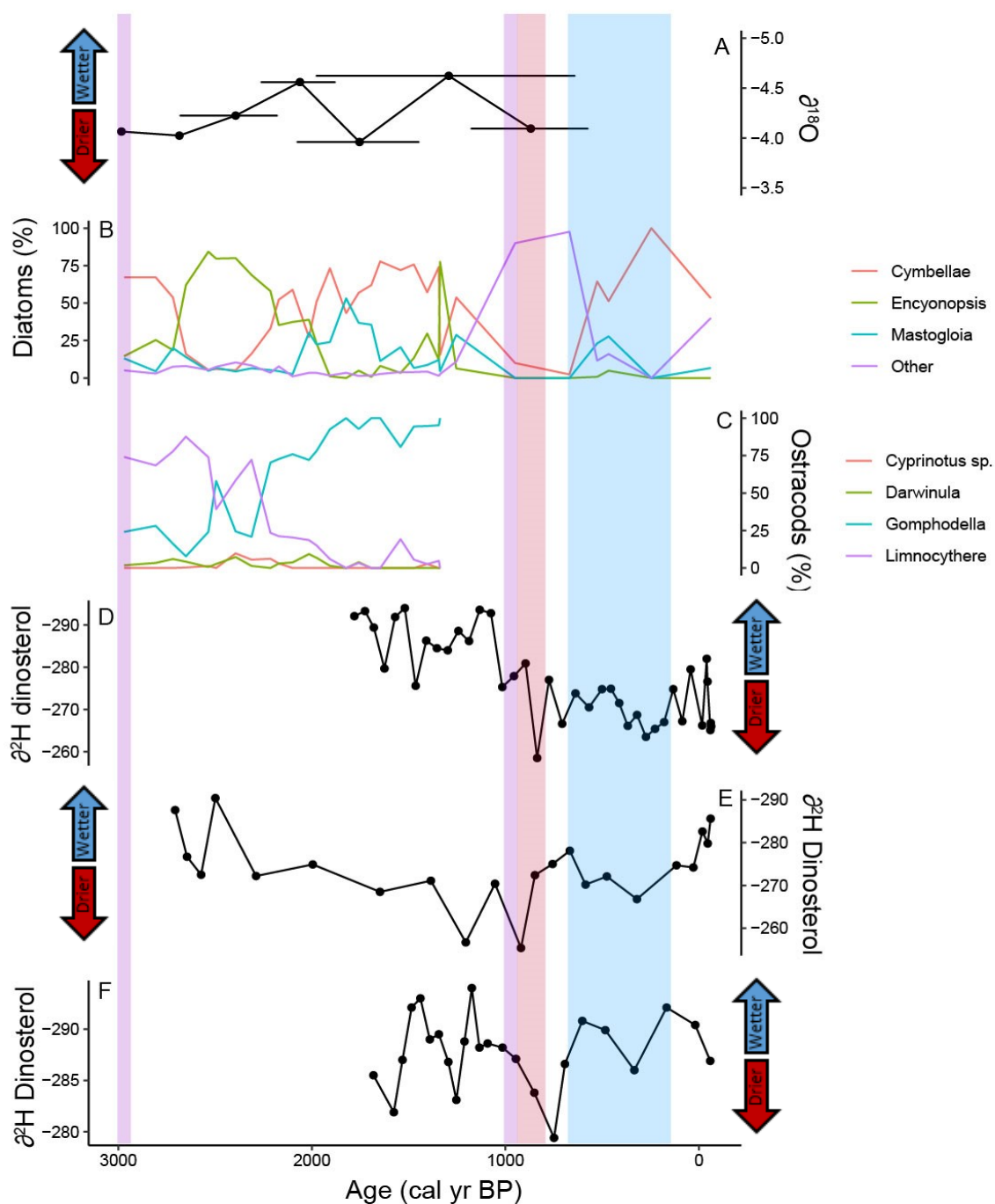


Figure 9.2: Comparison between palaeo records from Melanesia and Western Polynesia over the past 3,000 years. A – Emaotfer Swamp  $\delta^{18}\text{O}$  record from Efate, Vanuatu (this thesis), B – Diatom record from Emaotfer Swamp, Vanuatu (Wirrmann et al, 2011), C – Ostracod record from Emaotfer Swamp, Vanuatu (Wirrmann et al, 2011), D -  $\delta^2\text{H}$ -dinosterol (‰ VSMOW) biomarker record from Lake Emaotul, Vanuatu (Maloney et al, 2022). E -  $\delta^2\text{H}$ -dinosterol (‰ VSMOW) biomarker record from Lake Lanoto'o, Samoa (Maloney et al, 2022), F –  $\delta^2\text{H}$ -dinosterol (‰ VSMOW) biomarker record from Lac Lanutavake, Wallis (Maloney et al, 2022). Purple boxes denote the start of two

waves of human migration, the red box denotes start of dry period, the blue box denotes start of wetter condition.

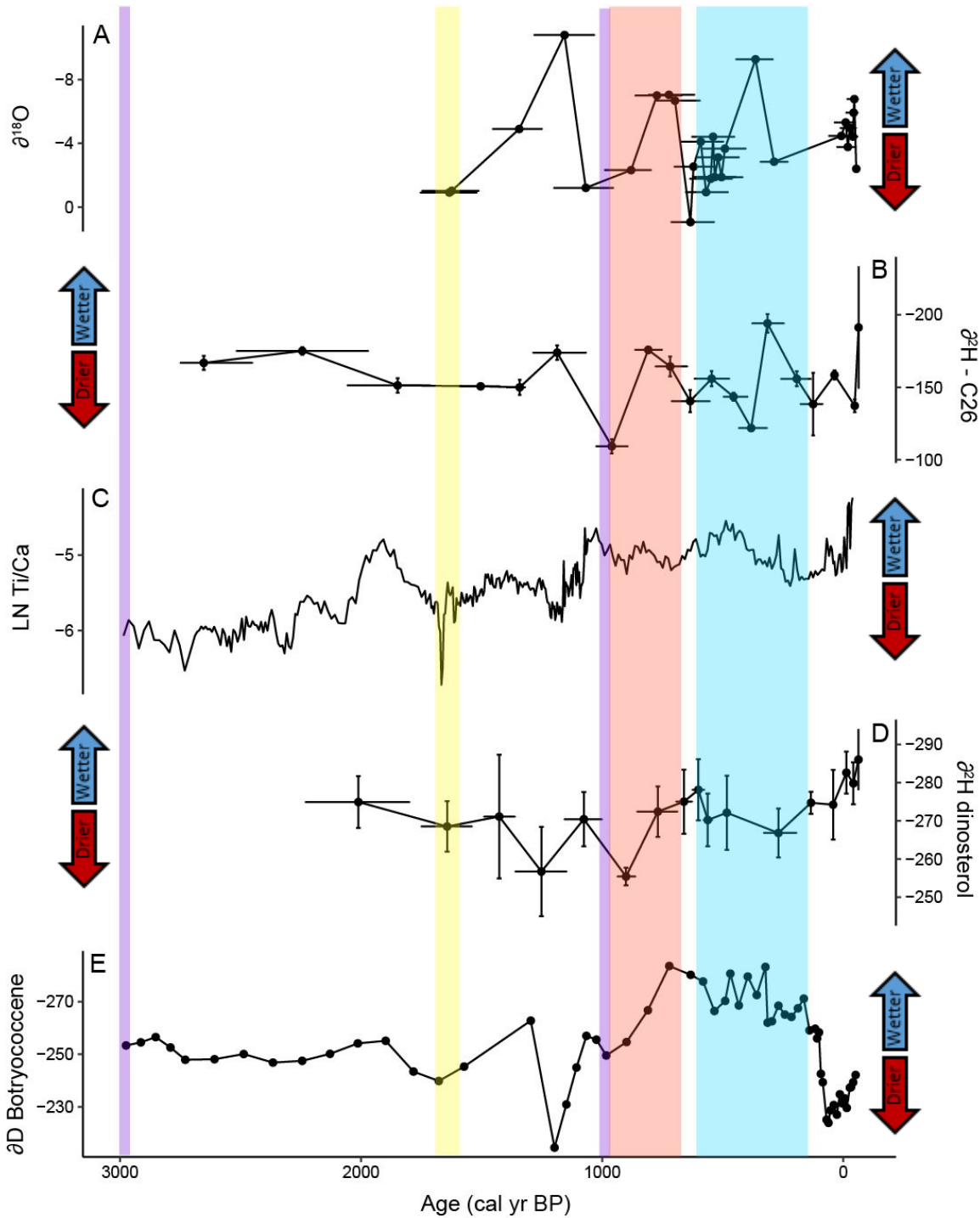


Figure 9.3: Comparison between palaeo records from Polynesia. A - Lake Tiriara  $\delta^{18}\text{O}$  record from Mangaia, Southern Cook Islands (this thesis), B -  $\delta^2\text{H}$  Dinosterol (‰ VSMOW) record from Lake Teroto - Atiu, Southern Cook Islands (Sear et al, 2020), C - Ti/Ca record from Apu Bay, Society Islands (Toomey et al, 2016), D -  $\delta^2\text{H}$  Dinosterol (‰ VSMOW) record from Lake Lanoto'o - Upolu, Samoa (Sear et al, 2020) and E - Botryococcene

(‰) from Lake Junco – Galapagos Zhang et al, 2014) .The red and blue rectangles denote the MCA and LIA periods respectively. The purple lines represent the timing of the two waves of human migration in the tropical South Pacific. Yellow denotes the tsunami layer event timing from the Mangaia sequence.

### **9.2.3 Palaeoenvironmental change in the MCA-LIA transition c. 1300 AD**

There is evidence for a second dry period about 300 years after the initial colonisation of Eastern Polynesia across multiple records. The  $\delta^{18}\text{O}$  record from Lake Tiriara and the  $\delta^2\text{H}$   $\text{C}_{26}$  leaf wax from Atiu (Sear *et al.*, 2020), show a significant shift toward dry conditions in the transition period between the MCA and the LIA (Figure 9.3). We know from archaeology that the population turned to cannibalism between 1390 AD and 1470 AD. Kirch (2017b) theorised that this indicated that there was pressure on the population during this period, possibly due to a resource depression that occurred between the Tangatatau (1300-1400 AD) and Ngaaitutaki (1400-1600 AD) phases in the Tangatatau sequence. Further afield, Maloney et al (2022) found the same signal in a lake sequence from Efate in Vanuatu where there was an almost 20 ‰ drop in dinosterol values or 2 mm/day change within the MCA-LIA transition (Figure 9.3-D), indicating that it is possible that this event too was felt elsewhere within the tropical South Pacific. In Wallis, the record from Lac Lanutavake (Maloney et al, 2022) there is also a relatively rapid drop in precipitation through the MCA, which reaches its absolute lowest values during the MCA-LIA transition (Figure 9.2-F). The agreement of the  $\delta^{18}\text{O}$  record from Lake Tiriara with other records within the same locality but also within the wider region provides confidence in the interpretation of the  $\delta^{18}\text{O}$  as a hydroclimate signal and demonstrates that a regional drying phase occurred during the start and progression of the colonisation of the east pacific by Polynesians.

### **9.2.4 Palaeoenvironmental change surrounding the LIA c.650-100 yr BP through to present**

There is a divergence between the records across the LIA. Again, the Mangaia and Atiu records show a similar pattern of rainfall change with the LIA starting with relatively drier

conditions before shifting towards wetter conditions in the latter half of the period. Whereas the Samoan record shows a continuous drying trend throughout the LIA and only from  $134 \pm 15$  cal yr BP do conditions start to get wetter, which persists through to the present day. However, the error bars associated with the data from Samoa mean that there is a higher level of uncertainty around the direction of change as the range of possible values could potentially be lower indicating a drop rather than an increase in the precipitation rates. Conversely, the errors on the  $\delta^{18}\text{O}$  and dinosterol record from Atiu are much smaller, meaning greater relative confidence can be ascribed to these records. Taken together and accounting for analytical and age model uncertainties, the combined records point to a shift to dry conditions around the time of the second wave of migration into the east Pacific. There is also strong evidence for a second dry period that started in the transition period between the MCA and the LIA and persisted into the beginning of the LIA. However, further work needs to be done to refine the timing of these dry periods as the errors on some of these data sets mean that it is difficult to precisely identify when these changes in hydroclimate occurred.

### **9.3 Was drought/changing hydroclimate a driver of human migration in the tropical South Pacific during the late Holocene?**

When discussing drought in relation to the records presented in this thesis, do we really have the resolution to pick out individual drought events? The carbon isotope record from Swallow Lagoon in Australia, which sits at the edge of the western Pacific has generated a record that could pick out individual drought events, but it is unique in its resolution. A majority of the records from the tropical Pacific do not have the resolution to pick up individual short-term drought events (annual or inter-annual) so most of the changes discussed thus far are looking at more long-term shifts (decadal, multi-decadal or even centennial) in overall hydroclimate. Only the stalagmite records such as the ones from the Solomon Islands (Maupin *et al.*, 2014) and Vanuatu (Partin *et al.*, 2013) have the resolution to pick up such changes but they are limited in terms of time scale, only going back to a maximum of 600 years. Nevertheless, these lower resolution records particularly from swamps and lakes can offer important insights into the larger, more regional changes in hydroclimate, reflecting changes in the mean state or longer-term

changes in overall precipitation (e.g. Smittenberg *et al.*, 2011; Zhang, Leduc and Sachs, 2014; Sear *et al.*, 2020; Maloney *et al.*, 2022).

The model results presented in Chapter 8 suggest that drought has a more significant impact upon a population once it starts to reach the carrying capacity threshold of the island they inhabit. The model results also suggest that the severity, which is a combination of both duration and intensity, is more important than frequency in terms of the impact it has on food availability and the associated population dynamics. Those impacts become more severe as the population density on the island increases. The amount of available food per person declines as the population starts to reach the maximum carrying capacity of the island leaving no room for mitigation of impacts. Considering this, this section seeks to bring together the palaeoenvironmental data both new and existing with archaeological records from the existing literature and the model outputs generated in this thesis to consider whether drought was a driver of human migration in the tropical South Pacific during the late Holocene.

### **9.3.1 Drought and the first wave of migration into Remote Oceania c. 3000 yr BP**

The first wave of human migration into remote Oceania occurred approximately 3,000 yr BP. The data generated from Emaotfer Swamp does suggest a slight change towards a drier hydroclimate during this period based on the current age model. As discussed, the  $\delta^{18}\text{O}$  do not show any extreme fluctuations during this period. However, overall conditions are getting drier during this time (approximately 3000-2300 yr ago) and other records that date back to that first wave of migration and beyond show conditions become relatively drier. Other records from the western-central South Pacific such as the record from Lake Lanoto'o in Samoa (Hassall, 2017) suggests that conditions were actually wetter than they had been previously so during the first wave of migration into remote Oceania, climatic conditions were not showing patterns that would bring about resource stress on islands. The higher resolution quantitative record from Australia suggests that perhaps there was a shift around 3,200 yr BP toward a drier mean state and rainfall became much more variable (Barr *et al.*, 2019). However, these patterns are not universally seen in the Pacific record either due to resolution or perhaps their proximity

to the SPCZ means that the signal is different compared with those records at the periphery of the western Pacific. The lack of records and the resolution on the current records available, including the one presented in this study, makes it difficult to identify the changes in hydroclimate across the South Pacific around the period of the first wave of migration into remote Oceania. Based on current evidence, it does appear that there is a potential connection between climate and the first wave of migration by the Lapita into Remote Oceania. However, the timing and rate of change are still debatable and require additional work to refine. The islands in Melanesia have the lowest minimum distance between islands compared with other regions of the Pacific (Montenegro, Callaghan and Fitzpatrick, 2014). The relatively short distances between a large number of uninhabited islands could have been the primary driver of the first Lapita wave of migration through Melanesia (Bedford and Spriggs, 2014) as the islands offered new lands and new resources for the Lapita civilisation if climatic conditions cause resource stress.

### **9.3.2 Drought and the “Long Pause”**

One of the key questions surrounding the timing of human migration into the Pacific is why there is such a long gap - dubbed within the literature as the “long pause” - between the first wave into Remote Oceania and the second wave from Western Polynesia through to the three pinnacles of the Polynesian Triangle (Irwin, 1992; Thomas, 2008; Burley and Addison, 2014; Kirch, 2017a).

In Kirch’s (2012) paper on the Kohala agricultural system and his monograph (2017b) on the socio-ecological system of Mangaia, he suggests that the size or productivity of the land are not important factors in the overall population dynamics and the population would reach stochastic equilibrium within approximately 250 years after arrival.

Stochastic equilibrium is where food availability drops to a level where there is not enough food to meet the requirements of the population. Based on this, Kirch (2017b) finds evidence from the archaeological sequence at Mangaia, specifically the decline in pig bone density and the increase in interpersonal violence, indicating food stress, supports this hypothesis of stochastic equilibrium on Mangaia toward the end of the Tangatatau phase and the start of the Ngaaitutaki phase, approximately 1390 - 1470 AD. There is evidence to suggest that this same pressure was being placed upon other South

Pacific archipelagos as the work conducted by Nunn and colleagues (Nunn, 2000a; Nunn and Britton, 2001; Goff and Nunn, 2016) suggests a 1300 AD event that caused conflict, motivated the building of fortifications and saw the development of complex social structures across the Pacific. These changes occurred around the timeframe suggested by Kirch as the time it would take for the islands to reach close to maximum carrying capacity following initial colonisation and exhibit similar behaviours to those on Mangaia.

If so, following the first wave of migration, why was there such a long pause between human colonisation of the west Pacific and the second wave of migration? If we see similar changes occurring at similar timescales following the movement of humans into Eastern Polynesia despite this region consisting of a range of different island types, then would the populations in Melanesia and Western Polynesia reach this stochastic equilibrium well before the second wave of migration? Would we not see evidence of changes in human behaviour whether that be to migrate eastward for new lands/resources or resort to inter-personal conflict? The timescales are very different and the islands in Melanesia are typically much larger (Thomas, 2008), so perhaps this difference in the time to reach stochastic equilibrium is a question of scale contrary to what Kirch *et al* (2012) suggested, which is a potential question for future research.

Based on current research however, it seems as though it could not only be population driven, otherwise there would be evidence of a population crunch in Melanesia and Western Polynesia and an earlier start to the second wave of migration across to Eastern Polynesia. In Chapter 8, the 2,000-year scenario has some level of consistent rainfall for the first 500 years using corrected variations on the Lanoto'o rainfall data. The different scenarios run showed the peak in food availability hits at about 250-300 years, but it can take between 125 and 500 years for Mangaia to reach stochastic equilibrium depending on the rainfall scenario and the shift into stochastic equilibrium was likely brought about by shifts in the climate toward drier conditions. Stochastic equilibrium is found once the population has started to reach the maximum carrying capacity of the island. The patterns of change in Hawaii that Kirch (2017b) felt could also be applied to Mangaia but equally, the model presented in this thesis can be applied to other islands. Not to suggest that the Mangaia socio-ecological system could reflect the larger Pacific islands such as Suva, Apia and Espiritu Santo for example, but parallels and comparisons can be drawn

between this model and other similar islands such as Ulawa in the Solomon Islands or Lakeba in Fiji. Further modelling experiments simulating conditions on some of the bigger islands such as Suva, Apia and Espiritu Santo could help fill this knowledge gap. Currently there is no archaeological evidence to suggest any population stress or changes in behaviour as is seen later during the onset of the MCA, which is discussed in more detail in the next section.

One explanation for this long pause is changing seafaring technology. The Lapita were able to cover thousands of kilometres of ocean using the seafaring technology available 3,000 yr BP to cover thousands of kilometres of open ocean enabling them to colonise all the way eastward to Samoa and Tonga. The eastward extent of the Lapita migration illustrates the boundary of a region in the Pacific - stretching from 191°–194° - that is relatively bereft of islands. The Cook Islands, which were considered these “gateway” islands to Eastern Polynesia (Allen and Wallace, 2007), were particularly isolated from the Lapita occupied islands (Thomas, 2008). To compound this, as one moves eastward across the Pacific the wind conditions become worse for travel toward Polynesia from Melanesia (Irwin, 1992). In summary, movement of the Polynesians eastward required longer crossings under increasingly unfavourable wind conditions (Montenegro, Callaghan and Fitzpatrick, 2014) in an Ocean where interisland distances increased by a factor of 2+, and island elevations and area reduced (Thomas, 2008; Irwin *et al.*, 2022).

Some suggest that this void was overcome over time with a technological change in seafaring technology and new canoes and outriggers allowed for these difficult conditions (Anderson and O’Connor, 2008; Irwin, 2008; Thomas, 2008; Irwin *et al.*, 2022). However, Montenegro *et al.* (2014) examined all of these factors and found that indigenous knowledge of the region and climatic oscillations that occur cyclically were the key to successful migration rather than advances in technology. Typically, wind conditions in the Pacific are not conducive to eastward migration into Polynesia as the trade winds blow from east to west. During El Niño - which brings drier conditions to south western Pacific and wetter to the Galapagos (Atwood and Sachs, 2014; McGree *et al.*, 2016) - the wind conditions in the Pacific become reversed from “normal” and blow from west to east (Murphy, Power and McGree, 2014). This provides conditions conducive for eastward sailing and would allow Pacific islanders to sail east to new islands (Anderson *et al.*, 2006;

Goodwin *et al*, 2014; Montenegro *et al*, 2014). This would suggest that technology was not the decisive factor in the timing of the long pause.

Another explanation could be the environmental conditions and availability of resources on the islands. Work conducted by Anderson (2001) specifically looked at the more remote islands of the Pacific and argues that the diversity and abundance of faunal resources does deplete for sub-tropical islands however, this does not consider the wider patterns of resources change across the Pacific west to east but rather north to south by focusing on the sub-tropical islands. There is a decrease in range of biota on islands the further away from land masses they are (Thomas, 2008) so as humans migrate eastward there will be a reduction in the range of faunal and plant resources. The major divide in terms of biogeography in the Pacific is across the Tonga Trench (Stoddart, 1992; Thomas, 2008) which sits in a similar geographical position as the land void (Montenegro, Callaghan and Fitzpatrick, 2014). In terms of the physical characteristics of islands. Those in Melanesia and Western Polynesia are typically bigger with examples such as Suva, Upolu, Viti Levu and Espiritu Santo. Larger islands offer more land and resources for founding populations and these islands are also typically higher so receive a higher proportion of rainfall due to orographic effects (Irwin, 2008; Thomas, 2008). The islands of the western Pacific also offer a greater variety of environments compared to Eastern Polynesia (Thomas, 2008). The eastward limit of the first Lapita migration also marks the break where further eastward islands become smaller and have a lower elevation with lower levels of rainfall (Thomas, 2008). In terms of the impacts of sea-level on island habitability that was suggested by (Dickinson, 2003), this had stabilised across the Pacific by 1600 BP at the latest (Burley and Addison, 2014) so this was not a barrier for at least 1000 years prior to the onset of the 2<sup>nd</sup> migration wave.

However, a number of islands in Fiji and Tonga sit within a similar range of environmental settings as some of the islands of the Cook Islands suggesting it would have been relatively easy for the Lapita to adapt to these islands (Thomas, 2008). Thomas (2008) argued that the Lapita from Fiji, Samoa and Tonga used these nearby islands to acclimatise to the more extreme conditions of marginal Polynesia whilst benefiting from the support of home settlements. However, there is no evidence that the colonisation strategy changed between the migration into Melanesia and the migration into Polynesia.

Both waves of migration see this focus initially on the wild and marine resources readily available on these islands to new colonisers and then over time a shift toward cultigens and eventually agricultural intensification following population growth (e.g. Tonga (Burley, 1998; Burley and Addison, 2014), Samoa (Quintus and Cochrane, 2018a), Cook Islands (Kirch, 1994, 2017b), Vanuatu, Wallis and Futuna (Kirch, 1994)). It has been suggested that Mangaia and other islands in the Southern Cooks would have proven relatively difficult to colonise particularly due to their makatea barrier and it was likely that there was not a permanent population immediately but colonisation included periodic visits to prepare the island for occupation (Kirch, 2017b; Sear *et al.*, 2020). However, this likely only occurred during the onset of this second wave into the Cooks around 1000 AD based on current evidence. Furthermore, there were several islands where environmental conditions were similar to that of Western Polynesia so would not have been so different to those already colonised and yet they remained untouched until almost 2000 years later. It has also been suggested that unlike the larger volcanic or composite high islands, the physical characteristics and resource availability of atoll and makatea islands across the Pacific are consistent and offer no significant differences between western and eastern Polynesia (Thomas, 2008). This begs the questions, what were humans learning for 2000 years that they did not already know?

Another factor to consider alongside the seafaring challenges and island characteristics is the climatic changes during this period. Based on the current available data from this thesis and existing records from the literature, there is some evidence for a shift toward drier conditions during the time of the Lapita migrations into western Polynesia (Samoa/Tonga/Fiji). If we look to the palaeo records, there is a slight enrichment in  $\delta^{18}\text{O}$  around 3200 to 2600 yr BP and other proxies such as TN and TOC also point toward drier conditions at Emaotfer Swamp. Other records from the tropical Pacific also point to a drying or dry phase including records from Fournier Swamp in New Caledonia (Wirrmann, Sémah and Chacornac-Rault, 2006), Apu Bay in French Polynesia (Toomey, Donnelly and Tierney, 2016), Lake Teroto in the Cook Islands (Hassall, 2017) and giant clams from Espiritu Santo in Vanuatu (Duprey *et al.*, 2014).

In terms of El Niño activity during the past 3000 years, there is a small window where there were a low number of ENSO events resulting in the threshold required for changing

wind direction not being met around 2000 yr BP – this would hinder further eastward migration. However, from 3000-2400 yr BP and 1600-1000 yr BP there were a sufficient number of ENSO events to allow for eastward migration (Anderson, Chappell, *et al.*, 2006). Interestingly, Barr *et al.*'s (2019) suggestion of the occurrence of longer and more intense El Niños causing an increase in the frequency of drier periods from ~2600 to 2000 cal yr BP also theoretically expands the windows for migration eastward compared to the record put forward by Anderson (2006). Goodwin *et al.* (2014) looked at climate windows for Polynesian voyaging but focused on time periods following the start of the second millennium AD and found conditions during the MCA allowed migration to the remotest parts of the Polynesian triangle. To answer the question surrounding the length of the “long pause” and the timing of the second wave of migration, future work should consider the possible windows of migration throughout the “long pause” to indicate whether El Niño conditions in the MCA were the driver of that second wave of migration into Eastern Polynesia. Earlier data from Anderson (2006) and more recent data from Barr *et al.* (2019) currently suggests that this is not the case and that El Niño conditions were high enough at other stages of the “long pause” to allow for migration eastward.

The speed of the first wave of migration into remote Oceania indicates that Lapita populations were subject to rapid growth though not so fast as to trigger a population derived resource depression (Hunt and Lipo, 2017) and it can be assumed that this growth continued into the “long pause” period. Evidence thus far suggests that either Pacific Islanders had the capacity to reach further eastward during that long pause but decided not to or there were significant barriers that deterred Pacific Islanders from venturing further. It would suggest that there was no incentive to move until an additional layer of pressure or a notable change was added to trigger that second wave of migration around 1000 AD. The evidence provided by Goff and Nunn (2016) includes examples from Melanesia and Western Polynesia as well as Eastern Polynesia. It is clear that there was a factor that was impacting island groups across the South Pacific all at the same time that was bringing about social change and changing human behaviour.

### 9.3.3 Drought and the second wave of migration into Eastern Polynesia c. 1000 yr BP

As discussed in section 9.2.2, there was a shift in many records across the Pacific toward dry conditions at the onset of the MCA at approximately 1000 yr BP. This change to dry conditions is seen in records from Vanuatu (Maloney *et al.*, 2022, this thesis), Samoa (Hassall, 2017; Sear *et al.*, 2020; Maloney *et al.*, 2022), and Atiu (Hassall, 2017; Sear *et al.*, 2020) and Mangaia in Cook Islands (this thesis). These records are picking up a long-term drought or overall shift in the mean state for around two hundred years rather than short-term droughts though these shorter-term events would be amplified.

In Chapter 8, for the 2,000 year scenario, which uses quantitative data from Samoa that is corrected to more closely match precipitation patterns on Mangaia, includes two fairly successive dry periods with the first beginning in year AD 590 and shifting back toward wetter conditions by year AD 810 and the second dry period begins around year AD 900 and reaches its maximum amplitude at around year AD 1050 when conditions start to become wetter again. Whilst the recurrent drought does mean that the population drop in the first drought means the populations overall are smaller, in a majority of scenarios the population does recover – only those with mean rainfall +10% of the error and below did not see a robust recovery between the two droughts. Nevertheless, the relative impact of the drought on a range of population sizes provides information on the impact this dry period had on island populations. This second shift in hydroclimate around AD 1000 taken from a record in Samoa (Hassall, 2017) is reflected in many records across the Pacific including sequences from Vanuatu, Samoa and Wallis (Maloney *et al.*, 2022; Strandberg *et al.*, 2023), Cook Islands (Hassall, 2017; Sear *et al.*, 2020), Easter Island (Roman *et al.*, 2021). The model results indicate that a drought during that time on islands that were close to the agricultural carrying capacity would have had a profound impact on the food security of the island, which in turn drives a downward turn in population due to the reduction in food availability. The socio-hydrological model results in Chapter 8 indicates that the pressure of climatic changes on an island working at full capacity could have produced significant effects on the island population and could have acted as a driver of migration as an adaptation strategy for these prehistoric societies. The reconstruction of the impacts of the 1000 yr BP dry conditions on Mangaia saw the

population essentially being wiped out following two dry periods, at the most extreme scenario. Even at the upper limits of the corrected dinosterol mm/year values saw a population drop between 22-62% during this time.

In terms of the impact of hydroclimate on the subsequent colonisation of Eastern Polynesia, the 1000-year model which replicates as closely as possible, the hydroclimate conditions and the island when humans arrived on Mangaia around 1000 AD. Though these peaks and troughs of population change would be less amplified with the inclusion of wild and marine resources in the model as food sources, the model suggests that poor climatic conditions may have led to the delay in developing agricultural resources which lead to the period of stress in-between the Tangatatau phase and the Ngaatutaki phase (Kirch, 2017b).

If we consider whether drought played a role in timing of human migration in the tropical South Pacific, it is important to consider the evidence of human behaviour during this time as an indicator of potential pressure on early Pacific society. To that end, an archaeological summary picking out the key cultural changes in Melanesia and Polynesia from 3000 yr BP through to present is included in Figure 9.4. This summary expands on the one offered by Goff and Nunn (2016) by looking back further to changes occurring prior to 900 cal yr BP and also including additional and key archipelagos such as Vanuatu, Tonga, Cook Islands and New Caledonia. Several have also been removed including Hawaii, Micronesia, Timor and Palau to specifically focus on the South Pacific region that is SPCZ sensitive.

It is difficult to draw more substantial conclusions concerning environmental change and the archaeological sequences from the western Pacific. In several archipelagos there are incomplete cultural sequences dating all the way back to colonisation. In Vanuatu, it is thought that a number of archaeological sites have been lost to volcanic activity in the area (Bedford and Spriggs, 2014). Whereas, in Samoa, it is thought that evidence from Early Lapita sites are likely lost to the ocean due to subsidence on the western side of the archipelago (Rieth and Hunt, 2008).

It is also worth considering that there were societal changes occurring in Melanesia and Western Polynesia around 1000 AD. When Goff and Nunn (2016) conducted their study

on rapid societal change as a proxy for regional environmental forcing, they focused around the AD 1300 event as per their hypothesis and they didn't consider any earlier evidence such as around the second period of migration where our archaeological sequences are more intact. In the lead up to this period between 1500 and 1000 yr BP in Samoa the relatively understudied and little understood Samoan "Dark Ages" occurred (Rieth and Hunt, 2008; Burley and Addison, 2014) and at 1000 yr BP there is a shift towards monument building and expansion of settlements. This also coincides with a period of social contraction in Fiji evidenced by drop in the amount of pottery sourced from outside island groups (Cochrane, 2014). In Tonga, there is a shift to monument and fortification building around 1000 AD (Kirch, 1984; Burley and Addison, 2014). In New Caledonia, 1000 AD is when the rise of the Traditional Kanak cultural complex, which coincides with isolation in some islands, the construction of monuments, permanent settlements inland alongside an intensification of agriculture (Sand, 2014). This connection between societal change and changing climatic conditions was also explored in a study focused on French Polynesia that found that the unpredictable oscillations in rainfall across space and time were likely connected to socio-political changes in prehistoric Marquesan society (Allen, 2010).

Goff and Nunn (2016) used similar social changes and archaeological evidence from around 1300 AD as a proxy for environmental change across the Pacific. If we take up their hypothesis that societal perturbation can be used as a proxy for environmental change then there is clearly some kind of disturbance occurring around 1000 AD as it is being felt across multiple island groups. As discussed in the previous section, there is evidence that around the time of the second wave of migration in the Pacific there was a shift to drier conditions both in Melanesia and within Polynesia. Alongside this archaeological evidence of societal change occurring in multiple countries across the Pacific - which has been suggested as a proxy for environmental change - we also have evidence from multiple palaeo-environmental archives including both the Emaotfer and Tiriara sites studied in this thesis. The palaeo data indicates that there was a significant shift in the hydroclimate that our socio-ecological model suggests could have had major implications for island populations and clearly made waves through societies across Melanesia and Polynesia.

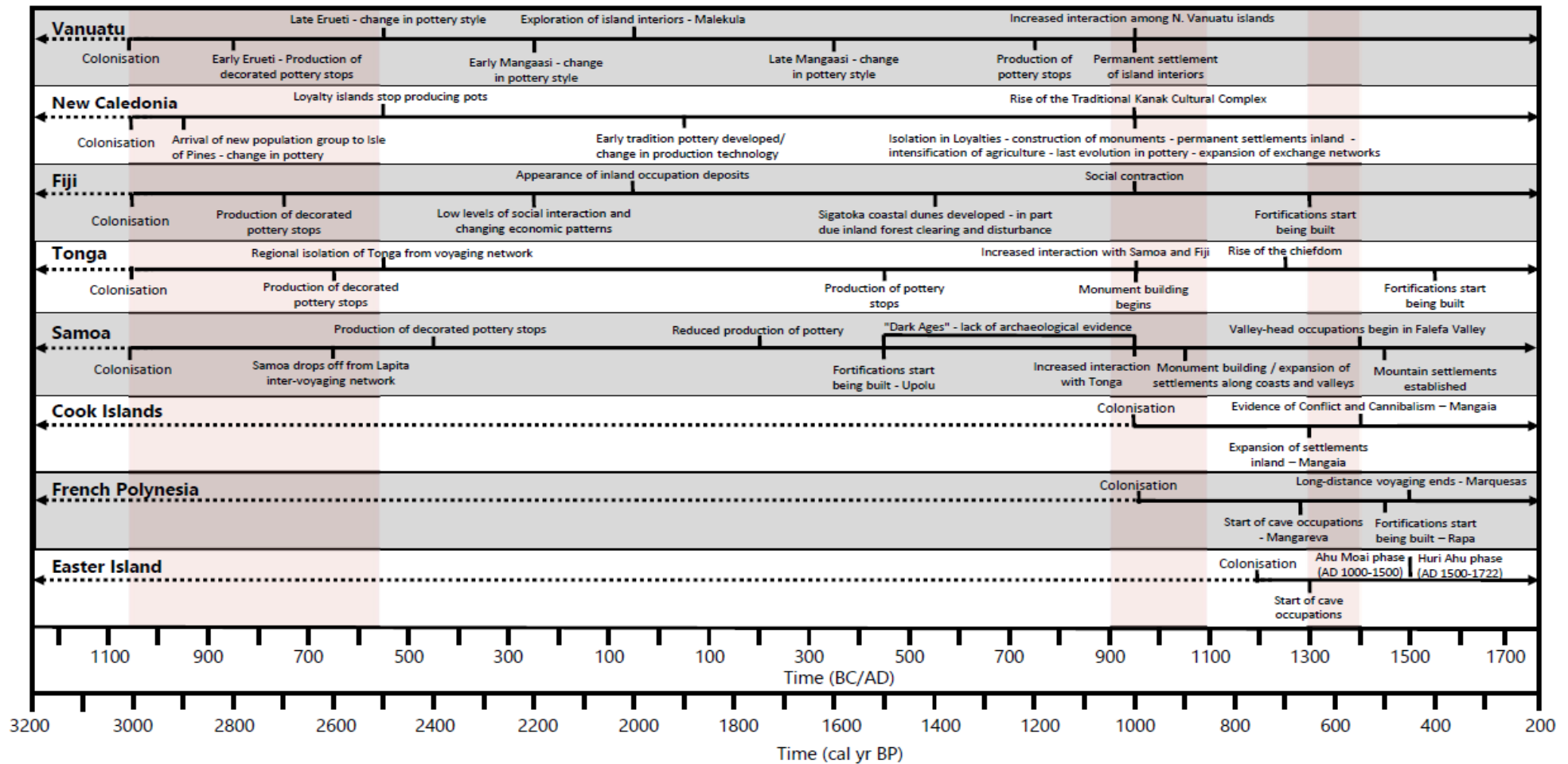


Figure 9.4: Main features of the archaeological records of major archipelagos of the tropical South Pacific. Information taken from sources listed in appendix B – redrawn and adapted from Goff and Nunn (2016). Red boxes denote drier hydroclimate conditions as suggested by the Emaotfer and Mangaia sediment sequences.

### 9.3.4 Drought and subsequent colonisation of Eastern Polynesia - 1300 AD event

One of the key findings from the Mangaia sequence was the occurrence of a dry period in zone-M5 occurring between 1316-1459 ± 88 cal yr BP. This shift to dry conditions is also seen in other records in the Pacific such as Vanuatu (Maloney *et al.*, 2022), Samoa (Hassall, 2017; Maloney *et al.*, 2022) and other records in the Southern Cook Islands (Sear *et al.*, 2020). This evidence all suggests that around AD 1300 during the transition between the MCA and the LIA there was a shift to drier conditions. As discussed in chapter 3, there is an existing body of literature that has studied the so-called “1300 AD event” that occurred in the tropical Pacific but theoretically was a global event with examples from North America (Benson *et al.*, 2007), Central America (DeMenocal, 2001) and Africa (Huffman, 2009). Known as a period of significant climatic variability with notable drops in temperature and sea level, the 1300 AD event is theorised to have had impacts on Pacific society (Nunn, 2003; Goff and Nunn, 2016). These palaeoenvironmental archives from across a range of island groups in the Pacific appear to confirm this theoretical 1300 AD event though specifically identify a shift in hydroclimate to drier conditions rather than changes in temperature or sea level. Contrarily, Nunn attributes higher rates of erosion to an increase in precipitation during this period but as evidenced in the Mangaia record presented in this thesis and across other sites in the Pacific, the higher rate of erosion is typically attributed to human disturbance in the catchment rather than increasing rainfall (Sear *et al.*, 2020).

However, other work conducted by Fitzpatrick (2010) argues that there is a range of data from across the Pacific that does not conform to this 1300 AD event theory. He uses Palau as an example of one such place and suggests that the 1300 AD event is clouded in climate deterministic ideas and does not consider the wider geographical context but only individual localised examples. Palau sits north of the equator above the ITCZ – not part of the SPCZ climate system inferring different climate dynamics to those experienced by islands in the South Pacific where rainfall patterns are dominated by the SPCZ (Sachs *et al.*, 2018; Brown *et al.*, 2020). So perhaps the suggestion that this event was a Pacific wide event is an overstatement or at least the impacts were felt in different ways in different regions. Higgins *et al.* (2020) found that the period 1310 to 1330 CE saw the largest

eastward shift in the SPCZ, which was larger than the major dry period observed at the start of the MCA.

The reality is that by approximately 1300 AD all of the islands of the Pacific had been colonised (Wilmshurst *et al.*, 2011; Ioannidis *et al.*, 2021) so there was no mechanism to relieve stress from over-population. Previously, islanders had utilised resources from their own islands as well as smaller neighbouring islands and exchanged resources through inter-island networks. However, following 1300 AD there was a notable drop in long-distance voyaging between islands (Weisler *et al.*, 2016). When all islands are populated and reaching the absolute island capacity and there is nowhere to go, islanders have turned to other mechanisms in order to release some of that pressure of rapid growth. Mechanisms such as building fortifications to defend key resource (Marais, 1990; Best, 1993; Field, 2004; Field and Lape, 2010), outbreaks of conflict (Nunn, 2000a; Field and Lape, 2010; Goff and Nunn, 2016), cannibalism or infanticide (Erickson and Gowdy, 2000; Antón and Steadman, 2003; Kirch, 2007, 2017b). Changes in climate and rapid population growth with no mechanism for relief may have altered human behaviour and their priorities to focus on developing agriculture and protection of resources (Allen and Craig, 2009).

As seen in the socio-hydrological model of Mangaia in Chapter 8, there is a range of possible precipitation scenarios. The lower the rate of precipitation the slower the growth of the population following arrival as the lower level of precipitation affects the yields of taro. Not as important following initial arrival but as these populations become established, agriculture grows in importance and the model results suggest that lowering rainfall levels have implications for crop production and population dynamics. This is seen in the model outputs shown in Figure 8.10 as precipitation rates continue to fall from around 350 to 600 years post colonisation, which sees a notable lowering of the agricultural carrying capacity of the island during this period. If this change did occur in Pacific history and there is already pressure from growing populations and no mechanism for release then this would explain the changes in human behaviour during this time to include cannibalism, conflict and fortification.

It is difficult to say whether this AD 1300 event occurred across the whole of the Pacific based on the data currently available. However, Vanuatu, Samoa and the Cook Islands all sit within the SPCZ zone and so perhaps this AD 1300 event had some impact upon the

precipitation patterns during this period, which is why a number of records from this region are showing similar changes. Work done by Hassall (2017) investigated SPCZ dynamics during the Holocene and found that between 725-150 cal yr BP the SPCZ had either contracted and/or migrated northwest. Furthermore, Hassall (2017) also identifies the transition period between the MCA and the LIA as an East Pacific El Niño dominated period where a number of the data sets used to make conclusions about precipitation and temperature in some of the original work surrounding this 1300 AD event were from the peripheral Pacific basin (Nunn, 2000a, 2000b). It is clear that further work needs to be done to refine the timing of hydroclimate changes in the tropical South Pacific.

### **9.4 Summary**

In summary, it seems clear that climate has been an important part of the Pacific island system especially throughout the human history of the region. The unique island environment with limitations on space and movement means that when human populations start to reach the absolute carrying capacity of these landscapes the impact of climatic change is felt much more deeply. Evidence surrounding the first wave of migration into remote Oceania by the Lapita is currently lacking though the current theory is that climate was potentially somewhat drier in that part of Pacific human history. The second wave of migration and the societal change in the 10<sup>th</sup> and 12-13<sup>th</sup> century represent two breaking points in Pacific history where climatic and demographic pressures came to a head resulting in major consequences for Pacific society.

## Chapter 10 Conclusions

This chapter will start with an overview of the aims of this thesis and the steps taken to see those aims through to fruition. Following this, a summary of the main findings covering some of the key topics of the thesis will be presented followed by recommendations for future work. The chapter will conclude with some final thoughts on the bigger picture of climate change in the Pacific and our understanding of the environmental context of human history in the tropical South Pacific.

### 10.1 Overview

The aims of this thesis were as follows:

- Reconstruct late Holocene hydroclimate over the past 3000 years from lacustrine sediments using a multi-proxy approach.
- Understand how climate likely impacted on food security and population dynamics in prehistoric Polynesia.
- Assess the new and existing evidence on whether drought played a role in the prehistoric migrations within the tropical South Pacific.

This thesis has presented palaeoenvironmental records for both Emaotfer Swamp and Lake Tiriara and assessed their use as hydroclimate archives by analysing the palaeoenvironmental changes these lakes have experienced over the past 9200 and 2780 years respectively. This has been achieved by using a multi-proxy approach including a mix of inorganic and organic stable isotopes, sedimentology, XRF geochemistry and diatom analysis. For the first time,  $\delta^{18}\text{O}$  has been used on terrestrial lake records from the tropical South Pacific to reconstruct hydroclimate changes through the Holocene. The use of oxygen isotopes in carbonates offer the possibility of producing higher resolution precipitation records though suitable sites can be difficult to identify and like Lake Tiriara, not all sedimentary sequences have the benefit of continuous precipitation of carbonate. This thesis has also offered up a new socio-ecological system dynamics model built around the Mangaian system due to the excellent archaeological record available for comparison from the Tangatatau Rockshelter. This has allowed for experimentation with a range of precipitation scenarios based on our current understanding of Mangaian

rainfall characteristics and the exploration of outcomes based on a palaeo rainfall scenario going back 2,000 years. Finally, the assessment of a range of palaeoclimate records from across the tropical South Pacific alongside archaeological evidence and the outputs from the socio-ecological model has shown that climate has been an important part of the Pacific island system especially throughout the human history of the region. Whilst the first wave of human migration into the Pacific likely was possibly driven by climate, the second wave of migration and the societal change in the C14th and C15th represent two breaking points in Pacific history where it is clear that climatic and demographic pressures came to a head resulting in major consequences for Pacific society.

## 10.2 Main Findings

Below are some of the main findings brought out through this thesis project. They are separated into some of the key themes described throughout the chapters and are as follows:

### 10.2.1 Environmental/Climatic change in Vanuatu over the Holocene

- The  $\delta^{18}\text{O}$ ,  $\delta^{13}\text{C}_{\text{inorganic}}$  and Ti/inc records in the Emaotfer Swamp sequence all suggest a relatively short-lived wet event around 8.2kyr event - c. 7159 - 8250 cal yr BP. The same wet signal is also seen in the record from the original Lake Lanoto'o (in Samoa) proxy reconstructions such as TOC and Ti/inc (Hassall, 2017) supporting Hassall's (2017) suggestion that the 8.2kyr event resulted in an expansion or SW shift of the SPCZ as Vanuatu sits just south of the SPCZ zone. However, updated age model data now put that wet event at around 9200 yr BP.
- The  $\delta^{18}\text{O}$  and terrestrial XRF proxies in the Emaotfer Swamp record all indicate a move toward drier conditions around approximately 6736-6121  $\pm$  415 cal yr BP. There is a paucity of records from the tropical South Pacific that date back beyond the Common Era. Two records that cover this time period show agreement on this change in hydroclimate from records in Samoa and the Cook Islands (Hassall, 2017). Hassall (2017) suggests that this dry period is due to a contraction or north-west migration of the SPCZ between 6,900-5,700 cal yr BP.

- Another dry period that occurred no earlier than 2012-2288 cal yr BP and likely ended approximately 499 - 629 cal yr BP with the initiation of peat growth in the basin, indicating a shift back to wetter conditions. In the lead up to the transition of Emaotfer Swamp from a marl lake to a peatland, there was a marked decrease in the rate of accumulation that represents either a hiatus in the sediments that requires further refinement in terms of chronology or a significant slowdown in productivity. Other records from Efate support this interpretation as they also indicate that there was a shift to dry conditions around 1000 AD that saw changes in rainfall, vegetation and ecology (Maloney *et al.*, 2022; Strandberg *et al.*, 2023).

### 10.2.2 Environmental/climatic change in the Southern Cook Islands over the Late Holocene

- The  $\delta^{18}\text{O}$  record from Lake Tiriara indicates that dry conditions dominate around 1067-881  $\pm$  135 cal yr BP, which coincides with the arrival of humans to Mangaia (Kirch, 2017b). This finding is supported by other records from the region, including the Southern Cook Islands (Sear *et al.*, 2020) and the Society Islands (Toomey, Donnelly and Tierney, 2016).
- The  $\delta^{18}\text{O}$  and Ca/inc records indicate that there was another shift toward dry conditions on Mangaia around 647-470  $\pm$  102 cal yr BP, which coincides with the postulated 1300 AD event hypothesised by Nunn and colleagues (Nunn, 2000a; Nunn and Britton, 2001; Goff and Nunn, 2016). This also corresponds with the Tangatatau period in Mangaian history (Kirch, 2017b), which sees the peak in human activity on Mangaia and the intensification of agriculture evidenced by the peak in the charcoal record during this period.
- Within the Tiriara sequence, a relatively short-lived event sees a major change in a range of proxy signals, which has been interpreted as a palaeotsunami layer in zone M-2. This event layer is dated to 1572-1678  $\pm$  129 cal yr BP, which considering the age model error could correspond to palaeo-tsunami deposits found on Mangaia (Chagué-Goff *et al.*, 2016) and in Wallis and Futuna (Goff, Lamarche, *et al.*, 2011) that cite the potential source as the Tonga-Kermadec Trench.

- The XRF proxy Ti/inc should be utilised carefully as the relationship between rainfall and terrestrial input as measured by Ti/inc can change through time. Local changes within the basin can dominate over wider regional climate signal. This could be due to changes in sediment availability because of human activity or natural land cover change or, during dry conditions, the exposure of additional sediment as water levels drop.

### **10.2.3 Modelling Prehistoric Polynesian Island Life**

- Using a range of rainfall/drought scenarios based around our current understanding of the Mangaian rainfall patterns the socio-ecological model provided outputs that allowed for an assessment of the impact of drought on population dynamics. One of the key findings was that as the population density of the island increases, the impact of drought events on population dynamics increases across all levels of severity. The threshold of the population density where there is a significant shift in the impact of drought varies depending on the precipitation patterns but typically sits around 165 - 230 people per km<sup>2</sup> based on the scenarios presented in Chapter 8.
- The scenarios based upon the modern day Mangaian rainfall data also found that the severity of the drought rather than the return frequency drove the bigger changes in carrying capacity and population dynamics for Mangaia over a 1000-year period.
- Based on the palaeo scenarios that utilise a corrected version of a quantitative precipitation data set from Lake Lanoto'o in Samoa, changing precipitation levels impact on the timing and rate of population growth due to its role as a limiting factor of agricultural productivity. This then can hasten or delay the rate at which a population reaches stochastic equilibrium.

### **10.2.4 Hydroclimate change over key periods of human migration and colonisation**

- The first wave of human migration into the Pacific by the Lapita approximately 3000 yr BP was possibly driven by climate based on existing records. Current data from Emaotfer Swamp and other existing records from the region (Hassall, 2017;

Barr *et al.*, 2019) suggests that conditions were either relatively stable or were moving toward drier conditions in the lead up to and over the first wave of human migration. However, the paucity of records in the tropical South Pacific means that our understanding of hydroclimate change going back beyond the Common Era is still lacking.

- The second wave of human migration across the Pacific into Eastern Polynesia approximately 1000 yr BP was likely entangled with considerable changes in hydroclimate toward drier conditions. This is seen in both the Emaotfer Swamp, Lake Tiriara sequences and the wider Pacific region (Maloney *et al.*, 2022; Strandberg *et al.*, 2023). Similar shifts in hydroclimate are observed in records from Melanesia and Western Polynesia implying that this change likely affected large parts of the tropical Pacific region.
- The sequence from Lake Tiriara, Mangaia also suggests a second shift toward dry conditions at approximately  $647-470 \pm 102$  cal yr BP, which occurs approximately 300 years after initial colonisation of the island and coincides with the transition from the MCA to the LIA. Similarly, in the Emaotfer record, conditions were dry and only started to become wetter following the period 499 - 629 cal yr BP, allowing peat to develop in the Emaotfer basin. Other records from across the South Pacific region pick up a similar signal in records from Efate (Maloney *et al.*, 2022), Atiu (Sear *et al.*, 2020) and Wallis and Futuna (Maloney *et al.*, 2022), indicating that multiple island groups across the Pacific were seeing the same shifts in hydroclimate to drier conditions during this MCA-LIA transition.

### 10.2.5 Drought as a driver of migration

- The data produced from Emaotfer Swamp as part of this thesis and the limited number of existing records from the tropical South Pacific suggest that conditions leading up to and including the first wave of migration into the Pacific were getting somewhat drier though there is disagreement between records on this. There is currently limited evidence from the Pacific islands that suggest that climate may have played a role in the timing of the first wave of human migration into Remote Oceania, but further work is required to understand hydroclimate change during this time.

- A summary of archaeological data from across multiple island groups in the tropical South Pacific suggest that similar to the 1300 AD event (Goff and Nunn, 2016), there were notable changes in archaeological sequences across the region around 1000 AD. If we accept the hypothesis of Goff and Nunn (2016), these societal changes could be used as a proxy for changing climate. This evidence along with the growing body of palaeoenvironmental records from this time - indicating a shift toward dry conditions in a number of island groups - strongly suggest that climate did play a role in the timing of the second wave of human migration across the Pacific into Eastern Polynesia.
- Following on from that, archaeological records around AD 1300 also signify considerable environmental change (Goff and Nunn, 2016). As mentioned, in both the Emaotfer and Tiriara records as well as other palaeo sequences across the Pacific there was a dry period around the transition between the MCA and the LIA, at approximately AD 1300. Kirch (2017b) suggests this would be the approximate time period for islands to reach stochastic equilibrium following human arrival. The population model suggests that this would occur later due to the slowdown in growth due to unfavourable climatic conditions for taro intensification. However, this could represent a mismatch in the decline of wild resources and the onset of agricultural intensification. Nevertheless, this fits with archaeological evidence from the Tangatatau Rockshelter on Mangaia that suggests that a decrease in the number of pig bones and an increase of interpersonal violence toward the end of the 12<sup>th</sup> century represents a period of considerable stress (Kirch, 2017b). If so, this period represents a time in Mangaian prehistory when both population and environmental pressures are at play. These results support the theorised AD 1300 event hypothesised by Nunn and colleagues (Nunn, 2000a; Nunn and Britton, 2001; Goff and Nunn, 2016).

### 10.3 Recommendations for future research

Taking into consideration the existing literature in this field and the main findings of this thesis, the following recommendations are made for future research:

- There has been a recent upturn in the number of palaeo records coming out of the tropical South Pacific. However, there is still a need for more high resolution, quantitative reconstructions of tropical South Pacific hydroclimate through the Late Holocene – particularly around the period of the second wave of migration and 1300 AD – along with a robust chronology to refine the timing and rate of these changes.
- At present, there is a paucity of palaeoclimate records from the tropical South Pacific that go back beyond the Common Era. Future work should focus on developing records that cover the first wave of human migration into Remote Oceania. This will build up our understanding of hydroclimate across the Holocene in the tropical South Pacific and provide a climatic context that we can use to understand the role of climate in the early human history of the Pacific.
- This study has highlighted the mystery surrounding the timing of the “Long Pause” between the first and second waves of migration. Future work could investigate the “long pause” duration on a range of different fronts including modelling of voyaging windows through the period, modelling different island systems to establish when they may reach a population crunch and also developing palaeo records in key areas such as Melanesia to establish the environmental context of this period of Pacific human history. The aim would be to establish what the key trigger of that second wave of migration was and why it was around 2,000 years after the first.
- The socio-ecological model presented in this thesis offers an experimental framework within which to explore the complex interactions between climate and human society on small islands. However, as discussed in section 8.7.6, there are a number of limitations to the model in terms of how it represents the Manganian socio-ecological system. Future work could look at developing a more complex and comprehensive model of socio-ecological island systems. This could involve incorporating aspects such as technological advances, availability of wild resources, complex population dynamics and a better representation of soil types and mixed cultivation strategies.

## 10.4 Final Thoughts

To conclude, it is important not to fall into the research bias of the palaeoclimatological community of over-stating the role of climate in Pacific human history. Despite being a region that has to handle a highly variable climate in small pockets of land, a vast majority of the islands have been continuously occupied since they were colonised (Anderson, 2001), speaking to the Pacific Islander's adaptability and resilience in the face of difficult conditions. However, there is little doubt that prehistoric Pacific Island life was intrinsically tied to a mix of wild, marine and cultivated resources, which in turn are intrinsically tied to environmental factors. Drought plays a role in the Late Holocene Pacific Island life, but it is not the only character at play, others include factors such as technological development, social complexity, population growth, and geographic constraints as well as many others. It is important to highlight each character in turn; this thesis has attempted to shine a light on a character – climate - that hitherto has been relatively neglected in the story of prehistoric human migration of the Pacific region.

We know that small islands states share common characteristics that make them vulnerable to climatic change such as their “size, limited resources, exposure to natural hazards, water resources vulnerable to changing sea levels, isolation both geographical and economic, high pop densities and growth rates, relatively poorly developed infrastructure and limited funds and human resource skill” (IPCC, 2001). Currently, there is “low confidence in the direction of change” of drought in the Pacific Ocean in the observed changes over the period 1951 to 2015 (Mycoo *et al.*, 2022, p. 2052). Going forward, the Central Pacific region is projected to have up to 30% drop in precipitation whilst the West Pacific region is expected to have a slight increase in precipitation of up to 8% (Mycoo *et al.*, 2022). However, it is also projected that there will be more frequent extreme ENSO events across the Pacific region, which are associated with significant changes in rainfall and the occurrence of drought.

Whilst this thesis has looked back to reflect on how past climate impacted on prehistoric Pacific society, palaeoenvironmental studies have an important part to play in developing our current understanding of how rainfall patterns have changed in the Pacific region and how they may change in the future. The palaeoenvironmental findings from both this thesis and within the existing literature show that the hydroclimate of the tropical Pacific

has been much drier in the past compared to what we have observed in the past century. The model presented in Chapter 8 could be adapted to look at the impact of projected climate change on islands that are heavily dependent upon subsistence cropping. Outputs from the model suggest that increasing magnitude is the key drought characteristic that impacts on population dynamics and agricultural carrying capacity and this is stepped up again when combining an increase in magnitude with increasing frequency and intensity. In the Central Pacific region, the projected drying along with more extreme ENSO events means that severe drought is likely to be more frequent and more intense. This will have substantial impacts on agriculture and those dependent upon it for subsistence, this is especially true for those islands that may have high population densities that are reaching the limit of what their island can sustain.



## Appendix A Palaeo-precipitation records

Table 10.1: Table of studies included in the map in the literature review that focus on hydroclimate in tropical South Pacific used in **Error! Reference source not found.**

Author & Year	Type of record	Length of Record	Max age (yr BP)
Horrocks et al (2015)	Lake	30000	30000
Le Bec et al (2000)	Coral	40	40
Gorman et al (2012)	Coral	165	165
Conroy et al (2014)	Lake	1	1
Duprey et al (2012)	Coral	6500	200
Rustic et al (2015)	Marine	1009	950
Mann et al (2008)	Lake	5600	5600
Stott et al (2004)	Marine	10000	10000
Smittenberg et al (2011)	Saline Lake	10000	10000
Nurhati et al (2011)	Coral	1020	70
Bagnato et al (2005)	Coral	225	174
Osborne et al (2014)	Coral	215	157
Partin et al (2013)	Stalagmite	450	400
Zhang et al (2014)	Lake	9200	9000
Nelson and Sachs (2016)	Saline Lake	2000	2000
Wirrman et al (2011)	Swamp/Lake	6886	6825
Margalef et al (2014)	Swamp	70850	70850
Rasbury and Aharon (2006)	Stalagmite	260	210
Kilbourne et al (2004)	Coral	65	30
Dassie et al (2014)	Coral	254	200
Cobb et al (2003)	Coral	150	1000
Linsley et al (2004)	Coral	100	150
Saez et al (2009)	Lake	34000	34000
Restrepo et al (2012)	Lake	2690	2690
Conroy et al (2008)	Lake	9110	9110

Appendix A

<b>Duprey et al (2014)</b>	Marine	1500	3800
<b>Canellas-Bolta et al (2012)</b>	Lake	34000	34000
<b>Wirrman et al (2006)</b>	Lake	2000	2000
<b>Sear et al (2020)</b>	Lake	2000	2000
<b>Rull et al (2015)</b>	Swamp	2500	2500
<b>Atwood and Sachs (2014)</b>	Lake	3000	3000
<b>Maupin et al (Maupin <i>et al.</i>, 2014)</b>	Stalgmite	600	600
<b>Wirrman et al (2011)</b>	Swamp	3500	3500
<b>Thompson et al (2017)</b>	Saline Lake	6100	6100

## Appendix B Archaeology data sources

Table 10.2: Archaeology figure sources used in Figure 9.4 – adapted and updated from Field and Lape (2010)

<b>Author &amp; Year</b>	<b>Region</b>	<b>Country/State</b>
<b>Anderson et al (2006)</b>	Melanesia	Fiji
<b>Best (1993)</b>	Melanesia	Fiji
<b>Clark and Anderson (2009b)</b>	Melanesia	Fiji
<b>Cochrane (2004)</b>	Melanesia	Fiji
<b>Dickinson et al (1998)</b>	Melanesia	Fiji
<b>Field (2003, 2004)</b>	Melanesia	Fiji
<b>Field and Lape (2010)</b>	Melanesia	Fiji
<b>Kirkendall (1998)</b>	Melanesia	Fiji
<b>O’Day et al. (2004)</b>	Melanesia	Fiji
<b>Rechtman (1992)</b>	Melanesia	Fiji
<b>Cochrane (2018)</b>	Melanesia	New Caledonia
<b>Sand (2014)</b>	Melanesia	New Caledonia
<b>McCoy and Cleghorn (1988)</b>	Melanesia	Solomon Islands
<b>Thomas et al (2001)</b>	Melanesia	Solomon Islands
<b>Bedford (2006)</b>	Melanesia	Vanuatu
<b>Bedford and Spriggs (2008)</b>	Melanesia	Vanuatu
<b>Bedford and Spriggs (2014)</b>	Melanesia	Vanuatu
<b>Rainbird (1996)</b>	Micronesia	FSM
<b>Allen and Craig (2009)</b>	Polynesia	Cook Islands
<b>Allen and Wallace (2007)</b>	Polynesia	Cook Islands
<b>Best (1993)</b>	Polynesia	Cook Islands
<b>Kirch (2017b)</b>	Polynesia	Cook Islands
<b>Sear et al (2020)</b>	Polynesia	Cook Islands
<b>Weisler et al (2016)</b>	Polynesia	Cook Islands
<b>Kennett et al (2006)</b>	Polynesia	French Polynesia
<b>Kirch (1984)</b>	Polynesia	Hawai’i (USA)

Appendix B

<b>Kolb and Dixon (2002)</b>	Polynesia	Hawai'i (USA)
<b>Rieth et al (2011)</b>	Polynesia	Hawai'i (USA)
<b>Allen (1994)</b>	Polynesia	New Zealand
<b>Davidson (1987)</b>	Polynesia	New Zealand
<b>Wilmshurst et al (2008)</b>	Polynesia	New Zealand
<b>Best et al (1989)</b>	Polynesia	Samoa
<b>Burley et al (2011)</b>	Polynesia	Samoa
<b>Gosling et al (2020)</b>	Polynesia	Samoa
<b>Pearl (2004)</b>	Polynesia	Samoa
<b>Burley (1998)</b>	Polynesia	Tonga
<b>Burley et al (2011)</b>	Polynesia	Tonga
<b>Burley et al (2015)</b>	Polynesia	Tonga
<b>Kirch (1984)</b>	Polynesia	Tonga
<b>Marais (1990)</b>	Polynesia	Tonga

## Appendix C Calibration values for the isotope measurements

Table 10.3: MCS and CCS calibration standards for inorganic isotopes  $\delta^{18}\text{O}$  and  $\delta^{13}\text{C}$ 

MCS			CCS		
Extraction #	$\delta^{13}\text{C}$ ‰ VPDB	$\delta^{18}\text{O}$ ‰ VPDB	Extraction #	$\delta^{13}\text{C}$ ‰ VPDB	$\delta^{18}\text{O}$ ‰ VPDB
CC93306	-0.71	-9.19	CC93311	-22.43	-13.49
CC93316	-0.71	-9.15	CC93321	-22.46	-13.59
CC93325	-0.70	-9.19	CC93331	-22.32	-13.28
CC93336	-0.74	-9.21	CC93341	-22.26	-13.34
CC93345	-0.67	-9.15	CC93361	-22.37	-13.38
CC93346	-0.70	-9.15	CC93371	-22.37	-13.43
CC93356	-0.71	-9.12	CC93381	-22.36	-13.40
CC93365	-0.70	-9.26	CC93391	-22.35	-13.42
CC93366	-0.64	-9.14	CC93401	-22.31	-13.47
CC93376	-0.72	-9.15	CC93411	-22.29	-13.26
CC93385	-0.75	-9.24	CC93421	-22.33	-13.39
CC93396	-0.73	-9.23	CC93431	-22.39	-13.38
CC93405	-0.68	-9.12	CC93441	-22.36	-13.26
CC93406	-0.69	-9.16	CC93451	-22.38	-13.51
CC93416	-0.68	-9.19	CC93461	-22.38	-13.38
CC93425	-0.74	-9.18	CC93471	-22.39	-13.42
CC93436	-0.70	-9.18	CC93481	-22.41	-13.31
CC93445	-0.73	-9.22	CC93491	-22.41	-13.36
CC93456	-0.74	-9.20	CC93501	-22.45	-13.41
CC93465	-0.66	-9.11	CC93511	-22.39	-13.44
CC93466	-0.71	-9.14	CC93521	-22.42	-13.38
CC93476	-0.73	-9.26	<b>Average</b>	<b>-22.37</b>	<b>-13.39</b>
CC93485	-0.68	-9.13	<b><math>\pm 1\sigma</math></b>	<b>0.05</b>	<b>0.08</b>
CC9386	-0.72	-9.28			
CC93496	-0.68	-9.10			
CC93505	-0.71	-9.15			
CC93506	-0.69	-9.19			
CC93516	-0.69	-9.22			
CC93525	-0.73	-9.12			
<b>Average</b>	<b>-0.70</b>	<b>-9.18</b>			
<b><math>\pm 1\sigma</math></b>	<b>0.03</b>	<b>0.05</b>			

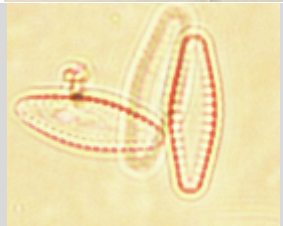
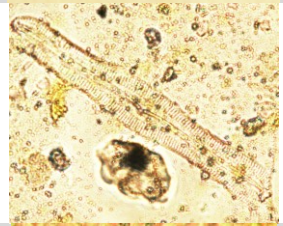
Table 10.4: BROC3 calibration standards for organic isotopes  $\delta^{13}\text{C}$  and  $\delta^{15}\text{N}$ .

<b>BROC3 - Broccoli</b>		
	<b><math>\delta^{13}\text{C}</math> ‰ VPDB</b>	<b><math>\delta^{15}\text{N}</math> ‰ AIR</b>
	-27.59	1.53
	-27.68	1.48
	-27.52	1.51
	-27.58	1.44
	-27.52	1.53
	-27.69	1.60
	-27.55	1.44
	-27.63	1.51
	-27.62	1.55
<b>Average</b>	-27.60	1.51
<b><math>\pm 1\sigma</math></b>	0.06	0.05

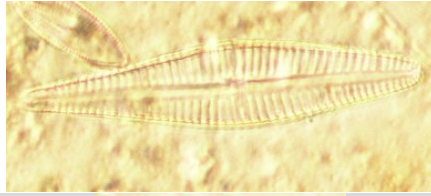
Table 10.5: Spirulina calibration standards for organic isotopes  $\delta^{13}\text{C}$  and  $\delta^{15}\text{N}$ .

<b>B2162 - Algae (Spirulina)</b>		
	<b><math>\delta^{13}\text{C}</math> ‰ VPDB</b>	<b><math>\delta^{15}\text{N}</math> ‰ AIR</b>
	-18.76	6.26
	-18.70	6.20
	-18.70	6.17
	-18.74	6.09
	-18.69	6.15
	-18.73	6.09
	-18.74	6.10
	-18.61	5.96
	-18.66	6.04
	-18.67	6.05
	-18.71	5.96
	-18.68	5.96
	-18.67	5.82
	-18.72	5.88
	-18.73	5.98
	-18.74	6.11
	-18.67	6.14
	-18.69	6.29
	-18.69	6.22
	-18.68	6.26
	-18.72	6.19
	-18.64	6.19
	-18.65	6.12
	-18.81	6.17
	-	6.03
	-	6.08
<b>Average</b>	-18.70	6.10
<b><math>\pm 1\sigma</math></b>	0.04	0.12

## Appendix D Diatom pictures

Type	Species	Image
A	<i>Rhoplalodia Gibberula</i>	
B	<i>Navicula spp.</i>	
C	<i>Pseudostaurosira Brevistriata</i>	
D	<i>Pinnularia major</i>	
E	<i>Achnanthes inflata</i>	
F	Unknown	
G	Unknown	
H	<i>Thalassiosira Weissflogii</i>	
I	<i>Nitzschia spp.</i>	No picture

**J** *Gomphonema* sp.



**K** *Achnanthes* sp.



**L** *Amphora coffeaformis*



## Appendix E R code for model metrics

For the socio-ecological model presented in chapter 8, the rainfall datasets were synthetically generated using a first order autoregressive model, often termed an AR(1) model. Below is the R code for synthetic rainfall data production:

```
n <- 1001
rho <- 0.9

x <- numeric(n)

x[1] <- rnorm(1)

for( i in 2:n ) {x[i] <- rnorm(1, 0.0, 1) + rho*x[i-1] }

x <- (x - mean(x)) / sd(x) # scale data to have (mean=0, sd=1)

a <- 250
b <- 3000
Rainfall <- (x - min(x)) / (max(x) - min(x)) * (b-a)+a #- only add on lower range value if it is not zero

Time <- c(0:1000)

All = data.frame(Time,Rainfall)

plot(Time, Rainfall, col="blue", type="l")

write_xlsx(list(Rainfall=All),"Rain_data.xlsx")
```

Next is the R code used to generate the drought and population metrics for the scenario and palaeo data sets once run through the model. Taken and adapted from and Hao *et al* (2017) Kuil *et al* (2016):

```
DI=matrix(t(Model_output$Rainfall),ncol=1)

PI=matrix(t(Model_output$Population), ncol=1)

thre<-1000
```

```

X0 <- rep(0, length(DI))
X0[DI < thre] <- 1
X1 <- c(0, X0, 0)
st <- c()
ed <- c()

for (i in 2:(length(X1) - 1)) { if (X1[i - 1] == 0 & X1[i] == 1) {st <- c(st, i - 1)}
  if (X1[i] == 1 & X1[i + 1] == 0) {ed <- c(ed, i - 1)}}

Duration <- ed - st + 1
Frequency <- length(Duration)
Severity <- matrix(nrow = Frequency, ncol = 1)

for (i in 1:Frequency) {Severity[i, 1] <- abs(sum(DI[st[i]:ed[i], 1] - thre))}

Max_pop_change <- rep(NA, length(st))

for (i in 1:length(st)) {Max_pop_change[i] <- (((min(PI[st[i]:ed[i]])/PI[st[i] - 1])*100) - 100)}

Recovery_time <- rep(NA, length(st))
min_pop <- rep(NA, length(st))
min_pop_index <- rep(NA, length(st))
Time_to_min_pop <- rep(NA, length(st))
T2R <- rep(NA, length(st))

for (i in 1:length(st)) {min_pop[i] <- min(PI[st[i]:ed[i]])
  min_pop_index[i] <- which(PI == min_pop[i])[1]
  Time_to_min_pop[i] <- min_pop_index[i] - st[i]

  T2R[i] <- min_pop_index[i] + which(PI[(min_pop_index[i]):length(PI)] >= PI[st[i]])[1]
  Recovery_time[i] <- T2R[i] - st[i]}

Total_land <- 52
Pop_density <- rep(NA, length(st))

for (i in 1:length(st)) {Pop_density[i] <- PI[st[i]]/ Total_land}

Result <- data.frame(st, ed, Duration, Frequency, Severity, Time_to_min_pop, T2R,
  Max_pop_change, min_pop_index, Recovery_time, Pop_density)

```

## List of References

- Aguilera, P. A. *et al.* (2011) 'Bayesian networks in environmental modelling', *Environmental Modelling and Software*. Elsevier Ltd, 26(12), pp. 1376–1388. doi: 10.1016/j.envsoft.2011.06.004.
- Allen, B. (1971) 'Wet-field Taro Terrace on Mangaia, Cook Islands', *Journal of the Polynesian Society*, 80(3), pp. 371–378.
- Allen, B. J. (1969) *The Development of Commercial Agriculture on Mangaia: Social and Economic Change in a Polynesian Community*. Massey University.
- Allen, M. S. (2006) 'New Ideas about Late Holocene Climate Variability in the Central Pacific', *Current Anthropology*, 41(3), pp. 521–535. doi: 10.1086/504168.
- Allen, M. S. (2010) 'Oscillating climate and socio-political process: The case of the Marquesan Chieftdom, Polynesia', *Antiquity*, 84(323), pp. 86–102. doi: 10.1017/S0003598X00099786.
- Allen, M. S. *et al.* (2011) 'New pollen, sedimentary, and radiocarbon records from the marquesas islands, east polynesia: Implications for archaeological and palaeoclimate studies', *Holocene*, 21(3), pp. 473–484. doi: 10.1177/0959683610385726.
- Allen, M. S. (2014) 'Marquesan Colonisation Chronologies and Post-Colonisation Interaction: Implications for Hawaiian Origins and the "Marquesan Homeland" Hypothesis', *Journal of Pacific Archaeology*, 5(2), pp. 1–17.
- Allen, M. S. (2015) *Dietary Opportunities and Constraints on Islands*, *The Oxford Handbook of the Archaeology of Diet*. doi: 10.1093/oxfordhb/9780199694013.013.2.
- Allen, M. S. and Craig, J. A. (2009) 'Dynamics of Polynesian Subsistence : Insights from Archaeofauna and Stable Isotope Studies, Aitutaki, Southern Cook Islands', *Pacific Science*, 63(4), pp. 477–506. doi: 10.2984/049.063.0403.
- Allen, M. S. and Mcalister, A. (2013) 'Early Marquesan Settlement and Patterns of Interaction : New Insights from Hatiheu Valley , Nuku Hiva Island', *Journal of Pacific Archaeology*, 4(1), pp. 90–109.
- Allen, M. S. and Wallace, R. (2007) 'New evidence from the east polynesian gateway: Substantive and methodological results from Aitutaki, Southern cook Islands', *Radiocarbon*, 49(3), pp. 1163–1179. doi: 10.1017/S0033822200043095.
- Allen, M. W. (1994) *Warfare and economic power in simple chiefdoms: The development of*

## List of References

*fortified villages and polities in Mid-Hawkes's Bay, New Zealand*. University of California.

Anderies, J. M. (1998) 'Culture and human agro-ecosystem dynamics: The Tsembaga of New Guinea', *Journal of Theoretical Biology*, 192(4), pp. 515–530. doi: 10.1006/jtbi.1998.0681.

Anderies, J. M. and Hegmon, M. (2011) 'Robustness and resilience across scales: Migration and resource degradation in the prehistoric U.S. Southwest', *Ecology and Society*, 16(2). doi: 10.5751/ES-03825-160222.

Anderson, A. (1995) 'Current approaches in East Polynesia colonisation research', *Journal of the Polynesian Society*, 104(1), pp. 110–132.

Anderson, A. (2001) 'No Meat on that Beautiful Shore: The Prehistoric Abandonment of Subtropical Polynesian Islands', *International Journal of Osteoarchaeology*, 23, pp. 14–23.

Anderson, A. (2002) 'Faunal Collapse, Landscape Change and Settlement History in Remote Oceania', *World Archaeology*, 33(3), pp. 375–390. doi: 10.1080/0043824012010743.

Anderson, A., Chappell, J., *et al.* (2006) 'Prehistoric maritime migration in the Pacific islands: An hypothesis of ENSO forcing', *Holocene*, 16(1), pp. 1–6. doi: 10.1191/0959683606hl901ft.

Anderson, A., Roberts, R., *et al.* (2006) 'Times of Sand : Sedimentary History and Archaeology at the Sigatoka Dunes , Fiji', *Geoarchaeology - An International Journal*, 21(2), pp. 131–154. doi: 10.1002/GEA.

Anderson, A. (2014) 'Seafaring in Remote Oceania: Traditionalism and Beyond in Maritime Technology and Migration', *The Oxford Handbook of Prehistoric Oceania*, 474(1957), pp. 1–22.

Available at:

<http://www.oxfordhandbooks.com/view/10.1093/oxfordhb/9780199925070.001.0001/oxfordhb-9780199925070-e-003>.

Anderson, A. J. *et al.* (2019) 'New excavations at Fa'ahia (Huahine, Society Islands) and chronologies of central East Polynesian colonization', *Journal of Pacific Archaeology*, 10(1), pp. 1–14. Available at: <https://pacificarchaeology.org/index.php/journal/article/view/279>.

Anderson, A. and O'Connor, S. (2008) 'Indo-Pacific Migration and Colonization - Introduction', *Asian Perspectives*, 47(1), pp. 2–11.

Andrews, J. E., Riding, R. and Dennis, P. F. (1997) 'The stable isotope record of environmental and climatic signals in modern terrestrial microbial carbonates from Europe', *Palaeogeography, Palaeoclimatology, Palaeoecology*, 129, pp. 171–189.

- Antón, S. C. and Steadman, D. W. (2003) 'Mortuary patterns in burial caves on Mangaia, Cook Islands', *International Journal of Osteoarchaeology*, 13(3), pp. 132–146. doi: 10.1002/oa.667.
- Appleby, P. G. and Oldfield, F. (1978) 'The calculation of lead-210 dates assuming a constant rate of supply of unsupported  $^{210}\text{Pb}$  to the sediment', *Catena*, 5(1), pp. 1–8. doi: 10.1016/S0341-8162(78)80002-2.
- Atwood, A. R. (2015) *Mechanisms of Tropical Pacific Climate Change During the Holocene*. University of Washington.
- Atwood, A. R. *et al.* (2021) 'Data-Model Comparisons of Tropical Hydroclimate Changes Over the Common Era', *Paleoceanography and Paleoclimatology*, 36(7), pp. 1–30. doi: 10.1029/2020PA003934.
- Atwood, A. R. and Sachs, J. P. (2014) 'Separating ITCZ- and ENSO-related rainfall changes in the Galápagos over the last 3 kyr using D/H ratios of multiple lipid biomarkers', *Earth and Planetary Science Letters*. Elsevier B.V., 404, pp. 408–419. doi: 10.1016/j.epsl.2014.07.038.
- Australian Bureau of Meteorology and CSIRO (2011) *Climate Change in the Pacific : Scientific Assessment and New Research - Volume 1 : Regional Overview*. Available at: <https://www.pacificclimatechangescience.org/wp-content/uploads/2013/08/Climate-Change-in-the-Pacific.-Scientific-Assessment-and-New-Research-Volume-1.-Regional-Overview.pdf>.
- Australian Government Bureau of Meteorology (2023) *Pacific Climate Change Portal*. Available at: <http://www.bom.gov.au/climate/pccsp/> (Accessed: 22 March 2023).
- Axtell, R. L. *et al.* (2002) 'Population growth and collapse in a multiagent model of the Kayenta Anasazi in Long House Valley', *Proceedings of the National Academy of Sciences of the United States of America*, 99(SUPPL. 3), pp. 7275–7279. doi: 10.1073/pnas.092080799.
- Bagnato, S. *et al.* (2005) 'Coral oxygen isotope records of interdecadal climate variations in the South Pacific Convergence Zone region', *Geochemistry, Geophysics, Geosystems*, 6(6), pp. 1–8. doi: 10.1029/2004GC000879.
- Barr, C. *et al.* (2019) 'Holocene El Niño–Southern Oscillation variability reflected in subtropical Australian precipitation', *Scientific Reports*, 9(1), pp. 1–9. doi: 10.1038/s41598-019-38626-3.
- Barton, C. M. *et al.* (2012) 'Looking for the future in the past: Long-term change in socioecological systems', *Ecological Modelling*, 241, pp. 42–53. doi: 10.1016/j.ecolmodel.2012.02.010.
- Barton, C. M. *et al.* (2016) 'Experimental socioecology: Integrative science for anthropocene

## List of References

- landscape dynamics', *Anthropocene*. Elsevier B.V., 13, pp. 34–45. doi: 10.1016/j.ancene.2015.12.004.
- Barton, D. N. *et al.* (2012) 'Bayesian networks in environmental and resource management', *Integrated Environmental Assessment and Management*, 8(3), pp. 418–429. doi: 10.1002/ieam.1327.
- Basener, W. *et al.* (2008) 'Rat instigated human population collapse on easter island', *Nonlinear dynamics, psychology and life sciences*, 12(3), pp. 227–240.
- Battarbee, R. W. *et al.* (2002) 'Diatoms', in *Tracking environmental change using lake sediments*. Dordrecht: Springer, pp. 155–202.
- Bayliss-Smith, T. P. and Hviding, E. (2015) 'Landesque capital as an alternative to food storage in Melanesia: Irrigated taro terraces in New Georgia, Solomon Islands', *Environmental Archaeology*, 20(4), pp. 425–436. doi: 10.1179/1749631414Y.0000000049.
- Le Bec, N. *et al.* (2000) 'A coral  $\delta^{18}\text{O}$  record of ENSO driven sea surface salinity variability in Fiji (south-western tropical Pacific)', *Geophysical Research Letters*, 27(23), pp. 3897–3900. doi: 10.1029/2000GL011843.
- Bedford, S. and Spriggs, M. (2008) 'Northern Vanuatu as a Pacific crossroads: The archaeology of discovery, interaction, and the emergence of the "ethnographic present"', *Asian Perspectives*, 47(1), pp. 95–120. doi: 10.1353/asi.2008.0003.
- Bedford, S. and Spriggs, M. (2014) 'The Archaeology of Vanuatu : 3,000 Years of History across Islands of Ash and Coral', in Cochrane, E. E. and Hunt, T. L. (eds) *The Oxford Handbook of Prehistoric Oceania*. Oxford: Oxford University Press, pp. 162–184.
- Bedford, S., Spriggs, M. and Regenvanu, R. (2006) 'The Teouma Lapita site and the early human settlement of the Pacific Islands', *Antiquity*, 80(310), pp. 812–828. doi: 10.1017/S0003598X00094448.
- Bell, R. G. *et al.* (2004) *Tsunami hazard for the Bay of Plenty and Eastern Coromandel Peninsula*.
- Below, R., Grover-kopec, E. and Dilley, M. (2007) 'Documenting Drought-Related Disasters', *Journal of Environment & Development*, 16(3), pp. 328–344.
- Bennion, H., Appleby, P. G. and Phillips, G. L. (2001) 'Reconstructing nutrient histories in the Norfolk Broads, UK: implications for the role of diatom-total phosphorus transfer functions in shallow lake management', *Journal of Paleolimnology*, 26, pp. 181–204.

- Benson, L. V. *et al.* (2007) 'Possible impacts of early-11th-, middle-12th-, and late-13th-century droughts on western Native Americans and the Mississippian Cahokians', *Quaternary Science Reviews*, 26(3–4), pp. 336–350. doi: 10.1016/j.quascirev.2006.08.001.
- Best, S. (1993) 'At the halls of the mountain kings. Fijian and Samoan fortifications: comparison and analysis', *Journal of the Polynesian Society*, 102(4), pp. 385–447.
- Best, S., Leach, H. and Witter, D. (1989) *Report on the second phase of fieldwork at the Tatagamatau site, American Samoa, July-August 1988.*
- Bird, B. W. *et al.* (2011) 'Holocene tropical South American hydroclimate revealed from a decadal resolved lake sediment  $\delta^{18}\text{O}$  record', *Earth and Planetary Science Letters*. Elsevier B.V., 310(3–4), pp. 192–202. doi: 10.1016/j.epsl.2011.08.040.
- Bird, M. I. *et al.* (2020) 'Stable isotope proxy records in tropical terrestrial environments', *Palaeogeography, Palaeoclimatology, Palaeoecology*. Elsevier, 538(October 2019), pp. 1–22. doi: 10.1016/j.palaeo.2019.109445.
- Birdsell, J. B. (1957) 'Some population problems involving Pleistocene man.', *Cold Spring Harbor Symposia on Quantitative Biology*, 22, pp. 44–69.
- Birks, H. H. and Birks, H. J. B. (2006) 'Multi-proxy studies in palaeolimnology', *Vegetation History and Archaeobotany*, 15(4), pp. 235–251. doi: 10.1007/s00334-006-0066-6.
- Blard, P. H. *et al.* (2011) 'Lake highstands on the Altiplano (Tropical Andes) contemporaneous with Heinrich 1 and the Younger Dryas: New insights from  $^{14}\text{C}$ , U-Th dating and  $\delta^{18}\text{O}$  of carbonates', *Quaternary Science Reviews*. Elsevier Ltd, 30(27–28), pp. 3973–3989. doi: 10.1016/j.quascirev.2011.11.001.
- Blockley, S. *et al.* (2018) 'The resilience of postglacial hunter-gatherers to abrupt climate change', *Nature Ecology and Evolution*. Springer US, 2(5), pp. 810–818. doi: 10.1038/s41559-018-0508-4.
- Blockley, S. P. E. *et al.* (2014) 'Tephrochronology and the extended intimate (integration of ice-core, marine and terrestrial records) event stratigraphy 8-128kab2k', *Quaternary Science Reviews*. Elsevier Ltd, 106, pp. 88–100. doi: 10.1016/j.quascirev.2014.11.002.
- Boiseau, M. *et al.* (1998) 'Atmospheric and oceanic evidence of El Niño-Southern Oscillation events in the south central Pacific Ocean from coral stable isotopic records over the last 137 years', *Paleoceanography*, 13(6), pp. 671–685. doi: 10.1029/98PA02502.
- Boyle, J. F. (2001) 'Inorganic Geochemical Methods in Palaeolimnology', in Last, W. M. and Smol,

## List of References

J. P. (eds) *Tracking Environmental Change Using Lake Sediments*. Kluwer Academic Publishers, pp. 83–141.

Boyle, J. F., Chiverrell, R. C. and Schillereff, D. (2015) 'Approaches to water content correction and calibration for  $\mu$ XRF core scanning: comparing X-ray scattering with simple regression of elemental concentrations.', in Croudace, I. W. and Rothwell, R. G. (eds) *Micro-XRF studies of sediment cores*. London: Springer, pp. 373–392.

Bradley, R. (2015) 'Lake sediments Sampling', in *Paleoclimatology*. 3rd edn. Elsevier Inc., pp. 319–344. doi: 10.1016/B978-0-12-386913-5.00009-0.

Bradley, R. S. (2015) *Paleoclimatology: Reconstructing Climates of the Quaternary*. 3rd edn. Oxford: Elsevier.

Brander, B. J. A. and Taylor, M. S. (1998) 'The Simple Economics of Easter Island : A Ricardo-Malthus Model of Renewable Resource Use', *The American Economic Review*, 88(1), pp. 119–138. Available at: [https://aae.wisc.edu/aae641/Ref/Brander\\_Taylor\\_Easter\\_Island\\_AER\\_1998.pdf](https://aae.wisc.edu/aae641/Ref/Brander_Taylor_Easter_Island_AER_1998.pdf).

Brandt, G. and Merico, A. (2015) 'The slow demise of Easter Island: Insights from a modeling investigation', *Frontiers in Ecology and Evolution*, 3(FEB), pp. 1–12. doi: 10.3389/fevo.2015.00013.

Brenner, M. *et al.* (1999) 'Stable isotope ( $\delta^{13}\text{C}$  and  $\delta^{15}\text{N}$ ) signatures of sedimented organic matter as indicators of historic lake trophic state', *Journal of Paleolimnology*, 22(2), pp. 205–221. doi: 10.1023/A:1008078222806.

Brown, J. R. *et al.* (2020) 'South Pacific Convergence Zone dynamics, variability and impacts in a changing climate', *Nature Reviews Earth and Environment*. Springer US, 1(10), pp. 530–543. doi: 10.1038/s43017-020-0078-2.

Bruhl, J. J. and Wilson, K. L. (2007) 'Towards a Comprehensive Survey of C3 and C4 Photosynthetic Pathways in Cyperaceae', *Aliso*, 23(1), pp. 99–148. doi: 10.5642/aliso.20072301.11.

Burley, D. *et al.* (2015) 'Bayesian modeling and chronological precision for Polynesian settlement of Tonga', *PLoS ONE*, 10(3), pp. 1–14. doi: 10.1371/journal.pone.0120795.

Burley, D. V. (1998) 'Tongan archaeology and the Tongan past, 2850-150 B.P.', *Journal of World Prehistory*, 12(3), pp. 337–392. doi: 10.1023/A:1022322303769.

Burley, D. V., Sheppard, P. J. and Simonin, M. (2011) 'Tongan and Samoan volcanic glass: PXRF analysis and implications for constructs of ancestral Polynesian society', *Journal of Archaeological Science*. Elsevier Ltd, 38(10), pp. 2625–2632. doi: 10.1016/j.jas.2011.05.016.

- Burley, D. V and Addison, D. J. (2014) 'Tonga and Sāmoa in Oceanic Prehistory : Contemporary Debates and Personal Perspectives', in Cochrane, E. E. and Hunt, T. L. (eds) *Oxford Handbook of Prehistoric Oceania*. Oxford: Oxford University Press, pp. 231–251.
- Burn, M. J. and Palmer, S. E. (2014) 'Solar forcing of Caribbean drought events during the last millennium', *Journal of Quaternary Science*, 29(8), pp. 827–836. doi: 10.1002/jqs.2660.
- Burnett, A. P. *et al.* (2011) 'Tropical East African climate change and its relation to global climate: A record from Lake Tanganyika, Tropical East Africa, over the past 90+kyr', *Palaeogeography, Palaeoclimatology, Palaeoecology*. Elsevier B.V., 303(1–4), pp. 155–167. doi: 10.1016/j.palaeo.2010.02.011.
- Burns, W. C. G. (2001) 'Pacific Island Developing Country Water Resources and Climate Change', *The World's Water 2002-2003*, (Tutangata 1996), pp. 113–132.
- Cadd, H. R. *et al.* (2018) 'Development of a southern hemisphere subtropical wetland (Welsby Lagoon, south-east Queensland, Australia) through the last glacial cycle', *Quaternary Science Reviews*. Elsevier Ltd, 202, pp. 53–65. doi: 10.1016/j.quascirev.2018.09.010.
- Cai, W. *et al.* (2014) 'Increasing frequency of extreme El Niño events due to greenhouse warming', *Nature Climate Change*. Nature Publishing Group, 4(2), pp. 111–116. doi: 10.1038/nclimate2100.
- Cai, W. *et al.* (2015) 'Increased frequency of extreme La Nina events under greenhouse warming', *Nature Climate Change*, 5(2), pp. 132–137. doi: 10.1038/nclimate2492.
- Cañellas-Boltà, N. *et al.* (2012) 'Macrofossils in Raraku Lake (Easter Island) integrated with sedimentary and geochemical records: Towards a palaeoecological synthesis for the last 34,000 years', *Quaternary Science Reviews*. Elsevier Ltd, 34, pp. 113–126. doi: 10.1016/j.quascirev.2011.12.013.
- Cañellas-Boltà, N. *et al.* (2016) 'Vegetation dynamics at Raraku Lake catchment (Easter Island) during the past 34,000years', *Palaeogeography, Palaeoclimatology, Palaeoecology*. Elsevier B.V., 446, pp. 55–69. doi: 10.1016/j.palaeo.2016.01.019.
- Cantonati, M. *et al.* (2021) 'Recent and subfossil diatom assemblages as indicators of environmental change ( including fish introduction ) in a high-mountain lake', *Ecological Indicators*. Elsevier Ltd, 125, p. 107603. doi: 10.1016/j.ecolind.2021.107603.
- Chagué-Goff, C. *et al.* (2011) 'Expanding the proxy toolkit to help identify past events - Lessons from the 2004 Indian Ocean Tsunami and the 2009 South Pacific Tsunami', *Earth-Science Reviews*. Elsevier B.V., 107(1–2), pp. 107–122. doi: 10.1016/j.earscirev.2011.03.007.

## List of References

- Chagué-Goff, C. *et al.* (2016) 'Late Holocene record of environmental changes, cyclones and tsunamis in a coastal lake, Mangaia, Cook Islands', *Island Arc*, 25(5), pp. 333–349. doi: 10.1111/iar.12153.
- Chase, A. F. and Scarborough, V. (2014) 'Diversity, Resiliency and IHOPE-Maya: Using the Past to Inform the Present', *Archaeological Papers of the American Anthropological Association*, 24, pp. 1–10. doi: 10.1126/SCIENCE.369.6507.1069-I.
- Chen, S. H. and Pollino, C. A. (2012) 'Good practice in Bayesian network modelling', *Environmental Modelling and Software*. Elsevier Ltd, 37, pp. 134–145. doi: 10.1016/j.envsoft.2012.03.012.
- Clark, G. and Anderson, A. (2009a) 'Site chronology and a review of radiocarbon dates from Fiji', in Clark, G. and Anderson, A. (eds) *The Early Prehistory of Fiji*. ANU E Press, pp. 153–182. doi: 10.22459/ta31.12.2009.07.
- Clark, G. and Anderson, A. (2009b) *The early prehistory of Fiji*. ANU E Press.
- Clayton, R. N. and Degens, E. T. (1959) 'Use of carbon isotope analyses of carbonates for differentiating fresh-water and marine sediments.', *AAPG Bulletin*, 43(4), p. pp.890-897.
- Cobb, K. M. *et al.* (2003) 'El Nino/Southern Oscillation and tropical Pacific climate during the last millennium', *Nature*, 424(July), pp. 271–276. doi: 10.1038/nature01779.
- Cochrane, E. E. (2004) *Explaining cultural diversity in ancient Fiji: The transmission of ceramic variability*. University of Hawai'i. doi: 10.1017/S0165115300023299.
- Cochrane, E. E. (2014) 'Ancient Fiji : Melting Pot of the Southwest Pacific', in Cochrane, E. E. and Hunt, T. L. (eds) *The Oxford Handbook of Prehistoric Oceania*. Oxford: Oxford University Press, pp. 206–230.
- Cochrane, E. E. (2018) 'The Evolution of Migration: the Case of Lapita in the Southwest Pacific', *Journal of Archaeological Method and Theory*. *Journal of Archaeological Method and Theory*, 25(2), pp. 520–558. doi: 10.1007/s10816-017-9345-z.
- Cocquyt, C. and De Wever, A. (2002) 'Epiphytic diatom communities on herbarium material from Lake Naivasha and Lake Sonachi, Eastern Rift Valley, Kenya', *Belg. Journ. Bot.*, 135(1), pp. 38–49.
- Cohen, A. S. (2003) *Paleolimnology: the history and evolution of lake systems*. New York: Oxford University Press. doi: <https://doi.org/10.1093/oso/9780195133530.001.0001>.
- Combettes, C., Sémah, A. M. and Wirrmann, D. (2015) 'High-resolution pollen record from Efate Island, central Vanuatu: Highlighting climatic and human influences on Late Holocene vegetation

- dynamics', *Comptes Rendus - Palevol. Academie des sciences*, 14(4), pp. 251–261. doi: 10.1016/j.crpv.2015.02.003.
- Commendador, A. S. *et al.* (2013) 'A stable isotope ( $\delta^{13}\text{C}$  and  $\delta^{15}\text{N}$ ) perspective on human diet on Rapa Nui (Easter Island) ca. AD 1400–1900', *American Journal of Physical Anthropology*, 152(2), pp. 173–185. doi: 10.1002/ajpa.22339.
- Conroy, J. L. *et al.* (2008) 'Holocene changes in eastern tropical Pacific climate inferred from a Galápagos lake sediment record', *Quaternary Science Reviews*, 27(11–12), pp. 1166–1180. doi: 10.1016/j.quascirev.2008.02.015.
- Conroy, J. L. *et al.* (2014) 'Climate influences on water and sediment properties of Genovesa Crater Lake, Galápagos', *Journal of Paleolimnology*, 52(4), pp. 331–347. doi: 10.1007/s10933-014-9797-z.
- Conte, E. and Molle, G. (2014) 'Reinvestigating a key site for Polynesian prehistory: New results from the Hane dune site, Ua Huka (Marquesas)', *Archaeology in Oceania*, 49(3), pp. 121–136. doi: 10.1002/arco.5037.
- Cook Islands Statistics Office (2018) *Census of Population and Dwellings 2016*. Cook Islands.
- Cook, J. (1821) *The Three Voyages of Captain James Cook Round the World*. London: A&R Spottiswoode. Available at: <https://www.gutenberg.org/files/62095/62095-h/62095-h.htm#b2c1>.
- Croudace, I. W. (2010) *Determination of  $^{210}\text{Po}$  in sediments and other solid matrices*. Southampton.
- Cuna, S., Pop, D. and Hosu, A. (2001) 'Carbon and Oxygen Isotope Ratios in Rona Limestone, Romania', *Studia Universitatis Babeş-Bolyai, Geologia*, 46(1), pp. 139–152. doi: 10.5038/1937-8602.46.1.11.
- Cuven, S., Francus, P. and Lamoureux, S. (2011) 'Mid to Late Holocene hydroclimatic and geochemical records from the varved sediments of East Lake, Cape Bounty, Canadian High Arctic', *Quaternary Science Reviews*. Elsevier Ltd, 30(19–20), pp. 2651–2665. doi: 10.1016/j.quascirev.2011.05.019.
- Dalrymple, G. B., Jarrard, R. D. and Clague, D. A. (1975) 'K-Ar ages of some volcanic rocks from the Cook and Austral Islands', *Bulletin of the Geological Society of America*, 86(10), pp. 1463–1467. doi: 10.1130/0016-7606(1975)86<1463:KAOSVR>2.0.CO;2.
- Dalton, T. R. and Coats, R. M. (2000) 'Could institutional reform have saved Easter Island?', *Journal*

## List of References

of *Evolutionary Economics*, 10(5), pp. 489–505. doi: 10.1007/s001910000050.

Dalton, T. R., Coats, R. M. and Asrabadi, B. R. (2005) 'Renewable resources, property-rights regimes and endogenous growth', *Ecological Economics*, 52(1), pp. 31–41. doi: 10.1016/j.ecolecon.2004.03.033.

Darling, W. *et al.* (2006) 'Isotopes in Water', in *Isotopes in palaeoenvironmental research*. Dordrecht: Springer, pp. 1–66.

Darling, W. G. (2004) 'Hydrological factors in the interpretation of stable isotopic proxy data present and past: A European perspective', *Quaternary Science Reviews*, 23(7–8), pp. 743–770. doi: 10.1016/j.quascirev.2003.06.016.

Dassie, E. P. *et al.* (2014) 'A Fiji multi-coral oxygen isotope composite approach to obtaining a more accurate reconstruction of the last two-centuries of the ocean-climate variability in the South Pacific Convergence Zone region', *Paleoceanography*, 29(12), pp. 1196–1213. doi: 10.1002/2013PA002591.

Dassié, E. P. *et al.* (2018) 'Spatiotemporal variability of the South Pacific convergence zone fresh pool eastern front from coral-derived surface salinity data', *Journal of Climate*, 31(8), pp. 3265–3288. doi: 10.1175/JCLI-D-17-0071.1.

Davidson, J. (1987) 'The Paa Maaori Revisited', *The Journal of the Polynesian Society*, 96(1), pp. 7–26.

Davies, S. J., Lamb, H. F. and Roberts, S. J. (2015) 'Micro-XRF Core Scanning in Palaeolimnology: Recent Developments', in Croudace, I. W. and Rothwell, R. G. (eds) *Micro-XRF Studies of Sediment Cores: Applications of a non-destructive Tool for the Environmental Sciences*. London: Springer, pp. 189–226.

Dearing, J. A. (1999a) *Environmental Magnetic Susceptibility: Using the Bartington MS2 System*. Kenilworth: Chi Publishing.

Dearing, J. A. (1999b) 'Holocene environmental change from magnetic proxies in lake sediments', in Maher, B. A. and Thompson, R. (eds) *Quaternary Climates, Environments and Magnetism*. Cambridge University Press, pp. 231–278. doi: 10.1017/cbo9780511535635.008.

DeMenocal, P. B. (2001) 'Cultural responses to climate change during the late holocene', *Science*, 292(5517), pp. 667–673. doi: 10.1126/science.1059827.

Dickinson, W. *et al.* (2013) 'Petrography of Temper Sands in 112 Reconstructed Lapita Pottery

- Vessels from Teouma (Efate): Archaeological implications and relations to other Vanuatu tempers', *Journal of Pacific Archaeology*, 4(2).
- Dickinson, W. R. *et al.* (1998) 'Geomorphic and Archaeological Landscapes of the Sigatoka Dune Site, Viti Levu, Fiji: Interdisciplinary Investigations', *Asian Perspectives*, 37(1), pp. 1–31.
- Dickinson, W. R. (2003) 'Impact of mid-Holocene hydro-isostatic highstand in regional sea level on habitability of islands in Pacific Oceania', *Journal of Coastal Research*, 19(3), pp. 489–502.
- Dinapoli, R. J. and Morrison, A. E. (2017) 'Human behavioural ecology and Pacific archaeology', *Archaeology in Oceania*, 52(1), pp. 1–12. doi: 10.1002/arco.5124.
- Ding, Z. *et al.* (2018) 'System dynamics versus agent-based modeling: A review of complexity simulation in construction waste management', *Sustainability*, 10(7), pp. 1–13. doi: 10.3390/su10072484.
- Dinsley, J. M., Gowing, C. J. B. and Marriott, A. L. (2019) *Natural and Anthropogenic Influences on Atmospheric Pb-210 Deposition and Activity in Sediments - A Review*. Nottingham.
- Dixon-Jain, P. *et al.* (2014) *Pacific Island Groundwater and Future Climates*.
- Dong, X. *et al.* (2008) 'Tracking eutrophication in Taihu Lake using the diatom record: Potential and problems', *Journal of Paleolimnology*, 40(1), pp. 413–429. doi: 10.1007/s10933-007-9170-6.
- Donlan, J. (2018) *Land Cover Assessment of Efate Island, Vanuatu*.
- Dunbar, E. *et al.* (2016) 'AMS 14C dating at the Scottish Universities Environmental Research Centre (SUERC) radiocarbon dating laboratory', *Radiocarbon*, 58(1), pp. 9–23. doi: 10.1017/RDC.2015.2.
- Duncan, D. (2011) *Freshwater under Threat: Pacific Islands Vulnerability Assessment of Freshwater Resources to Environmental Change*. doi: ISBN: 978-92-807-3132-3.
- Dunning, N. P. *et al.* (2002) 'Arising from the Bajos: The evolution of a neotropical landscape and the rise of Maya civilization', *Annals of the Association of American Geographers*, 92(2), pp. 267–283. doi: 10.1111/1467-8306.00290.
- Duprey, N. *et al.* (2012) 'Early mid-Holocene SST variability and surface-ocean water balance in the southwest Pacific', 27, pp. 1–12. doi: 10.1029/2012PA002350.
- Duprey, N. *et al.* (2014) 'Isotopic records from archaeological giant clams reveal a variable climate during the southwestern Pacific colonization ca. 3.0ka BP', *Palaeogeography, Palaeoclimatology,*

## List of References

- Palaeoecology*. Elsevier B.V., 404, pp. 97–108. doi: 10.1016/j.palaeo.2014.04.002.
- El-Daoushy, F., Olsson, K. and Garcia-Tenorio, R. (1991) 'Accuracies in Po-210 determination for lead-210 dating', *Hydrobiologia*, 214(1), pp. 43–52. doi: 10.1007/BF00050930.
- Ellison, J. C. (1993) 'Caves and Speleogenesis of Mangaia, Cook Islands', *Atoll Research Bulletin*, 417, pp. 1–25.
- Ellison, J. C. (1994) 'Palaeo-lake and Swamp Stratigraphic Records of Holocene Vegetation and Sea-level Changes, Mangaia, Cook Islands', *Pacific Science*, 48(1), pp. 1–15.
- Erickson, J. D. and Gowdy, J. M. (2000) 'Resource use, institutions, and sustainability: A tale of two Pacific Island cultures', *Land Economics*, 76(3), pp. 345–354. doi: 10.2307/3147033.
- Evans, G. *et al.* (2019) 'A multi-proxy  $\mu$ -XRF inferred lake sediment record of environmental change spanning the last ca. 2230 years from Lake Kanono, Northland, New Zealand', *Quaternary Science Reviews*, 225. doi: 10.1016/j.quascirev.2019.106000.
- FAO (1996) *Ecocrop 1. Crop Environmental Requirements Database*. Rome.
- Field, J. S. (2003) *The evolution of competition and cooperation in Fijian prehistory: Archaeological research in the Sigatoka Valley*. University of Hawai'i.
- Field, J. S. (2004) 'Environmental and climatic considerations: A hypothesis for conflict and the emergence of social complexity in Fijian prehistory', *Journal of Anthropological Archaeology*, 23(1), pp. 79–99. doi: 10.1016/j.jaa.2003.12.004.
- Field, J. S. and Lape, P. V. (2010) 'Paleoclimates and the emergence of fortifications in the tropical Pacific islands', *Journal of Anthropological Archaeology*, 29(1), pp. 113–124. doi: 10.1016/j.jaa.2009.11.001.
- Filatova, T., Polhill, J. G. and van Ewijk, S. (2016) 'Regime shifts in coupled socio-environmental systems: Review of modelling challenges and approaches', *Environmental Modelling and Software*. Elsevier Ltd, 75, pp. 333–347. doi: 10.1016/j.envsoft.2015.04.003.
- Finlay, J. C. and Kendall, C. (2007) 'Stable Isotope Tracing of Temporal and Spatial Variability in Organic Matter Sources to Freshwater Ecosystems', in Michener, R. and Lajtha, K. (eds) *Stable Isotopes in Ecology and Environmental Science*. Second Edi. Oxford: Blackwell Publishing Ltd, pp. 283–333. doi: 10.1002/9780470691854.ch10.
- Folland, C. K. *et al.* (2002) 'Relative influences of the Interdecadal Pacific Oscillation and ENSO on the South Pacific Convergence Zone', *Geophysical Research Letters*, 29(13), p. 1643. doi:

10.1029/2001GL014201.

Font, E. *et al.* (2010) 'Identification of tsunami-induced deposits using numerical modeling and rock magnetism techniques: A study case of the 1755 Lisbon tsunami in Algarve, Portugal', *Physics of the Earth and Planetary Interiors*. Elsevier B.V., 182(3–4), pp. 187–198. doi:

10.1016/j.pepi.2010.08.007.

Food and Agriculture Organization (FAO) (2010) 'Building Resilience To Climate Change: Root Crop and Fishery Production', p. 130.

Foucher, A. *et al.* (2021) 'A worldwide meta-analysis (1977–2020) of sediment core dating using fallout radionuclides including  $^{137}\text{Cs}$  and  $^{210}\text{Pbxs}$ ', *Earth System Science Data*, 13(10), pp. 4951–4966. doi: 10.5194/essd-13-4951-2021.

Freund, M. B. *et al.* (2019) 'Higher frequency of Central Pacific El Niño events in recent decades relative to past centuries', *Nature Geoscience*. Springer US. doi: 10.1038/s41561-019-0353-3.

Fritz, S. C. *et al.* (2010) 'Diatoms as indicators of hydrologic and climatic change in saline lakes', in Smol, J. P. and Stoermer, E. F. (eds) *The diatoms: applications for the environmental and Earth sciences*. 2nd edn. Cambridge: Cambridge University Press, pp. 186–208.

Gagliardi, L. M. *et al.* (2019) 'Reduced Rainfall Increases Metabolic Rates in Upper Mixed Layers of Tropical Lakes', *Ecosystems*, 22(6), pp. 1406–1423. doi: 10.1007/s10021-019-00346-0.

Gasse, F. (2002) 'Diatom-inferred salinity and carbonate oxygen isotopes in Holocene waterbodies of the western Sahara and Sahel (Africa)', *Quaternary Science Reviews*, 21(7), pp. 737–767. doi: 10.1016/S0277-3791(01)00125-1.

Gasse, F. and Fontes, J. C. (1989) 'Palaeoenvironments and palaeohydrology of a tropical closed lake (Lake Asal, Djibouti) since 10,000 yr B.P.', *Palaeogeography, Palaeoclimatology, Palaeoecology*, 69(C), pp. 67–102. doi: 10.1016/0031-0182(89)90156-9.

GeoCore (2023) *GeoCore Sediment Coring System*. Available at: <https://www.geo-core.com/> (Accessed: 3 April 2023).

Gill, W. W. (1894) *From Darkness to Light in Polynesia with illustrative clan songs*. London: The Religious Tract Society.

Giordano, R. and Liersch, S. (2012) 'A fuzzy GIS-based system to integrate local and technical knowledge in soil salinity monitoring', *Environmental Modelling and Software*. Elsevier Ltd, 36, pp. 49–63. doi: 10.1016/j.envsoft.2011.09.004.

## List of References

- Goff, J. (2008) *Tsunami Hazard Assessment for the Hawkes Bay Region*. Christchurch.
- Goff, J., Chagué-Goff, C., *et al.* (2011) 'Palaeotsunamis in the Pacific Islands', *Earth-Science Reviews*, 107, pp. 141–146.
- Goff, J., Lamarche, G., *et al.* (2011) 'Predecessors to the 2009 South Pacific tsunami in the Wallis and Futuna archipelago', *Earth-Science Reviews*. Elsevier B.V., 107(1–2), pp. 91–106. doi: 10.1016/j.earscirev.2010.11.003.
- Goff, J., McFadgen, B. G., *et al.* (2012) 'Palaeotsunamis and their influence on Polynesian settlement', *Holocene*, 22(9), pp. 1067–1069. doi: 10.1177/0959683612437873.
- Goff, J., Chagué-Goff, C., *et al.* (2012) 'Progress in palaeotsunami research', *Sedimentary Geology*. Elsevier B.V., 243–244, pp. 70–88. doi: 10.1016/j.sedgeo.2011.11.002.
- Goff, J. and Nunn, P. D. (2016) 'Rapid societal change as a proxy for regional environmental forcing: Evidence and explanations for Pacific island societies in the 14–15th centuries', *Island Arc*, 25(5), pp. 305–315. doi: 10.1111/iar.12117.
- Goodwin, I. D., Browning, S. A. and Anderson, A. J. (2014) 'Climate windows for Polynesian voyaging to New Zealand and Easter Island', *Proceedings of the National Academy of Sciences*, 111(41), pp. 14716–14721. doi: 10.1073/pnas.1408918111.
- Gorman, M. K. *et al.* (2012) 'A coral-based reconstruction of sea surface salinity at Sabine Bank, Vanuatu from 1842 to 2007 CE', *Paleoceanography*, 27(3), pp. 1–13. doi: 10.1029/2012PA002302.
- Gosling, W. D. *et al.* (2020) 'Human occupation and ecosystem change on Upolu (Samoa) during the Holocene', *Journal of Biogeography*, (October 2019), p. jbi.13783. doi: 10.1111/jbi.13783.
- Haffke, C. and Magnúsdóttir, G. (2013) 'The South Pacific Convergence Zone in three decades of satellite images', *Journal of Geophysical Research Atmospheres*, 118(19), pp. 10839–10849. doi: 10.1002/jgrd.50838.
- Hajdas, I. *et al.* (2021) 'Radiocarbon dating', *Nature Reviews Methods Primers*, 1(1). doi: 10.1038/s43586-021-00058-7.
- Hamilton, B. K. and Kahn, J. G. (2007) 'Pre-Contact Population in the 'Opunohu Valley, Mo'orea An Integrated Archaeological and Ethnohistorical Approach', in Kirch, P. V. and Rallu, J. L. (eds) *The Growth and Collapse of Pacific Island Societies: Archaeological and Demographic Perspectives*. University of Hawai'i Press, pp. 129–159.
- Hao, Z. *et al.* (2017) 'An integrated package for drought monitoring, prediction and analysis to aid

- drought modeling and assessment', *Environmental Modelling and Software*. Elsevier Ltd, 91, pp. 199–209. doi: 10.1016/j.envsoft.2017.02.008.
- Hassall, J. D. (2017) *Static or dynamic: reconstructing past movements of the South Pacific Convergence Zone*. University of Southampton. doi: 10.1016/0041-2678(70)90288-5.
- Heaton, T. J. *et al.* (2021) 'Radiocarbon: A key tracer for studying Earth's dynamo, climate system, carbon cycle, and Sun', *Science*, 374(6568). doi: 10.1126/science.abd7096.
- Heckbert, S. (2013) 'MayaSim : An Agent-Based Model of the Ancient Maya Social-Ecological System', *Journal of Artificial Societies and Social Simulation*, 16(4), pp. 1–10.
- Heikkilä, M. *et al.* (2010) 'Sediment isotope tracers from Lake Saarikko, Finland, and implications for Holocene hydroclimatology', *Quaternary Science Reviews*. Elsevier Ltd, 29(17–18), pp. 2146–2160. doi: 10.1016/j.quascirev.2010.05.010.
- Heiri, O., Lotter, A. F. and Lemcke, G. (2001) 'Loss on ignition as a method for estimating organic and carbonate content in sediments: reproducibility and comparability of results', *Journal of Paleolimnology*, 25, pp. 101–110. doi: 10.1016/0009-2541(93)90140-E.
- Hernández, A. *et al.* (2010) 'ENSO and solar activity signals from oxygen isotopes in diatom silica during late glacial-Holocene transition in central Andes (18°S)', *Journal of Paleolimnology*, 44(2), pp. 413–429. doi: 10.1007/s10933-010-9412-x.
- Hernández, A. *et al.* (2013) 'Climate, catchment runoff and limnological drivers of carbon and oxygen isotope composition of diatom frustules from the central andean altiplano during the Lateglacial and Early Holocene', *Quaternary Science Reviews*. Elsevier Ltd, 66, pp. 64–73. doi: 10.1016/j.quascirev.2012.10.013.
- Hernández, A. *et al.* (2020) 'Modes of climate variability : Synthesis and review of proxy-based reconstructions through the Holocene', *Earth-Science Reviews*. Elsevier, 209(June), pp. 1–31. doi: 10.1016/j.earscirev.2020.103286.
- Herrscher, E. *et al.* (2018) 'Multi-isotopic analysis of first Polynesian diet (Talasiu, Tongatapu, Kingdom of Tonga)', *Journal of Archaeological Science: Reports*, 18(January), pp. 308–317. doi: 10.1016/j.jasrep.2018.01.012.
- Heyerdahl, T. (1950) 'The Voyage of the Raft Kon-Tiki', *The Royal Geographical Society (with the Institute of British Geographers)*, 115(1), pp. 20–41. Available at: <https://www.jstor.org/stable/1789016>.

## List of References

- Heyng, A. M. *et al.* (2012) 'Environmental changes in northern New Zealand since the Middle Holocene inferred from stable isotope records ( $\delta^{15}\text{N}$ ,  $\delta^{13}\text{C}$ ) of Lake Pupuke', *Journal of Paleolimnology*, 48(2), pp. 351–366. doi: 10.1007/s10933-012-9606-5.
- Higgins, P. A. *et al.* (2020) 'One Thousand Three Hundred Years of Variability in the Position of the South Pacific Convergence Zone', *Geophysical Research Letters*, 47(17), pp. 1–11. doi: 10.1029/2020GL088238.
- Higley, M. C., Conroy, J. L. and Schmitt, S. (2018) 'Last Millennium Meridional Shifts in Hydroclimate in the Central Tropical Pacific', *Paleoceanography and Paleoclimatology*, 33(4), pp. 354–366. doi: 10.1002/2017PA003233.
- Hiroa, T. R. (Peter B. (1934) *Mangaian Society*. Bernice P. Honolulu, Hawaii: Bishop Museum Press. Available at: <https://nzetc.victoria.ac.nz/tm/scholarly/tei-BucMangi.html>.
- Hixon, S. W. *et al.* (2019) 'The ethnohistory of freshwater use on Rapa Nui (Easter Island, Chile)', *Journal of the Polynesian Society*, 128(2), pp. 163–189. doi: 10.15286/jps.128.2.163-189.
- Holden, J. (2017) *An introduction to physical geography and the environment*. London: Pearson Education Ltd.
- Horrocks, M. *et al.* (2015) 'A plant microfossil record of Late Quaternary environments and human activity from Rano Aroi and surroundings, Easter Island', *Journal of Paleolimnology*, 54(4), pp. 279–303. doi: 10.1007/s10933-015-9852-4.
- Huang, W. (1979) *Comparative Food Values of Sweet Potatoes in Hawaii*. 42.
- Huffman, T. N. (2009) 'A cultural proxy for drought: ritual burning in the Iron age of Southern Africa', *Journal of Archaeological Science*. Elsevier Ltd, 36(4), pp. 991–1005. doi: 10.1016/j.jas.2008.11.026.
- Hunt, T. L. and Lipo, C. P. (2006) 'Late Colonization of Easter Island', *Science*, 311(March), pp. 1603–1607.
- Hunt, T. L. and Lipo, C. P. (2008) 'Evidence for a shorter chronology on Rapa Nui (Easter Island)', *Journal of Island and Coastal Archaeology*, 3(1), pp. 140–148. doi: 10.1080/15564890801990797.
- Hunt, T. L. and Lipo, C. P. (2017) 'The last great migration : Human colonization of the remote Pacific Islands', in Boivin, N., Crassard, R., and Petraglia, M. (eds) *Human Dispersal and Species Movement: From Prehistory to Present*. Cambridge: Cambridge University Press, pp. 194–216. doi: 10.1017/9781316686942.009.

- Ioannidis, A. G. *et al.* (2021) 'Paths and timings of the peopling of Polynesia inferred from genomic networks', *Nature*, 597(7877), pp. 522–526. doi: 10.1038/s41586-021-03902-8.
- IPCC (2001) *Climate Change 2001: Impacts, Adaptation & Vulnerability*. Edited by J. J. McCarthy *et al.* Cambridge: Cambridge University Press. Available at: <http://www.ipcc.ch/ipccreports/tar/wg2/index.htm>.
- IPCC (2022) *Climate Change 2022: Impacts, Adaptation, and Vulnerability. Contribution of Working Group II to the Sixth Assessment Report of the Intergovernmental Panel on Climate Change*. Edited by H.-O. Pörtner *et al.* Cambridge, United Kingdom: Cambridge University Press.
- Irwin, G. (1992) *The Prehistoric Exploration and Colonisation of the Pacific*. Cambridge: Cambridge University Press.
- Irwin, G. (2008) 'Pacific Seascapes , Canoe Performance , and a Review of Lapita Voyaging with Regard to Theories of Migration', *Asian Perspectives*, 47(1), pp. 12–27.
- Irwin, G. *et al.* (2022) 'The sailing performance of ancient Polynesian canoes and the early settlement of East Polynesia', *Archaeology in Oceania*, 0, pp. 1–17. doi: 10.1002/arco.5277.
- Jakeman, A. J., Letcher, R. A. and Norton, J. P. (2006) 'Ten iterative steps in development and evaluation of environmental models', *Environmental Modelling and Software*, 21(5), pp. 602–614. doi: 10.1016/j.envsoft.2006.01.004.
- Jankaew, K. *et al.* (2008) 'Medieval forewarning of the 2004 Indian Ocean tsunami in Thailand', *Nature*, 455(7217), pp. 1228–1231. doi: 10.1038/nature07373.
- Johnson, T. C. *et al.* (2016) 'A progressively wetter climate in southern East Africa over the past 1.3 million years', *Nature*. Nature Publishing Group, 537(7619), pp. 220–224. doi: 10.1038/nature19065.
- Kahn, J. G. (2014) 'Colonization , Settlement , and Process in Central Eastern Polynesia', in Cochrane, E. E. and Hunt, T. L. (eds) *Oxford Handbook of Prehistoric Oceania*. Oxford: Oxford University Press, pp. 353–374.
- Kahn, J. G., Horrocks, M. and Nieuwoudt, M. K. (2014) 'Agriculture, Domestic Production, and Site Function: Microfossil Analyses and Late Prehistoric Landscapes of the Society Islands', *Economic Botany*, 68(3), pp. 246–263. doi: 10.1007/s12231-014-9274-7.
- Kahn, J. G. and Sinoto, Y. (2017) 'Refining the Society Islands Cultural Sequence: Colonisation Phase and Developmental Phase Coastal Occupation on Mo'orea Island', *The Journal of Polynesian*

## List of References

*Society*, 126(1), pp. 33–60.

Kalfatak, D. and Jaensch, R. (2014) *Directory of Wetlands of Vanuatu*.

Kamatani, A. (1982) 'Dissolution rates of silica from diatoms decomposing at various temperatures', *Marine Biology*, 68(1), pp. 91–96. doi: 10.1007/BF00393146.

Kaniewski, D., Guiot, J. and Van Campo, E. (2015) 'Drought and societal collapse 3200years ago in the Eastern Mediterranean: A review', *Wiley Interdisciplinary Reviews: Climate Change*, 6(4), pp. 369–382. doi: 10.1002/wcc.345.

Kelly, R. A. *et al.* (2013) 'Selecting among five common modelling approaches for integrated environmental assessment and management', *Environmental Modelling and Software*. Elsevier Ltd, 47, pp. 159–181. doi: 10.1016/j.envsoft.2013.05.005.

Kennett, D. *et al.* (2006) 'Prehistoric human impacts on Rapa, French Polynesia', *Antiquity*, 80(308), pp. 340–354. doi: 10.1017/s0003598x00093662.

Kilbourne, K. H. *et al.* (2004) 'El Niño-Southern Oscillation-related salinity variations recorded in the skeletal geochemistry of a *Porites* coral from Espiritu Santo, Vanuatu', *Paleoceanography*, 19(4), pp. 1–8. doi: 10.1029/2004PA001033.

Kinaston, R., Bedford, S., *et al.* (2014) 'Diet and human mobility from the lapita to the early historic period on Uripiv Island, Northeast Malakula, Vanuatu', *PLoS ONE*, 9(8). doi: 10.1371/journal.pone.0104071.

Kinaston, R., Buckley, H., *et al.* (2014) 'Lapita diet in remote oceania: New stable isotope evidence from the 3000-year-old Teouma site, Efate Island, Vanuatu', *PLoS ONE*, 9(3), pp. 1–18. doi: 10.1371/journal.pone.0090376.

Kirch, P. V. (1984) *The evolution of the Polynesian chiefdoms*. Cambridge: Cambridge University Press.

Kirch, P. V. (1994) *The wet and the dry: irrigation and agricultural intensification in Polynesia*. Chicago: University of Chicago Press.

Kirch, P. V. (2007) 'Three islands and an archipelago: Reciprocal interactions between humans and island ecosystems in Polynesia', *Earth and Environmental Science Transactions of the Royal Society of Edinburgh*, 98(1), pp. 85–99. doi: 10.1017/S1755691007000011.

Kirch, P. V. *et al.* (2010) 'The Onemea site (Taravai Island, Mangareva) and the human colonization of Southeastern Polynesia', *Archaeology in Oceania*, 45(2), pp. 66–79. doi: 10.1002/j.1834-

4453.2010.tb00081.x.

Kirch, P. V. *et al.* (2012) 'Building and testing models of long-term agricultural intensification and population dynamics: A case study from the Leeward Kohala Field System, Hawai'i', *Ecological Modelling*. Elsevier B.V., 227, pp. 18–28. doi: 10.1016/j.ecolmodel.2011.11.032.

Kirch, P. V. (2017a) *On the Road of the Winds*. 2nd editio. London: University of California Press, Ltd.

Kirch, P. V. (2017b) *Tangatatau Rockshelter: The Evolution of an Eastern Polynesian Socio-Ecosystem*. Los Angeles: Cotsen Institute of Archaeology Press.

Kirch, P. V *et al.* (1995) 'Prehistory and Human Ecology in Eastern Polynesia : Excavations at Tangatatau Rockshelter , Mangaia , Cook Islands', *Archaeology in Oceania*, 30(2), pp. 47–65.

Kirch, P. V (1997) 'Microcosmic Histories: Island Perspectives on "Global" Change', *American Anthropologist*, 99(1), pp. 30–42.

Kirkendall, M. A. (1998) *Demographic change on Matuku island, Fiji in response to infectious diseases introduced at European contact*. University of Hawai'i.

Kokociński, M. *et al.* (2009) 'Diatom assemblages in 26 December 2004 tsunami deposits from coastal zone of Thailand as sediment provenance indicators', *Polish Journal of Environmental Studies*, 18(1), pp. 93–101.

Kolb, M. J. and Dixon, B. (2002) 'Landscapes of War: Rules and Conventions of Conflict in Ancient Hawai'i (And Elsewhere)', *American Antiquity*, 67(3), pp. 514–534. doi: 10.2307/1593824.

Krammer, K. and Lange-Bertalot, H. (1991) *Süßwasserflora von Mitteleuropa*. Edited by H. Ettl *et al.* Stuttgart, Germany.: Gustav Fisher Verlag.

Kuil, L. *et al.* (2016) 'Conceptualizing socio-hydrological drought processes: The case of Maya collapse', *Water Resources Research*, 52, pp. 6222–6242. doi: 10.1111/j.1752-1688.1969.tb04897.x.

Kuil, L. *et al.* (2019) 'Learning from the Ancient Maya: Exploring the Impact of Drought on Population Dynamics', *Ecological Economics*. Elsevier, 157, pp. 1–16. doi: 10.1016/j.ecolecon.2018.10.018.

Kurita, N. (2013) 'Water isotopic variability in response to mesoscale convective system over the tropical ocean', *Journal of Geophysical Research Atmospheres*, 118(18), pp. 10376–10390. doi: 10.1002/jgrd.50754.

## List of References

- Kylander, M. E. *et al.* (2011) 'High-resolution X-ray fluorescence core scanning analysis of Les Echets (France) sedimentary sequence: New insights from chemical proxies', *Journal of Quaternary Science*, 26(1), pp. 109–117. doi: 10.1002/jqs.1438.
- Kylander, M. E. *et al.* (2012) 'Recommendations for using XRF core scanning as a tool in tephrochronology', *Holocene*, 22(3), pp. 371–375. doi: 10.1177/0959683611423688.
- Ladd, S. N. *et al.* (2021) 'Leaf Wax Hydrogen Isotopes as a Hydroclimate Proxy in the Tropical Pacific', *Journal of Geophysical Research: Biogeosciences*, 126(3). doi: 10.1029/2020JG005891.
- Ladefoged, T. N., Flaws, A. and Stevenson, C. M. (2013) 'The distribution of rock gardens on Rapa Nui (Easter Island) as determined from satellite imagery', *Journal of Archaeological Science*. Elsevier Ltd, 40(2), pp. 1203–1212. doi: 10.1016/j.jas.2012.09.006.
- Lamb, A. L. *et al.* (2000) 'A 9000-year oxygen and carbon isotope record of hydrological change in a small Ethiopian crater lake', *The Holocene*, 10(2), pp. 167–177.
- Lamb, A. L. *et al.* (2002) 'Climatic and non-climatic effects on the  $\delta^{18}\text{O}$  and  $\delta^{13}\text{C}$  compositions of Lake Awassa, Ethiopia, during the last 6.5 ka', *Quaternary Science Reviews*, 21(20–22), pp. 2199–2211. doi: 10.1016/S0277-3791(02)00087-2.
- Lamb, A. L. *et al.* (2005) 'A comparison of the palaeoclimate signals from diatom oxygen isotope ratios and carbonate oxygen isotope ratios from a low latitude crater lake', *Palaeogeography, Palaeoclimatology, Palaeoecology*, 223, pp. 290–302. doi: 10.1016/j.palaeo.2005.04.011.
- Langdon, P. G. *et al.* (2010) 'Lacustrine evidence of early-holocene environmental change in northern Iceland: A multiproxy palaeoecology and stable isotope study', *Holocene*, 20(2), pp. 205–214. doi: 10.1177/0959683609354301.
- Laut, L. *et al.* (2019) 'Diatoms from the most hypersaline lagoon in Brazil: Vermelha lagoon', *Continental Shelf Research*. Elsevier Ltd, 181(April), pp. 111–123. doi: 10.1016/j.csr.2019.05.001.
- Lee, C. T. and Tuljapurkar, S. (2008) 'Population and prehistory I: Food-dependent population growth in constant environments', *Theoretical Population Biology*, 73(4), pp. 473–482. doi: 10.1016/j.tpb.2008.03.001.
- Leng, M. J. (2006) *Isotopes in Palaeoenvironmental Research*. Netherlands: Springer.
- Leng, M. J. and Henderson, A. C. G. (2013) 'Recent advances in isotopes as palaeolimnological proxies', *Journal of Paleolimnology*, 49, pp. 481–496. doi: 10.1007/s10933-012-9667-5.
- Leng, M. J. and Marshall, J. D. (2004) 'Palaeoclimate interpretation of stable isotope data from

- lake sediment archives', *Quaternary Science Reviews*, 23(7–8), pp. 811–831. doi: 10.1016/j.quascirev.2003.06.012.
- Leppard, T. P. (2019) 'Anthropocene Dynamics in the Prehistoric Pacific', *Nature and Culture*, 14(2), pp. 119–146. doi: 10.3167/nc.2019.140202.
- Li, H. C. and Ku, T. L. (1997) ' $\delta^{13}\text{C}$ - $\delta^{18}\text{O}$  covariance as a paleohydrological indicator for closed-basin lakes', *Palaeogeography, Palaeoclimatology, Palaeoecology*, 133(1–2), pp. 69–80. doi: 10.1016/S0031-0182(96)00153-8.
- Linsley, B. K. *et al.* (2004) 'Geochemical evidence from corals for changes in the amplitude and spatial pattern of South Pacific interdecadal climate variability over the last 300 years', *Climate Dynamics*, 22(1), pp. 1–11. doi: 10.1007/s00382-003-0364-y.
- Liutkus, C. M. *et al.* (2005) 'Paleoenvironmental interpretation of lake-margin deposits using  $\text{d}^{13}\text{C}$  and  $\text{d}^{18}\text{O}$  results from early Pleistocene carbonate rhizoliths, Olduvai Gorge, Tanzania', *Geology*, 33(5), pp. 377–380. doi: 10.1130/G21132.1.
- Van Loon, A. F. *et al.* (2014) 'How climate seasonality modifies drought duration and deficit', *Journal of Geophysical Research Atmospheres*, 119, pp. 4640–4656. doi: 10.1038/175238c0.
- Van Loon, A. F. (2015) 'Hydrological drought explained', *Wiley Interdisciplinary Reviews: Water*, 2(4), pp. 359–392. doi: 10.1002/WAT2.1085.
- Lorrey, A. *et al.* (2012) 'Reconstructing the South Pacific Convergence Zone Position during the Presatellite Era: A La Niña Case Study', *Monthly Weather Review*, 140(11), pp. 3653–3668. doi: 10.1175/mwr-d-11-00228.1.
- Lowe, D. J. (2011) 'Tephrochronology and its application: A review', *Quaternary Geochronology*. Elsevier B.V, 6(2), pp. 107–153. doi: 10.1016/j.quageo.2010.08.003.
- Lowe, J. J. *et al.* (2015) 'The RESET project: Constructing a European tephra lattice for refined synchronisation of environmental and archaeological events during the last c. 100 ka', *Quaternary Science Reviews*, 118, pp. 1–17. doi: 10.1016/j.quascirev.2015.04.006.
- Lucero, L. J., Gunn, J. D. and Scarborough, V. L. (2011) 'Climate change and classic maya water management', *Water (Switzerland)*, 3(2), pp. 479–494. doi: 10.3390/w3020479.
- Maloney, A. E. *et al.* (2019) 'Reconstructing precipitation in the tropical South Pacific from dinosterol 2H/1H ratios in lake sediment', *Geochimica et Cosmochimica Acta*. Elsevier Ltd, 245, pp. 190–206. doi: 10.1016/j.gca.2018.10.028.

## List of References

- Maloney, A. E. *et al.* (2022) 'Contrasting Common Era climate and hydrology sensitivities from paired lake sediment dinosterol hydrogen isotope records in the South Pacific Convergence Zone', *Quaternary Science Reviews*. Elsevier Ltd, 281, p. 107421. doi: 10.1016/j.quascirev.2022.107421.
- Mamo, B. L., Brock, G. A. and Gretton, E. J. (2013) 'Deep sea benthic foraminifera as proxies for palaeoclimatic fluctuations in the New Caledonia Basin, over the last 140,000years', *Marine Micropaleontology*. Elsevier B.V., 104(September 2001), pp. 1–13. doi: 10.1016/j.marmicro.2013.08.002.
- Mann, D. *et al.* (2008) 'Drought, vegetation change, and human history on Rapa Nui (Isla de Pascua, Easter Island)', *Quaternary Research*, 69(1), pp. 16–28. doi: 10.1016/j.yqres.2007.10.009.
- Mann, M. E. *et al.* (2009) 'Global signatures and dynamical origins of the little ice age and medieval climate anomaly', *Science*, 326(5957), pp. 1256–1260. doi: 10.1126/science.1177303.
- Marais, A. P. (1990) *Kolo Velata: An analysis of west Polynesian fortifications*. University of California, Berkeley. Available at: [http://cyber.usask.ca/login?url=https://search.proquest.com/docview/304216493?accountid=14739&bdid=6497&\\_bd=v1h5R87UR0yNZzULVS6iL6ibP5g%3D](http://cyber.usask.ca/login?url=https://search.proquest.com/docview/304216493?accountid=14739&bdid=6497&_bd=v1h5R87UR0yNZzULVS6iL6ibP5g%3D).
- Margalef, O. *et al.* (2014) 'Environmental processes in Rano Aroi (Easter Island) peat geochemistry forced by climate variability during the last 70kyr', *Palaeogeography, Palaeoclimatology, Palaeoecology*. Elsevier B.V., 414, pp. 438–450. doi: 10.1016/j.palaeo.2014.09.025.
- Mark, M. V. (1976) *The Relationship between Ecology and Myth in Mangaia*. University of Otago, Dunedin.
- Matisoo-Smith, E. (2015) 'Ancient DNA and the human settlement of the Pacific: A review', *Journal of Human Evolution*, 79, pp. 93–104. doi: 10.1016/j.jhevol.2014.10.017.
- Maupin, C. R. *et al.* (2014) 'Persistent decadal-scale rainfall variability in the tropical South Pacific Convergence Zone through the past six centuries', *Climate of the Past*, 10(4), pp. 1319–1332. doi: 10.5194/cp-10-1319-2014.
- Maxson, C. *et al.* (2021) 'Ecology and climate sensitivity of a groundwater-fed lake on subtropical North Stradbroke Island (Minjerrabah), Queensland, Australia over the last 7500 years', *Journal of Paleolimnology*. Springer Netherlands, 9. doi: 10.1007/s10933-021-00222-9.
- McCoy, P. C. and Cleghorn, P. L. (1988) 'Archaeological excavations on Santa Cruz (Nendö), southeast Solomon Islands: summary report', *Archaeology in Oceania*, 23(3), pp. 104–115. doi: 10.1002/j.1834-4453.1988.tb00197.x.

- McGree, S., Schreider, S. and Kuleshov, Y. (2016) 'Trends and variability in droughts in the Pacific islands and Northeast Australia', *Journal of Climate*, 29(23), pp. 8377–8397. doi: 10.1175/JCLI-D-16-0332.1.
- Merico, A. (2017) 'Models of easter island human-resource dynamics: Advances and gaps', *Frontiers in Ecology and Evolution*, 5(DEC), pp. 1–7. doi: 10.3389/fevo.2017.00154.
- Merlin, M. D. (1991) 'Woody Vegetation on the Raised Coral Limestone of Mangaia', *Pacific Science*, 45(2), pp. 131–151.
- Meyers, P. A. (2003) 'Application of organic geochemistry to paleolimnological reconstruction: a summary of examples from the Laurentian Great Lakes', *Organic Geochemistry*, 34(2), pp. 261–289.
- Meyers, P. A. and Ishiwatari, R. (1993) 'Lacustrine organic geochemistry-an overview of indicators of organic matter sources and diagenesis in lake sediments', *Organic Geochemistry*, 20(7), pp. 867–900. doi: 10.1016/0146-6380(93)90100-P.
- Meyers, P. A. and Lallier-Vergès, E. (1999) 'Lacustrine sedimentary organic matter records of Late Quaternary paleoclimates', *Journal of Paleolimnology*, 21(3), pp. 345–372. doi: 10.1023/A:1008073732192.
- Meyers, P. A. and Teranes, J. L. (2001) 'Sediment Organic Matter', in Last, W. M. and Smol, J. P. (eds) *Tracking Environmental Change Using Lake Sediments. Volume 2: Physical and Geochemical Methods*. Dordrecht: Kluwer Academic Publishers, pp. 239–269.
- Mishra, A. K. and Singh, V. P. (2010) 'Review paper A review of drought concepts', *Journal of Hydrology*. Elsevier B.V., 391, pp. 202–216. doi: 10.1016/j.jhydrol.2010.07.012.
- Montenegro, A., Callaghan, R. T. and Fitzpatrick, S. M. (2014) 'From west to east: Environmental influences on the rate and pathways of Polynesian colonization', *Holocene*, 24(2), pp. 242–256. doi: 10.1177/0959683613517402.
- Mulrooney, M. A. (2013) 'An island-wide assessment of the chronology of settlement and land use on Rapa Nui (Easter Island) based on radiocarbon data', *Journal of Archaeological Science*. Elsevier Ltd, 40(12), pp. 4377–4399. doi: 10.1016/j.jas.2013.06.020.
- Murphy, B. F., Power, S. B. and McGree, S. (2014) 'The varied impacts of El Niño-southern oscillation on Pacific Island climates', *Journal of Climate*, 27(11), pp. 4015–4036. doi: 10.1175/JCLI-D-13-00130.1.

## List of References

Mycoo, M. *et al.* (2022) 'Small Islands', in Pörtner, H.-O. *et al.* (eds) *Climate Change 2022: Impacts, Adaptation and Vulnerability. Contribution of Working Group II to the Sixth Assessment Report of the Intergovernmental Panel on Climate Change*. Cambridge: Cambridge University Press, pp. 2043–2121. doi: 10.1017/9781009325844.017.2043.

National Environment Service Government of Cook Islands (2021) *National Water, Sanitation and Climate Outlook*. Cook Islands.

Navarro, J. N. and Lobban, C. S. (2009) 'Freshwater and marine diatoms from the western Pacific islands of Yap and Guam, with notes on some diatoms in Damselish territories', *Diatom Research*, 24(1), pp. 1–34. doi: 10.1080/0269249X.2009.9705787.

Neale, R. and Slingo, J. (2003) 'The Maritime Continent and its role in the global climate: A GCM study', *Journal of Climate*, 16(5), pp. 834–848. doi: 10.1175/1520-0442(2003)016<0834:TMCAIR>2.0.CO;2.

Nelson, D. B. and Sachs, J. P. (2016) 'Galápagos hydroclimate of the Common Era from paired microalgal and mangrove biomarker 2H/1H values', *Proceedings of the National Academy of Sciences of the United States of America*, 113(13), pp. 3476–3481. doi: 10.1073/pnas.1516271113.

Nemeth, K., Cronin, S. J. and White, J. D. L. (2007) 'Kuwae Caldera and Climate Confusion', *The Open Geology Journal*, 1(1), pp. 7–11. doi: 10.2174/187426290701017092.

Newman, M. *et al.* (2016) 'The Pacific decadal oscillation, revisited', *Journal of Climate*, 29(12), pp. 4399–4427. doi: 10.1175/JCLI-D-15-0508.1.

NIWA (2023) *Interdecadal Pacific Oscillation*. Available at: <https://niwa.co.nz/node/111124> (Accessed: 11 April 2023).

NOAA (2022) *Ocean Exploration*. Available at: <https://oceanexplorer.noaa.gov/facts/pacific-size.html> (Accessed: 21 November 2022).

Nunn, P. and Britton, J. M. R. (2001) 'Human-Environment Relationships in the Pacific Islands around A. D. 1300', *Environment and History*, 7(1), pp. 3–22.

Nunn, P. D. (2000a) 'Environmental Catastrophe in the Pacific Islands around A.D. 1300', *Geoarchaeology - An International Journal*, 15(7), pp. 715–740. doi: 10.1002/1520-6548(200010)15:7<715::AID-GEA4>3.0.CO;2-L.

Nunn, P. D. (2000b) 'Illuminating Sea-Level Fall around AD 1220-1510 (730-440 cal yr BP) in the Pacific Islands: Implications for Environmental Change and Cultural Transformation', 56(1), pp.

46–54.

Nunn, P. D. (2003) 'Revising ideas about environmental determinism: Human-environment relations in the Pacific Islands', *Asia Pacific Viewpoint*, 44(1), pp. 63–72. doi: 10.1111/1467-8373.00184.

Nunn, P. D. *et al.* (2016) 'Classifying Pacific islands', *Geoscience Letters*. Springer International Publishing, 3(1). doi: 10.1186/s40562-016-0041-8.

Nunn, P. D. and Kumar, R. (2018) 'Understanding climate-human interactions in Small Island Developing States (SIDS) Implications for future livelihood sustainability', *International Journal of Climate Change Strategies and Management*, 8(1), pp. 80–95. doi: 10.1108/17568690910955603.

Nurhati, I. S., Cobb, K. M. and Di Lorenzo, E. (2011) 'Decadal-scale SST and salinity variations in the central tropical pacific: Signatures of natural and anthropogenic climate change', *Journal of Climate*, 24(13), pp. 3294–3308. doi: 10.1175/2011JCLI3852.1.

NWS (2023) *Hydroclimate*. Available at: [https://www.weather.gov/safety/drought-hydroclimate#:~:text=What is Hydroclimate%3F,hydrological \(or water\) cycle](https://www.weather.gov/safety/drought-hydroclimate#:~:text=What%20is%20Hydroclimate%3F,hydrological%20(or%20water)%20cycle). (Accessed: 11 April 2023).

O'Connor, S. and Hiscock, P. (2014) *The peopling of Sahul and Near Oceania*, *The Oxford Handbook of Prehistoric Oceania*. Available at: <http://www.oxfordhandbooks.com/view/10.1093/oxfordhb/9780199925070.001.0001/oxfordhb-9780199925070-e-002%0Ahttp://oxfordhandbooks.com/view/10.1093/oxfordhb/9780199925070.001.0001/oxfordhb-9780199925070-e-002>.

O'Day, S. J., O'Day, P. and Steadman, D. W. (2004) 'Defining the Lau Context: Recent Findings on Nayau, Lau Islands, Fiji', *New Zealand Journal of Archaeology*, 25, pp. 31–56.

Oehlert, A. M. and Swart, P. K. (2014) 'Interpreting carbonate and organic carbon isotope covariance in the sedimentary record', *Nature Communications*. Nature Publishing Group, 5, pp. 1–7. doi: 10.1038/ncomms5672.

Oldfield, F. and Appleby, P. G. (1984) 'Empirical testing of <sup>210</sup>Pb-dating models for lake sediments', in Hayworth, E. Y. and Lund, J. W. G. (eds) *Lake Sediments and Environmental History*. Leicester, UK: Leicester University Press, pp. 93–124.

Osborne, M. C. *et al.* (2014) 'A 215-yr coral  $\delta^{18}\text{O}$  time series from Palau records dynamics of the West Pacific Warm Pool following the end of the Little Ice Age', *Coral Reefs*, 33(3), pp. 719–731.

## List of References

doi: 10.1007/s00338-014-1146-1.

Owen, R. B. *et al.* (2004) 'Swamps, springs and diatoms: Wetlands of the semi-arid Bogoria-Baringo Rift, Kenya', *Hydrobiologia*, 518(1–3), pp. 59–78. doi: 10.1023/B:HYDR.0000025057.62967.2c.

Palacios, O., Barcelo, J. A. and Delgado, R. (2022) 'Exploring the role of ecology and social organisation in agropastoral societies : A Bayesian network approach', *PLoS ONE*, 17(10), pp. 1–29. doi: 10.1371/journal.pone.0276088.

Palanisamy, P. *et al.* (2018) 'Taro (*Colocasia esculenta*): An overview', ~ 156 ~ *Journal of Medicinal Plants Studies*, 6(4), pp. 156–161.

Parkes, A. (1994) *Holocene environments and vegetational change on four Polynesian islands*. University of Hull.

Partin, J. W. *et al.* (2013) 'Multidecadal rainfall variability in south pacific convergence zone as revealed by stalagmite geochemistry', *Geology*, 41(11), pp. 1143–1146. doi: 10.1130/G34718.1.

Pawley, A. (2007) 'The origins of Early Lapita culture: the testimony of historical linguistics', in Bedford, S., Sand, C., and Connaughton, S. P. (eds) *Oceanic Explorations: Lapita and Western Pacific Settlement*. Canberra: ANU E Press, pp. 17–49.

Pearl, F. B. (2004) 'The chronology of mountain settlements on Tutuila, American Samoa', *Journal of the Polynesian Society*, 113(4), pp. 331–348.

Peng, Y. *et al.* (2015) 'Journal of geophysical research', *Journal of geophysical research*, 120(4449), pp. 7573–7585. doi: 10.1002/2015JD023104.

Perry, G. L. W. W. and O'Sullivan, D. (2018) 'Identifying Narrative Descriptions in Agent-Based Models Representing Past Human- Environment Interactions', *Journal of Archaeological Method and Theory*, 25(3), pp. 795–817. doi: 10.17608/k6.auckland.5327944.

Petchey, F. *et al.* (2014) 'Radiocarbon dating of burials from the Teouma Lapita cemetery, Efate, Vanuatu', *Journal of Archaeological Science*, 50(1), pp. 227–242. doi: 10.1016/j.jas.2014.07.002.

Pezzey, J. C. V. and Anderies, J. M. (2003) 'The effect of subsistence on collapse and institutional adaptation in population-resource societies', *Journal of Development Economics*, 72(1), pp. 299–320. doi: 10.1016/S0304-3878(03)00078-6.

Philippsen, B. (2013) 'The freshwater reservoir effect in radiocarbon dating', *Heritage Science*, 1(1), pp. 1–19. doi: 10.1186/2050-7445-1-24.

- Power, S. *et al.* (1999) 'Inter-decadal modulation of the impact of ENSO on Australia', *Climate Dynamics*, 15(5), pp. 319–324. doi: 10.1007/s003820050284.
- Puleston, C. O. and Tuljapurkar, S. (2008) 'Population and prehistory II: Space-limited human populations in constant environments', *Theoretical Population Biology*, 74(2), pp. 147–160. doi: 10.1016/j.tpb.2008.05.007.
- Quinn, T. M., Taylor, F. W. and Crowley, T. J. (2006) 'Coral-based climate variability in the Western Pacific Warm Pool since 1867', *Journal of Geophysical Research: Oceans*, 111(11), pp. 1–11. doi: 10.1029/2005JC003243.
- Quinn, T. M., Taylor, F. W. and Crowley, T. J. (2017) 'A 173 year stable isotope record from a tropical South Pacific coral', *The Journal of Neuroscience*, 37(47), pp. 11335–11352. doi: 10.1523/JNEUROSCI.1223-17.2017.
- Quintus, S. and Cochrane, E. E. (2018a) 'Pre-Contact Samoan Cultivation Practices in Regional and Theoretical Perspective', *Journal of Island and Coastal Archaeology*. Taylor & Francis, 13(4), pp. 474–500. doi: 10.1080/15564894.2017.1285835.
- Quintus, S. and Cochrane, E. E. (2018b) 'The prevalence and importance of niche construction in agricultural development in Polynesia', *Journal of Anthropological Archaeology*. Elsevier, 51(July), pp. 173–186. doi: 10.1016/j.jaa.2018.06.007.
- Rainbird, P. (1996) 'A place to look up to: A review of Chuukese hilltop enclosures', *The Journal of Polynesian Society*, 105(4), pp. 461–478.
- Rainbird, P. (2002) 'A message for our future? The Rapa Nui (Easter Island) ecodisaster and Pacific island environments', *World Archaeology*, 33(3), pp. 436–451. doi: 10.1080/00438240120107468.
- Ramage, C. (1995) *Forecasters Guide to Tropical Meteorology - Air Weather Technical Report 240 (updated)*. Scott AFV, IL: Air Weather Service.
- Ramage, C. S. (1995) *Forecasters Guide to Tropical Meteorology - AWS TR 240 updated*. Scotts Air Force Base, IL.
- Rao, S. *et al.* (1987) 'Isotopic studies on sea water intrusion and interrelations between water bodies: some field experiments', in IAEA (ed.) *Isotope Techniques in Water Resources Development*. Austria: IAEA, p. 836.
- Rasbury, M. and Aharon, P. (2006) 'ENSO-controlled rainfall variability records archived in tropical stalagmites from the mid-ocean island of Niue, South Pacific', *Geochemistry, Geophysics*,

## List of References

*Geosystems*, 7(7). doi: 10.1029/2005GC001232.

Rechtman, R. B. (1992) *The Evolution of Sociopolitical Complexity in the Fiji Islands*. University of California.

Reed, J. M. (1998) 'Diatom preservation in the recent sediment record of Spanish saline lakes: Implications for palaeoclimate study', *Journal of Paleolimnology*, 19(2), pp. 129–137. doi: 10.1023/A:1007948600780.

Reepmeyer, C. (2021) 'Modelling prehistoric social interaction in the south-western Pacific: a view from the obsidian sources in northern Vanuatu. In From Field to Museum—Studies from Melanesia in Honour of Robin Torrence, ed. Jim Specht, Val Attenbrow, and Jim Allen', *Technical Reports of the Australian Museum online*, 34(34), pp. 137–148. doi: 10.3853/j.1835-4211.34.2021.1748.

Reilly, M. P. J. (2009) *Ancestral Voices from Mangaia: A history of the Ancient Gods and Chiefs*. Auckland: The Polynesian Society.

Restrepo, A. *et al.* (2012) 'Impacts of climate variability and human colonization on the vegetation of the Galápagos Islands', *Ecology*, 93(8), pp. 1853–1866. doi: 10.1890/11-1545.1.

Reuveny, R. and Decker, C. S. (2000) 'Easter Island: Historical anecdote or warning for the future?', *Ecological Economics*, 35(2), pp. 271–287. doi: 10.1016/S0921-8009(00)00202-0.

Rieth, T. M. *et al.* (2011) 'The 13th century polynesian colonization of Hawai'i Island', *Journal of Archaeological Science*, 38(10), pp. 2740–2749. doi: 10.1016/j.jas.2011.06.017.

Rieth, T. M. and Hunt, T. L. (2008) 'A radiocarbon chronology for Samoan prehistory', *Journal of Archaeological Science*, 35, pp. 1901–1927. doi: 10.1016/j.jas.2007.12.001.

Riou, B. *et al.* (2020) 'Backwash sediment record of the 2009 South Pacific Tsunami and 1960 Great Chilean Earthquake Tsunami', *Scientific Reports*, 10(1), pp. 1–13. doi: 10.1038/s41598-020-60746-4.

Rohling, E. J. and Palike, H. (2005) 'Centennial-scale climate cooling with a sudden cold event around 8,200 years ago', *Nature*, 434(April).

Roman, M. *et al.* (2021) 'A multi-decadal geochemical record from Rano Aroi (Easter Island/Rapa Nui): Implications for the environment, climate and humans during the last two millennia', *Quaternary Science Reviews*, 268. doi: 10.1016/j.quascirev.2021.107115.

Roman, S., Bullock, S. and Brede, M. (2017) 'Coupled Societies are More Robust Against Collapse:

- A Hypothetical Look at Easter Island', *Ecological Economics*. The Authors, 132, pp. 264–278. doi: 10.1016/j.ecolecon.2016.11.003.
- Rongo, T., Bush, M. and Van Woesik, R. (2009) 'Did ciguatera prompt the late Holocene Polynesian voyages of discovery?', *Journal of Biogeography*, 36(8), pp. 1423–1432. doi: 10.1111/j.1365-2699.2009.02139.x.
- Rothwell, R. G. and Croudace, I. W. (2015) 'Micro-XRF Studies of Sediment Cores: A Perspective on Capability and Application in the Environmental Sciences', in Rothwell, R. G. and Croudace, I. W. (eds) *Micro-XRF Studies of Sediment Cores: Applications of a non-destructive Tool for the Environmental Sciences*. London: Springer, pp. 1–24.
- Rull, V. *et al.* (2015) 'Late Holocene vegetation dynamics and deforestation in Rano Aroi: Implications for Easter Island's ecological and cultural history', *Quaternary Science Reviews*, 126(SEPTEMBER), pp. 219–226. doi: 10.1016/j.quascirev.2015.09.008.
- Rustic, G. T. *et al.* (2015) 'Dynamical excitation of the tropical Pacific Ocean and ENSO variability by Little Ice Age cooling', *Science*, 350(6267), pp. 1537–1541. doi: 10.1126/science.aac9937.
- Ryves, D. B. *et al.* (2006) 'Physical and chemical predictors of diatom dissolution in freshwater and saline lake sediments in North America and West Greenland', *Limnology and Oceanography*, 51(3), pp. 1355–1368. doi: 10.4319/lo.2006.51.3.1355.
- Sachs, J. P. *et al.* (2009) 'Southward movement of the Pacific intertropical convergence zone AD 1400-1850', *Nature Geoscience*, 2(7), pp. 519–525. doi: 10.1038/ngeo554.
- Sachs, J. P. *et al.* (2018) 'Southward Shift of the Pacific ITCZ During the Holocene', *Paleoceanography and Paleoclimatology*, 33(12), pp. 1383–1395. doi: 10.1029/2018PA003469.
- Sáez, A. *et al.* (2009) 'Glacial to Holocene climate changes in the SE Pacific. The Raraku Lake sedimentary record (Easter Island, 27°S)', *Quaternary Science Reviews*, 28(25–26), pp. 2743–2759. doi: 10.1016/j.quascirev.2009.06.018.
- Sand, C. (2014) 'Archaeology of a Piece of Gondwanaland : The Past of New Caledonia Archaeology of a Piece of Gondwanaland : The Past of New Caledonia', in Cochrane, E. E. and Hunt, T. L. (eds) *The Oxford Handbook of Prehistoric Oceania*. Oxford: Oxford University Press, pp. 185–205.
- Santos, G. M. *et al.* (2007) 'Ultra small-mass AMS 14C sample preparation and analyses at KCCAMS/UCI Facility', *Nuclear Instruments and Methods in Physics Research, Section B: Beam Interactions with Materials and Atoms*, 259(1), pp. 293–302. doi: 10.1016/j.nimb.2007.01.172.

## List of References

- El Sawah, S. *et al.* (2012) 'Using system dynamics for environmental modelling: Lessons learnt from six case studies', *iEMSs 2012 - Managing Resources of a Limited Planet: Proceedings of the 6th Biennial Meeting of the International Environmental Modelling and Software Society*, pp. 1367–1374.
- El Sawah, S. *et al.* (2017) 'An overview of the system dynamics process for integrated modelling of socio-ecological systems: Lessons on good modelling practice from five case studies', *Environmental Modelling and Software*. Elsevier Ltd, 93, pp. 127–145. doi: 10.1016/j.envsoft.2017.03.001.
- de Scally, F. A. (2008) 'Historical tropical cyclone activity and impacts in the Cook Islands', *Pacific Science*, 62(4), pp. 443–459. doi: 10.2984/1534-6188(2008)62[443:HTCAAI]2.0.CO;2.
- Schabetsberger, R. *et al.* (2009) 'Losing the bounty? Investigating species richness in isolated freshwater ecosystems of oceania', *Pacific Science*, 63(2), pp. 153–179. doi: 10.2984/049.063.0201.
- Schroeder, T. T. A. (2009) 'Climate on Islands', in Gillespie, R. G. and Clague, D. A. (eds) *Encyclopedia of Islands*. London: University of California Press, Ltd., pp. 171–174.
- Schulze, J. *et al.* (2017) 'Agent-based modelling of social-ecological systems: Achievements, challenges, and a way forward', *Jasss*, 20(2). doi: 10.18564/jasss.3423.
- Schwalb, A., Burns, S. J. and Kelts, K. (1999) 'Holocene environments from stable isotope stratigraphy of ostracods and authigenic carbonate in Chilean Altiplano Lakes', *Palaeogeography, Palaeoclimatology, Palaeoecology*, 148(1–3), pp. 153–168. doi: 10.1016/S0031-0182(98)00181-3.
- Sear, D. A. *et al.* (2020) 'Human settlement of East Polynesia earlier, incremental, and coincident with prolonged South Pacific drought', *PNAS*, 117(16), pp. 8813–8819. doi: 10.1073/pnas.1920975117.
- Secretariat of the Pacific Community (2011) 'Food security in the Pacific and East Timor and its vulnerability to climate change A report to the Australian Government Department of Climate Change and Energy Efficiency'. Available at: <http://creativecommons.org/licenses/by/3.0/au/>.
- Secretariat of the Pacific Community (2020) 'Pacific Island Populations 2020'. doi: 10.1007/978-94-007-0753-5\_675.
- Shanahan, T. M. *et al.* (2007) 'Simulating the response of a closed-basin lake to recent climate changes in tropical West Africa ( Lake Bosumtwi , Ghana )', *Hydrological Processes*, 21, pp. 1678–1691. doi: 10.1002/hyp.

- Shanahan, T. M. *et al.* (2009) 'Atlantic forcing of persistent drought in West Africa', *Science*, 324(5925), pp. 377–380. doi: 10.1126/science.1166352.
- Shapiro, C. H. (2020) *The Function of Prehistoric Agricultural Systems in Sāmoa : A GIS Analysis of Resilience to Flooding*. Ohio State University.
- Sheffield, J. and Wood, E. F. (2008) 'Projected changes in drought occurrence under future global warming from multi-model, multi-scenario, IPCC AR4 simulations', *Climate Dynamics*, 31(1), pp. 79–105. doi: 10.1007/s00382-007-0340-z.
- Sims, P. A. (1996) *An Atlas of British Diatoms*. Biopress Ltd.
- Smittenberg, R. H. *et al.* (2011) 'Compound-specific D/H ratios of the marine lakes of Palau as proxies for West Pacific Warm Pool hydrologic variability', *Quaternary Science Reviews*, 30(7–8), pp. 921–933. doi: 10.1016/j.quascirev.2011.01.012.
- Spriggs, M. J. T. (1984) 'Taro Irrigation Techniques in the Pacific', in Chandra, S. (ed.) *Edible Aroids*. Oxford: Clarendon Press, pp. 123–135.
- Stansell, N. D. *et al.* (2020) 'A lake sediment stable isotope record of late-middle to late Holocene hydroclimate variability in the western Guatemala highlands', *Earth and Planetary Science Letters*. Elsevier B.V., 542, p. 116327. doi: 10.1016/j.epsl.2020.116327.
- Sterman, J. D. (2002) *System Dynamics: Systems Thinking and Modeling for a Complex World*.
- Stoddart, D. R. (1992) 'Biogeography of the tropical Pacific', *Pacific Science*, 46(2), pp. 276–293.
- Stoddart, D. R., Woodroffe, C. D. and Spencer, T. (1990) 'Mauke, Mitiaro and Atiu: geomorphology of Makatea Islands in the southern Cooks', *Atoll Research Bulletin*, 339–346(341). doi: 10.5479/si.00775630.341.1.
- Stoermer, E. F. and Smol, J. P. (2010) 'Applications and uses of diatoms: prologue', in Stoermer, E. F. and Smol, J. P. (eds) *The diatoms: Applications for the environmental and earth sciences*. 2nd edn. Cambridge: Cambridge University Press, pp. 3–10.
- Stott, L. *et al.* (2004) 'Decline of surface temperature and salinity in the western tropical pacific ocean in the holocene epoch', *Nature*, 431(7004), pp. 56–59. doi: 10.1038/nature02903.
- Strandberg, N. A. *et al.* (2023) 'Island ecosystem responses to the Kuwae eruption and precipitation change over the last 1600 years ', *Frontiers in Ecology and Evolution*, 11, pp. 1–14. doi: 10.3389/fevo.2023.1087577.

## List of References

- Stuiver, M. and Polach, H. A. (1977) 'Radiocarbon Reporting of  $^{14}\text{C}$  data', *Radiocarbon*, 19(3), pp. 355–363.
- Sylvestre, F. *et al.* (1995) 'Lake levels in the southern Bolivian Altiplano ( $19^{\circ}$ - $21^{\circ}\text{S}$ .) during the Late Glacial based on diatom studies', *International Journal of Salt Lake Research*, 4(4), pp. 281–300. doi: 10.1007/BF01999113.
- Talbot, M. R. (1990) 'A review of the palaeohydrological interpretation of carbon and oxygen isotopic ratios in primary lacustrine carbonates', *Chemical Geology: Isotope Geoscience Section*, 80(4), pp. 261–279. doi: 10.1016/0168-9622(90)90009-2.
- Talbot, M. R. (2001) 'Nitrogen Isotopes in Palaeolimnology', *Tracking Environmental Change Using Lake Sediments*, 2, pp. 401–439. doi: 10.1007/0-306-47670-3\_15.
- Temple-Brown, C. (2018) *When did Humans First Colonise Mangaia? - A Sediment Core Analysis*. University of Southampton.
- Terry, J. P., Kostaschuk, R. A. and Garimella, S. (2006) 'Sediment deposition rate in the Falefa River basin, Upolu Island, Samoa', *Journal of Environmental Radioactivity*, 86(1), pp. 45–63. doi: 10.1016/j.jenvrad.2005.07.004.
- Thomas, T. (2008) 'The long pause and the last pulse: Mapping East Polynesian colonisation', in Clark, G., Leach, F., and O'Connor, S. (eds) *Islands of Inquiry: Colonisation, seafaring and the archaeology of maritime landscapes*. Canberra: Australian National University Press, pp. 97–112. doi: 10.22459/ta29.06.2008.07.
- Thomas, T., Sheppard, P. and Walter, R. (2001) 'Landscape , Violence and Social Bodies : Ritualized Architecture in a Solomon Islands Society', *The Journal of the Royal Anthropological Institute*, 7(3), pp. 545–572.
- Thompson, C. S. (1986) *The climate and weather of the Southern Cook Islands*. Wellington.
- Thompson, D. M. *et al.* (2017) 'Tropical Pacific climate variability over the last 6000 years as recorded in Bainbridge Crater Lake, Galápagos', *Paleoceanography*, 32(8), pp. 903–922. doi: 10.1002/2017PA003089.
- Tibby, J. *et al.* (2007) 'Diatom – salinity relationships in wetlands : assessing the influence of salinity variability on the development of inference models', *Hydrobiologia*, 591, pp. 207–218. doi: 10.1007/s10750-007-0803-6.
- Till, C. *et al.* (2018) 'Understanding climate-induced migration through computational modeling: A

- critical overview with guidance for future efforts', *Journal of Defense Modeling and Simulation*, 15(4), pp. 415–435. doi: 10.1177/1548512916679038.
- Tiwari, M., Singh, A. K. and Sinha, D. K. (2015) 'Stable Isotopes: Tools for understanding past climatic conditions and their application in chemostratigraphy', in Mu, R. (ed.) *Chemostratigraphy: concepts, techniques and application*. Amsterdam: Elsevier, pp. 65–92.
- Toomey, M. R., Donnelly, J. P. and Tierney, J. E. (2016) 'South Pacific hydrologic and cyclone variability during the last 3000 years', *Paleoceanography*, 31(4), pp. 491–504. doi: 10.1002/2015PA002870.
- Troy, T. J., Pavao-Zuckerman, M. and Evans, T. P. (2015) 'Debates—Perspectives on socio-hydrology: Socio-hydrologic modeling: Tradeoffs, hypothesis testing, and validation', *Water Resources Research*, 51, pp. 4806–4814. doi: 10.1029/eo064i046p00929-04.
- United Nations (1983) *Ground Water in the Pacific Region, Natural Resources/Water Series No.12*. New York.
- United Nations (2012) *Weathering Uncertainty: Traditional knowledge for climate change assessment and adaptation*. Available at: [www.unutki.org](http://www.unutki.org).
- Valentin, F. *et al.* (2006) 'Dietary patterns during the late prehistoric/historic period in Cikobia island (Fiji): insights from stable isotopes and dental pathologies', *Journal of Archaeological Science*, 33(10), pp. 1396–1410. doi: 10.1016/j.jas.2006.01.012.
- Valentin, F. *et al.* (2010) 'Lapita subsistence strategies and food consumption patterns in the community of Teouma (Efate, Vanuatu)', *Journal of Archaeological Science*. Elsevier Ltd, 37(8), pp. 1820–1829. doi: 10.1016/j.jas.2010.01.039.
- Valero-Garcés, B. L. *et al.* (1997) 'Holocene Climate in the Northern Great Plains Inferred from Sediment Stratigraphy, Stable Isotopes, Carbonate Geochemistry, Diatoms, and Pollen at Moon Lake, North Dakota', *Quaternary Research*, 48(3), pp. 359–369. doi: 10.1006/qres.1997.1930.
- Ventana Systems, I. (2015) *Vensim Software*. Available at: <https://vensim.com/vensim-software/> (Accessed: 21 June 2022).
- VNSO (2009) *Vanuatu National Statistics Office 2009 Census Reports*. Available at: <http://www.vnso.gov.vu>.
- VNSO (2016) *Vanuatu National Statistics Office 2016 Census Reports*. Available at: <http://www.vnso.gov.vu>.

## List of References

- Weisler, M. I. *et al.* (2016) 'Cook Island artifact geochemistry demonstrates spatial and temporal extent of pre-European interarchipelago voyaging in East Polynesia', *Proceedings of the National Academy of Sciences of the United States of America*, 113(29), pp. 8150–8155. doi: 10.1073/pnas.1608130113.
- Weltje, G. J. *et al.* (2015) 'Prediction of Geochemical Composition from XRF Core Scanner Data: A New Multivariate Approach Including Automatic Selection of Calibration Samples and Quantification of Uncertainties', in Croudace, I. W. and Rothwell, R. G. (eds) *Micro-XRF Studies of Sediment Cores, Developments in Paleoenvironmental Research*. London: Springer, pp. 507–534.
- White, I. *et al.* (2007) 'Climatic and Human Influences on Groundwater', *Soil Science*. doi: 10.2136/vzj2006.0092.
- van der Wiel, K. *et al.* (2015) 'A dynamical framework for the origin of the diagonal South Pacific and South Atlantic Convergence Zones', *Quarterly Journal of the Royal Meteorological Society*, 141(691), pp. 1997–2010. doi: 10.1002/qj.2508.
- Williams, J. (1837) *A Narrative of Missionary Enterprises in the South Sea Islands*. Cambridge, United Kingdom: Cambridge University Press. Available at: <https://www.cambridge.org/core/books/narrative-of-missionary-enterprises-in-the-south-sea-islands/CFF44B9335D97D033F6FCC54E62FF5B5>.
- Wilmshurst, J. M. *et al.* (2008) 'Dating the late prehistoric dispersal of Polynesians to New Zealand using the commensal Pacific rat', *Proceedings of the National Academy of Sciences of the United States of America*, 105(22), pp. 7676–7680. doi: 10.1073/pnas.0801507105.
- Wilmshurst, J. M. *et al.* (2011) 'High-precision radiocarbon dating shows recent and rapid initial human colonization of East Polynesia', *Proceedings of the National Academy of Sciences of the United States of America*, 108(5), pp. 1815–1820. doi: 10.1073/pnas.1015876108.
- Wirrmann, D., Eagar, S. H., *et al.* (2011) 'First insights into mid-Holocene environmental change in central Vanuatu inferred from a terrestrial record from Emaotfer Swamp, Efaté Island', *Quaternary Science Reviews*. Elsevier Ltd, 30(27–28), pp. 3908–3924. doi: 10.1016/j.quascirev.2011.10.003.
- Wirrmann, D., Sémah, A. M., *et al.* (2011) 'Mid- to late Holocene environmental and climatic changes in New Caledonia, southwest tropical Pacific, inferred from the littoral plain Gouaro-Déva', *Quaternary Research*, 76(2), pp. 229–242. doi: 10.1016/j.yqres.2011.04.007.
- Wirrmann, D., Sémah, A. M. and Chacornac-Rault, M. (2006) 'Late Holocene paleoenvironment in

- northern New Caledonia, southwestern Pacific, from a multiproxy analysis of lake sediments', *Quaternary Research*, 66(2), pp. 213–232. doi: 10.1016/j.yqres.2006.04.002.
- Wood, B. L. (1967) 'Geology of the Cook Islands', *New Zealand Journal of Geology and Geophysics*, 10(6), pp. 1429–1445. doi: 10.1080/00288306.1967.10423227.
- Wood, C. P. (1978) 'Petrology of Atiu and Mangaia, Cook Islands (note)', *New Zealand Journal of Geology and Geophysics*, 21(6), pp. 767–771. doi: 10.1080/00288306.1978.10425206.
- Wyman, D. A. *et al.* (2021) 'Coeval Drying Across the Central Tropical Pacific Over the Last Millennium', *Paleoceanography and Paleoclimatology*, 36, pp. 1–15. doi: 10.1029/2021PA004311.
- Yacobaccio, H. D. and Morales, M. (2005) 'Mid-Holocene environment and human occupation of the Puna', *Quaternary International*, 132, pp. 5–14. doi: 10.1016/j.quaint.2004.07.010.
- Yan, D. *et al.* (2006) 'A quantitative knowledge-based model for designing suitable growth dynamics in rice', *Plant Production Science*, 9(2), pp. 93–105. doi: 10.1626/pp.9.93.
- Yonekura, N. *et al.* (1988) 'Holocene fringing reefs and sea-level change in Mangaia Island, Southern Cook Islands', *Palaeogeography, Palaeoclimatology, Palaeoecology*, 68(2–4), pp. 177–188. doi: 10.1016/0031-0182(88)90038-7.
- Zaborska, A. *et al.* (2007) 'Intercomparison of alpha and gamma spectrometry techniques used in  $^{210}\text{Pb}$  geochronology', *Journal of Environmental Radioactivity*, 93(1), pp. 38–50. doi: 10.1016/j.jenvrad.2006.11.007.
- Zhang, D. D. *et al.* (2011) 'The causality analysis of climate change and large-scale human crisis', *Proceedings of the National Academy of Sciences of the United States of America*, 108(42), pp. 17296–17301. doi: 10.1073/pnas.1104268108.
- Zhang, Z., Leduc, G. and Sachs, J. P. (2014) 'El Niño evolution during the Holocene revealed by a biomarker rain gauge in the Galápagos Islands', *Earth and Planetary Science Letters*. Elsevier B.V., 404, pp. 420–434. doi: 10.1016/j.epsl.2014.07.013.